საქართველოს მეცნიერებათა ეროვნული აკადემიის მაცნე
PROCEEDINGS OF THE GEORGIAN NATIONAL ACADEMY OF SCIENCES
ИЗВЕСТИЯ НАЦИОНАЛЬНОЙ АКАДЕМИИ НАУК ГРУЗИИ

ქიმიის სერია

CHEMICAL SERIES

СЕРИЯ ХИМИЧЕСКАЯ

ISSN – 0132 – 6074

ტომი
2016 № 3 **Volume 42**
Том

თბილისი – TBILISI – ТБИЛИСИ

საქართველოს მეცნიერებათა ეროვნული აკადემიის მაცნე
PROCEEDINGS OF THE GEORGIAN NATIONAL ACADEMY OF SCIENCES
ИЗВЕСТИЯ НАЦИОНАЛЬНОЙ АКАДЕМИИ НАУК ГРУЗИИ

ქიმიის სერია
CHEMICAL SERIES
СЕРИЯ ХИМИЧЕСКАЯ

ISSN – 0132 – 6074

ტომი
Volume 42 № 3
Том

ჟურნალი დაარსდა 1975 წელს
The Journal is founded in 1975
Журнал основан в 1975 году

წელიწადში 4 ნომერი
4 numbers annually
4 номера в год

თბილისი – **TBILISI – ТБИЛИСИ**

2016

შოთა რუსთაველის ეროვნული სამეცნიერო ფონდი
SHOTA RUSTAVELI NATIONAL SCIENCE FOUNDATION

ჟურნალის მიმდინარე ნომერი დაიბეჭდა შოთა რუსთაველის ეროვნული სამეცნიერო ფონდის ფინანსური მხარდაჭერით (CG16_i_2_48)

* 2540 Olentagy River Road, P.O. Box 3012, Columbus, OH 43210-0012, USA, American Chemical Society
** LERL TECHINFORMI, http://www.tech.org.ge; www.tech.caucasus.net

საერთაშორისო სამეცნიერო კონფერენცია

„თანამედროვე კვლევები და მათი გამოყენების პერსპექტივები ქიმიაში, ქიმიურ ტექნოლოგიასა და მომიჯნავე დარგებში“

რჩეული სტატიების ქართული რეზიუმეები
ნაწილი I

International Scientific Conference

"MODERN RESEARCHES AND PROSPECTS OF THEIR USE IN CHEMISTRY, CHEMICAL ENGINEERING AND RELATED FIELDS"

Featured articles
Part I

Международная научная конференции «СОВРЕМЕННЫЕ ИССЛЕДОВАНИЯ И ПЕРСПЕКТИВЫ ИХ ПРИМЕНЕНИЯ В ХИМИИ, ХИМИЧЕСКОЙ ТЕХНОЛОГИИ И СМЕЖНЫХ ОБЛАСТЯХ» Резюме избранных статей Часть I

საქართველოს მეცნიერებათა ეროვნული აკადემიის მაცნე, ქიმიის სერია 2016 ტ. 42 №3
Proceedings of the Georgian National Academy of Sciences, chemical series 2016 v. 42 No 3
ИЗВЕСТИЯ НАЦИОНАЛЬНОЙ АКАДЕМИИ НАУК ГРУЗИИ, Серия химическая 2016 т. 42 № 3

საერთაშორისო სამეცნიერო კონფერენცია

„თანამედროვე კვლევები და მათი გამოყენების პერსპექტივები ქიმიაში, ქიმიურ ტექნოლოგიასა და მომიჯნავე დარგებში“

მიძღვნილი რაფიელ აგლაძის არაორგანული ქიმიისა და ელექტროქიმიის ინსტიტუტის დაარსების 60 წლის იუბილეს
2016 ქლის 21-23 სექტემბერი, ურეკი, საქართველო

რჩეული სტატიები
ნაწილი I

International Scientific Conference

“MODERN RESEARCHES AND PROSPECTS OF THEIR USE IN CHEMISTRY, CHEMICAL ENGINEERING AND RELATED FIELDS”

Dedicated to the 60th anniversary of R.Agladze Institute of Inoeranic Chemistry and Electrohemistry
September 21-23, 2016, Ureki, Georgia

Featured articles
Part I

Международная научная конференции

«СОВРЕМЕННЫЕ ИССЛЕДОВАНИЯ И ПЕРСПЕКТИВЫ ИХ ПРИМЕНЕНИЯ В ХИМИИ, ХИМИЧЕСКОЙ ТЕХНОЛОГИИ И СМЕЖНЫХ ОБЛАСТЯХ»

посвященная 60-летию основания Института неорганической химии и электрохимии им. Р.И.Агладзе
21-24 сентября 2016 года, Уреки, Грузия

Избранные статьи
Часть I

Conference programm

	WEDNESDAY, 21 SEPTEMBER
13:00 – 15:00	**Registration,** *Lobby of the Hotel Kolkhida*
15:00 – 16:00	**Welcome address,** *Hall A*
16:00 – 16:30	**Coffee break,** *Hall of the Hotel Kolkhida*
	PLENARY, *Hall A*
	Chair: **Dr.N. Vaszilcsin,** University Politehnica Timisoara, Romania
16:30 – 17:00	**V. Beschkov**, Institute of Chemical Engineering, Bulgarian Academy of Sciences, Bulgaria
	BIOWASTE AND HYDROGEN SULFIDE – PERSPECTIVE RENEWABLE FUELS
17:00 – 17:30	**V. Tsitsishvili,** Ivane Javakhishvili Tbilisi State University, Petre Melikishvili Institute of Physical and Organic Chemistry, Georgia
	NEW GENERATION ZEOLITIC ADSORBERS
19:00 – 21:00	**Welcome Reception,** *Café of the Hotel Kolhida*
	THURSDAY, 22 SEPTEMBER
	PLENARY, *Hall A*
	Chair: **Dr. V. Beshkov**, Institute of Chemical Engineering, Sofia, Bulgaria
8:30 – 9:00	**K. Dossumov,** Center of Physical and Chemical Methods of Research and Analysis al-FarabyKazNU, Kazakhstan
	CONVERSION OF METHANE OVER THE OXIDE CATALYSTS
9:00 – 9:30	**T. Agladze,** Georgian Technical University, Georgia
	NOVEL TECHNOLOGY PLATFORM FOR SYNTHESIS OF MULTIFUNCTIONAL HYBRID NANOCOMPOSITES
9:30 – 10:00	**N. Vaszilcsin,** University Politehnica Timisoara, Romania
	ENHANCEMENT OF CATHODIC HYDROGEN EVOLUTION REACTION USING PROTON CARRIERS
10:00 – 10:30	**Coffee break**
	NEW METHODS FOR ECOLOGICAL AND RADIATION SAFETY, MEDICAL AND AGRARIAN RESEARCHES, *Hall A*
	Chair: **Dr. S. Kirillov**, Joint Department of Electrochemical Energy System, Kyiv, Ukraine
	Co – chair: **Dr. M. Tsitsagi,** TSU Petre Melikishvili Institute of Physical and Organic Chemistry, Georgia
10:30 – 10:45	**A. Mansourizadeh,** Department of Chemical Engineering, Islamic Azad University, Iran
	OILY WASTE WATER TREATMENT USING BLEND PSF-SPEEK HOLLOW FIBER MEMBRANE
10:45 – 11:00	**M. Tsitsagi,** TSU Petre Melikishvili Institute of Physical and Organic Chemistry, Georgia
	UTILIZATION OF AGRO-INDUSTRIAL WASTE MATERIALS BY USING SEQUENTIAL SUPERCRITICAL FLUID AND ULTRASOUND EXTRACTION METHODS

11:00 – 11:15	**S.A. Kirillov**, Joint Department of Electrochemical Energy Systems, Ukraine
	PHOSPHATE SCAVENGERS FOR REMEDIATION OF GROUNDWATERS AND TREATMENT OF HYPERPHOSPHATAEMIA IN ANIMALS AND HUMANS: REVIEW AND COMPARISON
11:15 – 11:30	**A. Surmava,** M. Nodia Institute of Geophysics, Georgia
	NUMERICAL SIMULATION OF DISTRIBUTION OF ARSENIC DISCHARGED TO TSKHENISTSKALI AND LUKHUNI RIVERS FROM INDUSTRIAL WASTE
11:30 – 11:45	**M. Mirtskhulava**, National Center for disease control and Public health, Georgia
	ULTRASOUND IN MEDICINE, BIOLOGY, BIOTECHNOLOGY
11:45 – 12:00	**V. Elisashvili**, Agricultural University of Georgia, Georgia
	INTEGRATED LIGNOCELLULOSE BIOREFINERY EXPLOITING WOOD-ROTTING FUNGI POTENTIAL
12:00 – 12:15	**D. Gventsadze**, LEPL R. Dvali Institute of Machine Mechanics, Georgia
	TECHNOLOGY OF ECO-FRIENDLY HIGH TEMPERATURE HEAT-INSULATOR MATERIALS ON THE BASIS OF LIQUID GLASS AND FOAMED PERLITE
12:15 – 13:15	**Free time**
	Chair: **Dr. E.H. Ismailov**, Institute of Petrochemical Processes, Baku, Azerbaijan
	Co-chair: **T. Chachibaia,** TSU, Tbilisi, Georgia
13:15 – 13:30	**T. Chachibaia,** TSU Faculty of Medicine, Georgia, University of Santiago de Compostela, Spain
	NMR TECHNOLOGY FOR ASSESSMENT OF SOCIETAL, ENVIRONMENTAL AND CHEMICAL RISKS OF AMMONIUM NITRATE
13:30 – 13:45	**I. Chikvaidze,** TSU, Georgia
	REGARDING SOME STEPS OF E. FISCHER REACTION MECHANISM
13:45 – 14:00	**E.H. Ismailov**, Institute of Petrochemical Processes of Azerbaijan National Academy of Sciences, Azerbaijan
	HYDROGENATION OF CARBON DIOXIDE OVER Fe-Zr/Al AND Fe-Ni/Al OXIDE CATALYSTS
14:00 – 14:15	**T. Varazi,** Durmishidze Institute of Biochemistry and Biotechnology of Agricultural University of Georgia, Georgia
	ABOUT ALGAE SPIRULINA'S ECOLOGICAL POTENTIAL FOR THEIR APPLICATION REMEDIATION TECHNOLOGIES
14:15 – 14:30	**V. Bakhtadze**, R. Agladze Institute of Inorganic Chemistry and Electrochemistry, Georgia
	OXIDE-MANGANESE CATALYSTS FOR SOLVING OF ECOLOGICAL PROBLEMS
14:30 – 14:45	**M. V. Panchvidze**, TSU, R. Agladze Institute of Inorganic Chemistry and Electrochemistry, Georgia

	ABOUT RADIOPROTECTIVE PROPERTIES OF SULFUR-ORGANIC COMPOUNDS
14:45 – 15:00	**N. Kvirkvelia**, TSU R. Agladze Institute of Inorganic Chemistry and Electrochemistry, Georgia
	OZONE USE IN AGRICULTURE
15:00 – 15:15	**I. Chitrekashvili,** TSU, PetreMelikishvili Institute of Physical and Organic Chemistry, Georgia
	STRUCTURAL CHANGES OF POLYPHENYLENEOXIDES IN THE PROCESS OF FRICTION
15:15 – 16:15	**STUDENT SESSION, *Hall A***
	Chair: **MSc**. **M. Soselia**, IICE, Georgia
15:15 – 15:30	**K. Kharaishvili**, TSU, Georgia
	SEPARATION OF ENANTIOMERS WITH SUPERFICIALLY POROUS SILICA MODIFIED WITH POLYSACCHARIDE DERIVATIVES AS EFFECTIVE CHIRAL STATIONARY PHASES IN HIGH-PERFORMANCE LIQUID CHROMATOGRAPHY
15:30 – 15:45	**M. Shavgulidze**, Iv. Beritashvili Experimental Biomedicine Centre, Georgia
	CHANGES OF LEARNING MOTIVATIONAL AND EMOTIONAL BEHAVIOR AND PASSIVE AVOIDANCE IN DEPRESSIVE RATS
15:45 – 16:00	**L. Khvichia,** AkakiTsereteli State University
	QUANTITATIVE DETERMINATION OF TOTAL MANGANESE IN ZESTAFONI SOIL AND DRINKING WATER AND ABNORMALITIES CAUSED BY ITS ABUNDANCE
16:00 – 16:15	**Z. Samkharadze**, TSU R. Agladze Institute of Inorganic Chemistry and Electrochemistry
	OXIDATION OF MANGANESE NITRATE SOLUTIONS BY OZONE - AIR MIXTURE
16:15 – 16:45	**Coffee break**
	NANO PROCESSES AND NANOTECHNOLOGIES, *Hall B*
	Chair: **Dr. G.Ya. Kolbasov**, V.I. Vernadskii Institute of General and Inorganic Chemistry of National, Academy of Sciences of Ukraine, Ukraine
	Co-chair: **Dr. N. Nioradze**, TSU, IICE, Georgia
10:30 – 10:45	**O. Ruzimuradov**, Turin Polytechnic University in Tashkent, Uzbekistan
	SECOND-GENERATION POROUS TiO_2 BASED PHOTOCATALYTIC NANOMATERIALS: SYNTHESIS AND PROPERTIES
10:45 – 11:00	**L. Tsereteli**, Max Planck Institute of Colloids and Interfaces, Germany
	AN ACCURATE COARSE-GRAINED MODEL FOR POLYSACCHARIDES IN SOLUTION
11:00 – 11:15	**M. Ersoz,** Selcuk University, Advanced Technology Research&Application Center, Turkey
	NANOSTRUCTURE FABRICATION BY USING OF BLOCK COPOLYMERS
11:15 – 11:30	**V. Bregadze**, TSU, Andronikashvili Institute of Physics, Georgia
	SORPTION CHARACTERISTICS OF ORGANIC MATERIALS IN METAL ION REDUCTION REACTION AND NANOTECHNOLOGY
11:30 – 11:45	**M. Rukhadze,** TSU, Faculty of Exact and Natural Sciences, Georgia

	STUDY OF STRUCTURE OF CONFINED WATER NANODROPLETS
11:45 – 12:00	**G.Ya. Kolbasov**, V.I. Vernadskii Institute of General and Inorganic Chemistry of National Academy of Sciences of Ukraine, Ukraine
	NANOMATERIALS AND PHOTOELECTROCHEMICAL SYSTEM FOR PRODUCTION OF SOLAR HYDROGEN
12:00 – 12:15	**N. Nioradze**, TSU, R. Agladze Institute of Inorganic Chemistry and Electrochemistry, Georgia
	SCANNING ELECTROCHEMICAL MICROSCOPY OF NANOSTRUCTURED CARBON MATERIALS
12:15 – 13:15	**Free time**
	ENERGY SOURCES, CONVERSION AND STORAGE, *Hall B*
	Chair: **Dr. M. N. Abdikarimov,** KazNTU, Kazakhstan
	Co-chair: Dr. **G. Tsagareli,** TSU, R. Agladze Institute of Inorganic Chemistry and Electrochemistry, Georgia
13:15 – 13:30	**E. Kachibaia**, TSU R. Agladze Institute of Inorganic Chemistry and Electrochemistry, Georgia
	SPINELS $LiM_XNi_{0.5-X}Mn_{1.5}O_4$ – TYPE (M=CO+CR, AL AND CU; $0<X\leq0.4$) AS PROMISING CATHODE MATERIALS FOR Li- ION BATTERIES
13:30 – 13:45	**M. N. Abdikarimov**, KazNTU, Kazakhstan
	PHOTOVOLTAIC MODULE
13:45 – 14:00	**S.I. Abasov,** Institute of Petrochemical Processes of Azerbaijan National Academy of Sciences, Azerbaijan
	THE FORMATION OF INTERMOLECULAR C-C BONDS AS A FUNCTION OF TEMPERATURE WITH PARTICIPATION OF C3-C4 ALKANE
14:00 – 14:15	**P. Nikoleishvili**, TSU R. Agladze Institute of Inorganic Chemistry and Electrochemistry, Georgia
	SYNTHESIS OF TiO_2 NANOTUBES BY Ti FOIL ELECTROCHEMICAL DISSOLUTION FOR DYE-SENSITIZED PHOTOELECTROCHEMICAL SOLAR CELL
14:15 – 14:30	**N. Khetsuriani,** TSU, Institute of Physical and Organic Chemistry, Georgia
	PRODUCTION OF BIODIESEL USING SUPERCRITICAL FLUIDS TECHNOLOGY
14:30 – 14:45	**G. Tsagareli,** TSU, R. Agladze Institute of Inorganic Chemistry and Electrochemistry, Georgia
	THE PREPARATION OF THE ACTIVE MANGANESE DIOXIDE POWDER BY ELECTROCHEMICAL METHOD FOR CURRENT SOURCES
15:15 – 16:15	**STUDENT SESSION, *Hall A***
16:15 – 16:45	**Coffee break**
16:45 – 17:45	**POSTER SESSION, Hotel Kolkhida Lobby**

	FRIDAY, 23 SEPTEMBER
	PLENARY, *Hall A*
	Chair: **Dr. V. Tsitsishvili**, TSU Petre Melikishvili Institute of Physical and Organic Chemistry,, Tbilisi, Georgia
8:30 – 9:00	**G. A. Tsirlina**, Moscow State University, Russia
	PLATINUM FREE ELECTROCATALYSTS BASED ON MANGANESE OXIDES FOR ELECTROCHEMICAL DEVICES
9:00 – 9:30	**S. A. Kirillov,** Joint Department of Electrochemical Energy Systems, Ukraine
	HIGH-RATE LITHIUM-ION BATTERIES: RECENT ADVANCES
9:30 – 10:00	**T. Marsagishvili,** R. Agladze Institute of Inorganic chemistry and Electrochemistry, Georgia
	SOME ASPECTS OF MODELING OF PHOTOCATALYSIS PROCESS
10:00 – 10:30	**Coffee break**
	NEW METHODS FOR ECOLOGICAL AND RADIATION SAFETY, MEDICAL AND AGRARIAN RESEARCHES, *Hall A*
	Chair: **Dr. L. Gorniak**, Industrial Chemistry Research Institute, Warsaw, Poland
	Co-chair: **Dr. I. Rubashvili**, Aversi-Rational Ltd, Quality Control Laboratory, Georgia
10:30 – 10:45	**M. N. Abdikarimov,** KazNTU, Kazakhstan
	INVESTIGATION OF POSSIBLE CHEMICAL WASTE DISPOSAL
10:45 – 11:00	**L. M. Gorniak,** Industrial Chemistry Research Institute, Warsaw, Poland
	CHEMICAL SECURITY AS A SYNTHESIS OF SCIENCES
11:00 – 11:15	**M. Labartkava,** University "Geomedi", Georgia
	THE USE OF MODERN PHYSICAL-CHEMICAL METHODS OF SUBSTANCE ANALYSIS IN THE ANALYSIS OF GEORGIAN RED WINE
11:15 – 11:30	**M. Nalbandyan,** NAS RA Institute of Geological Sciences, Yerevan, Armenia
	TECHNOLOGY OF PURIFICATION OF IRRIGATION WATER WITH A HIGH SALT CONTENT IN ORDER TO PREVENT SECONDARY SALINIZATION OF ARARAT VALLEY
11:30 – 11:45	**Ch. Stahl**, NaralexMaschinen UG, Germany
	BIO BRIQUETTES POTENTIAL IN GERMANY
11:45 – 12:00	**V.V. Tkach**, Chernivtsi National University, Ukraine
	A MATHEMATICAL REPRESENTATION OF ELECTROANALYTICAL FUNCTION OF THE SAFRANIN-MODIFIED RADICALLY-PRETREATED MATERIAL TO HYDROQUINONIC COMPOUNDS
12:00 – 12:15	**I. Rubashvili**, Aversi-Rational Ltd, Quality Control Laboratory, Georgia
	DEVELOPMENT AND VALIDATION OF SAMPLING AND QUANTITATIVE DETERMINATION METHODS OF CARVEDILOL RESIDUES USING HIGH PERFORMANCE LIQUID CHROMATOGRAPHY FOR CLEANING VALIDATION

12:15 – 13:15	**Free time**
	Chair: **Dr. N. Durgaryan**, Institute of Geological Sciences of NAS of Armenia, Yerevan, Armenia
	Co-chair: **Dr**. **M. Mantskava**, Society of Rheology, I. Beritashvili Center of Experimental Biomedicine, Georgia
13:15 – 13:30	**M. Karchkhadze**, TSU, Georgia
	ENANTIOSEPARATION OF CHIRAL ANTIMYCOTIC DRUGS IN HIGH-PERFORMANCE LIQUID CHROMATOGRAPHY WITH POLYSACCHARIDE-BASED CHIRAL COLUMNS
13:30 – 13:45	**N. Durgaryan**, Yerevan State University, Yerevan, Armenia
	SYNTHESES OF NH2/NH2 CAPPED ANILINE OLIGOMERS AND THEIR DERIVATIVES
13:45 – 14:00	**M. Mantskava**, Society of Rheology, I. Beritashvili Center of Experimental Biomedicine, Georgia
	THE SIGNIFICANCE OF THE NEW PROPERTIES OF BEMIPARIN FOR APPLIED MEDICINE
14:00 – 14:15	**A. Mskhiladze,** Faculty of Natural Sciences and Healthcare, Sokhumi State University, Georgia
	SOME CHARACTERISTICS OF THE SEPARATION OF ENANTIOMERS OF BETA-BLOCKER DRUGS USING POLYSACCHARIDE BASED CHIRAL COLUMNS IN HPLC
	FUNDAMENTAL AND TECHNOLOGICAL ASPECTS OF PROCESSING OF MINERAL PRODUCT AND SECONDARY RAW MATERIALS
	Chair: **Dr. G. Magalashvili**, GTU, Tbilisi, Georgia
	Co-chair: **Dr. Ali A. Jazie**, Alqadissiya University, Iraq
10:30 – 10:45	**L. Gurchumelia**, TSU, R. Agladze Institute of Inorganic Chemistry and Electrochemistry
	ELABORATION OF NEW TYPES, ECO-SAFE, INEXPENSIVE, HIGHLY EFFICIENT FIRE- PROTECTIVE MATERIALS
10:45 – 11:00	**G. Zakharov,** Ferdinand Tavadze Institute of Metallurgy and Materials Science
	OBTAINING LIGATURES FROM FINE GRAINED PARTICLES OF MANGANESE WASTE BY TECHNOLOGY -SHS METALLURGY
11:00 – 11:15	**D. Gogoli**, TSU R. Agladze Institute of Inorganic Chemistry and Electrochemistry
	ELECTRODEPOSITION AND CHARACTERIZATION OF Mn-Cu-Zn ALLOYS FOR CORROSION PROTECTION COATINGS
11:15 – 11:30	**L.G. Shamanauri**, R. Dvali Institute of Machine Mechanics
	COMPOSITES BASED ON POLYESTER LACQUER AND MINERAL FILLERS
11:30 – 11:45	**Ali A. Jazie,** Alqadissiya University, Iraq
	OPTIMIZATION OF BIODIESEL PRODUCTION FROM MUSTARD OIL
11:45 – 12:00	**G. Magalashvili,** Georgian Technical University
	ASCERTAINMENT OF THE MECHANISM OF FORMING OF ZONAL CONCENTRIC “AGATE STRUCTURES”

12:00 – 12:15	**B. Godibadze**, LEPL, G. Tsulukidze Mining Institute, Georgia
	EXPLOSIVE CONSOLIDATION OF Cu–W COMPOSITES IN HOT CONDITION
12:15 – 13:15	**Free time**
	Chair: **Dr. A. Peikrishvili**, F. Tavadze Institute of Metallurgy and Materials Science, IICE, Georgia
	Co-chair: **Dr. T. E. Machaladze,** TSU, R. Agladze Institute of Inorganic Chemistry and Electrochemistry
13:15 – 13:30	**A. Peikrishvili**, F. Tavadze Institute of Metallurgy and Materials Science, IICE, Georgia
	SHOCK WAVE ASSISTED CHEMICAL REACTIONS AND CONSOLIDATION OF Ta-Al INTERMETALIC COMPOUNDS
13:30 – 13:45	**L. Gabunia**, Caucasian Alexander Tvalchrelidze Institute of Mineral Resources, Georgia
	RESEARCH OF THE POSSIBILITY OF RECEIVING ACID AND HEAT-RESISTANT CONTINUOUS FIBER GLASS WITH USE OF MANGANIFEROUS WASTE PRODUCTS
13:45 – 14:00	**T. Machaladze,** TSU, R. Agladze Institute of Inorganic Chemistry and Electrochemistry
	THERMAL CHARACTERISTICS OF SPINEL-TYPE COMPLEX OXIDES $Me_{1-X}Zn_XFe_2O_4$ (WITH Me= Cu OR Mg)
14:00 – 14:15	**E. Shapakidze**, TSU, Caucasian A. TvalchrelidzeInstitite of Mineral Resources, Georgia
	RESEARCH OF INFLUENCE OF THE MODIFYING BaO AND SO_3 OXIDES ON PROPERTIES OF CEMENT CLINKER
14:15 – 15:15	**POSTER SESSION, *Hotel Kolkhida Lobby***
	ROUND TABLE; *Hall A*
15:15 – 15:30	**L. Chobanyan**, Georgian Technical University, Institute
	TECHINFORMI ANALYSIS OF SCIENTIFIC PRODUCTIVITY AT THE MESO- AND MACRO-LEVELS
15:30 – 16:00	**M. Kutsia,** National Intellectual Property Center of Georgia – Sakpatenti
	PATENTING IN CHEMISTRY
16:00 – 16:15	**Discussion**
16:15 – 17:15	**CLOSING THE CONFERENCE, *Hall A***

FUEL CELLS FOR ENVIRONMENTAL PURPOSES. PART I. SULFIDE AND NITRATE DRIVEN FUEL CELL

E. Razkazova-Velkova, M. Martinov, S. Stefanov, V. Beschkov
Institute of Chemical Engineering-Bulgarian Academy of Sciences
Akad. G. Bonchev, str. Bld.103, 1113 Sofia, Bulgaria
razkazova_velkova@bas.bg

Hydrogen sulfide and nitrates are persistent pollutants from various origins – domestic, industrial and natural. There are different methods for their elimination, but most of them are expensive and energy inefficient. The present study is an attempt for their removal with energy generation at the same time. By recombination of the waste fluxes of sulfides and nitrates the treatment of both of them can be achieved. The sulfides are oxidized to sulfates and the nitrates are reduced to nitrogen. The milestones in the processes for creating such a fuel cell are the choices of optimal design of the fuel cell and effective electrodes for minimizing the internal losses.
In this investigation a configuration that consists of two concentrically arranged compartments separated by a membrane situated at the bottom of the inner unit was studied. The experiments were carried out with different electrodes and improved electroconductivity of the solutions by adding NaCl. A commercially available Celgard 3510 membrane was used. The electrical resistance of the fuel cell was decreased from 850 to 76 Ω after using pyrolysed activated paddling and activated carbon instead of graphite rods for electrodes. The results for the depletion of the waste substances as well as the electrical indicators are given.
Key words: Fuel cells, nitrates, sulfides, wastewater treatment.

Introduction

The main sources of sulfides are the petroleum, coal gasification and natural gas industries. Another big source is the conversion of wood to pulp by the Kraft process. Naturally sulfides are formed in closed basins due to the anaerobic decomposition of sulfur-containing organic matter, in volcanic gases, mineral springs, sewage systems etc.

Due to their high toxicity they are threatening to humans' and animals' health and their high chemical reactivity is causing corrosion to metal and concrete parts.

The possibilities for their disposal and decomposition can be divided mainly as follows:

Processes for adsorption of the sulfides from fluids (they can be combined with their oxidation) [1-5], wet scrubbing processes [6-8], oxidation with strong chemical oxidants [9], precipitation with metals [10] biological oxidation [11].Thermal and electrochemical methods for decomposition [12,13] are also investigated as an alternative. The Claus process is a well studied and classical method for hydrogen sulfide and sulfur dioxide decomposition to elemental sulfur and even though attempts are made to lower the operation temperature by selective catalysts it is still quite an expensive method. Studies in recent years show an increased interest for hydrogen sulfide as an alternative fuel in fuel cells [13]. Microbiological fuel cells are also investigated [14]. In many cases elemental sulfur is obtained as end product from decomposition of hydrogen sulfide. It is not a desirable product because of its low commercial price. In a fuel cell it is better to convert the sulfide to sulfate ion instead of elemental sulfur, because there is a transfer of eight electrons instead of only two thus obtaining four times more energy. Moreover the sulfate ions occur in natural water sources and are harmless in a wide range of concentrations.

Nitrates are identified as one of the dangerous pollutants in waters. Sources of wastewaters contaminated with nitrates are animal farms, households, petroleum industry and others. The conventional processes used to eliminate nitrate from water are ion exchange, reverse osmosis and electro-dialysis.

Materials and methods

The model solutions of sulfides and nitrates were obtained by dissolving analytical grade of $Na_2S.9H_2O$ and KNO_3. Analytical grade of NaCl was used for improving the conductivity of the sulfide solution.

The concentrations of sulfides were determined photometrically with N,N-diethyl-n-phenylenediamine in presence of Fe(III) with formation of methylene blue [15, 16]. This method increases the sensitivity of the determination in comparison with the method when using N,N-dimethyl-n-phenylenediamine.

The determination of nitrates was conducted UV-spectrophotometrically by the method proposed by Goldman&Jacobs [17]. UWR-UV-1600PC spectrophotometer was used for this analysis.

The selected configuration of the cell consists of two concentrically arranged compartments separated by a membrane situated at the bottom to the indoor unit (***Fig. 1***). Celgard 3501 membrane was used with a diameter 0.02 m^2. The volume of the two compartments was equal – 0.3 l.

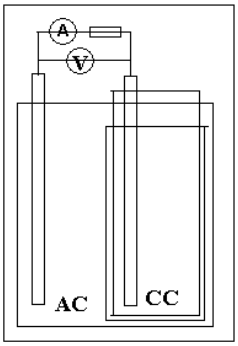

Fig. 1. Scheme of the construction of the fuel cell.
AC-anode compartment; CC-cathode compartment.

Several sets of experiments were carried out:

1) The first was varying different types of electrodes.

- Five graphite rods into the anode compartment and one into cathode on. Each one has a surface area of 0.02 m^2;
- Pyrolyzed activated paddling with surface area 0.1 m^2 in the anode compartment and one graphite rod into the cathode one.

2) After that using the same electrodes in the anode compartment investigation was carried out with 0.3 l of activated carbon (AC-Fujikasau, Japan, 680 m^2/g.) into the cathode compartment and one graphite rod for electrical connection.

3) In order to increase the electroconductivity of the solution NaCl with concentration 16.5 g/l was added to the solution in the anode compartment in the last set of experiments varying the electrodes and the presence of activated carbon. The last set of experiments also has a practical importance for the Black Sea which is of the same salinity and is a virtually inexhaustible source of hydrogen sulfide.

The pyrolyzed activated paddling was obtained from commercially available polyester tissue after its pyrolyzation with simultaneous activation by patented method [18]. It has a specific surface area of 208 m^2/g analyzed using BET method.

Results and Discussion

The intended reactions were as follows:

Anode: $S^{2-} + 6OH^- = SO_3^{2-} + 3H_2O + 6e^-$

$SO_3^{2-} + 2OH^- = SO_4^{2-} + H_2O + 2e^-$

Net anode reaction: $S^{2-} + 8OH^- = SO_4^{2-} + 4H_2O + 8e^-$

Cathode: $NO_3^- + H_2O + 3e^- = NO_2^- + 2OH^-$;

$NO_2^- + 2H_2O + 2e^- = 1/2N_2 + 4OH^-$

Net cathode reaction: $NO_3^- + 3H_2O + 5e^- = 1/2N_2 + 6OH^-$

The above reactions show that the 8 electrons generated in the anode compartment are more than the 5 required for the reactions in the cathode one. To avoid that imbalance the experiments were carried out at an approximate ratio of sulfide to nitrate ions 5:8 (125:200mg/l).

In order to evaluate the influence of the electrodes, the activated carbon (AC) added into cathode compartment and the improved conductivity by adding NaCl experiments for determination of the resistance of the cell were carried out. This parameter is identified by measuring the current and the voltage produced by the cell varying the external resistance. The slope of the plot in coordinates current-voltage gives the resistance of the cell. The external resistance was changed from 1000 to 0. 1 Ω. Table 1 summarizes the obtained results.

Table 1. Electrical resistance of the fuel cell for different electrodes and conditions

Type of electrode	Experimental Conditions		
	Without AC and NaCl	AC without NaCl	AC and NaCl
Graphite (GR)	850.68 Ω	292.56 Ω	182.42 Ω
Pyrolyzed paddling (PP)	650.72 Ω	165.34 Ω	76.42 Ω

In ***Fig. 2 (a)*** the electricity power as a function of the currant for the best results for both electrodes are presented. Further experiments were carried with these two configurations.

With regard to the resulting electrical power we have more than 6 times improved performance when using electrodes made from pyrolyzed padding compared to graphite rods for equal external working surfaces. It can be explained with the very large internal surface of the PP electrodes.

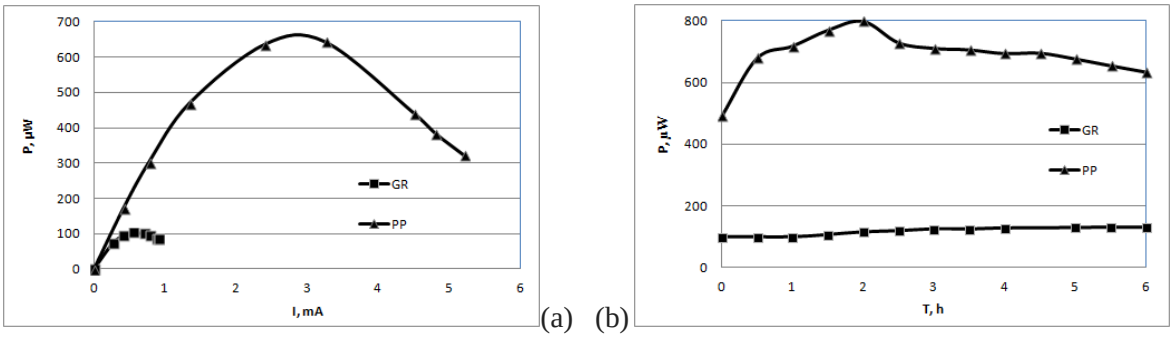

(a) (b)

Fig. 2 Electrical power as a function of the current (a) and time (b)

Figure (***Fig 2(b)***) represents the obtained power of the fuel cell as function of time. The results were taken with external resistance of 100 Ω. In this experiment as well there is about five times improved performance of PP electrodes compared to GR electrodes due to the same reasons. The peak in the curve of the PP electrodes is due to adsorption of sulfide ions in the pores of the electrode. The gradual increase reaches a maximum after 2 hour when the electrode is completely saturated and over time performance decreases due to reduced concentration of "fuel".

A comparison of the depletion of sulfides and nitrates in the different configuration of the fuel cells is shown on ***Fig 3 (a)*** and ***(b)*** respectively.

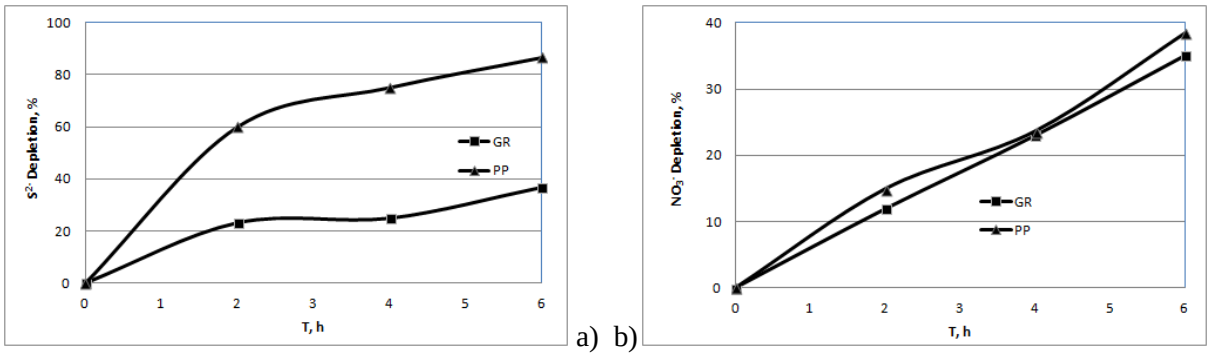

a) b)

Fig. 3. Depletion of sulfide and nitrate ions using different configuration of fuel cells.

The use of PP electrodes in the anode compartment increases the rate of oxidation of sulfides twice and over the course of a 6 hour experiment the concentration is reduced by up to 90% of the initial one ***(Fig 3(a)).*** Unfortunately, the reduction of nitrates in the cathode compartment (***Fig 3(b***)) is progressing at a lower rate over the course of the experiment with less than 40% reduction compared to the initial one. Our future efforts will be focused in this direction.

Conclusions

It has been demonstrated that fuel cells can be successfully used for environmental purposes, while harvesting some electrical energy at the same time. For improving their operational characteristics new type of electrodes with incorporated catalysts for reduction and oxidation can be used. This is going to increase both characteristics - environmental (the rate of depletion of the hazardous ions) and energy (the electrical power) of the fuel cell.

Acknowledgement. **This work was accomplished within the project E02-15/12.12.2014 of National Science Fund, Ministry of Education, and Science, Republic of Bulgaria**

ლიტერატურა - REFERENCES – ЛИТЕРАТУРА

1. Cotrino R., A.D. Levine, P. Amitzoglou, J. S. Perone, Removal of Hydrogen Sulfide from Groundwater Using Packed-Bed Anion Exchange Technology,C., Florida Water Resourses Journal, (2007) pp. 22-25.
2. Seredych M., T.J. Bandosz, Sewage sludge as a single precursor for development of composite adsorbents/catalysts, Chem. Eng. J. 128, (2007), pp.59-67
3. Yasyerli S., I. Ar, G. Dogu, T. Dogu, Removal of hydrogen sulfide by clinoptilolite in a fixed bed adsorber, Chem. Eng. Process. 41 (9), (2002), pp.785–792.
4. Yasyerli S., G. Dogu, I. Ar, T. Dogu, Dynamic analysis of removal and selective oxidation of H2S to elemental sulfur over Cu–V and Cu–V–Mo mixed oxides in a fixed bed reactor, Chem. Eng. Sci. 59 (2004),pp.4001–4009.
5. Primavera A., A. Trovarelli, P. Andreussi, G. Dolcetti, The effect of water in the low-temperature catalytic oxidation of hydrogen sulfide to sulfur over activated carbon, Appl. Catal. A 173, (1998) pp.185–192.
6. Ball, T. and Veldman, R. Improve gas treating. Chem. Eng. Prog., (1991), 87, 67-12.
7. Wang R., , Investigation on a new liquid redox method for H_2S removal and sulfur recovery with heteropoly compound, Sep. Purif. Technol. 31, (2003), pp. 111–121.
8. West, J. R.,Sulfur recovery. In: Kirk-Othmer, Encyclopedia of Chemical Technology. Vol. 22 (Grayson, M. and Eckroth, D., eds.).John Wiley & Sons, New York, (1983), pp. 267-297.
9. Tomar M., Abdullah, T.H.A., Evaluation of chemicals to control the generation of malodorous hydrogen-sulfide in wastewater. Water Res. 28,(1994), pp. 2545–2552;
10. Henze, M., Harremoe¨ s, P., la Cour Jansen, J., Arvin, E., Wastewater Treatment: Biological and Chemical Processes,second ed. Springer, Berlin, (1997)
11. Nemati, M., Mazutinec, T.J., Jenneman, G.E., Voordouw, G., Control of biogenic H2S production with nitrate and molybdate. J. Ind. Microbiol. Biotechnol. 26, (2001), pp. 350–355.
12. Gerçe Özgül l, A. Savas Koparal, Ülker Bakır Öğütveren, , Removal of hydrogen sulfide by electrochemical method with a batchwise operation, Separation and Purification Technology 62, (2008), pp.656–660.
13. Zhai Lin-Feng, Wei Song, Zhong-Hua Tong, Min Sun, A fuel-cell-assisted iron redox process for simultaneous sulfur recovery and electricity production from synthetic sulfide wastewater, Journal of Hazardous Materials 243, (2012), pp.350– 356
14. Cai Jing, Ping Zheng, Simultaneous anaerobic sulfide and nitrate removal in microbial fuel cell, Bioresource Technology 128, (2013), pp.760–764.
15. W. Fresenins, G. Jander, Handbook for Anal. Chem., Springer 4th edn., 1967.
16. M. G. Bapat, B. Z. Scharma, Anal. Chem. 157, 258 (1957).
17. 18. Goldman, E., R. Jcobs, “Determination of nitrates by ultraviolet absorption”, J. Am. Water Works Assoc., 53 (1961) , pp.187-191.
18. Ljutzkanov L., Atanasov A., Method for Treatment of Carbon-Containing Materials, BG patent № 63594 /26.06.2002

თბური ელემენტები ეკოლოგიური მიზნებისათვის

ე. რაზკაზოვა-ველკოვა, მ. მარტინოვ, ს. სტეფანოვ, ვ. ბეშკოვ
ქიმიური ტექნოლოგიის ინსტიტუტი - ბულგარეთის მეცნიერებათა აკადემია
razkazova_velkova@bas.bg

რეზიუმე

გოგირდწყალბადი და ნიტრატები წარმოადგენენ სხვადასხვა წარმოშობის (საყოფაცხოვრებო, სამრეწველო, ბუნებრივ) მუდმივი დაბინძურების წყაროს. მათი განადგურების სხვადასხვა მეთოდები არსებობს, რომელთა უმრავლესობა არის ძვირი და ენერგეტიკული თვალსაზრისით არაეფექტური. წარმოდგენილი კვლევა არის ამ ნარჩენების ლიკვიდაციის მცდელობა ენერგიის ერთდროული გენერირებით. სულფიდების და ნიტრატების შემცველი ნარჩენების რეკომბინაციით შესაძლებელია მივაღწიოთ ორივეს გადამუშავებას. სულფიდები იჟანგება სულფატებამდე და ნიტრატები დაიყვანება აზოტამდე. ასეთი თბური ელემენტის შექმნის პროცესში მთავარი მომენტებია - ამ ელემენტისთვის ოპტიმალური დიზაინისა და ეფექტური ელექტროდების შერჩევა შიდა დანაკარგების შესამცირებლად.

ТОПЛИВНЫЕ ЭЛЕМЕНТЫ В ЭКОЛОГИЧЕСКИХ ЦЕЛЯХ

Е.Разказова-Велкова, М.Мартинов, С.Стефанов, В.Бешков
Институт химической технологии, Академия наук Болгарии
razkazova_velkova@bas.bg

РЕЗЮМЕ

Сероводород и нитраты являются источниками постоянного загрязнения различного происхождения (бытовые, промышленные, естественные). Существуют различные методы их устранения, большинство которых обходятся дорого и неэффективны с энергетической точки зрения. Представленное исследование является попыткой ликвидации этих отходов с одновременным генерированием энергии. Рекомбинацией потоков, загряненных сульфидами и нитратами, возможна переработка обоих. Сульфиды окисляются до сульфатов, нитраты восстанавливаются до азота. Основным моментом в процессе создания таких топливных элементов является подбор оптимального дизайна и эффективных электродов для уменьшения внутренних потерь.

В данной работе была изучена конфигурация топливного элемента, состоящая из двух концентрических отделений, разделенных мембраной. Эксперименты были проведены с использованием различных электродов и растворов с улучшенной электропроводностью, что было достигнуто добавлением NaCl в раствор. Использовалась коммерчески доступная мембрана Celgard 3510. Электрическое сопротивление топливного элемента было уменьшено от 850 до 76 ом после использования пиролитического активированного перемешивания и активированного угля для электродов вместо прутков графита. Показаны результаты по уменьшению отходов, а также электрические индикаторы.

MULTIFUNCTIONAL INORGANIC CORE-SHELL HYBRID NANOPARTICLES; SYNTHESIS AND APPLICATIONS

M.Donadze, M.Gabrichidze, P.Toidze, T.Agladze
Georgian Technical University
Institute of Green & Sustainable Chemistry

Binary and ternary multifunctional hybrid "core (Ag)-shell (Mn, Cr oxides)" nanoparticles were synthesized by means of heterogeneous oxidation of oleic acid ligand (stabilizer of Ag NPs) by Mn and Cr oxides precursors. High catalytic activity of AgMnOx nanoparticles toward carbon monoxide oxidation reaction as well as bactericidal action in relation of gram-positive and gram-negative bacteria was observed

Introduction

Metal based core-shell nanoparticles (NPs) as a research object has attracted attention owing to their unique catalytic, biomedical, magnetic and electric properties compared to their bulk counter parts. Surface functionalisation of free – standing metal NPs by coupling with another metal oxide provides means to prepare hybrid nanoparticles which are emerging multifunctional nanoscale materials that facilitate divers application of one the same material in various fields.

The common bottom – up synthesis of inorganic composites involves formation of primary building blocks e.g. metal NPs of desired size and shape and use various nano -architectonic strategies to design multifunctional hybrids. The frequently used seed – mediated growth (SMG) nano-architectonics strategy involves ligand stabilized metal NPs used as seeds to deposit the oxide component on the top of metal NPs (fig. 1).

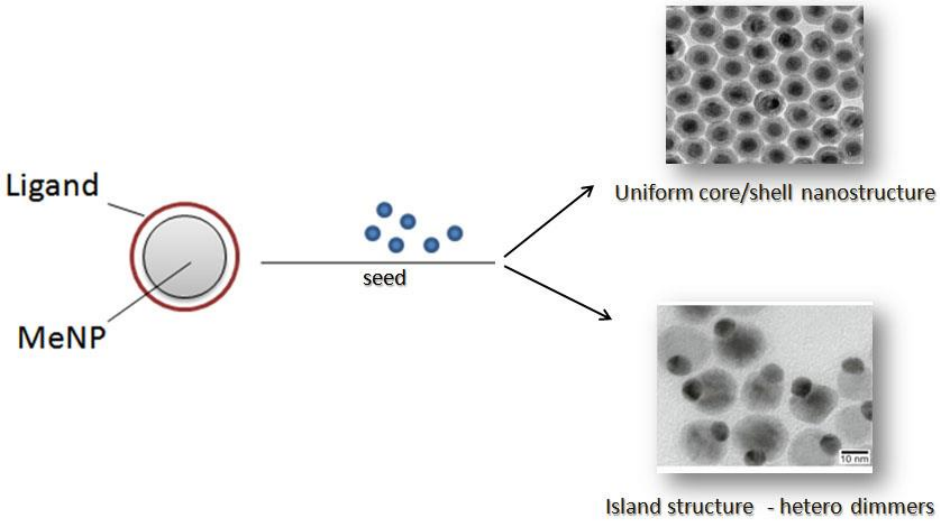

Fig. 1. Schematics of seed mediated synthesis of hybrid nanoparticles

According to classical hetero epitaxial grows theory when material A is deposited over a preexisting seed substrate of a different material B, total Gibbs free surface energy change:

$$\Delta G_s = \gamma_A - \gamma_B + \gamma_{A/B}$$

Where γ_A is surface energy of seed substrate, γ_B is surface energy of deposited material, $(\gamma_A - \gamma_B)$ is solid –solution interfacial energy of colloidal nanoparticles in liquid media and $\gamma_{A/B}$ is strain related to solid / solid interfacial energy which depends on the bounding strength and degree of crystallographic compatibility.

Two limiting cases can be considered:

Frank –van der Merwe growth model: $\gamma_B < \gamma_A$ + good lattice matching ($\Delta\gamma_{1/2}$ is small), yields spherical M_AM_BOx core/shell structures, fig.2 (1-3).

$$\Delta G_s > 0$$

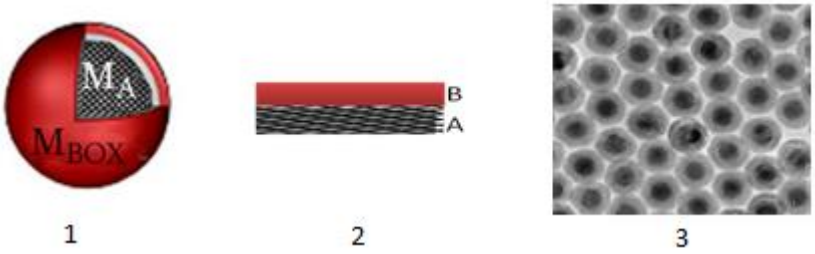

1 2 3

Volmer-Weber growth model: $\gamma_B > \gamma_A$ ɔoore lattice matching ($\Delta\gamma_{1/2}$ is high) yields dumbell $M_AM_BO_x$ systems of yolk structures, fig.2 (4-6)

$$\Delta G_s < 0$$

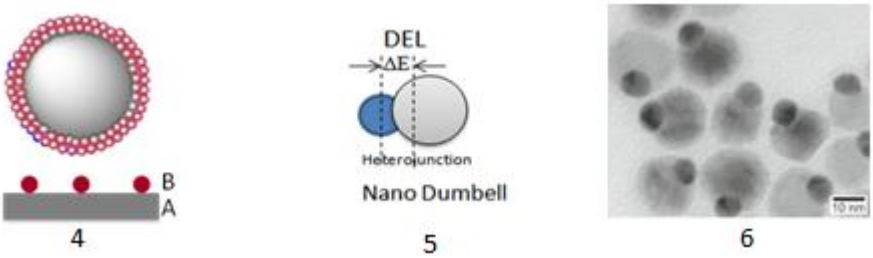

4 5 6

Fig. 2. Schematic (1, 4) and TEM (3, 6) images of core/shell (1-4) and dumbell (4-6) $M_AM_BO_x$ nanostructurs

Though a number successful synthesis of hybrid structures has been reported application of SMG method for integration of two or more dissimilar materials in a single core/shell system is still a challenging task, due to complexity of accounting for structural matching of components. Major drawbacks of dumbbell structures are:

- Materials properties are modified only in a narrow region close to the heterojunction (Fig.2,5)
- Growth inhibition and crystal instability owing to crystal strain induced by lattice mismatch
- Aggregation or corrosion of metal NPs due to loss of stabilizing shell

Our goal was to develop alternative nanoarchitectonic strategy free from above drawbacks. Focus was on integration of the dissimilar metal-metal oxide nanoparticles in stable homogeneous core-shell structures. Formation of $M_AM_BO_x$ core-shell nano structure via direct oxidation of ligand by metal oxide precursor was studded (Fig.3).

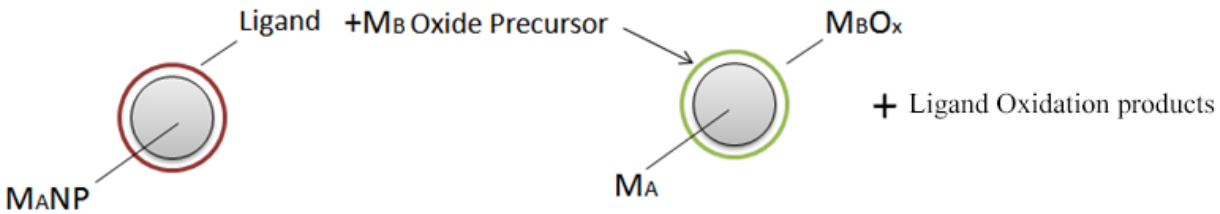

Fig. 3. Schematics of synthesis of M_AM_BOx hybrid by ligand oxidative substitution reaction

Binary (AgMnOx and AgCrOx) and ternary (AgCrMnOx) hybrids were synthesized using oleic acid stabilized Ag NPs as building blocks and potassium permanganate and potassium dichromate as oxide precursors.

Experimental

Chemicals and instruments. The reagents used in present study were purchased from Sigma-Aldrich unless otherwise specified and used without purification. Optical properties of silver and$AgMnO_2$NPs were characterized by UV spectroscopy in a range (200-600) nm (Carry 100, Varian). Chemical interactions of ligand with NPs and permanganate ions were studied by FT-IR spectroscopy in a range (400-4000) cm^{-1} with resolution of 0, 5 cm^{-1} (Thermo Nicolet, Avatar370) using KBr technique. Size, shape and chemical

composition of NPs were estimated from TEM (Tesla BS 500) and SEM (JSM-6510LV) images and EDS data. The samples were prepared by placing small drops of a sole onto the carbon coated copper grid. The size distribution of NPs in a sole was evaluated from laser beam dynamic light scattering (DLS) data (Zetasizer-Nano, Malvern). Prior to measurements as prepared soles were diluted with hexane 1:8. The structural and thermal stability properties were characterized by XRD (Dron 4) and thermo- gravimetric analysis (TGA, Derivatograph Q-1500D).In both cases soles were initially evaporated at ambient temperatures (5 hours), residual powder (1 g) was used as a sample. Concentration of Ag and K in the liquid and solid phases was measured by inductively coupled plasma optical emission spectrometer (ICP-OES, Varian). Concentration of MnO_2 in the reaction mixture was determined by the redox titration method [1]. The consumption of permanganate ion in oleic acid oxidation reaction was controlled by optical absorbance of solution by photo colorimeter (KFK 2) using light absorbance calibration curves.

Preparation of soles of Ag NPs. The soles of silver NPs in a hexane were synthesized using the electrochemical reactor consisting of a sacrificial silver anode (99, 9% purity), and aluminum (99, 9%) ring cathode which upon rotation crosses immiscible layers of an aqueous (0, 05 M $AgNO_3$, doubled distilled water) and organic (Hexane, 1% oleic acid) solvents [2]. The experimental setup allows silver ions formed at the anode to discharge at the cathode surface poisoned by a surfactant (OA) which adsorbs at sites favorable for silver adatoms and inhibits the growth of silver nanoclusters. The latter being weakly adsorbed at the surface and strongly bounded to amphiphile OA molecules are easily washed out from the cathode upon rotation forming the stable soles of Ag-OA core-shell NPs in hexane. In a previous study [2], we demonstrated the ability to tune a particle size by variation in residence time τ_r, during which a metal cluster formed at a ring cathode in an aqueous electrolyte is allowed to adsorb amphiphile molecules of a surfactant from an organic phase. In a present study we carried out electrosynthesis at cathode current density 7500 A cm^{-1}, ring cathode rotation rate 960 rev.min^{-1}, electrolyte temperature 20°C and τ_r = 36 s, which leads to the formation of an Ag-OA sole containing 0,54 gl^{-1} NPs with an average particle size of 10-12 nm.

Preparation of binary and ternary hybrids.

To prepare binary AgMnOx nanocomposite 100 ml sole of Ag NPs in a hexane was mixed with 40 ml 0, 2 M $KMnO_4$ aqueous solution under vigorous shaking during 1 hour (until discoloring of permanganate solution) at ambient temperature. After separation of organic and aqueous phases by centrifugation (0, 5 hour, 8,000 rev min^{-1}) sole of spherical $AgMnO_x$ particles consisting from, wt. %: 29, 2 Ag, 28, 16 MnO2, 4, 4 5 K and 38, 19 OA oxidation products was obtained.

To prepare triple AgCrMnOx nanocomposite 25 ml aqueous solution of $K_2Cr_2O_7$ (2M) and 50 ml ethanol was added to 250ml silver sole (0,06M) in hexane and stirred 55°C, 20 hours. 25ml aqueous $KMnO_4$ (2M) was added to the mixture and stirred 1 hour at ambient temperature. After 24 hours aging and filtration, separated solid residual was dried at ambient temperature 4 hour and calcinated at400°C, 2 hour. According to EDS data the final composite consisted from wt. %: 15, 6 Ag, 46, 5 Mn and 5, 3 Cr.

Preparation of water filter and evaluation of bactericidal activity.

Woven textile materials (FHRC10EMB) was impregnated by AgMnOx sole in ultrasonic bath (100 Watt, frequency 40 KHz) during 1 hour and dried 4 hour. Bactericidal activity was tested against gram-positive (streptococcus and staphylococcus) and gram-negative (Escherichia coli, Pseudomonas aeruginosa, Proteus) bacteria introduced in a water of drinking quality. Microbial strains (G. Eliava Institute of Bacteriophages, Microbiology and Virusology) were tested according to standard method [3].

Preparation of catalysts and evaluation of catalytic activity.

Samples for catalytic tests were prepared by 1 hour impregnation of supporting material,1 g calcium aluminosilicate ($CaAl_2Si_2O_8$), 2,5 mm grain size in ultrasonic bath (100 Watt, frequency 40 KHz, 1 hour) containing 5 ml Ag-OA sole. The catalytic activity toward CO oxidation reaction was studied by standard test procedure at 0, 6 g catalyst load and continuous flow of CO/CO_2 mixture at a rate of 30,000 h^{-1}. The CO conversion degree α was calculated according to equation:

$$\alpha = \frac{a-b}{a} \times 100\% \quad (2)$$

where **a** and **b** are respectively concentrations (%) of CO and CO_2, controlled by gas chromatography (Gasochrom 3101).

Characterization of AgOA, $AgMnO_x$ and Ag $CrMnO_x$ NPs

Optical absorption spectra. UV-vis spectra of OA in a hexane with and without addition of the $KMnO_4$ are shown at Fig.4. Soon after permanganate addition the characteristic for OA absorption peak at 233 nm (Fig.4 a.1) shifts to 368 nm and a number of new peaks in red region characteristic of intermediate OA oxidation products are formed (Fig. 4b). At prolong action of permanganate ions the main peak splits to a series of peaks (386-361 nm) characteristic for oleats and the manganese dioxide (360 nm) [4-7] (Fig. 4 a.2).

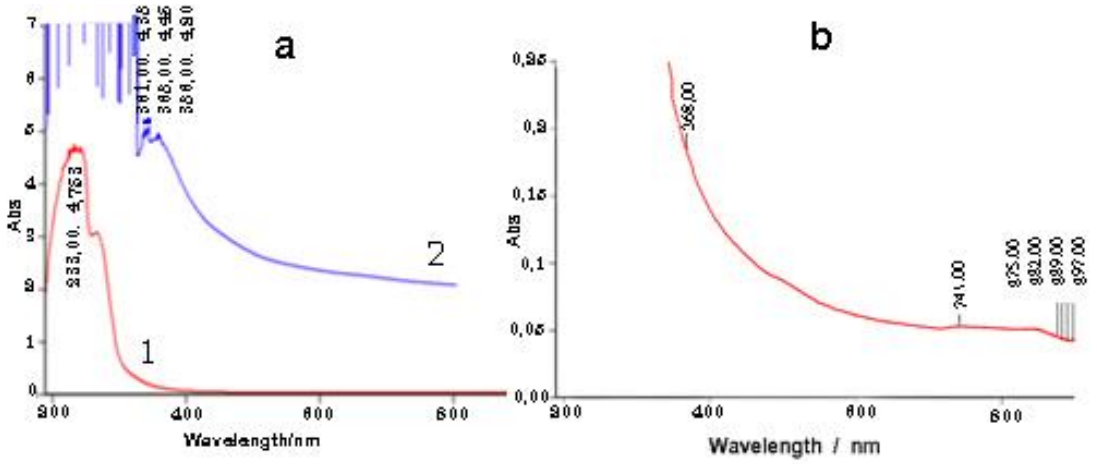

Fig. 4. UV spectra of OA: a1. In hexane. b. In hexane, 5 min after $KMnO_4$ addition. a2. 20 min after addition

The UV-vis spectra of OA caped silver nanoparticles with and without addition of permanganate are shown at fig. 5. At initial stage of a MnO_4^- - Ag-OA interaction depression and broadening of characteristic for 10-12 nm size Ag NPs peak (404 nm, Fig. 5 a.1) caused by overlapping of MnO_2 and Ag peaks and appearance of peaks characteristic for oxidized organic products are observed (Fig. 5 b). Appearance of twin peaks after 20 min, contact of reagents appearance at 359 and 378 nm (Fig. 5 a. 2) indicates the formation of AgMnOx nanocmposite.

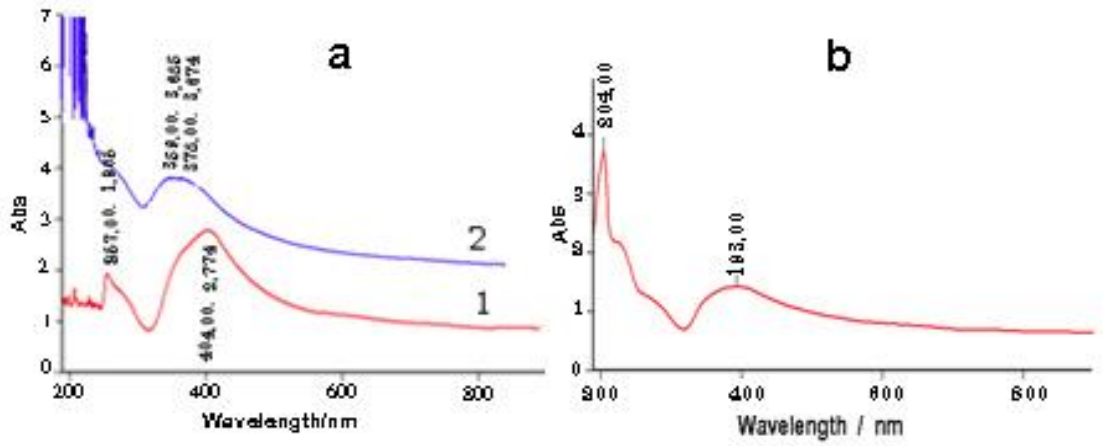

Fig. 5. UV-vis spectra: a 1. Ag-OA nanosoles in hexane b. 5 min after permanganate addition 1 b. 20 min after permanganate addition

FT-IR Spectroscopy

Earlier it was shown that the most remarkable effect of Ag-OA interaction is disappearance of the peak at 1712 cm^{-1}, assigned to C=O stretch bound and appearance of two new bounds at 1635 and 1380 cm^{-1} which are characteristic of the asymmetric and symmetric carboxylate stretch [2]. These effects were interpreted as evidence of OA bonding to silver via two symmetrically coordinate oxygen atoms of the carboxylate head.

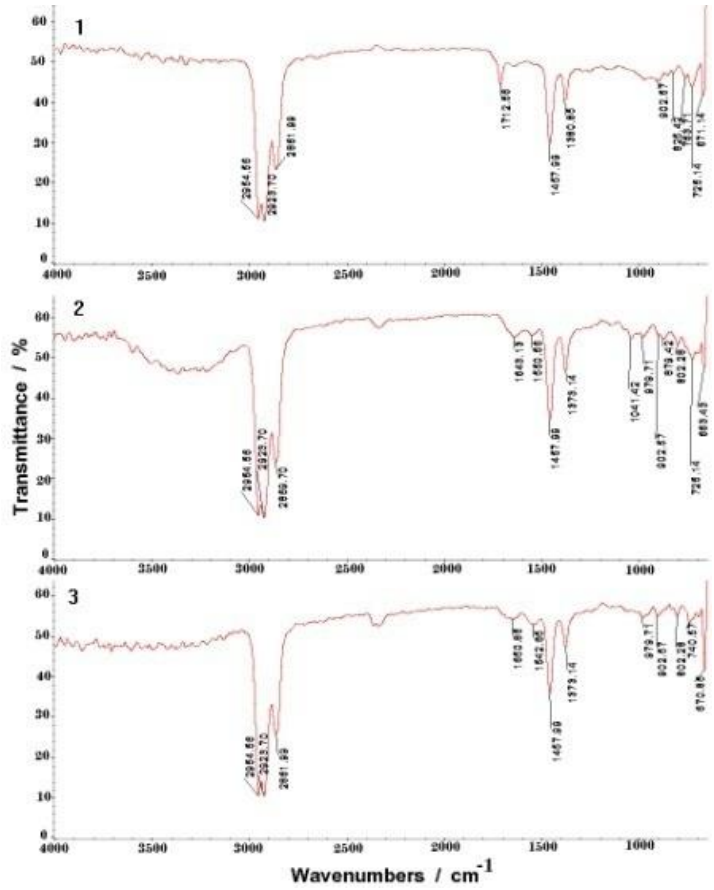

The FT-IR spectra of Ag-OA soles in a hexane with and without additions of permanganate ions are shown at Fig.6. It follows from these spectra that permanganate addition results in vanishing of the peak at 1712 cm^{-1}, and appearance of two new peaks at 1643, 13 and 1650 nm which only slightly change the position in time (Fig. 6,1-3). A new absorption peak appeared at 802, 28 $cm^{-1}$is assumed to be associated with MnO bending vibrations of [MnO_6] octahedral in MnO_2 [5]. The disappearance of peak assigned to a C=O stretch and appearance of two new bounds indicates the rearrangement of stretching modes of a carboxylate owing to interaction with both silver and manganese oxide components of the composite. The formation of a peak at 1041, 42 cm^{-1} which disappears in time is in line with modification of UV-vis spectra in time, pointing to formation of short live intermediates of OA oxidation reaction.

Fig. 6. FT-IR spectra: 1 – Ag-OA sole in hexane. 2 – 5 min, and 3 – 20 min after addition of permanganate

XRD Spectrometry

The structural properties of Ag NPs prior and post oxidation of OA shell as well as of MnO_2 were characterized by XRD spectra (Fig.7. 1 - 4). The XRD patterns of as prepared silver sole demonstrate amorphous character of the material. The size of the silver particles calculated according to Debye Sheerer equation is about 18 nm (Fig. 7.1). After the calcinations at 400°C a fine dispersion of a crystalline phase with increased to 150 nm crystal size was observed (not shown). The X-ray diffraction records of a MnO_2 prepared by interaction of an aqueous potassium permanganate (40 ml 0, 2 M) and a 1% solution of OA in a 100 ml hexane illustrates an amorphous character of colloidal MnO_2 (a broad diffraction peak located around 20º, Fig. 7.2). The diffraction maximum at 37º is in agreement with the peak characteristic to δ MnO_2 (JCPDS № 80-1098) [6, 7]. The X-ray diffraction patterns of as prepared Ag-MnO_2 shows that low crystallinity is characteristic also of the composite nanoparticles (18 nm size). A spectrum contains peaks characteristic for both individual MnO_2 [6, 8, 9] and silver NPs (Fig. 7.3) proving formation of chemical bounds between components of the composite. After calcination at 800 ºC the X-ray patterns show clear crystalline structure of the composite with increased particle size up to 95 nm (Fig. 7. 4). As expected, calcination at elevated temperatures favors particles aggregation.

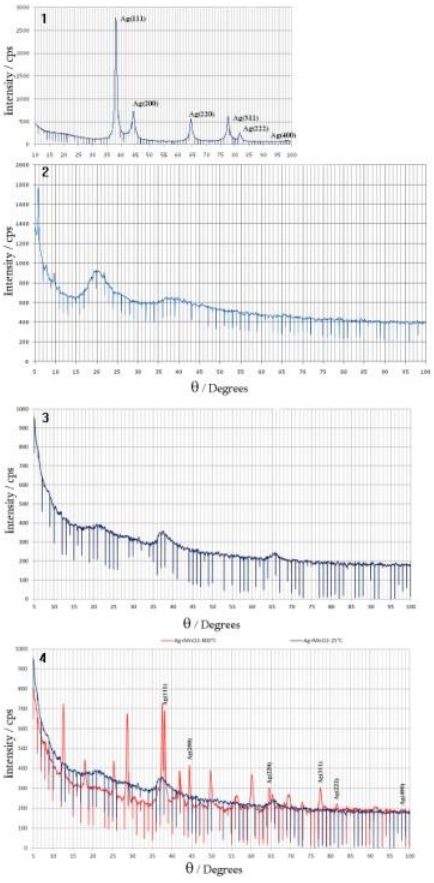

Fig. 7. XRD patterns of: 1. As prepared Ag-OA NPs. 2. MnO_2 prepared via permanganate reduction by bulk OA. 3. As prepared $AgMnO_x$ NPs, 4. $AgMnO_x$ NPs after calcination at 800ºC, 2 hour.

Size distribution, SEM and TEM images of binary and ternary nanocomposits

Size distribution of nanoparticles measured by laser beam dynamic light scattering technique as well as SEM and TEM images of AgMnOx and $AgCrMnO_x$ nanohybrids are shown at figures 8 and 9.

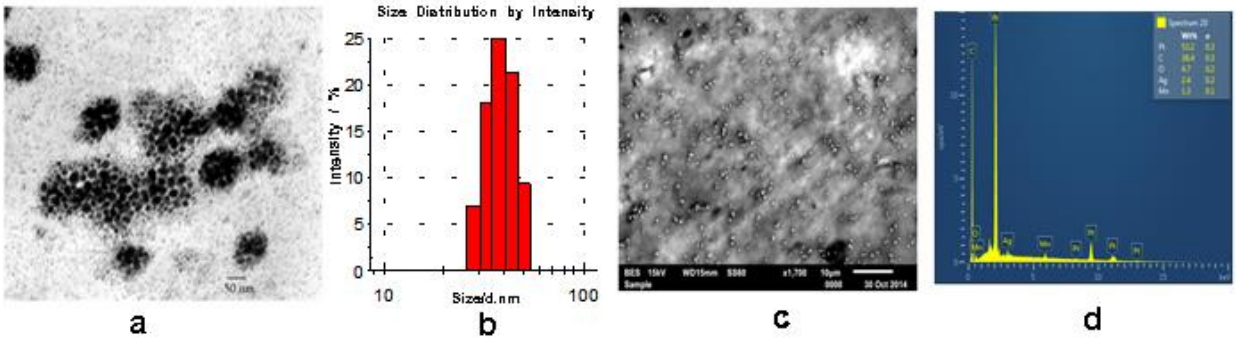

Fig. 8. a.TEM images of Ag-MnO_2 particles b. Histogram of particle size distribution c. SEM images of Ag-MnO_2 particles and d. EDS analysis of the sole obtained after centrifugation (8000 rpm)

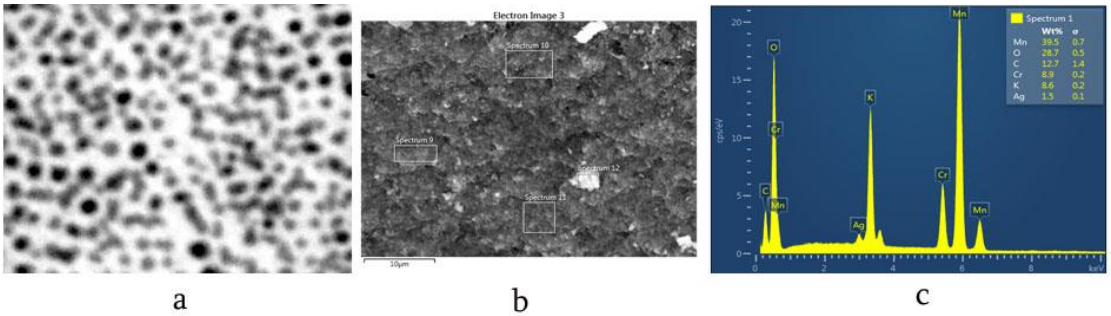

Fig. 9. a.TEM images of $AgCrMnO_x$ particles.b.SEM images of $AgCrMnO_x$ particles and c. EDS analysis of the sole obtained after centrifugation (8000 rpm)

It follows from these data that nanocomposite has spherical core/shell structure with average size of nanoparticles -6, 2 (±1, 0) nm.

Thermogravimetric analysis

The thermal gravimetric analysis (TGA) was performed to characterize the thermal stability of AgMnOx nanocomposites and to compare to that of Ag-OA NPs (Fig. 10). It follows from these data that both particles lose about 40 % of their weight below 500ºC owing to evaporation of oleic acid and products of its oxidation. A shift of exothermic DTA peaks at 350 ºC and 450 ºC to the higher temperatures in case of Ag-MnO_2 indicates stronger bonding of organic molecules to the core center of the composite nanoparticles.

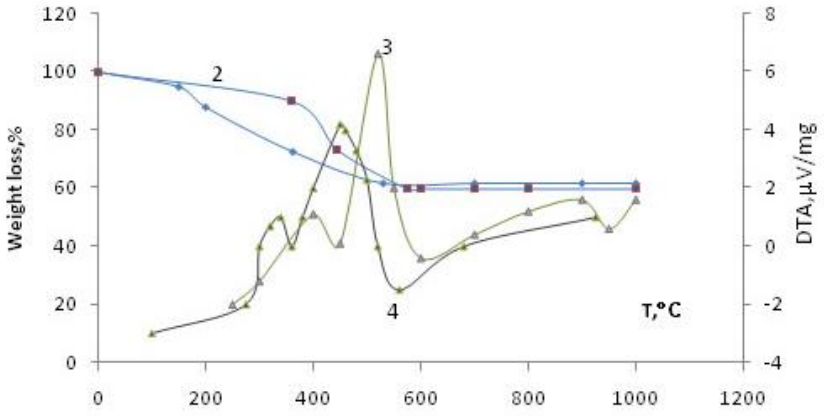

Fig.10. TGA (1, 2) and DTA (3, 4) curves of Ag-OA NPs (1, 3) and $AgMnO_x$ nanocomposites (2, 4)

Kinetics of permanganate reduction

Kinetics of MnO_2 formation was studied by tracing decrease of the permanganate concentration in a reaction mixture containing Ag-OA sole in hexane and aqueous solution of potassium permanganate. To evaluate the effect of OA-Ag bonding on OA oxidation interaction of permanganate ion with OA also was studied. Time courses of both systems at various rates of stirring of solution are presented at Fig. 11. It follows from these data that reduction of permanganate ions increases with an increase of stirring rate up to 1000 rpm, indicating mass transport limitations at lower stirring rates. Oxidation of oleic acid is quite fast reaction and both homogeneous (curve 1, 3, 5) and heterogeneous (curve 2, 4, 6) reactions follow the same kinetic regulations. The overall process involves three consecutive stages characterized by different rate constants. The silver core displays clear catalytic properties toward permanganate reduction reaction.

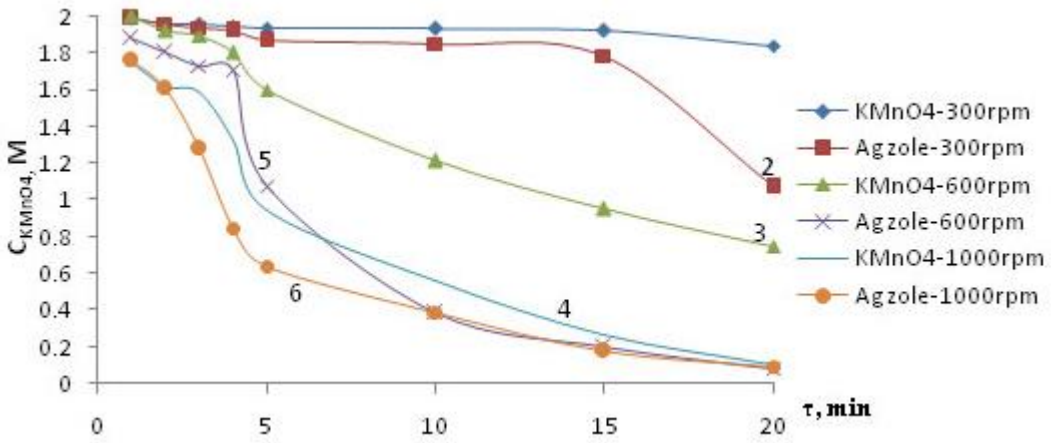

Fig. 11. Time courses of potassium permanganate concentration in oleic acid (1vol. %) and Ag-OA zole (0,0065M) at 25 ^{0}C

It is interesting to compare the kinetic data obtained in our study with studies performed in similar systems. The majority results relate to identification of the intermediates of OA oxidation. While there is consensus on composition of the final products (manganese dioxide, pelargonic and azelaic acids) views on the nature and composition of intermediates diverge [10, 11-13]. The detailed study of oxidation kinetics of a monolayer of oleic acid spread over aqueous permanganate solution performed by use of radiotracers reveals complex character of OA oxidation reaction which involves rapid formation of intermediate *cis-epoxy* acid in OA monolayer (rate constant k_1) and its farther fission yielding *azelaic* and *nonanoic* acids (rate constant-k_2) instantaneously dissolved into an aqueous subphase [13]. It is assumed that the overall rate of oxidation reaction is determined by rate (k_3) of parallel step of desorption of intermediate acid into an underlying subphase. Though above conclusions relates to conditions differed from that of the present study an assumption on a slow transfer of intermediates through the organic –aqueous interface seems applicable to the system under investigation.

Kinetics of bacteria removal

Fig. 12 represents time courses of concentration of gram-positive (streptococcus and staphylococcus) and gram-negatives (Escherichia coli, Pseudomonas aeruginosa, Proteus) bacteria in a water passed though the woven filter impregnated by hybrid nanoparticles. The results indicate that $AgMnO_x$ nanocomposite display strong antibacterial activity resulting in almost 100% removal of all tested pathogens from water.

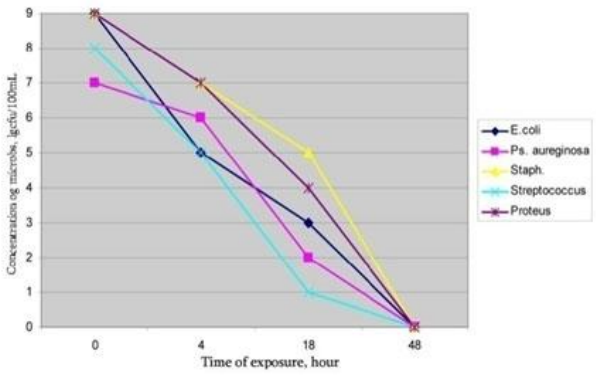

Fig. 12. Antibacterial activity of the $AgMnO_x$ hybrid NPs

The kinetics of bacteria removal was evaluated from variation in bacteria concentration (lg cfu/100 ml) in a sample (10 ml) extracted from filtration loop at water flow rate 3 l/h.

Catalysis of CO conversion

Data on comperative assessment of catalytic activity of Ag NPs and $AgMnO_x$ composities toward CO oxidation reaction are shown at Fig.13. Both oxidation curves follow almost similar patterns indicating the similarity of reacton kinetics. The composite catalyst displays higher activity: CO oxidation starts below the ambient temperature and full conversion degree is achieved at lower temperatures. The beneficial action of manganese oxide additives to noble metal catalysts is commonly attributed to the ability of MnO_x to supply mobile oxygen for reoxidation of core catalyst [14]. In the same way an improvement of catalytic activity of silver nanoparticles by introduction of MnO_2 can be reasonable explained by facilitation of oxygen transfer from the manganese oxide shell to the silver core.

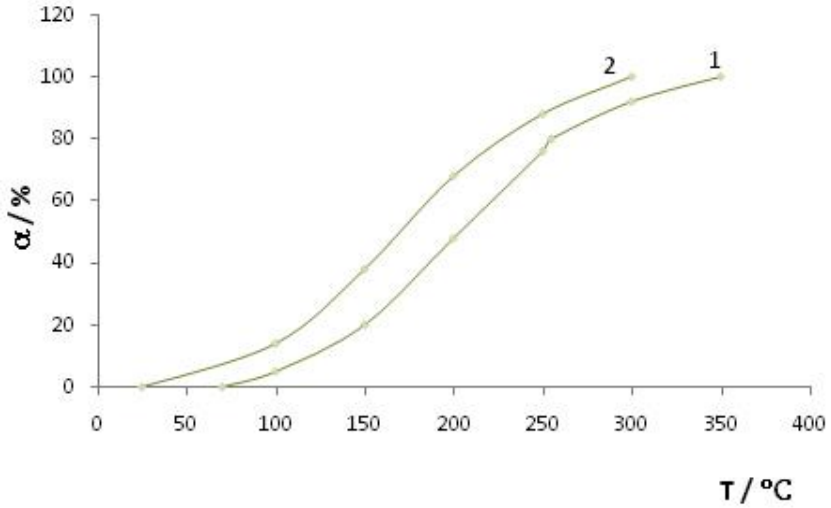

Fig. 13. Temperature dependance of CO conversion catalyzed by as prepared catalyst: 1. Ag NPs. 2. $AgMnO_x$ NPs

Conclusion

$AgMnO_x$ and $AgCrMnO_x$ hybrid nanoparticles were synthesized following novel bottom up two-step strategy which involves the electrochemical formation of oleic acid caped silver nanoparticles and substitution of oleic acid shell by MnO_2 via interfacial chemical reduction of a precursor, the potassium permanganate. At elevated temperatures amorphous $AgMnO_x$ nanocomposite loses organic components and acquires crystallinity.The kinetic study reveals the three step reduction process catalyzed by silver core. The bactericidic and catalytic properties of $AgMnO_x$ hybrids were also tested. The results revealed that filters composed from the hybrid material removes almost 100% gram-negative and gram-positive bacteria from contaminated water and converts CO to CO_2 with improved activity owing to ability of MnO_2 to provide rapid supply of oxygen for reoxidation of the silver core. The proposed strategy was successfully applied for preparation of $AgCrMnO_x$ tripple nanocomposite.

ლიტერატურა - REFERENCES – ЛИТЕРАТУРА

1. ASTM E465-11, Standard test methods for determination of Manganese(IV) in Manganese ores by redox titrimetry
2. T.Agladze, M. Donadze, M. Gabrichidze, P. Toidze, J. Shengelia, N. Boshkov and T, N. Tsvetkova: Synthesis and Size Tuning of Metal Nanoparticles, Z. Phys.Chem., 2013, 227,1187-1198.
3. American Public Health Association (APHA). Standard Methods for Examination of Water and Wastewater, 20th ed.; APHA: Washington, DC, USA, 1998.
4. D.Jaganyi, M.Altaf and I.Wekesa: Synthesis and characterization of whisker-shaped MnO2 nanostructure at room temperature, Appl Nanosci, 2013, 3, 329-333.
5. **S.**Allabad, F.A.Syed, M.E.Assal, M.Khan, A.Alwart and M.R.H. Siddqui:Oxidation Communications, 2013,(3),778-791.

6. Abulikemu Abulizi, Guo Hai Yang, Kenji Okitsu, Jun-Jie Zhu: Synthesis of MnO2 nanoparticles from sonochemical reductionof MnO_4 in water under different pH conditions Ultrasonics Sonochemistry, 2014, 21(5), 1629–1634.
7. Oxide Nanostructures: Growth, Microstructures, and Properties, Ed. Avanish Kumar Srivastava, 2013.
8. M.R. Mahmoudiana, Y. Aliasa, W.J. Basiruna, Pei Meng Woia, M. Sookhakian: Facile preparation of MnO_2nanotubes/reduced graphene oxide nanocomposite for electrochemical sensing of hydrogen peroxide, Sensor and Actuators B: 2014, 201,526-534.
9. D.Moradkhani, M. Malekzadeh, E. Ahmadi: Nanostructured MnO_2 synthesized via methane gas reduction of manganese ore and hydrothermal precipitation methods, Trans. Nonferrous Met. Soc., 2013, 23, 134-139.
10. N.Garti, and E. Avni: Permanganate Oxidation of Oleic Acid Using. Emulsion Tehnology, JAOCS 1981 58 (8), 840-841.
11. J. T. Davies and E. K. Rideal: Interfacial Phenomena, Academic Press, New York, 1961 134 (3490), 1611-1612
12. Doaa Muayad, Saadon Abdulla Aowda and Abbas A-Ali Drea: Simulation Study of Oxidation for Oleic acid by $KMnO_4$ Using Theoretical Calculations, Journal of Applicable Chemistry , 2013, 2 (1), 42-49
13. Makio Iwahashi, Kunihiko Toyoki, Toshiyuki Watanabe and Mitsuo Muramatsu: Radiotracer study on oxidation of oleic acid monolayer on aqueous permanganate solution, Journal of Colloid and Interface Science, 1981, 79(1), 21-32.
14. G.G. Xia, Y.G. Yin, W.S. Willis, J.Y. Wang, S.L. Suib: Efficient Stable Catalysts for Low Temperature Carbon Monoxide Oxidation, Journal of Catalysis, 1999, 185, 91-105.

ბირთვი-გარსის ტიპის მულტიფუნქციური არაორგანული ჰიბრიდული ნანონაწილაკები; სინთეზი და გამოყენება

მ.დონაძე, მ.გაბრიჩიძე, პ.თოიძე, თ.აგლალაძე
საქართველოს ტექნიკური უნივერსიტეტის მწვანე და მდგრადი ქიმიის ინსტიტუტი, თბილისი, საქართველო

რეზიუმე

მანგანუმის და ქრომის ოქსიდების პრეკურსორების მიერ ვერცხლის ნანონაწილაკების მასტაბილეზებელი ლიგანდის (ოლეინმჟავა)ჰეტეროგენული დაჟანგვის რეაქციის გამოყენებით სინთეზირებულ იქნა „ბირთვი(Ag)-გარსი(MO_x)“ ტიპის ორ - ($AgMnO_x$) და სამ - ($AgCrMnO_x$) კომპონენტიანი მულტიფუნქციური ჰიბრიდული ნანომასალები. დადგენილი იქნა $AgMnO_x$-ის მაღალი კატალიზური და ანტიბაქტერიული აქტივობა შესაბამისად ნახშირბადის მონოოქსიდის დაჟანგვის და გრამდადებითი და გრამუარყოფითი ბაქტერიების მიმართ.

ДВУХ И ТРЁХ КОМПОНЕНТНЫЕ МУЛЬТИФУНКЦИОНАЛЬНЫЕ НЕОРГАНИЧЕСКИЕ НАНОГИБРИДНЫЕ МАТЕРИАЛЫ ТИПА «ЯДРО-ОБОЛОЧКА»; СИНТЕЗ И ПРИМЕНЕНИЕ

М.А.Донадзе, М.С.Габричидзе, П.Л.Тоидзе, Т.Р.Агладзе
Институт зелёной и устойчивой химии Грузинского технического университета, Тбилиси, Грузия

РЕЗЮМЕ

Двух (AgMnOx) и трёх (AgCrMnOx) компонентные мультифункциональные наногибридные материалы типа «ядро (Ag)-оболочка (оксиды Mn и Cr)» были синтезированы методом гетерогенного окисления, стабилизирующего наночастицы серебра лиганда (олеиновой кислоты) прекурсорами оксидов марганца и хрома. Была установлена высокая каталитическая и антибактериальная активность AgMnOx в отношении реакций, соответственно, окисления монооксида углерода и грамположительных и грамотрицательных бактерий.

MODELING OF PHOTOCATALYTIC PROCESSES

T.Marsagishvili, M.Machavariani, G.Tatishvili, N.Ananiashvili, M.Gachechiladze, J.Metreveli, E.Tskhakaia
R.Agladze Institute of Inorganic Chemistry and Electrochemistry of Iv.Javakhishvili Tbilisi State University

Photocatalysis or action upon the chemical reaction by photons is of interest as for theoretical, so for practical use. Model system – condensed medium with dissolved reagents was studied in the present work. Methods of theoretical and mathematical physics, particularly, multiparticle temperature Green functions of polarization operators of condensed medium were used during theoretical calculations of chemical reactions. Numerical values of reorganization energy, transition dipole moment, the reorganization energy of the quantum subsystem, etc. are obtained.

Photocatalysis [1-4] or action upon the chemical reaction by photons (of visible range or short-range ultraviolet, as a rule) is of interest as for theoretical, so for practical use. Photocatalysis implies existence of such substances, which participate in chemical processes, but do not exist in the end product of the chemical process. Participation of catalysts in the process is realized by two mechanisms:

1. According to the first mechanism the catalyst absorbs light photon and transits into an excited state. Thereafter, catalyst, which is in an excited state promotes thepassing of chemical process and becomes an additional energy source for chemical catalytic process.
2. According to the second mechanismthe whole photocatalytic process passes as one elementary act - the catalyst absorbs light photon and chemical system transits from initial state into final state, without transition of the catalyst into excited state. In spite of the fact, that in both cases the same product is obtained, these two mechanisms differ from each other by the rate of the process and by the rate constant calculation method.

During theoretical calculations[5-7]of chemical reactions we use methods of theoretical and mathematical physics, particularly, multiparticle temperature Green functions of polarization operators of condensed medium (medium involves impurity particles and catalysts).

We consider model system, which is condensed medium with dissolved reagents. In order to neglect direct interaction of one type ofthe reagents with each other and to consider the interaction of the group of the particles, which brings tothe reaction we suppose, that concentration of the particles-reagents is sufficiently low. It is assumed also, that the photon flux acts upon the system. In addition, it is supposed, that interactionof reagents with the medium has either weak character, so that the medium does not change the structure of the reagents, or is so strong, that reagents form complexes and just these complexes are considered asreagents.

Polarizable particles, placed in amorphous solid medium(condensed medium) form intermediate bonds with medium. These particles are partially polarized and their frequency spectra andgeometric structure are different from gaseous phase at that.

We consider a charge transfer processesbetween dipole-active polarizable(electron and infra-red polarization)particles in the nonregular condensed medium whenthe interaction of reagents with photons' field, interaction of condensed medium with the electromagnetic field of reagents and interaction of polarizations of fluctuations with static field and intramolecular vibrations of reagents are taken into account.

Such approaches allow calculation of vibrational spectrum of reagent and values of the equilibrium distances of chemical bonds.

Calculation of probability of the charge transfer process with photon absorption and transition of an electron in final state may be carried out in general form in model approximations.

It is assumed, that a number of vibrational degrees of freedom at the beginning and at the end of the process is the same. Even with this assumption general expression for the rate constant has rather bulky character. For simplicity, we'll study the case when intramolecular oscillations may be considered as classical.

The rate constant of the phototransfer process can be expressed as:

$$K = \sum_{\sigma=1}^{2} \frac{\left|L^{\sigma}{}_{fi}(\vec{R}^*,\psi^*)\right|^2}{\sqrt{\left|\psi''_{\theta\theta}\right|}} \phi^{\sigma}\Phi(\vec{R}^*,\psi^*)U(\vec{R}^*,\Psi^*)\exp\Big\{-\beta\theta^*(\Delta F-\hbar\omega^{\sigma})-\psi^m(\vec{R}^*,\psi^*;\theta)-$$

$$-\beta\sum_{n=1}^{N}E_{rn}\frac{\theta^*(1-\theta^*)\omega_n^i\omega_n^f}{(1-\theta^*)(\omega_n^i)^2+\theta^*(\omega_n^f)^2}-\theta\sum_{k=1}^{N}\ln(\omega_n^f/\omega_n^i)-\theta^*\ln\Bigg[1+\beta\sum_{k=1}^{N}(G_k(\vec{R}^*,\psi^*)+$$

$$+\frac{\omega_k^f}{\omega_k^i}\overline{G}_k(\vec{R}^*,\psi^*))\frac{\sqrt{2E_{rk}\omega_k^i}}{\omega_k^f}\Bigg]\Big\}(2\pi)^{1/2}\Bigg[\prod_{s=1}^{N}\frac{\omega_s^i}{\sqrt{(1-\theta^*)(\omega_s^i)^2+\theta^*(\omega_s^f)^2}}\Bigg]\Big\{1+$$

$$\sum_{k=1}^{N}\Bigg[G_k(\vec{R}^*,\psi^*)+\frac{\omega_k^f}{\omega_k^i}\overline{G}_k(\vec{R}^*,\psi^*)\Bigg](\beta\theta^*-F_{\omega}(\theta^*))\sqrt{2E_{rk}\omega_k^i}\,\theta^*(\omega_k^f)^2\Big[(1-\theta^*)(\omega_k^i)^2+$$

$$\theta^*(\omega_k^f)^2\Big]^{3/2}\Big\};$$

whereE_{rn} is reorganization energy of n-th intramolecular degree of freedom of adsorbable particle, and ωis frequency of intramolecular vibration at the beginning and at the end of the process correspondingly; ϕ^{σ} is the distribution function of photonswith energy *h*ν. The values of the coordinates of reagents $R^*$and the angles of their orientation ψ^*in the transitional configuration and "Brensted" factor of symmetry θ^*depends on photon polarization σ, the quantity $1/\sqrt{\left|\psi''_{\theta\theta}\right|}$ is the width of the integral over θ, and saddle point θ^* may be found from equation:

$$\beta(\Delta F-h\nu)+\frac{\partial\psi^m(R^*,\psi^*;\theta)}{\partial\theta}+\frac{\partial}{\partial\theta}\sum_{k=1}^{N}\beta E_{rk}\frac{\theta(1-\theta)\omega_k^i\omega_k^f}{(1-\theta)(\omega_k^i)^2+\theta(\omega_k^f)^2}+\ln\prod_{k=1}^{N}\frac{\omega_k^f}{\omega_k^i}+$$

$$\ln\Bigg\{1+\beta\sum_{k=1}^{N}\Bigg[G_k\left(\vec{R}^*,\psi^*\right)+\frac{\omega_k^f}{\omega_k^i}\overline{G}_k\left(\vec{R}^*,\psi^*\right)\Bigg]\frac{\sqrt{2E_{rk}\omega_k^i}}{\omega_k^f}\Bigg\}=0$$

In this formula L_{fi} is resonance integral of interaction of reagents (some particle or group of particles) with photons (dipole moment of charge phototransfer). ΔF is the free energy of the process, ω-intramolecular vibrational frequencies of the reagents.The matrix element and the functions G and $\overline{G}$are calculated with the use of the wave functions in frames of concrete model for reagents. The resonance integral L_{fi}may be considered as some phenomenological parameter. The arguments of this resonance integral describegeometric characteristics of the process. The function $\Phi(\vec{R}^*,\psi^*)$ is the distribution function of reagents. Model function may be selected as this function. The distribution function of reagentshas most simple form for homogeneous systems.

The reorganization energy of the medium for charge transfer processes may be determined by the expression:

$$E_r^m\left(\vec{R},\psi\right)=-\frac{1}{2}\int d\vec{r}d\vec{r}'\Delta E_i\left(\vec{r};\vec{R},\psi\right)g^{R}{}_{ik}\,(\vec{r},\vec{r}';\omega=0)\Delta E_k(\vec{r}';\vec{R},\psi)$$ Here $\Delta E_i\left(\vec{r};\vec{R},\psi\right)$is the change

of system's electrostatic field strength during the transfer process and Green function $g^R$is a temporal function of polarization fluctuations' operators of amorphous solid and liquid at finite temperature T=1/β.

In factorization approximation for function g^Rwe have:

$$g_{ik}{}^{R}\,(\vec{r},\vec{r}';\omega)=g_{ik}{}^{R}\,(\vec{r},\vec{r}';\omega=0)\,f(\omega).$$

The reorganization function of the medium can be expressed as:

$$\Psi^m(\vec{R}^*,\psi^*,\theta)=E_r^m\frac{2}{\hbar}\int_{-\infty}^{\infty}d\omega f(\omega)\frac{sh\dfrac{\beta\omega(1-\theta)}{2}\,sh\dfrac{\beta\omega\theta}{2}}{\omega^2 sh\dfrac{\beta\omega}{2}}$$

When taking integrals over r and r' it is necessary to consider the geometry of the channel and the circumstance, that as effects of spatial dispersion of medium (function g(r,r')), so the effects of frequency dispersion (function F(ω)) must be described by different model functions for amorphous condensed medium.

Everything that is connected with medium reorganization must be considered during calculation. The functions adduced in [3] were used as model functions for description of effects of frequency and spatial dispersion of medium. As conducted calculations have shown, carrying out of the analytical calculations to the end is impossible and it is necessary to conduct numerical integration.

The expression for rate constant will appreciably simplify if interaction of intramolecular vibrations of particle with polarization fluctuations of medium will be neglected.

For ease of the analysis the rate constant may be written as:

$$K = \sum_{\sigma}^{2} \left| L_{fi}^{\sigma} \right|^2 \phi_{\sigma}^{\nu} N \exp\left\{ -\beta\theta_{\sigma}^{*}\Delta F + \frac{h}{2\pi}\nu\beta\theta_{\sigma}^{*} - \psi_{\sigma}^{m}\left(\theta_{\sigma}^{*}\right) - \psi_{\sigma}^{V}\left(\theta_{\sigma}^{*}\right) - \psi_{\sigma}^{mV}\left(\theta_{\sigma}^{*}\right) \right\}$$

$\Psi^{\nu}(\vec{R}^{*},\psi^{*};\theta)$ and $\Psi^{m\nu}(\vec{R}^{*},\psi^{*};\theta)$ are reorganization functions of the vibration system and have rather complicated form. Electron resonance integral of the transition into excited state $\left|L_{fi}{}^{\sigma}(\vec{R}^{*},\psi^{*})\right|$ is calculated as non-diagonal matrix element of interaction of reagents with photons(by electron wave-functions of initial and final states of the system). Function $N(\vec{R}^{*},\psi^{*};\theta;\omega_{n})$ is calculated for concrete processes with consideration of geometry of the particles.

Obtained analytic expressions may be used for finding of analytic expression of optical density of the process.

We use the method, which is analogous to Lambert-Beer law for optical density D:

$$D = ln\left(\frac{I_0}{I}\right) = \kappa d$$

where I_0 is light intensity on input of the measuring cell of thickness d, I is light intensity on the output of the cell.Proportionality coefficient κmay be substituted by extinction coefficient ε_a of particle adsorption:

$$\kappa = \sum_{a} C_a \varepsilon_a$$

where $C_a$is concentration of a-type particles.

More information may be obtained from the form of the absorption curve (photon absorption by the system as function of photon energy).

In case of implementation of extinction coefficient notion during electron transfer process between reagents, the following expression will be obtained:

$$\varepsilon = h\nu \left| L_{fi}^{\sigma} \right|^2 \phi^{\nu} A^{\nu} \exp\left\{ -\beta\theta^{*}\Delta F + \frac{h}{2\pi}\nu\beta\theta_{\sigma}^{*} - \psi^{m}\left(\theta^{*}\right) - \psi^{V}\left(\theta^{*}\right) - \psi^{mV}\left(\theta^{*}\right) \right\}$$

Consideration of this correlation allows realization of the analysis for wide range of the processes.To this effect it is necessary to select concrete model, to simplify analytically general expressions in the framework of this model and to compare with experimental data. Whereupon it is possible to obtain numerical values of reorganization energy, transition dipole moment, reorganization of the quantum subsystem, etc.

In case when distribution function of reagents is known the last expression allows calculation of transition dipole moment and accordingly evaluation of transition interval, which is important during investigation of the complicated systems.

ლიტერატურა – REFERENCES – ЛИТЕРАТУРА

1. Amy L Linsebigler ,Guangquan Lu , John T Yates. *Chem Rev.* 1995;95(3):735–758.
2. Wu CH and Chang CL. Journal of hazardous materials. 2006;128 (2–3):265–72. doi:10.1016/j.jhazmat. 2005.08.013.PMID 16182444.
3. Xing J, Fang WQ, Zhao HJ and Yang HG. Chem Asian J. 2012;7:642–657.

4. Xuan J and Xiao WJ. Visible-Light Photoredox Catalysis. AngewChemInt Ed. 2012;51: 6828.
5. Dogonadze R. R. and Marsagishvili T. A., in: The Chemical Physics of Solvation, Part A, Ed. R. Dogonadze, Elsevier Publ. Co., Amsterdam, 1985, p. 39.
6. Platzman P.M., Wolff P.A., Waves and interactions in solid state plasmas, Academic Press, N.Y., London, 1973.
7. Marsagishvili T.A., Heterogeneous process of charge transfer and phototransfer with participation of dipole particles. Journal of Electroanal. Chem., 1998, v. 450, p. 47-53.

ფოტოკატალიზური პროცესების მოდელირება

თ.მარსაგიშვილი, მ.მაჭავარიანი, გ.ტატიშვილი, ნ.ანანიაშვილი,
მ.გაჩეჩილაძე, ჯ.მეტრეველი, ე.ცხაკაია
ივანე ჯავახიშვილის თბილისის სახელმწიფო უნივერსიტეტის
რაფიელ აგლაძის არაორგანული ქიმიისა და ელექტროქიმიის ინსტიტუტი

რეზიუმე

ფოტოკატალიზი ანუ ზემოქმედება ქიმიურ რეაქციაზე ფოტონების საშუალებით წარმოადგენს ინტერესს როგორც თეორიული, ასევე პრაქტიკული თვალსაზრისით. მოცემულ სამუშაოში შესწავლილია მოდელური სისტემა - კონდენსირებული გარემო მასში გახსნილი რეაგენტებით. ქიმიური რეაქციების თეორიული გათვლების დროს გამოიყენება თეორიული და მათემატიკური ფიზიკის მეთოდები, კერძოთ, კონდენსირებული გარემოს პოლარიზაციის ოპრერატორების მრავალნაწილაკიანი ტემპერატურული გრინის ფუნქციები. მიღებულია რეორგანიზაციის ენერგიის, გადასვლის დიპოლური მომენტის, კვანტური ქვესისტემის რეორგანიზაციის ენერგიის და სხვ. რიცხვითი მნიშვნელობები.

МОДЕЛИРОВАНИЕ КАТАЛИТИЧЕСКИХ ПРОЦЕССОВ

Т.Марсагишвили, М.Мачавариани, Г.Татишвили, Н.Ананиашвили, М.Гачечиладзе,
Дж.Метревели, Е.Цхакая
Тбилисский государственный университет им. И. Джавахишвили
Институт неорганической химии и электрохимии им. Р.Агладзе

РЕЗЮМЕ

Фотокатализ или воздействие на химическую реакцию с помощью фотонов представляет интерес как с теоретической, так и с практической точки зрения. В данной работе была изучена модельная система – конденсированная среда с растворенными в ней реагентами.При теоретических расчетах химических реакций используются методы теоретической и математической физики, в частности, многочастичные температурные функции Грина операторов поляризации конденсированной среды. Получены численные значения энергий реорганизации, дипольного момента перехода, энергии реорганизации квантовой подсистемы и др.

NEW GENERATION ZEOLITIC ADSORBERS

Vladimer Tsitsishvili, Nanuli Dolaberidze, Maia Alelishvili, Manana Nijaradze, Nato Mirdzveli
Petre Melikishvili Institute of Physical and Organic Chemistry
of Ivane Javakhishvili Tbilisi State University, 0186, 31 Politkovskaia str., Tbilisi, Georgia
v.tsitsishvili@gmail.com

The synthesis of new generation zeolite materials by hydrothermal transformation of natural Georgian clinoptilolite-heulandite treated by HCl water solution and suspended in NaOH solution was investigated. Products were characterized by SEM-EDS, XRD, and FTIR analyses. Investigartion demonstrated that synthesis of zeolites with high silicon content (mordenite-like materials) could be carried our directly from aged gels having suitable chemical composition, but obtaining of materials with high aluminum content (**LTA** type synthetic zeolitic material) is possible in two steps: hydrothermal crystallization of the same natural zeolite firstly to the sodalite structure with Si/Al=1, followed by re-crystallization of sodalite in the NaA zeolite; in both cases morphology of crystallites generally depends on conditions of crystallization.

Introduction. Wide application of zeolites in industry, agriculture, environmental protection and other areas led to interest in new synthetic materials with zeolite-like molecular sieve, sorption, ion exchanging, catalytic, and other properties. Through the synthesis wide range of structures can be obtained, not existing in nature or possessing different properties. For example, synthetic mordenite has the ability to accept ions or molecules larger than 4.5Å, while natural mordenit deprived this ability. On the other hand, due to the well-developed mesoporous structure, natural zeolites have a number of useful properties, including possibility to bond macromolecules and even microorganisms. Synthetic zeolites are usually prepared in the form of crystallites with sizes ranging from hundreds of nanometers ("nano-zeolites") to tens of micrometers, without secondary porosity. However, the mesoporous structure can be reproduced synthetically.
The aim of present work was to demonstrate modern possibilities to carry out synthesis of zeolitic materials with different sizes of crystallites, as well as with suitable system of pores and channels.

Experimental. Preparation of synthetic zeolite material was carried out using Georgian natural clinoptilolite-heulandite-containing rock from the Rkoni plot of Tedzami deposit [1] having chemical composition $(Na_{3.3}K_{1.15}Ca_{0.75}Mg_{0.25}[Me]_{0.55})(Al_{7.0}Si_{29.3}O_{72})\cdot 22.5H_2O$ (Me = Cu, Zn, Ba, Sc according to EDS data), characterized by X-ray diffraction pattern, IR spectrum, water adsorption capacity and thermal analysis data, and belonging to the Na,K,Ca,Mg-form of the **HEU** (UPAC chemical formula $|Ca_4(H_2O)_{24}|$ **[**$Al_8Si_{28}O_{72}$]) type natural zeolites.
Processing of raw in target material includes following steps:
Treatment of raw material & preparation of suspension. Clinoptilolite-heulandite-containing rock powder was treated at room temperature by 20% HCl water solution under stirring, washed by water before the complete disappearance of Cl^- ions, and dried in owen at 100-105ºC; water suspension of treated material was prepared with the solid to liquid ratio of 1 : 3.
Gel formation. Prepared suspension was treated at room temperature by 10% NaOH water solution, solid to liquid ratio of 1 : 6, gel homogenization takes 30 minutes, details are given in [2]. General characteristics of target zeolitic material are in strong dependence on the chemical composition ($kNa_2O{:}mSiO_2{:}Al_2O_3{:}nH_2O$) of gel prepared for aging and crystallization: the SiO_2/Al_2O_3 ratio determines the type of microporous structure to be produced, and application of sodium hydroxide gives possibility to prepare nearly monocationic sodium forms; water content generally is rather high to ensure suitable physical properties (viscousity, etc.) for crystallization process, but water molecules are compulsory units to built zeolite structure and play a significant role.
Gel aging. Generally the process of gel aging at room temperature and without application of seed crystals takes several days, details are described in [3].
Crystallization. Crystallization of aged gel was carried out in the Teflon flasks at different temperatures up to 110ºC, duration of the process – up to 90 hours; both temperature and duration affect to crystalline sizes – low temperature prolonged synthesis gives high quality large crystals, high temperature fast crystallization is a way to produce "nano-zeolites" and their fibrous aggregates.

Separation and cleaning. Separation of produced crystalline material was carried out by filtration of mother solution, solid material was cleaned by water until pH 8.0-8.5, and dried at 90-100°C.

Synthesis of mordenite-like materials was carried out [4] from gels aged during one week and having chemical composition of SiO_2/Al_2O_3 = 9.8, Na_2O/SiO_2 = 0.08, H_2O/Na_2O = 250, but obtaining of materials with high aluminum content is impossible in single described stage.

However, preparation of synthetic zeolitic material of the type A (**LTA** structure) was carried out by two-stage re-crystallization of the same **HEU** type natural zeolite firstly to the sodalite (**SOD**) structure, and then in the target structure: **HEU → SOD → LTA**, in following steps: preparation and acid treatment of raw material; gel formation and its aging; hydrothermal crystallization; separation of intermediate **SOD** product, new gel formation without any acid or basic treatment, but including gel aging; crystallization and separation of target product, its washing and drying.

Chemical composition of prepared samples (Table 1) was determined by elemental analyses carried out using a Spectromom 381L plasma spectrometer and a Perkin-Elmer 300 atomic absorption spectrometer, as well as by energy dispersive X-ray (EDS) analysis. X-ray powder diffraction patterns were obtained from a DRON-4 diffractometer, employing the Cu-K_α line and scanning at 1^O per minute, FTIR spectra in the wavenumber range 4000-400 cm^{-1} were recorded on the Perkin-Elmer FTIR spectrometer (version 10.4.2) using the KBr pellet technique for sample preparation, SEM images were obtained by using Jeol JSM6510LV scanning electron microscope (parameters are given on figures) equipped with Oxford Instruments X-Max 20 analyzer for EDS. Water adsorption capacity was measured under static conditions (p/p_S=0.40, 20^OC).

Table 1. Chemical composition of prepared materials compared with UPAC chemical formula

Sample	Chemical composition	UPAC chemical formula
Synthetic mordenite	$(Na_{6.23}K_{0.51}Ca_{0.25}Mg_{0.12})(Al_{7.5}Si_{40.2}O_{96})\cdot 16.0H_2O$	$\lvert Na^+_8\ (H_2O)_{24}\rvert$ **[**$Al_8Si_{40}O_{96}$**]-MOR**
Synthetic sodalite	$(Na_{4.5}K_{0.6}Ca_{0.25}Mg_{0.1})(Al_{5.8}Si_{6.4}O_{24})\cdot 5.92H_2O$	$\lvert Na_8Cl_2\rvert$ **[**$Al_6Si_6\ O_{24}$**]-SOD**
Synthetic NaA	$(Na_{10.2}K_{0.4}Ca_{0.1}Mg_{0.3})(Al_{11.4}Si_{12.0}O_{48})\cdot 24.3H_2O$	$\lvert Na_{12}\ (H_2O)_{27}\rvert_8$ **[**$Al_{12}Si_{12}O_{48}$**]$_8$-LTA**

Results & discussion

Chemical composition of prepared materials is in a good accordance with corresponding chemical formula with the exception of small "lack" of the Al atoms in the frame; prepared materials are nearly pure Na-forms, in several EDS spectra traces of Cu and Zn have been observed, Ba and Sc are removed in full.

XRD. The framework type of prepared material was testified by X-ray powder diffraction patterns. (for synthetic mordenite see details in [4])No additional diffraction peak at $2\Theta = 7.74^o$ indicating the formation of the **BEA** type structure [5] or at $2\Theta = 15.8^o$ indicating the formation of analcime (reffered as $2\Theta = 16.3^o$ in [6]) as impurities have been observed in XRD of synthetic mordenite [4]; the main peaks of the **MOR** structure appear with high intensity in accordance with sufficient silica to alumina molar ratio and synthesis time. Influence of the silica to alumina molar ratio in gel on the synthesis time and crystallinity of synthesized mordenite is the same, as described in [7]. XRD patterns of **LTA** samples have been compared with calculated ones taken from the "Database of Zeolite Structures" of the International Zeolite Association (http://www.iza-structure.org/).

Table 3. **LTA** calculated XRD pattern (peaks over $0.09I_{max}$) compared with experimental

hkl	Calculated			Experimental	
	2Θ, degree	d, Å	I, $\%I_{max}$	2Θ, degree	I, $\%I_{max}$
200	7.178	12.3050	100.00	7.2	100
220	10.158	8.7009	51.31	10.1	78
222	12.449	7.1043	31.82	12.4	44
420	16.093	5.5030	20.30	16.2	42
600	21.648	4.1017	10.62	21.1	18
442			22.78	21.8	93
622	23.965	3.7101	44.34	24.0	1.56
640	26.089	3.4128	10.11	26.0	42
642	27.092	3.2886	41.01	26.9	1.50
820	29.915	2.9844	19.92	29.9	1.93
644			19.70		
840	32.315	2.7515	9.34	32.9	45
664	34.149	2.6234	27.06	34.2	1.20

Experimental XRD pattern has the same peculiarities mentioned in [8]: high intensity peaks at 2Θ = 7° and 10°, as well as at 2Θ = 24, 27, 30, and 34°. With the molar ratio Si/Al nearly equal to one, kaolin is considered as an ideal raw material for preparing NaA zeolite [9 and references therein], but **LTA** materials prepared from natural kaoline contain quartz (strong peak at 2Θ = 26.63°) and the **SOD** type zeolite (characteristic peaks at 2Θ = 14.14° (0.53), 24.62° (1.00), 31.96° (0.98), and 35.1° (0.78)) as impurities, not observed in XRD patterns of samples obtained by re-crystallization of **SOD** produced from **HEU**. No improvement in crystallinity like noted in [5] for high-silica zeolite A sample treated for five minutes with 12.5% NaOH solution at room temperature has been observed.

Developed zeolitic crystal microporous structure in synthesized samples has been confirmed also by comparatively high averaged value (5.30 mmole/g for **MOR** and 7.60 mmole/g for **LTA**) of water adsorption capacity under static conditions at the "plateau" pressure.

FTIR. Assignment of the main bands in mid infrared was made according to [10] distinguishing external and internal asymmetrical (ν_{asym}) and symmetrical (ν_{sym}) stretch vibrations of the TO_4 tetrahedra (T = Si or Al), results are given in the table 3.

Table 3. Peak positions in infrared spectra and their assignment

Measured peak position in cm^{-1}				**Assignment**
Mordenite		A		
3572	Broad	3467	Broad	Asymmetric stretching of OH group
3486	Broad			
1634		1648		Bending vibration of H–OH
1384		1510 – 1260	Peaks & Shoulders	Bending vibration of bridging –OH-O–
1222		1190	Shoulder	Internal ν_{asym}
1050	Broad	1008	Broad	External ν_{asym}
777		750	Shoulder	External ν_{sym}
727		704	Shoulder	Internal ν_{sym}
625		663		
581		552		Double ring vibration
575	Shoulder			
442		465		T-O bend vibration

SEM images (figures 1-2) show crystalline morphology of obtained samples. Produced mordenite prismatic crystals (figure 1, left) have width in a range of 0.15 – 0.45 μm and length up to 3 μm, mordenite fibrous aggregates (figure 1, right) are characterized by fiber diameter from 40 nm to 90 nm and length up to 10 μm, imitating non-regular mesoporous structure.

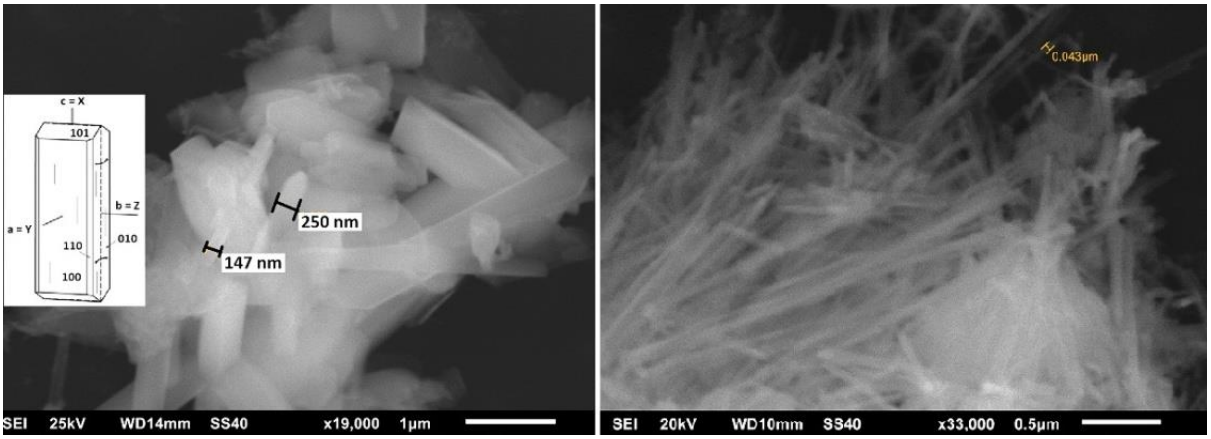

Fig. 1. Mordenite vertically striated prismatic crystals and fibrous aggregates

As compared with known methods using pure chemicals [11,12] and natural kaolin as a raw material [13], our method of the **HEU** type natural zeolite re-crystallization needs no organic template or seed crystals and takes nearly the same time to produce high quality micro crystals; fast crystallization results materials like described in [14] (fiber diameter 65 nm and length 7 μm), also prepared in the absence of organic template by hydrothermal method, but at higher temperature of 180°C (autoclave crystallization), and during a longer time, 120 hours, that may be due to the differences in the composition of synthesis mixture. SEM images of the sodium form NaA (figure 2) testify the possibility of obtaining both micrometric (average diameter 2 μm) and nanoscale crystallites depending on the crystallization rate and other parameters; selection of conditions makes possible to receive samples from fairly narrow distribution of the crystallite sizes.

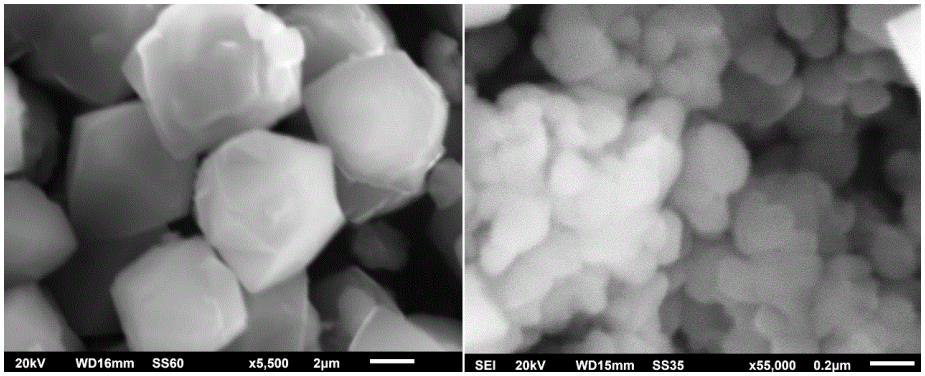

Fig. 2. NaA micro and nano crystals

The proposed methods are based on the use of natural silica-alumina raw materials and inexpensive reagents (HCl, NaOH), are characterized by the relative rapidity, low energy expenditures and low Sheldon's factor E.

ლიტერატურა – REFERENCES – ЛИТЕРАТУРА

1. V.Tsitsishvili, N.Dolaberidze, M.Alelishvili, G.Tsintskaladze, G.Sturua, D.Chipashvili, M.Nijaradze, N.Khazaradze. Adsorption and Thermal Properties of Zeolitic Rocks from Newly Investigated Deposit Plots in Georgia. Georgian Eng. News, 1998, No 2(6), p. 61-65.
2. V.Tsitsishvili, N.Dolaberidze, N.Mirdzveli, M.Alelishvili, N.Nijaradze, M.Suladze. Chemical Preparation of Nano-Sized Zeolite Materials. Study of Pre-Crystallization Processes. Proc. Georgian Nat. Acad. Sci., chem. ser., 2009, v. 35, No 2, p.197-200.
3. N.M.Dolaberidze, V.G.Tsitsishvili, N.A.Mirdzveli, M.O.Nijaradze, M.V.Alelishvili. Hydrothermal transformation of clinoptilolite to obtain fine-dispersed zeolite materials. In "Actual Problems of Adsorption Theory, Porosity and Selectivity", Materials of 2nd All-Russian Conference with International Participation, Moscow, 2015, p. 91.
4. V.Tsitsishvili, N.Dolaberidze, N.Mirdzveli, N.Nijaradze. MOR type synthetic zeolite material. Proc. Georgian Nat. Acad. Sci., chem. ser., 2016, v. 42, No 1, p.7-20.
5. G.T.Kokotailo, C.A.Fyfe. Zeolite structure analysis with powder X-ray diffraction and solid-state NMR techniques. The Rigaku Journal, 1995, v. 12, No 1, p. 3-10.
6. B.O.Hincapie, L.J.Garces, Q.Zhang, A.Sacco, S.L.Suib. Synthesis of mordenite nanocrystals. Micropor. Mesopor. Mat., 2004, v. 67, p. 19-26.
7. R.Merdekawati, R.Ediati, D.Prasetyoko. Effect of silica to alumina molar ratio on crystallinity of mordenite synthesized using rice husk ash and kaolin from Bangka Belitung. Proc. Internat. Conf. Satya Wacana Uni., Indonesia, 2015, p. BC.84-89.
8. A.Shoumkova, V.Stoyanova. SEM–EDX and XRD characterization of zeolite NaA, synthesized from rice husk and aluminium scrap by different procedures for preparation of the initial hydrogel. Journal of Porous Materials, 2013, v. 20, No 1, p. 249-255.
9. M.Gougazeh, J.-Ch.Buhl. Synthesis and characterization of zeolite A by hydrothermal transformation of natural Jordanian kaolin. Journal of the Association of Arab Universities for Basic and Applied Sciences, 2014, v. 15, p. 35-42.

10. E.M.Flanigen, H.Khatami, H.A.Seymenski. Characterization of zeolitic materials by IR spectroscopy. Adv. Chemistry Series, 101 (Editors E.M.Flanigen, L.B.Sand), American Chemical Society, Washington, 1971, p. 201-228.
11. L.B.Sand. Synthesis of large-port and small port mordenites. In "*Molecular Sieves*", Society of Chemical Industry, 1968, London, p. 71-77.
12. P.K.Bajpai. Synthesis of mordenite type zeolite. Zeolites, 1986, v. 6, is. 1, p. 2-8.
13. M.L.Mignoni, D.I.Petkowicz, N.R.C.Fernandes Machado, S.B.C.Pergher. Synthesis of mordenite using kaolin as Si and Al source. Applied Clay Science, 2008, v. 41, is. 1-2, p. 99-104.
14. H.M.Ali, M.E.Moustafa, E.A.Abdelrahman. Synthesis of mordenite zeolite in absence of organic template. Advanced Powder Technology, 2012, v. 23, is. 6, p. 757-760.

ახალი თაობის ცეოლითური ადსორბენტები

ვლადიმერ ციციშვილი, ნანული დოლაბერიძე, მაია ალელიშვილი, მანანა ნიჟარაძე, ნატო მირძველი
ივანე ჯავახიშვილის სახელობის თბილისის სახელმწიფო უნივერსიტეტის
პეტრე მელიქიშვილის ფიზიკური და ორგანული ქიმიის ინსტიტუტი
საქართველო, თბილისი 0186, ა.პოლიტკოვსკაიას ქ. 31 v.tsitsishvili@gmail.com

რეზიუმე

შესწავლილია ახალი თაობის ცეოლითური მასალების სინთეზის პროცესები საქართველოს ბუნებრივი ჰეილანდიტ-კლინოპტილოლიტის ჰიდროთერმული გარდაქმნის გზით, მისი წინასწარი მჟავური დამუშავებისა და ტუტე ხსნარში სუსპენდირების შემდეგ. მიღებული პროდუქტები დახასიათებულია მასკანირებელი ელექტრონილი მიკროსკოპიის, რენტგენული დიფრაქტომეტრიისა და ფურიე-ინფრაწითელი სპექტროსკოპიის მეთობით. ნაჩვენებია, რომ სილიციუმის მაღალი შემცველობის მასალების (მორდენიტის ტიპის ცეოლითები) მიღება შესაძლებელია ერთ სტადიაში, ხოლო ალუმინის შედარებით მაღალი შემცველობის (A ტიპის ცეოლითები) მასალების დასამზადებლად საჭიროა ჯერ Si/Al=1 მქონე სოდალიტის მიღება, რომელის შემდგომ უნდა გადაკრისტალდეს მიზნობრივი პროდუქტის მიღებით; ორივე შემთხვევაში კრისტალიტების მორფოლოგია და ზომები ძირითადად განისაზღვრება კრისტალიზაციის პირობებით.

ЦЕОЛИТНЫЕ АДСОРБЕНТЫ НОВОГО ПОКОЛЕНИЯ

В.Г.Цицишвили, Н.М.Долаберидзе, М.В.Алелишвили, М.О.Нижарадзе, Н.А.Мирдзвели
Институт физической и органической химии им. П.Г.Меликишвили Тбилисского государственного университета им. И.Джавахишвили, 0186, ул. А.Политковской 31, Тбилиси, Грузия
v.tsitsishvili@gmail.com

РЕЗЮМЕ

Исследован синтез цеолитных материалов нового поколения путем гидротермального превращения грузинского природного клиноптилолит-гейландита, обработанного соляной кислотой и суспендированного в щелочнон растворе. Полученные продукты охарактеризованы методами сканирующей электронной микроскопии, рентгеновской диффрактометрии и Фурье-ИК-спектрального анализа. Показано, что синтез высококремнистых цеолитов типа морденита возможен в одну стадию, в то время как для приготовления цеолитов со сравнительно высоким содержанием алюминия (цеолитов типа А) сперва требуется получение содалитовой структуры с Si/Al=1, которая затем перекристаллизуется в целевой продукт; в обоих случаях морфология и размеры кристаллитов в основном определяются условиями кристаллизации.

THERMAL CHARACTERISTICS OF SPINEL-TYPE COMPLEX OXIDES $Me_{1-x}Zn_xFe_2O_4$ (WITH Me=Cu OR Mg)

T.E.Machaladze, V.S.Varazashvili, M.S.Tsarakhov, M.G.Khundadze, T.A.Pavlenishvili, N.G.Lezhava, R.P.Jorbenadze

R.Agladze Institute of Inorganic Chemistry and Electrochemistry, Ivane Javakhishvili Tbilisi State University

tmachaladze@rambler.ru

Determination of Curie temperature, of coefficient of heat expansion and of electrical conductivity as well as X-ray and neutronographic researches belong to the methods by which the process of ferrite transition into thermodynamically stable state could be inferred.

Calorimetric methods for determination of heat capacity, at which in the compound the process of removal of metastable state takes place, is characterized by a number of advantages in comparison with other physical-chemical methods. This advantage is determined by the possibility of measuring of temperature and heat with a high degree of accuracy, by establishing of certain thermal conditions, by exact thermodynamical characteristics of initial and final states of the compound [1].

With increasing temperature some spinelssuffer disordering and tend to statistically random distribution in A- and B-sub-lattices of the cations. In the course of high-temperature hardening of such samples the maintenance of high-temperature metastable state is possible. In the process of heating of hardened spinel the state is attained when overcoming of activation barrier is possible and cations displacement begins to obtain the equilibrium state typical for mentioned temperature. In the course of thermodynamical researches this process is fixed at the curve of heat capacity as exothermic effect. Hardening effects are most pronounced for the spinels which are characterized by small difference between the energies of normal and reverse states. Solid solutions of copper-zinc and magnesium-zinc ferrites, investigated by us, belong to such compounds.

Ferrites of copper, magnesium, copper-zinc and magnesium-zinc were prepared by ceramic method from corresponding oxides of chemical purity . Detail information on synthesis and identification of ferrites is given in [2]. For maintenance of ions high-temperature distribution in crystalline lattice the sample was hardened from 1425K by throwing in ice water.

Calorimetric researches were performed at differential scanning microcalorimeter (SETARAM) – DSC-111 in temperature range from 300K to 900K. Calorimeter sensitivity was determined by means of Joule effect. The heat capacity of standard compound-synthetic corundum was measured for determination of research accuracy.

Comparison of obtained data with metrological measurements [3] has shown that the device accuracy is maximum in temperature range from 360K to 760K - ~0,2% and is minimum in the range from T<360K to T>760K - ~2%.

Experimental conditions were similar at calibration and measuring of ferrites heat capacity: scanning rate –3K/min, amplifier sensitivity – 1 mV.

Influence of thermal treatment on heat capacity is known only for copper ferrites [4]. We primarily in the practice investigated the effect of thermal treatment on heat capacity of solid solutions of the ferrites of magnesium, magnesium-zinc and copper-zinc. We have also investigated copper ferrite, synthesized by us, for comparison with the data of [4].

Repeat measurements of once hardened balanced samples have shown that the value of heat capacity is slightly exceeds the heat capacity of balanced samples in all cases. In transformation points the peaks of heat capacity are of more smooth shape and the transformation temperature range increases. All above-mentioned is indicative of the fact that the cooling of the samples by slow rate together with a calorimeter is sufficient to partial hardening of the sample under study. As a result the sample gains an excess internal energy which is reflected at the curve of heat capacity.

Copper ferrite – $CuFe_2O_4$. In Fig.1 the curves of heat capacity are given for the samples obtained by slow cooling and hardening of copper ferrite as well as for the reheated and hardened sample. The overall

picture up to T<Tc is principially coincident with the data of [5] and nearCurie temperature and above the considerable difference is observed.

At initial stage a small difference is observed between beat capacities of balanced (tetragonal) and hardened (metastable-cubic) ferrites. This fact may be explained by diversity of their crystalline latticies. Cations displacement and annealing of hardened samples begin at sufficiently low temperature (from ~330K). With increase of the temperature this process becomes intensive: at first the plateau is formed in the range from ~430K to ~480K, thereafter above 530K an exothermic effect is observed, which reflects the gradual formation of tetragonal copper ferrite from metastable cubic phase of hardened sample. This process is continued up to reasonably high temperatures since the curve of the heat capacity of hardened sample isn't connected with the equilibrium curve and is lower up to 900K. Slight endothermic effect at 600K is indicative of the transition of recently formed low-temperature modification to high-temperature cubic one. As is obvious, this process isn't completed in this case and corresponding endothermic effect can't overlap an exothermic effect of cations redistribution neither of mentioned area nor in the area of ferromagnetic transformation. Therefore the process of heat release and, respectively, the process of transition to equilibrium state in temperature range under study become uncompleted. This process takes place at higher temperatures. Hence, from obtained data it is impossible to estimate the reliable value of the transition from metastable state to stable one in the range of exothermic peak - (530-720)K. Summation of the amounts of released heat by means of DTA regime of scanning calorimeter and by integration of Cp-T function gives ΔH, which only partially reflects this process.

The picture of reheating of hardened sample confirms the suggestion that the formation of tetragonal phase at primary heating isn't complete. The peak of heat capacity at the temperature of the transition from tetragonal structure to cubic one is lower than for balanced sample. Moreover, as is seen, the equilibrium redistribution of the cations continues above 580K causing exothermic processes and partial overlapping of endothermic effect in the area of structural transformation (~600K) where the very small endothermic peak is observed.

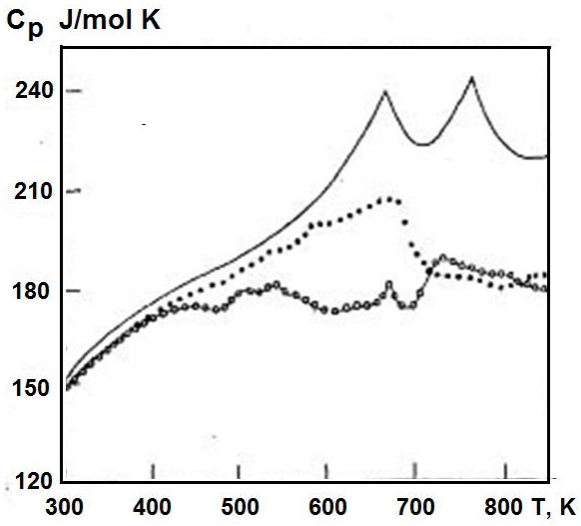

Fig. 1. Heat capacity of $CuFe_2O_4$ — – unhardened sample; • – hardened sample; o – rehardened sample

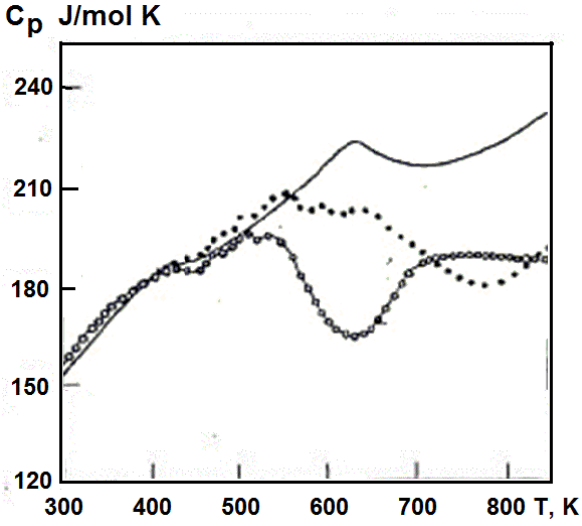

Fig. 2. Heat capacity of $Cu_{0.8}Zn_{0.2}Fe_2O_4$ — – unhardened sample; • – hardened sample; o – rehardened sample

$Cu_{0.8}Zn_{0.2}Fe_2O_4$. In Fig.2 the heat capacity of hardened sample is presented. As expected, for metastable phase with excess internal energy in the range from 300K to 400 K the heat capacity is slightly higher than for balanced sample. In copper-zinc ferrite of this composition the structural variations, caused by Yan-Teller cooperative effect, are missed. Therefore the sample retains a cubic structure even at high temperatures and for it only ferromagnetic transformation with a maximum at650K is characteristic.

For the ferrite of mentioned composition a reasonably hardening effect is typical. The stage of cations redistribution in A- and B – sub-lattices is observed as a plateau already above 430K and in the range from 550K to 760K the process of cations equilibrium redistribution proceeds by maximum intensity. Above 760K this process isn't completed since the heat capacity isn't equal to the value of the heat capacity of balanced sample and is significantly less. Along with it, there is a tendency to its reduction which is indicative of low intensity of ordering process. The fact that for the sample of copper ferrite as well as of copper-zinc ferrite the balancedredistribution isn't attained up to 900K is confirmed by reheating of hardened sample. In this case a slight excess of the heat capacity up to 560K in comparison with the balanced sample is indicative of relatively metastable state of the system. Above 580K the exothermic process is observed which is even less than in the case of first heating but nevertheless overlaps the ferromagnetic transformation which is expressed by a minor peak.

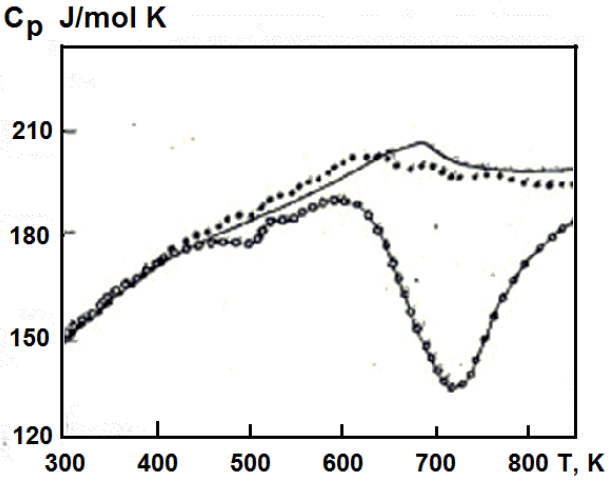

Fig. 3. Heat capacity of $MgFe_2O_4$
— – unhardened sample; • – hardened sample; o – rehardened sample

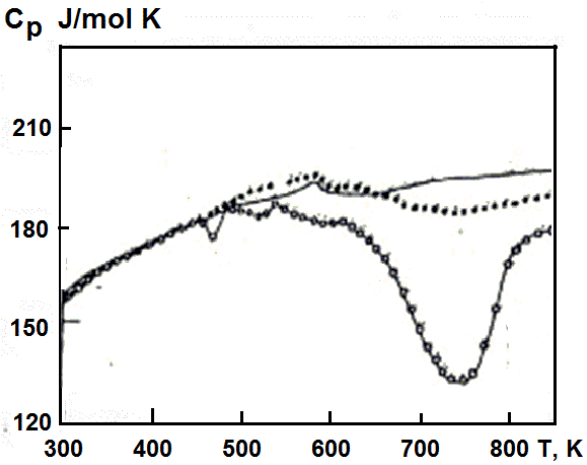

Fig. 4. Heat capacity of $Mg_{0.8}Zn_{0.2}Fe_2O_4$
— – unhardened sample; • – hardened sample; o – rehardened sample

$MgFe_2O_4$ and $Mg_{0.8}Zn_{0.2}Fe_2O_4$. In the case of the samples of magnesium ferrite and magnesium-zinc ferrite the picture is nearly similar (Fig.3 and 4). The heat capacity of hardened metastable samples of both ferrites is slightly exceeds the heat capacity of balanced sample. 500K may be considered as the initial temperature of exothermic peak and the phase of intensive redistribution of the cations is in the range from 600K to 900K. It is expected that mentioned process is continued even at high temperatures by less intensity. In magnesium ferrite, in contrast to copper-containing ferrites, the process of balanced ordering is more perfect which is confirmed by the results of reheating of hardened samples. The values of corresponding heat capacities are nearly coincident with the heat capacity of balanced sample and at the curve the ferromagnetic transformations are reflected. Obtained values of heat effect may be considered as the enthalpies of ordering process.

In the temperature range under study an incompleteness of the samples annealing process is determined by kinetic factor and is indicative of the necessity of increase of process duration than it possible at calorimetric experiment in scanning regime. The minimum of exothermic peaks are recommended as optimal temperatures of annealing.

In the table 1 the values of the enthalpies of the transition from metastable modification to stable one for the samples under study and the values of optimal temperatures of annealing of hardened samples are presented.

Table 1

Heat characteristics of the ferrites under study

Compound	ΔH J/mole	Effect temperature Range (K)	Annealing T_{opt} (K)
$CuFe_2O_4$	2150	430-720	630
$Cu_{0.8}Zn_{0.2}Fe_2O_4$	3100	430-760	660
$MgFe_2O_4$	6960	490-900	750
$Mg_{0.8}Zn_{0.2}Fe_2O_4$	4870	500-870	770

ლიტერატურა - REFERENCES – ЛИТЕРАТУРА

1. Kolesov V.G., Vorobiev V.N. Reports of Academy of Sciences of USSR, 1972, 205, 1358 (Russian)
2. Samadashvili I., Machaladze T. Proceesings of Georgian Academy of Sciences, Chem. series, 1998, 24, 1-4, 185-187 (Georgian)
3. Kelly K.K. High-Temperature Heat-Content, Heat Capacity and Entropy Data for the Elements and Inorganic Compaunds – Bureau of Mines Builetin, 584, 1960.
4. Reznitski L.A. Chemical Thermodynamics and Equilibrium. V.4 Moscow, MSU, 1978, 43.

შპინელის ტიპის რთული ოქსიდების $Me_{1-x}Zn_xFe_2O_4$ (Me=Cu, Mg) თერმული მახასიათებლები

თ.მაჩალაძე, ვ.ვარაზაშვილი, მ.ცარახოვი, მ.ხუნდაძე, თ.ფავლენიშვილი, ნ.ლეჟვა, რ.ჯორბენაძე
ივანე ჯავახიშვილის სახელობის თბილისის სახელმწიფო უნივერსიტეტის რ.აგლაძის არაორგანული ქიმიისა და ელექტროქიმიის ინსტიტუტი, 0186, მინდელის ქ.11, თბილისი, საქართველო

რეზიუმე

მეტასტაბილურ მდგომარეობაზე თერმული დამუშავების გავლენის დასადგენად შესწავლილია სპილენძ-თუთიისა და მაგნიუმ-თუთიის გამოწრთობილი ფერიტების თბოტვადობის ტემპერატურისაგან დამოკიდებულება. დადგენილია მეტასტაბილურიდან სტაბილურ მდგომარეობაში გადასვლის ენთალპიის მნიშვნელობები და წრთობის ეფექტის მოწვის ოპტიმალური ტემპერატურები.

ТЕРМИЧЕСКИЕ ХАРАКТЕРИСТИКИ СЛОЖНЫХ ОКСИДОВ ШПИНЕЛЬНОГО ТИПА $Me_{1-x}Zn_xFe_2O_4$ (Me=Cu, Mg)

Т.Е.Мачаладзе, В.С.Варазашвили, М.С.Царахов, М.Г.Хундадзе,
Т.А.Павленишвили, Н.Г.Лежава, Р.П.Джорбенадзе
Институт неорганической химии и электрохимии им. Р.И.Агладзе Тбилисского государственного университета им. И.Джавахишвили, 0186, ул. Миндели11, Тбилиси, Грузия

РЕЗЮМЕ

Для выявления влияния термической обработки на метастабильное состояние изучена температурная зависимость величины теплоемкости закаленных образцов медно-цинковых и магний-цинковых ферритов. Установлены значения энтальпий перехода из метастабильного состояния в стабильное и оптимальные температуры отжига эффектов закаливания.

DETERMINATION OF CONDITION OF COMPLETE SOLID SOLUBILITY IN THE SYSTEM $Li_{0,5}Fe_{2,5-x}Al_xO_4$ BY MEANS OF CALORIMETRIC INVESTIGATION OF EXCESS MIXING PARAMETERS ΔH_{mix}^{ex} AND ΔS_{mix}^{ex}

N.G.Lezhava, M.G.Khundadze, V.S.Varazashvili, T.E.Machaladze, T.A.Pavlenishvili, M.S.Tsarakhov

R.Agladze Institute of Inorganic Chemistry and Electrochemistry of Ivane Javakhishvili Tbilisi State University, 0186, Mindeli st.11, Tbilisi, Georgia

The energy of solid solubility of the system $Li_{0,5}Fe_{2,5}O_4 – Li_{0,5}Al_{2,5}O_4$ with general formula: $Li_{0.5}Fe_{2.5-x}Al_xO_4$ have been investigated using the method elaborated in laboratory by A Landia, in order to determine the borders of region of the broken solubility. On the base of the complex calorimeter experiments and semi-empirical calculation method, the phase diagram of state of investigated system was built and the top of the "dome of decomposition" of solid solution was fixed. The special thermal treatment provides receiving of single phase composition.

Introduction

In laboratory of thermochemistry by N.Landia the method of determination of the energy of spinels' solid solubility process was elaborated. This is the combination of calorimetric and semi-empirical calculation methods.

The systems Ni-Zn, Co-Zn, Li-Zn ferrites have been investigated using this method and results are published earlier [1-3].

The majority of ferrites and aluminates, as well as, molibdates and titanates are characterized by continuous solid solubility. But in some cases the continuous mutual dissolution of initial spinels breaks.

Since the compositions as intermediate complex compounds with valuable hi-tech properties often are found at the process of mutual solubility of simple spinels, it is very important to observe the process by means of thermodynamic parameters of mixing.

The high-temperature calorimetric dissolution method is the main experiment which allows study the mechanism of process of mixing.

The equilibrium state of solid solutions, as well as of any other systems is determined by aspiration to minimizing its free energy:

$\Delta G = \Delta H - T\Delta S = \Delta H + p\Delta V - T\Delta S.$

The process is directed by so called excess parameters of mixing:

$\Delta G_{mix}^{ex}(x_1\, x_2) = \Delta G_{s.sol}(x_1\, x_2) – [\Delta Gx_1 + \Delta Gx_2] = \Delta H_{mix} - T\Delta S_{mix}$,

$\Delta H_{mix}^{ex}(x_1\, x_2) = \Delta H_{s.sol}\,(x_1\, x_2) – [\Delta Hx_1 + \Delta Hx_2]$,

$\Delta S_{mix}^{ex}(x_1\, x_2) = \Delta S_{s.sol}\,(x_1\, x_2) – [\Delta Sx_1 + \Delta Sx_2]$, where

x_1 and x_2 – mole fraction of components,

$\Delta H_{s.sol}\,(x_1\, x_2)$ and $\Delta S_{s.sol}\,(x_1\, x_2)$ - thermodynamic parameters of solubility of complex spinels.

Calorimetric investigation of Lithiumferroaluminates' solid solutions with spinel structure

The object of the presented investigation is the system of solid solutions

$Li_{0,5}Fe_{2,5}O_4 – Li_{0,5}Al_{2,5}O_4$ with general formula: $Li_{0.5}Fe_{2.5-x}Al_xO_4$.

The nature of mixing of lithiumferroaluminate solid solutions is specific [4]. This system contains only one ferromagnetic Fe^{3+} ion. Nevertheless, it is characterized by several types of Neel's curves of dependence – magnetization/temperature (likely to nickelferroaluminates), and respectively - by ordered and disordered states of structure. In disordered state (quenched) in system continuous solubility is revealed. So, we have single-phased solid solutions at any ratio of initial components. However, in ordered (annealed) state we have discontinuous of the mutual solubility and two-phased mixture of initial components which appears near equi-molar composition.

The main calorimetric experiment was carried out on Hightemperature Differential Microcalorimeter Calve (Setaram) using the method high-temperature dissolution at 973K in a liquid melt of oxides ($9PbO.3CdO.4B_2O_3$) as the solvent. This method firstly was proposed by Jokokawa J.and Kleppa O.J. [5]. Later it was modified by Navrotky A. and Kleppa K [6] for determination of heat of formation of ferrites, aluminates and other spinel-structured compounds from corresponding oxides.

Since the value of enthalpy of mixing of spinels, almost an order of magnitude is less than enthalpy of formation of simple spinels from oxides, the higher accuracy and reproducibility of measurement of dissolving effect is needed. The purpose was achieved by means of special installation for dissolving of samples at Calve calorimeter, created in collaboration with scientists of department of mineralogy of Geological faculty of Moscow State University (Fig.1).

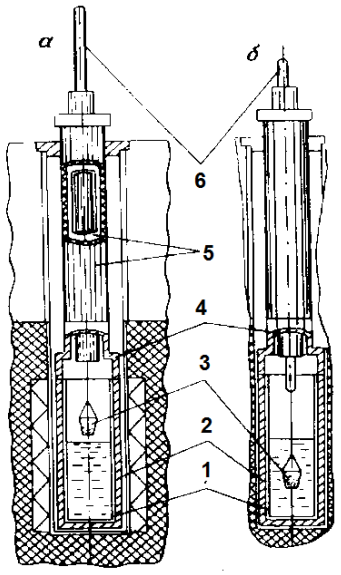

Fig. 1. Scheme of installation for high temperature dissolution at the Calve calorimeter

1. Platinum reaction vessel with solvent (1)
2. The nest (2) (from special alloy) for reaction platinum vessel with top (4)
3. Suspended little spoon with the sample under investigation (3)
4. Ceramic tubes (5) and
5. Mobile corundum rod (6)

The samples of initial components and intermediate compositions are prepared by ceramic method, identified by Chemical and X-ray analysis. The previous information about the functions $\Delta H = f(T)$, $C_p=f(T)$ and enthalpies of phase transformations are published earlier [7-8]. Together with the present results of high-temperature dissolution experiments they are necessary to calculate the excess thermodynamic parameters of mixing.

The important condition for carrying out such complex calorimetric investigation suggests - all this information should be taken from the same or absolutely identically prepared samples. This provides taking into account the factor of non-equilibrium and prehistory of samples under investigations. Knowing previously about the opportunity of decomposition of solid solution with ordered structure [4], we pretreated appropriately the sample $Li_{0,5}FeAl_{1,5}O_4$ before experiment. It was quenched in a stringent condition to fix disordered single-phased structure.

Obtained by dissolving of four compositions and two initial components in liquid oxide melt ($9PbO.3CdO.4B_2O_{3)}$ experimental data of $\Delta H_{dis}(973)$ are presented in Table1 and the concentration dependence of $\Delta H_{dis}(973)$ on Fig.2. Calibration of calorimeter was carried out before each series of dissolution throwing the pieces of platinum into liquid melt. Each sample was dissolved 5 times, standard error was estimated by formula: $S = \pm 2[(\sum\Delta i)2/n(n-1)]^{1/2}$, where Δ_I is deviation of each result of dissolution from the average ΔH_{dis}.

Table 1. Experimental data of dissolution of solid solutions $Li_{0,5}Fe_{2,5-x}Al_xO_4$

Number	Composition X	M_r	$\Delta H_{dis}(973)$kJ/mol	$\Delta H_{dis} \pm s$
1	0	207,18	59.65	± 0,45
2	0,5	192,67	59.56	± 0,59
3	1,0	178,24	55.65	± 0,90
4	1,5	163,82	49.22	± 0,45
5	2,0	149,40	49.20	± 0,52
6	2,5	134,92	52.12	± 0,82

As it is seen from Fig.2 the new portion of Al ions entering the structure of $Li_{0,5}Fe_{2,5}O_4$ decreases the value of ΔH_{dis} (973K). Obviously, the calculated values of mixing enthalpy of solid solution ΔH_{mix}^{ex973}

of $Li_{0,5}Fe_{2,5-x}Al_xO_4$ (x= 0,5; 1,0; 1,5; 2,0) will be positive. This is the first observed difference of this system compared with investigated earlier [1-3] systems, where ΔH_{mix}^{ex973} were negative.

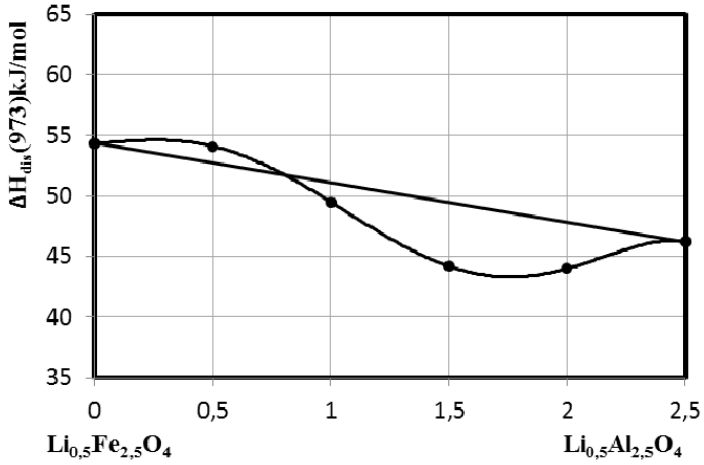

Fig. 2. Concentration dependence of enthalpy of dissolution ΔH_{dis} (973K)

The excess enthalpy of mixing ΔH_{mix}^{973} , as the difference between enthalpy of dissolving of the investigated composition of solid solution and the sum of initial pure components in relevant mole ratio is calculated by expression:

$$\Delta H_{mix}^{973} = [x\Delta H_{dis}^{973}(LiFe_2O_4+(1-x)\Delta H_{dis}^{973}LiAl_2O_4)] - \Delta H_{dis}^{973}Li_{0,5}Fe_{2,5-x}Al_xO_4$$

where x and 1-x are the mole fractions of components.

Availability of calorimetrically stated high-temperature functions $\Delta H = f(T)$, $C_p = f(T)$ and phase transformation enthalpy of each individual members of system $Li_{0,5}Fe_{2,5-x}Al_xO_4$ (0; 0,5; 1,0; 1,5; 2,0; 2,5) [8-9], allows us to calculate the standard mixing enthalpy - $\Delta H_{mix}^{ex\ 298}$

Calculated results are given on the Table 2 and Fig.3. The average value ΔH_{mix}^{973} have been estimated by means of statistical method of "errors accumulation". On the Table 2 and the Fig.3 curves (1) and (2) the concentration dependences of $\Delta H_{mix}^{ex\ 973}$ and $\Delta H_{mix}^{ex\ 298}$ respectively, are presented.

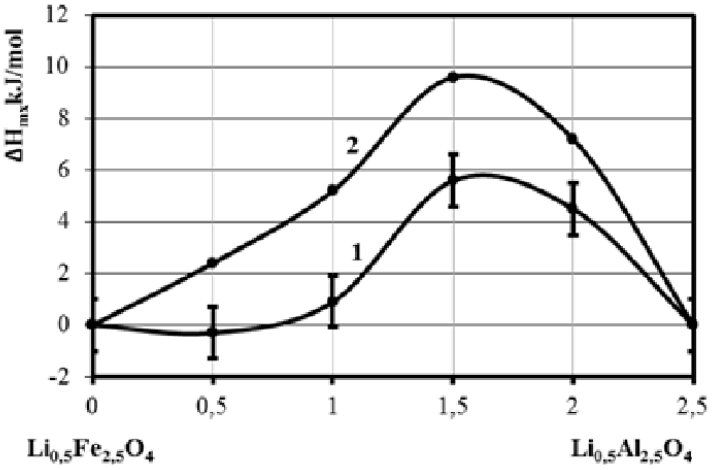

Fig.3 The excess enthalpy of mixing ΔH_{mix}^{ex973} (1) and ΔH_{mix}^{ex298} (2) of solid solution $Li_{0,5}Fe_{2,5-x}Al_xO_4$

Table 2. Mixing enthalpies - ΔH_{mix}^{ex298} and ΔH_{mix}^{ex973} of solid solution $Li_{0,5}Fe_{2,5-x}Al_xO_4$

Number	X	ΔH_{mix}^{ex973} kJ/mol	ΔH_{mix}^{ex298}kJ/mol
1	0,5	-0.37 ± 1,27	2.43
2	1,0	1.00 ± 1,14	4.60
3	1,5	5.92 ± 1,09	9.82
4	2,0	4.39 ± 1,33	6.59

Four systems [1-3] investigated earlier are characterized by negative ΔH_{mix}^{ex298}. Differently from this case they all contain sp^3 hybridized Zn^{2+} ion, which creates covalent bonds in spinel's structure using d-orbital of d^2sp^3 hybridized Ni, Fe and Co ions. The energy of these bonds is changed in dependence with concentration. This provides the negative signs of $\Delta H_{mix}^{ex\ 298}$ and according to "Isomorphic Theory of Solid Solubility" [7] leads to unlimited solubility of components.

That's why $ZnFe_2O_4$ often is used as a universal solvent in technology of ferrites.

As it is concerns to our case, both initial components of $Li_{0,5}Fe_{2,5-x}Al_xO_4$ solid solution are characterized by super-structural order [1:3] of Li^+/Fe^{3+} and Li^+/Al^{3+} ions in octahedral sub-lattices of spinel. During the process of mutual dissolution of lithium ferrite and lithium aluminate this order is destroyed. Solid solubility breaks and two-phase mixture should be appeared. To take into account the positive sign of only one fundamental energetic factor - ΔH_{mix}^{ex298}, which notes on impossibility of mutual solubility of initial components across the entire length of concentration, we can't identify the real process of mixing in the given system. Together with ΔH_{mix}^{ex298} it is necessary to know also entropy and free energy of mixing $\Delta S_{mix}^{ex\ 298}$ and as a result $\Delta G_{mix}^{ex\ 298}$

The excess entropy of mixing $\Delta S_{mix}^{ex\ 298}$ is the second fundamental parameter which is necessary to determine free energy of mixing $\Delta G_{mix}^{ex\ 298}$.

Since the mixing entropy ΔS_{mix}^{298} is the difference between entropy S of the given composition and the sum of entropies of initial pure components in corresponding mole ratio, for calculation of ΔS_{mix} the following expression should be used:

$$\Delta S_{mix} = S_{(solid\ sol)} - (S_x + S_{x-1}),\ \text{where}$$

$S_{(solid\ sol)}$, S_x and S_{x-1} are calculated by semi - empirical method D. Zagareishvili [10]:

$$S_{298}^{at} = 2{,}3\ \hat{C}_{p298}^{at} / (7{,}25 - 2{,}3\ \hat{C}_{p298}^{at})^{1/3},\ \text{where}$$

$$\hat{C}_{p298}^{at} = (C_{p298}^{at})^2 / [C_{p298}^{at} + 298\ (\partial C_p/\partial T)_{298}^{at}]$$

This method is based on the known and experimentally proved postulate that standard entropy can not be characterized universally and certainly only by means of heat capacity $C_{p298.}$

As a rule, in reality, to the same values of two or more substances's standard heat capacity C_{p298} corresponds the different values of S_{298}. It significantly depends on the rate of change of function $C_p=f(T)$ near the standard temperature, i.e. on the derivative $(\partial C_p/\partial T)_{298}$ of $C_p=f(T)$ at T= 298 (Table 3, Fig.4)

Table 3. Calculation of ΔS_{mix}, for solid solutions $Li_{0,5}Fe_{2,5-x}Al_xO_4$ [10]

Composition X	C_{p298}	$(\partial Cp/\partial T)^{at}_{298}$	$\hat{C}_{p298}$	S	ΔS_{mix}J/molK
0,5	17.37	0,0085	15.16	155	14
1.0	18.54	0,010	15.97	171	17
1,5	19.49	0,009	17.07	187	22
2,0	20.0	0,0054	18.51	210	33
00	15.8	0,0117	12.97	129	
2,5	21.8	0,0198	17.15	189	

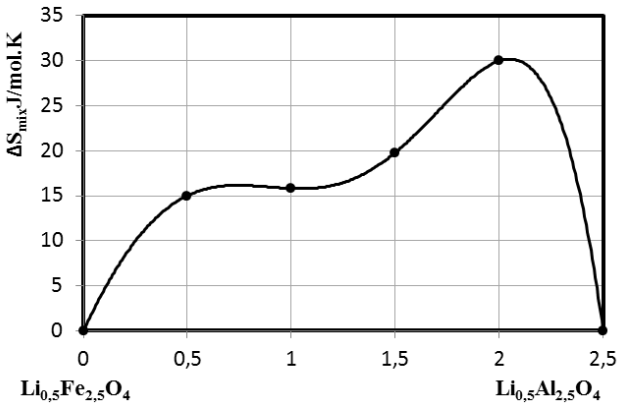

Fig. 4. The excess entropy of mixing ΔS_{mix}^{298} J/molK of solid solution $Li_{0,5}Fe_{2,5-x}Al_xO_4$ in dependence with concentration

The used semi-empirical calculation method of entropy ΔS_{mix}^{ex} has its advantage above other known calculation methods. First of all, it is based on experimental information about the nature of individual characteristic curvature of function $C_p = f(T)$ of investigated substance near standard temperature:

1. Systematic error of this method extinguished in difference type of expression

$$\Delta S_{mix} = S_{(soli\ sol)} - (S_x + S_{x-1})$$

2. The configuration disorder actually is frozen in function $C_p = f(T)$ measured at very low temperature, and as a result it contains much less information about redistribution of ions inside of spinel's structure in comparison with $C_p=f(T)$ measured near the room and ambient temperature.

3. The using of the method is justified also, because all needed experimental information: (Cp^{at}_{298} , $(\partial Cp/\partial T)^{at}_{298}$, ΔH_{mix}^{298}) are taken on the samples with the same prehistory. This fact is extremely important for such complex spinels with nonequivalent positions in the structural sublattices, as the solid solutions under investigation. In the Table 3 experimental and calculated data of determined ΔS_{mix}^{ex} J/molK are presented.

It is known that entropy of mixing is always positive. Even for ideal mixing of two simplest component configuration entropy $\Delta \mathbf{S_{conf}}$ is 1,38 entropy unit**.** For such complex system as $Li_{0,5}Fe_{2,5-x}Al_xO_4$ ΔS_{mix}^{ex} J/molK should be significantly bigger. As it is seen from the Table 3 and Fig. 4, it reaches about 30J/molK, and naturally it can gain the energy for creation and stabilization of solid solution.

The main advantage of this approach is: it excludes the need in special laborious low temperature calorimetric investigation of $C_p=f(T)$ for calculation ΔS_{mix}^{298}.

The analysis of obtained data on the light of second thermodynamics law, shows that in the area near to composition $Li_{0,5}Fe_{1,5}AlO_4$ the entropy of mixing ΔS_{mix}^{298} can not compensate the destructive influence of positive sign of ΔH_{mix}^{298} and in this region solid solubility is excluded.

It should be emphasized that needed information about $C_p=f(T)$ near ambient temperature and $C_{p298are}$ have been taken from [9], where the investigation were carried on the samples prepared absolutely identically as the samples used in present dissolving experiment.

Free energy of mixing $\Delta \mathbf{G_{mix}^{298}}$ according to the second law of thermodynamics includes two therms: ΔH_{mix} and $-T\Delta S_{mix}$.

Necessary experimental and calculated data are presented in Table 4 and Fig.5.

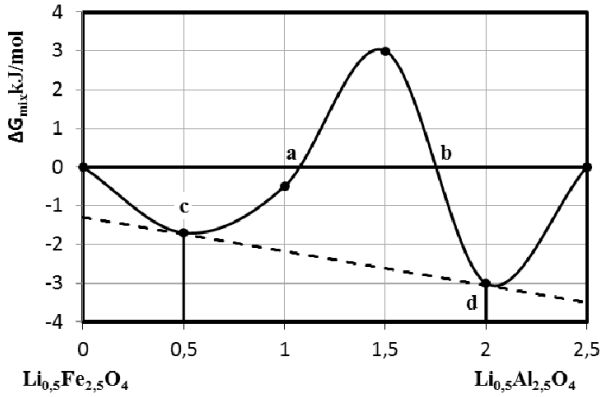

Fig. 5. Concentration dependence of the excess energy of mixing ΔG_{mix}^{298} of solid solution $L_{0,5}Fe_{2-x}Al_xO_4$

Table 4. Free energy of mixing ΔG_{mix}^{ex} kJ/mol of solid solution $Li_{0,5}Fe_{2,5-x}Al_xO_4$

Number	Composition x	ΔH_{mix} kJ/mol	$T\Delta S$ kJ/mol	$\Delta G_{mix} = \Delta H - T\Delta S$ kJ/mol
1	0,5	2.4	4.2	1.8
2	1,0	4.6	5.1	0.5
3	1,5	9.8	6.6	- 3.2
4	2,0	6.6	9.8	3.2

As it is seen from Fig.5 the free energy of mixing ΔG_{mix}^{ex298} changes its negative sign into positive in the region of concentration a - b ; [1,1<x<1,55; (22% – 63,5%)]. It means that here the solubility **is** completely excluded and composition (x =1,5) falls in two-phase area.

The common tangent's two projection (c and d) on the abscissa axes relates practically to x= 0,5 and x=2,0, actually to maximums of negative values of ΔG_{mix}^{ex298} .

According to Fig.5 we can judge about the character of change of free energy dependently on the structural peculiarity of system under investigation, also we can fix correctly the beginning and the end of the area of formation of two immiscible phases.In the work [4] enthalpies of order-disorder transformation have been studied and proved that for all compositions (except x=1,5 which is homogeneous only in disorder state) enthalpy of transformation reduces from the boundary components and became almost zero at the equimolar composition. The initial component $Fe^{3+}[Li_{0,5}Fe_{1,5}]O_4$ is characterized by super-structural ordering [1:3] inside octahedral sub-lattice of spinel, which begins to be destroyed as the ions Al^{3+} enter the structure at mixing process.

From the Fig.5 it is seen also that negative value of ΔG_{mix}^{ex298} from composition x=0,5 begins to decrease. That reflects the difficulties of dissolution tied with the process of violation of the super-structural order in both initial spinels which is accompanied by competition for octahedral positions of ions with equal preference energy to octahedral sublattice in oxygen surrounding, until the rivaling ions size factor prevails.

At x=1,1 the excess free energy of mixing ΔG_{mix}^{ex298} changes its sign into positive and keeps it until x=1,55 (ab segment on Fig.5. Then with recovering of super-structural [1:3] order in octahedral sub-lattice characterized for pure lithium aluminate, ΔG_{mix}^{ex298} of solid solution gains its negative sign and the solid solution is stabilized.

The results of investigation allow us to calculate ΔG_{mix}^{ex} in a wide temperature interval. Results are given in Table 5. So, on the basis of these data the state phase diagram of investigated solid solution is built Fig.6.

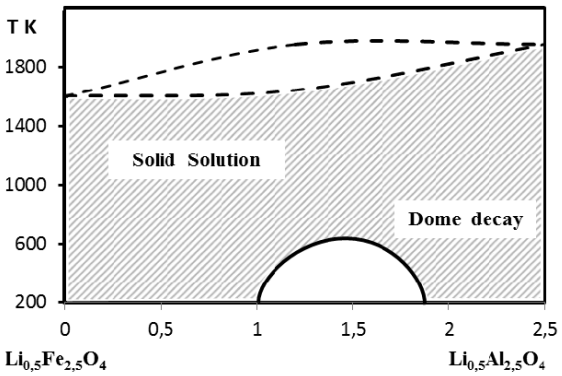

Fig. 6. The phase diagram of state of solid solution $Li_{0,5}Fe_{2,5-x}Al_xO_4$

Table 5. The temperature dependence ΔG_{mix} of solid solution $Li_{0,5}Fe_{2,5-x}Al_xO_4$

T, K \ X	0,5	1,0	1,5	2,0
298	-1.8	-0.5	3.2	-3.2
300	-1.8	-0.5	3.2	-3.3
400	-3.2	-2.2	1.0	-6.6
500	-4.6	-3.9	-1.2	-9.9
600	-5.9	-5.6	-3.4	-13.2
700	-7.4	-7.3	-5.6	-16.5
800	-8.7	-9.0	-7.8	-19.8
900	-10.2	-10.7	-9.9	-23.1
1000	-11.6	-12.4	-12.2	-26.4
1100	-12.9	-14.1	-14.4	-29.7
1200	-14.4	-15.8	-16.6	-33.0
1300	-15.8	-17.5	-18.8	-36.3
1400	-17.9	-19.2	-20.9	-39.6

From the phase diagram of state it is seen that the top of the "cupola of decomposition" of the solid solution is about 500K. This is the temperature above which the process of structural disordering inside the structure of composition $Li_{0.5}FeAl_{1.5}O_4$ begins and the one-phased solid solution can be received.

ლიტერატურა - REFERENCES – ЛИТЕРАТУРА

1. Лежава Н.Г., Дзагнидзе Н.Ш., Чачанидзе Г.Д., Термиинамические параметры смешения твердого Раствора $Ni_{1-x}Zn_xFe_2O_4$ // Изв. АН СССР Неорганические материалы – 1987.- т.23, N9.- с 1591 (Translated in English)
2. Лежава Н.Г., Дзагнидзе Н.Ш., Чачанидзе Г.Д., Калориметрическое определение термодинамических параметров смешения Т.Раствора $Li_{0.5-0.5x}Zn_xFe_{2.5-0.5x}O_4$ // Изв. АН СССР Неорганические материалы – 1989.- т.25, N4.- с. 656-658 (Translated in English)
3. Лежава Н.Г., Дзагнидзе Н.Ш., Димитриади В. Л., Чачанидзе Г.Д., Энергия смешения твердых растворов $Ni\ Fe_{2-x}\ Al_xO_4$ // Изв. АН СССР Неорганические материалы – 1992.- т.5, N4.- с. 1031-1033 (Translated in English)
4. Kato E. Phase transition of Lithium ferrospinel, Lithium ferroalumospinel solid solutions// Bull. Chem. Soc. Japan – 1959 – v. 32, N1. p.51
5. Jokokawa J., Kleppa O.J., A calorimetric study of the transformation of some Metastable modifications of Alumina to - Alumina // J.Phys.Chem. – 1964. –v.68, N11.-p.3246
6. Navrotsky A.,Kleppa O.I Thermodynamics of formation of simple spinels // J.Inorganic and nuclear chemistry.- 1968 – v.30, N3, p.479-498
7. Yrusov V.S The theory of isomorphic mixing // .M.: 'Nauka'. Publishing AS USSR – 1977. –p.13
8. Н.А.Ландия,Г.Д.Чачанидзе.,Н.Г.Лежава,В.С.Варазашвили,М.Г.Хундадзе. Калориметрическое исследование ΔH и ΔG разупорядочения $Li_{0,5}Fe_{2,5}Al_{0,5}O_4$ и $Li_{0,5}Fe_{1,5}AlO_4$ и влияние термической обработки на величину указанных параметров// Сообщение АН ГССР – 1980. т.98.№2.-353с. .
9. Хундадзе М.Г., Лежава Н.Г., Чачанидзе Г.Д., Ландия Н.А. Исследование термодинамических свойств $Li_{0,5}Fe_{2,5-x}Al_xO_4$ на адиабатическом калориметре смешения и ДСК калориметре //VIII Всесоюзная конференция по калориметрии и химической термодинамике. Иваново. – 1979. -403
10. Zagareishvili D.Sh. The calculation methods of thermal and elastic properties of crystal inorganic substances // T.: 'Meznіereba' Published 1970,- p.190.

უწყვეტი მყარი ხსნადობის პირობის განსაზღვრა $Li_{0,5}Fe_{2,5-x}Al_xO_4$ სისტემაში შერევის ჭარბი პარამეტრების ΔH_{mix}^{ex} და ΔS_{mix}^{ex} კალორიმეტრული კვლევის გზით

ნ.გ.ლეჟავა, მ.გ.ხუნდაძე, ვ.ს.ვარაზაშვილი, თ.ე.მაჩალაძე, თ.ა.ფავლენიშვილი. მ.ს.ცარახოვი

ივანე ჯავახიშვილის სახელობის თბილისის სახელმწიფო უნივერსიტეტის რ.აგლაძის არაორგანული ქიმიისა და ელექტროქიმიის ინსტიტუტი, 0186, მინდელის ქ.11, თბილისი, საქართველო

რეზიუმე

$Li_{0,5}Fe_{2,5-x}Al_xO_4$ მყარი ხსნარის მაგალითზე ნაჩვენებია მეთოდის სანდოობა. ხსნადობის წყვეტის საზღვრები თანხვდება ლიტერატურულ მონაცემებს. გარდა ამისა დაფიქსირდა მყარი ხსნარის „დაშლის თაღის" წვერო - ტემპერატურა 550K, რომლის ზემოთ იწყება საკვლევი მყარი ხსნარისთვის დამახასიათებელი „წესრიგი-უწესრიგობის" გარდაქმნა, ეს კი იძლევა საშუალებას სპეციალური თერმული დამუშავებით ვაკონტროლოთ მყარი ხსნარის ნებისმიერი კომპოზიციის ერთფაზიანობა. ამ მეთოდის გამოყენებით ჩვენ შეგვიძლია თვალი ვადევნოთ ნებისმიერი სისტემის შერევის მექანიზმს და უზრუნველვყოთ ნარევის ნაცვლად ერთფაზიანი კომპოზიციის მიღება.

ОПРЕДЕЛЕНИЕ УСЛОВИЯ НЕПРЕРЫВНОЙ ТВЕРДОЙ РАСТВОРИМОСТИ СИСТЕМЫ $Li_{0,5}Fe_{2,5-x}Al_xO_4$ ПУТЕМ КАЛОРИМЕТРИЧЕСКОГО ИССЛЕДОВАНИЯ ИЗБЫТОЧНЫХ ПАРАМЕТРОВ СМЕШЕНИЯ ΔH_{mix}^{ex} И ΔS_{mix}^{ex}

Н.Г.Лежава, М.Г.Хундадзе, В.С.Варазашвили, Т.Е.Мачаладзе, Т.А.Павленишвили, М.С.Царахов

Институт неорганической химии и электрохимии им. Р.И.Агладзе Тбилисского государственного университета им. И.Джавахишвили, 0186, ул. Миндели11, Тбилиси, Грузия

РЕЗЮМЕ

На примере твердого раствора $Li_{0,5}Fe_{2,5-x}Al_xO_4$ была доказана надежность метода. Границы разрыва растворимости совпадают с литературными данными. Кроме того, зафиксирована вершина *арки распада* твердого раствора – температура 550K, выше которой начинается характерное для исследуемого твердого раствора превращение *порядок-беспорядок*, что дает возможность с помощью специальной термической обработки контролировать процесс изготовления однофазной композиции твердого раствора. С помощью метода мы можем наблюдать механизм процесса смешения любой системы и предотвратить получение смеси вместо однофазной композиции.

OZONE IN AGRICULTURE

Rimzet Tushurashvili, Merab Panchvidze, Tsiuri Basiladze, Genrieta Shanidze, Manana Mamardashvili, Nino Kvirkvelia, Givi Khidesheli, Vazha Matsaberidze

R.Agladze Institute of Inorganic Chemistry and Electrochemistry of Ivane Javakhishvili Tbilisi State University, 0186, Mindeli st.11, Tbilisi, Georgia, ninokvirkve@gmail.com

The influence of ozone on certain agricultural crops, in particular on cucumber and tomato seeds, has been studied for the purpose of acceleratingtheir germinationand achieving an increase in yields. Prospects for ozone treatment of seeds using ozonisedwater and ozone-air mixture have been established. Besides, the influence of ozone-air mixtureon extension of storage life of tangerines has been studied and it has been established that daily treatment of tangerines with ozone-air mixture during their storage can extendtheir storage life to three months.

Very powerful and strong oxidation capability of ozonehas lately made it an element widely used in chemical, pharmaceutical and lightindustries as well as in medicine and agriculture – for the purposes ofproduct storage and product disinfectionduring storage. Various chemical agents are widely used to make seeds free from internal and external phytopathogenous micro flora before their sowing, to activate their natural processes and to protect plants during the process of their vegetation. However the positive effects of chemical agents have some negative impacts as well: environmental pollution caused by toxic chemicals and their accumulation in the soil and subsequently in the plants and their products.

Especially noteworthy is the fact that development of technologies that are based on using ozone is largely owed toozone being environmentally friendly. Unlike other oxidants, reactions cause ozone to decompose into oxygen molecules and oxygen atoms. All these products are known as the agents neither participating in pollution nor producing the carcinogenic substances that are produced in the process of oxidation by chlorine or fluoride. Ozone only remains in the air for several minutes and in water - for 1.5-2 hours. [1,2]

The purpose of the research was to study the influence of ozone on certain agricultural crops, in particular on cucumber and tomato seeds, for the purpose of accelerating their germination and achieving an increase in yields.

Ozone-air mixture flow was being produced using a 220 Watt Ozonator. The concentration of ozone in ozone-air mixture flow was 0.6 g/L, and in ozonised water - 3mg/L. The rate of ozone-air mixture flow was 2.4g/hour.

The influence of ozonized water and ozone-air mixture flow on cucumber and tomato seeds was studied for the purpose of evaluating the quality of their germination.In both cases the seeds were previously soaked in water for two hours. Ozonized waterwas produced by barbotaging ozone-air mixture flow into water until saturation. The treated seeds were put into Petri dishes on appropriate soil. 50 seeds were put into each Petri dish. After a week the quality ofgermination was evaluated.

The results showed that the quality of germination of the seeds treated with ozonized water, ozone-air mixture flow and potable water for potato seeds was 96%, 80% and 80%, respectively; and for cucumber seeds - 96%, 90% and 74%, respectively.

The colour of the leaves of the plant samples germinated from the seeds treated with ozonized water was darker green than that of the plant samples germinated from the seeds treated with ozone-air mixture flow and potable water.

After a week the seedlings were replanted from Petri dishes into the boxes full of soil. The seedlings were systematically watered with ozonized water and observed during the next four weeks. After the four weeks the damaged leaves on each plant sample were counted. In the case of cucumber samples treated with ozonized water andpotable water, the number of damaged leaves was approximately the same (9% and 10%, respectively), whereas in the case of potato samples the number of damaged leaves was - 12% and 24%, respectively.

Four weeks after being sown the heights of the seedlings as well as their leaf areaswere measured. The findings showed that heights and the leaf areas of the seedlings treated with ozonized water and ozone-air mixture flow exceeded those of the seedlings treated with potable water, namely,the heights of the cucumber seedlingswere 37 cm, 33 cm and 30 cm, respectively, and the leaf areas - 64 cm^2, 33 cm^2 and 28 cm^2, respectively (picture 1).

Many countries throughout the world face the problem of and are in search of the ways for extension of storage lifefor food products, in particular, for perishable fruit and vegetables. Ozone is a particularly effective disinfectant which fights molds, bacteria, viruses, toxins and other contaminators in air and in water and helps to remove them from surfaces. [3,4]

Georgia faces the similar problem of treatment and extension of storage life for citrus fruit, especially for tangerines. The harvest season in Georgia lasts for 1-1.5 months.

The longest storage life for citrus fruit is achieved by wrapping each fruit separately in a wrapping paper impregnated with diphenyl. Diphenyl is a petroleum product, which is considered to be a substance of mild toxicity,protecting the fruit from fungal infection. It is prohibited in the European Union and the United States as a carcinogen known to cause cancer.In some countries paraffin is added to diphenyl, i.e. boxes are impregnated with the mixture. Sometimes synthetic antiseptics are used and fungicides are applied to citrus peel. The above mentioned methods can substantially extend the storage time of citrus fruit.

Currently,new, environmentally friendly technologies are being introduced. The use of ozone is considered to be among one of the most important and effective methods.

It has been estimated that ozone does not have harmful effect on food products and does not cause a change in their nutritional value. In addition, the products maintain their delicate flavours.This is caused by the fact that ozone,as antiseptic, affects only the exterior surface of the product, and then it quickly decomposes to safe oxygen. [5]

In our case two lab-made ozonators of different capacities and product sterilization chambers were used to extend the storage life for tangerines.

In the experiment certain number of tangerines (ten) was placed in a sterilization chamber (№1), and ozone-air mixture was injected into the chamber. The time of exposure varied from 20 minutes to 60 minutes. During the exposure that lasted for 20-30 minutes the ozone-air mixture flow rate provided by the ozonator was 1gr/hour, whereas during the exposure that lasted for 60 minutesthe ozone-air mixture flow rate provided by the ozonator was 2-2.5 gr/hour. Simultaneously, the same number of tangerines (ten) was placed into a control chamber (№2).

At the first stage of the experiment, the tangerines were treated with ozone-air mixture flow for ten days (every other day, treated for 20 minutesper day). During this period the product loss in the chamber №1 was 2 out of 10 tangerines (20%), whereas in the control chamber №2 the product loss was 1 out of ten (10%). The findings indicated that it was necessary to prolong the time of exposure to ozone.

At the second stage of the experiment, after being treated with ozone-air mixture flow for 30 minutes per day (every other day, for the duration of ten days), the product loss in both chamberswas one tangerine out of ten. The results were the same in the case of 60 minutes per day treatment. The results revealed that increase in the amount of ozone has positive effects on the storage process. In view of the findings, anewdoubled capacity ozonatorwas developed in the laboratory.

At the third stage of the experiment, application of ozone-air mixture flow for 60 minutes per day using the new ozonator duration 10 days changed the picture: product loss in the chamber №1 was one tangerine, whereas in the control chamber (№2) product loss was 4 tangerines.

At the fourth stage of the experiment, application of ozone-air mixture flow for 60 minutes per day during 32 days resulted in no product loss in the chamber №1 and subsequently 40% of the

tangerines treated with ozone-air mixture flow maintained their initial quality, whereas all the tangerines in the chamber №2 were damaged (picture 2).

At the fourth stage of the experiment, the process of ozonation was ceased and the observation continued for the next 19 days. The tangerines, which were not damaged by the time the process of ozonation was ceased, maintained their initial quality for the next 3 weeks.

Thus, as a result of the experiment, it was found that daily treatment of tangerines with ozone-air mixture flow for 60 minutes per day can extend their storage life to three months, and after ceasingthe process of ozonation,the product maintains its quality for 3 weeks.

ლიტერატურა - REFERENCES – ЛИТЕРАТУРА

1. Кочеткова А.Р. «Технология консервирования тропических и субтропических фруктов и овощей», Киев-Одеса, «Высшая школа», 1989, с.352
2. Журнал «Овощи и фрукты», Киев, декабрь, 2014, с.57-60
3. Каснянчу В.Д.,Анистасенко В.А. «Безотходная технология переработки плодово-ягодного сырья», «Пищевая промышленность», 1978,№2, с.44-45
4. ხათუნაჭანუყვამე,“ლიმონის პერსპექტიულ-სამრეწველო ჯიშების ნაყოფების ქიმიური და ტექნოლოგიური თავისებურებანი’’, დისერტაცია, ქუთაისი, 2006, გვ. 71.
5. Гулакина Т.В., Коваленко Т.В., Бурова Т.Е. «Влияние периодического действия озона на некоторые компоненты химического состава картофеля/Совершенствование методов холодильного консервирования пищевих продуктов», ЛТИХП, 1983, с.36-41

ოზონის გამოყენება სოფლის მეურნეობაში

რიმზეტ თუშურაშვილი, მერაბ ფანჩვიძე, ციური ბასილაძე, გენრიეტა შანიძე,
მანანა მამარდაშვილი, ნინო კვირკველია, გივი ხიდეშელი, ვაჟა მაცაბერიძე
ივანე ჯავახიშვილის სახელობის თბილისის სახელმწიფო უნივერსიტეტი
რაფიელ აგლაძის არაორგანული ქიმიისა და ელექტროქიმიის ინსტიტუტი
თბილისი, საქართველო, ninokvirkve@gmail.com

რეზიუმე

შესწავლილია ოზონის გავლენა ზოგიერთი სასოფლო-სამეურნეო კულტურის, კერძოდ, კიტრისა და პომიდვრის თესლებზე, მათი აღმოცენების ინტენსიფიცირებისა და მოსავლიანობის ზრდის მიზნით. დადგენილია ოზონის გამოყენების პერსპექტიულობა თესლების ოზონიანი წყლითა და ოზონ-ჰაერის ნაკადით დამუშავებისას. ასევე, შესწავლილია ოზონ-ჰაერის ნარევის გავლენა მანდარინის შენახვის ვადის გახანგრძლივებაზე. დადგენილია, რომ ოზონ-ჰაერის ნარევით მანდარინის ყოველდღიური დამუშავებისას, შენახვის ვადა შეიძლება გახანგრძლივდეს 3 თვემდე.

ПРИМЕНЕНИЕ ОЗОНА В СЕЛЬСКОМ ХОЗЯЙСТВЕ

Р.Г.Тушурашвили, М.В.Панчвидзе, Ц.М.Басиладзе, Г.В.Шанидзе, М.И.Мамардашвили,
Н.М.Квирквелия, Г.И.Хидешели, В.Г.Мацаберидзе
Тбилисский Государственный Университет им. Ив. Джавахишвили
Институт неорганической химии и электрохимии им. Р.И. Агладзе
Тбилиси,Грузия, ninokvirkve@gmail.com

РЕЗЮМЕ

Изучено влияние озона на семена некоторых сельскохозяйственных культур (помидоров и огурцов) с целью интенсификации их прорастания иповышения урожайности. Также изучено влияние потока озонно-воздушной смеси на мандарины с целью увеличения срока их хранения.

Показано, что обработка семьян этих культур озонированной водой и озонно-воздушной смесью интенсифицирует их всхожесть, что выражается как в большей площади листьев растений, так и в большей высоте. Также установлено, что ежедневной обработкой мандаринов потоком озонно-воздушной смеси можно добиться увеличения срока их хранения до трех месяцев.

PRODUCTION OF POTASSIUM PERMANGANATE IN THE FLOW ELECTROLYZER

V.Kveselava
R.Agladze Institute of Inorganic Chemistry and Electrochemistry of Ivane Javakhishvili Tbilisi State University, 0186, Mindeli st.11, Tbilisi, Georgia

The paper presents the electrochemical process of oxidation of potassium manganate into permanganate ($KMnO_4$) in a flow reactor of tubular (hollow) shape. The internal surface of the stainless steel tube serves as an anode and a current-carrying wire, which is coaxially fixed inside of the tubeserves as a cathode. At high current densities to decrease cathode reduction obtained at the anode $KMnO_4$, the ratio of the cathode and anode surfaces should be 1:100. Therefore, the surface of the coaxially disposed wire was covered with an insulating material at some equal intervals. The current efficiency of the final product in the presented reactor was more than 80%.

Potassium permanganate is a universal oxidizing agent. Today it is industrially obtained by a combined semi-electrochemical two-step method: 1) production of potassium manganate from manganese ore; 2) electrochemical oxidation of manganate to potassium permanganate.

Production of potassium permanganate is realized in Germany (Bitterfeld), Czech Republic, USA, China and Russia (Saki).

The article gives an overview of the electrochemical oxidation of potassium manganate into permanganate in different design electrolyzers.

In Germany they use red- and green-alkaline variations of potassium permanganate manufacturing. In both methods, the production of potassium manganate and the oxidation of manganate into potassium permanganate proceed identically except the decomposition of starting manganese ore: in red-alkaline method the ore is processed by pure alkali, whereas in the green-alkaline - by 50% circulating KOH solution [1].

The red-alkaline method envisage the supply of unfiltered manganat melt (210 g/L K_2MnO_4 and 160 g/L KOH) and 1-2N KOH solution into an iron cylindrical electrolyzer with the capacity of 4 m^3. Between the nickel, nickel-copper alloy or nickel-plated steel sheet of anodes the iron cathode rods are placed. Electrolysis is carried out up to a conversion of 85-90% manganate into potassium permanganate. The cell is operating at of 5 kA and 2.2-2.5 V; at the anodic current density - 0.07 kA/m^2 and the cathodic current density - 0.7 kA/m^2. After electrolysis, the pulp is directed to carbonation. The rest of the K_2MnO_4 isdisproportionate to $KMnO_4$ and MnO_2. Raw permanganate is obtained after cooling and decantation of the pulp. It is further subjected to crystallization. The mother solution containing 750 g/L of K_2CO_3 was evaporated, cooled and filtered, and then the deposit of raw permanganate is sent to the crystallizer. The obtained $KMnO_4$ is centrifuged, dried, and is issued as a commodity product. $KMnO_4$ current efficiency is 60%. Remaining in the filtrate $KMnO_4$ (~1 g/L) is reduced by calcium formate to $MnO_2$and after re-filtration together with other impurities is separated as slime. Potassium in the filtrate is supplied to the consumer as a concentrated solution (750 g/L). This method gives about 1100 kg K_2CO_3 for every 1000 kg of $KMnO_4$.

In order to reduce the consumption of potash in Bitterfeld the green-alkaline method of producing $KMnO_4$ is used in parallel. The pulp obtained from the electrolysis is cooled and filtered to obtain raw permanganate crystals and green filtrate, which contains KOH, K_2CO_3, K_2MnO_4, silicates and aluminates. To remove silicates and aluminates the solution is passed through a heat exchanger and is treated with lime (CaO). The suspension is filtered; the filtrate is evaporated in two steps. At the first step the alkali concentration is adjusted to 600 g/L. A mixture of permanganate and potassium permanganate crystals returns to the electrolysis process. At the second step of evaporation the alkali concentration reaches 750 g/L. Potash formed on the expense of CO_2 air, is filtered and the filtrate containing 50% KOH is directed to the oxidation of the ore. The obtained potash crystals are dissolved in water.The solution is decolorized by calcium formate and is filtered. With the use of this option 200 kg of K_2CO_3 falls for every 1000 kg of $KMnO_4$.

In Czech Republic the electrolyzer for the production of $KMnO_4$ is a rectangular iron box (0.5 m^3) with six anodes and cathodes separated by the asbestos diaphragm.The electrolyte (90 g/L K_2MnO_4, 90 g/L KOH, 30 g/L K_2CO_3) is constantly supplied to the electrolyzer. After the pulp is cooled and centrifuged the

crystals containing 70% $KMnO_4$ are crystallized. Fugate is evaporated to a density of 1.2 g/ml and is cooled. The separated crystals of $KMnO_4$ are centrifuged.Heated to 60^0C manganatefugate flows into the second electrolytic cell. The pulp obtained after the electrolysis is cooled and is centrifuged. The $KMnO_4$ obtained at this stage makes 21% of the total product. 50% of the fugate is used to make the initial electrolyte and 50% - is evaporated to separate potassium permanganate which is 3% of the total product. The residual filtrate is evaporated to obtain a 50% KOH solution which contains an excess of K_2CO_3. The solution is treated with CaO and further centrifuged. Fugate used for the preparation of the initial electrolyte. Part KOH solution is used for decomposition of the ore and the other part is bleached [2].

In the town of Saki, to obtain $KMnO_4$the rectangular electrolytic cells are used with stainless steel anodes and cathodes arranged in parallel at a distance of 15 mm from each other. In the process of electrolysis gases are emitted through the fitting on the top of the bath. The electrolyte is fed from the bottom up with axially pump providing mixing of electrolyte and collection of the crystallized potassium permanganate in the so-called "pockets". Current load is 5-10 kA; cell voltage - 2.5-3.2 V; anodic current density - 0.08-0.09 kA/m^2, the ratio of the anodic and cathodic current densities - 1:10; $KMnO_4$ current efficiency - 80% [3].

In the USA (the company «Carus Chemical») there is a flow electrolizer for the production of $KMnO_4$ which consists of many individual bipolar cells. The base of the bipolar electrode consists of a steel sheet to one side of which a Monel wire working as anode is welded. The anode current density is 50-90 kA/m^2. The other side of the steel sheet presents perpendicularly welded steel pins that work as a cathode. The area between the pins is covered with an insulating material. Ratio of the anodic and cathodic current densities is 1:120-150. Moving of electrolyte and gases between the electrodes is provided by directing partitions. Electrolyte flows from one cell to another through the hole which is located between two adjacent cells. The electrolyzer consists of three series of 20 cells in each.The electrolyte with initial concentration of 120 g/L KOH, 53 g/L K_2MnO_4 and 30 g/L $KMnO_4$ is simultaneously supplied to all three series. The solution moves upwards. After passing of 20 cells the electrolyte with concentration of 128 g/L KOH, 24 g/L K_2MnO_4 and 53 g/L $KMnO_4$ flows out of each series and is sent to a separator as one stream. The cells are connected coherently, the voltage of each cell - 2.5-2.8 V, current - 1.2 A. After crystallization and centrifugation the mother solution is returned to various process steps, the potassium permanganate crystals are dried and packaged. Despite many advantages the described electrolyzer has a very complex structure [4].

For the organization of high-performance electrochemical processes the correct selection of the electrolyzer structure is considered to be one of the most important factors. This can be explained by the fact that for the production of the same product - potassium permanganate - electrolyzers of different designs are used.

The aim of the present work is to provide a simple and user-friendly design of the high performance electrolyzer for the production of potassium permanganate its testing on the laboratory scale.

Potassium manganate, used in our experiments, was provided by the laboratory of chemical processing of local resources and raw minerals. Potassium manganate consisted of 87.8% of K_2MnO_4, 9.4% of K_2CO_3, 0.16% of MnO_2. For electrosynthesis of potassium permanganate the potassium manganate was dissolved in a solution of potassium hydroxide.

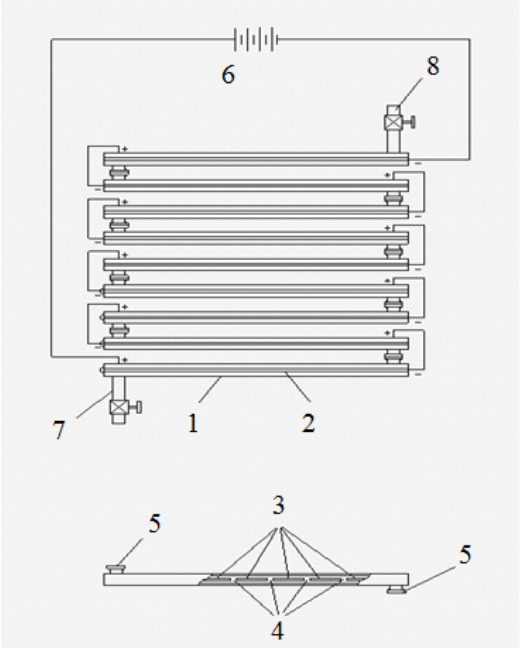

Figure. Flow electrolyzer for production of potassium permanganate

The electrolyzer consisted of tubular cells with circular cross section, the inner surface of which served as anodes (1). Conductive wires were coaxially mounted in the stainless steel tubular cells (2), their surface was coated at regular intervals with a dielectric material (3); the uncovered parts of the wire were the cathode (4). Thus, a ratio of the anodic and the cathodic current densities was as 1: 100, which minimizes the share of cathodic reduction of permanganate-manganate ions.

The cells are interconnected by tubes (5) made of insulating material (these tubes are attached to the beginning and to the end of each cell). Cells in the electrochemical network are connected in parallel.

The principle of the operation of electrolyzer is: electrolyte is supplied through the tube (7) to the bottom of the electrolytic cell by a centrifugal pump. Redox reactions accompanied by release of gases occur at the anode and the cathode. The electrolyte and gases move in parallel and are pumped through the connecting tube (5) in the subsequent cell, and finally in the last upper cell and through the outlet tube (8) into the separator, then enters the crystallizer and on the centrifuge to obtain the final product.

A single unit cell of the described electrolyzer was constructed for the production of potassium permanganate, the length - 4.26 m; diameter of the inner surface of the tube (anode) - 0.024 m; diameter of the cathode - 0.0035 m; distance between the anode and the cathode - 0.00975 m. The volume of electrolyte in the cell - 1.8 L. Composition of the initial solution: 53 g/L of K_2MnO_4, 30 g/L $KMnO_4$ and 120 g/L of KOH. The cell was connected to a power supply;current - A 30, cell voltage - 2.6 V;the anodic current density -93.5 mA/cm^2, the cathodic current density - 9500 A/m^2.The ratio between the anodic and cathodic current densities - 1:100. The centrifugal pumpwas placed in an intermediate steel tank with a thermometer and a mixer with horizontal blades. The electrolyte in the tank was heated to 70^{0}C. Through the feed tube he solution was getting into a cell and then back into thetank.The flow rate was 8.5 g/min. The duration of the electrolyte circulation was recorded;the electrolyte temperature at the output of the cell - 60-64^{0}C. The duration of electrolysis was 20 min. The $KMnO_4$current efficiency was 80.4%.

ლიტერატურა - REFERENCES – ЛИТЕРАТУРА

1. Ullmans Encyklopadie der technisheChemie, Hrsg.: W. Foerst. Bd. 12, 3 Aufl.Munchen, Derlin: Urban and Schwazenberg, 1969.
2. *Agladze G*. Electrosynthesis oxidants and electrochemical wastewater treatment. 1994, pp. 220.
3. Potassium permanganate production Regulations of Saki chemical plant. 1973.
4. *Carus M., Reidies A.*, US patents 2940821, 2940822, 2940823, 2908620, 1960.
5. *Agladze G., Kveselava V*. Electrolyzer for electrochemical processes. Ge P № 3437, 2003.

კალიუმის პერმანგანატის მიღება განდინარე ელექტროლიზერში

ვ.კვესელავა

ივანე ჯავახიშვილის სახელობის თბილისის სახელმწიფო უნივერსიტეტის რ.აგლაძის არაორგანული ქიმიისა და ელექტროქიმიის ინსტიტუტი, 0186, მინდელის ქ.11, თბილისი, საქართველო

რეზიუმე

სამუშაოში წარმოდგენილია მილისებრი გამდინარე რეაქტორი კალიუმის პერმანგანატის ($KMnO_4$) ელექტროსინთეზისათვის. უჟანგავი ფოლადის მილის შიდა ზედაპირი წარმოადგენდა ანოდს, ხოლო მილის შიგნით კოაქსიალურად განტავსებული დენგამტარი მავრთული – კათოდს. ანოდზე მიღებული $KMnO_4$-ის კათოდზე მაღალი დენის სიმკვრივის პირობებში აღდგენის შემცირების მიზნით კათოდური და ანოდური დენის სიმკვრივეების შეფარდება უნდა შეადგენდეს 1:100. ამისათვის კოაქსიალურად განთავსებული მავრთულის ზედაპირი გარკვეული თანაბარი ინტერვალით დაფარული იყო საიზოლაციო მასალით. წარმოდგენილ რეაქტორში მიზნობრივი პროდუქტის დენითი გამოსავალი შეადგენდა 80%-ზე მეტს.

ПОЛУЧЕНИЕ ПЕРМАНГАНАТА КАЛИЯ В ПРОТОЧНОМ ЭЛЕКТРОЛИЗЕРЕ

В.М.Квеселава

Институт неорганической химии и электрохимии им. Р.И.Агладзе Тбилисского государственного университета им. И.Джавахишвили, 0186, ул. Миндели11, Тбилиси, Грузия

РЕЗЮМЕ

В работе представлен проточный реактор трубчатой формы для электрохимического процесса окисления манганата калия в пермарганат ($KMnO_4$). Внутренняя поверхность трубы из нержавеющей стали служила анодом, коаксиально закрепленная внутри трубы токопроводящая проволока – катодом. С целью уменьшения при высоких плотностях тока катодного восстановления полученного на аноде $KMnO_4$, соотношение катодной и анодной плотностей тока должно составлять 1:100. Поэтому поверхность коаксиально расположенной проволоки через определенные равные интервалы покрывалась изоляционным материалом. Выход по току целевого продукта в представленном реакторе составил более 80%.

COMBINED HYDROMETALLURGICAL TREATMENT OF JOINT CHALCOPYRITE AND OXIDIZED MANGANESE CONCENTRATES

Lamzira Bagaturia, Boris Purtseladze, Nana Barnovi
R.Agladze Institute of Inorganic Chemistry and Electrochemistry of Ivane Javakhishvili Tbilisi State University, 0186, Mindeli st.11, Tbilisi, Georgia, lamzirabagaturia@mail.ru

The proposed joint hydrometallurgical processing of sulfide concentrate and the poor of manganese raw materials. Proven effectiveness of joint processing of copper-sulfide and manganese concentrates from the environmental point of view. It is shown that sulfide sulfur is partially transferred into the sediment in the form of free sulfur, partly in solution in the form of sulfuric acid, and therefore, it is possible the emission of sulfur dioxide in the atmosphere.

Developed and theoretically substantiated the process of joint processing of copper oxide and manganese concentrates, in which instead of the prior high-temperature reductive roasting is used, the reception of mechanical activation, the process includes the subsequent sulfuric acid leaching [1÷3].

Performed work on complex processing chalcopyrite concentrate in Madneuli and Chiatura manganese oxidized concentrate. For research was used chalcopyrite concentrate mineralogical composition of the concentrate are summarized in table 1 and Chiatura manganese concentrate the following chemical composition, %: Mn-32,5; MnO_2-29,84; $MnCO_3$ -29,2; SiO_2 -19; CaO – 5,75; Fe_2O_3 - 1,96; Al_2O_3 – 1,64; MgO – 1,58; H_2O – 1,85; P_2O_5- 0,55.

Table 1. The mineralogical content of the concentrate chalcopyrite

Name	content,%									
	Cu	Fe	S	SiO_2	CaO	MgO	Al_2O_3	H_2O	the others	sum
$CuFeS_2$	12,64	11,27	12,91							36,82
FeS_2		20,13	23,0							43,13
CuS	0,5		0,25							0,75
Cu_2S	0,61		0.154							0,764
$CaCO_3$					2,79				2,19	4,98
SiO_2				10,75						10,75
$MgCO_3$						0,45			0,49	0,94
$Al(OH)_3$							0,55		0,3	0,85

Chalcopyrite concentrate also contains precious metals gold -3,2 g/t, silver -14,6 g/t; for their selection, you need a full autopsy concentrates

In the concentrate the noble metals are present in the form of isomorphic. To separate them requires a complete autopsy of the concentrate.

The shows the efficiency in the environmental sense, the joint processing of chalcopyrite and manganese oxide concentrates [5]. Sulfur, containing in the mixture, partially passes into the in the form elementary sulfur, partially - in solution in the form of sulfuric acid, and accordingly, eliminates the pollution of the atmosphere by sulfur dioxide

The observations indicate that the gas phase in the form of SO_2 or H_2S from the slurry is not allocated.

Analysis of the sediment (table 2) obtained after sulfuric acid leaching the ground mixture chalcopyrite and oxidized manganese concentrate showed that the amount of sulfur in it slightly, it does not correspond to the amounts of sulfide sulfur.

Part of the sulfide sulfur in the sediment is transferred in the form of free sulfur [4], and the rest contributes to the formation of sulfuric acid. This conclusion is based on calculations: despite the fact that sulfuric acid added to the powder mixture, used to obtain sulfates of iron, manganese and impurity, its amount in solution is not reduced, but rather increases.

Table 2. The composition of the precipitate obtained after sulfuric acid leaching the ground mixture chalcopyrite and oxidized manganese concentrates; grind time – 2 h, the ratio of liquid:solid 10:1, the concentration of sulfuric acid 20%, (d=1,1400), leaching time – 3 h.

The composition of the sediment, %				
Fe	Mn	Cu	S_{common}	S_{free}
12,37	Traces	0,62	17,84	2,5

Table 3. The composition of solution obtained after sulfuric acid leaching of the mixture of jointly ground chalcopyrite and oxidized manganese concentrates; grind time – 2 h, the ratio of liquid:solid 10:1,the concentration of sulfuric acid 20%, (d=1,1400), leaching time – 3 h.

The composition of the solution, %			
Fe	Mn	Cu	H_2SO_{4free}
0,51	9,26	1,472	54,53

From table 3 it can be seen that a portion of sulfide sulfur is consumed for the formation of the sulfate ion.

The proposed technology gives the possibility of regeneration of sulfuric acid from the resulting solution and apply it to the first stage for leaching the ground mixture.

To reduce the ratio of liquid:solid and increase in the degree of leaching conducted countercurrent leaching.

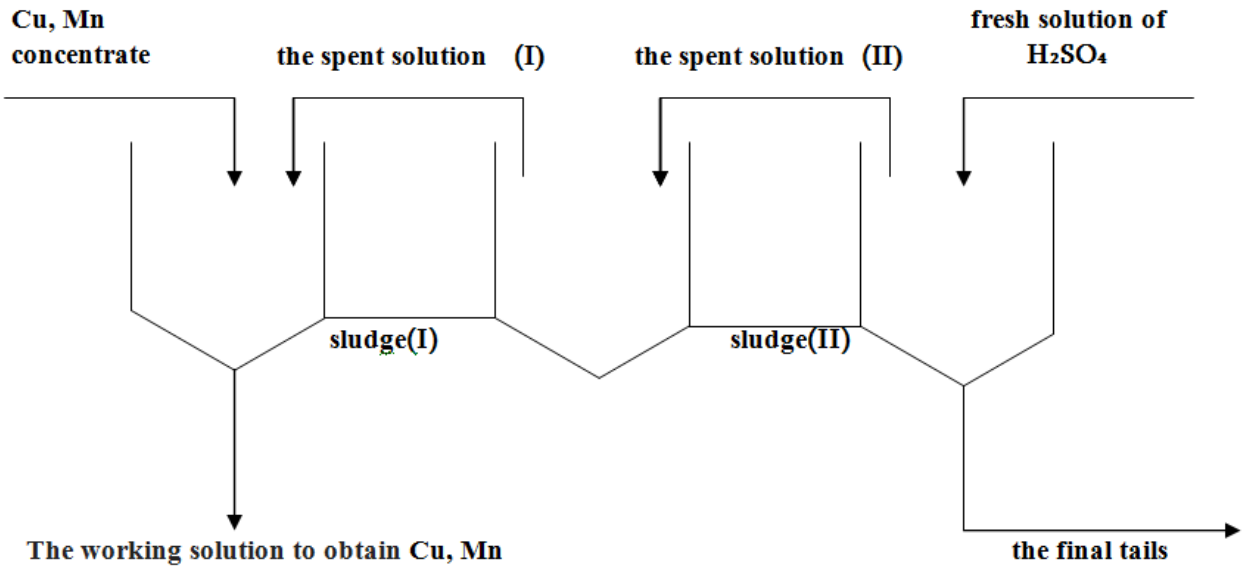

Diagram of countercurrent leaching.

The results confirm the advantages of countercurrent leaching. The copper recovery amounted to 99,7, but of manganese - 99,8%.

ლიტერატურა - REFERENCES – ЛИТЕРАТУРА

1. L. V. Bagaturia, V.N. Gaprindashvili, T.B. Janimanov, V.Sh. Tsveniashvili. Combined hydrometallurgical treatment of chalcopyrite and Mn concentrate. Bulletin of the Georgia Academy of sciences, 142, #1, 1991, p.85-88.
2. L. V. Bagaturia, V.N. Gaprindashvili.- Combined hydrometallurgical treatment of chalcopyrite and manganese oxide concentrates.- Proceedings of the Georgian Academy of Sciences, 19, #3-4, 993, p.135-137.
3. L.V.Bagaturia, V.N. Gaprindashvili, N.V.Barnovi, M.K. Gvelesiani, T.T.Lezhava. Opposite of current, sulfuric acid extraction of jointly activated studion of Halcopyrite and Manganum concentrates. Georgian chemical journal, Vol.11, #2, 2011, p. 135-137.

ქალკოპირიტისა და მანგანუმის ოქსიდური კონცენტრატების ერთობლივი ჰიდრომეტალურგიული გადამუშავება

ლამზირა ბაღათურია, ბორის ფურცელაძე, ნანა ბარნოვი

ივანე ჯავახიშვილის სახელობის თბილისის სახელმწიფო უნივერსიტეტის რ.აგლაძის არაორგანული ქიმიისა და ელექტროქიმიის ინსტიტუტი, 0186, მინდელის ქ.11, თბილისი, საქართველო

რეზიუმე

შემოთავაზებულია ქალკოპირიტისა და მანგანუმის ოქსიდური კონცენტრატების ერთობლივი ჰიდრომეტალურგიული გადამუშავება სასარგებლო კომპონენტების ამოღების მაღალი მაჩვენებლებით საწყის სტადიაზე მექანოქიმიური აქტივაციის ჩართვით. სამუშაო აქტუალურია ეკოლოგიური თვალსაზრისითაც, ატმოსფეროში არ ხდება მავნე აირების გამოყოფა, სულფიდური გოგირდის ნაწილი გადადის ნალექში ელემენტური გოგირდის სახით, ნაწილი - იხარჯება გოგირდმჟავას წარმოქმნაზე.

СОВМЕСТНАЯ ГИДРОМЕТАЛЛУРГИЧЕСКАЯ ПЕРЕРАБОТКА МЕДНОСУЛЬФИДНОГО И ОКИСЛЕННОГО МАРГАНЦЕВОГО КОНЦЕНТРАТОВ

Л.В.Багатурия, Б.Х.Пурцеладзе, Н.В.Барнова

Институт неорганической химии и электрохимии им. Р.И.Агладзе Тбилисского государственного университета им. И.Джавахишвили, 0186, ул. Миндели11, Тбилиси, Грузия

РЕЗЮМЕ

Разработан и теоретически обоснован процесс совместной переработки медьсодержащих и окисных марганцевых концентратов, в котором взамен предварительного высокотемпературного восстановительного обжига использован прием механической активации, процесс включает в себя последующее сернокислотное выщелачивание. Доказана эффективность совместной переработки медносульфидного и марганцевого концентратов с экологической точки зрения. Показано, что сульфидная сера частично переходит в осадок в виде свободной серы, частично – в раствор в виде серной кислоты, и, следовательно, исключена эмиссия сернистого газа в атмосфере.

OXIDATION OF MANGANEZE NITRATE SOLUTIONS BY OZONE – AIR MIXTURE

Boris Purtseladze, Marina Avaliani, Rusudan Chagelishvili, Lamzira Bagaturia, Zurab Samkharadze, Eter Shoshiashvili, Makvala Svanidze, Nana Barnovi, Marina Gvelesiani

R.Agladze Institute of Inorganic Chemistry and Electrochemistry of Ivane Javakhishvili Tbilisi State University, 0186, Mindeli st.11, Tbilisi, Georgia, rusudanch@yahoo.com

The developed chemical method of obtaining manganese dioxide, which consists in the oxidation of manganese-containing solutions by mixture of ozone – air with a formation of g-MnO_2. Simplicity, reliability, efficiency and the absence of ballast are those main features, which allows to create the waste-free production by means of ozone method.

The various methods of ozone production are available all over the world. In the most countries the ozonators are mainly manufactured, where the graphite or aluminum layer is applied on the inner side of milli-dielectric, which is placed in cylindrical stainless body. In ozonators as a result of supplying current is "quiet" discharge effects on the air with production of ozone [1].

Ozone synthesis may be realized by another method, where feeding is carried out in "cascaded" manner. In this case the current discharge is distributed at "needle" surface. There is no need in ozonator cooling by water and in air drying.

Over many years our laboratory and the firm "Hydrogen Technologist" are connected by official friendly relations. In 1980-th the ozonator construction was jointly elaborated, which is protected by author's certificate [2]. Ozonator worked under the action of photochemical , ultraviolet light and by "quiet" discharge. The disadvantage of ozonator involves a low efficiency. At now the firm "Hydrogen Technologist" made ozonators of new generation , which are introduced in various fields of Georgian industry.

The technology of the enrichment of Chiatura manganese-containing ores is tested, where the reduction-leaching process is realized in the reactor from the usual stainless steel by 40-45% nitric acid. Precipitation of admixture is carried out by ammonia. After filtration the silt is extracted from the system and ozone-air mixture is fed into manganese nitrate solution and formed γ-MnO_2 .

The chemistry of this processed is expressed by the following equations:

Leaching stage:

$$MnO+2HNO_3 \rightarrow Mn(NO_3)_2 + H_2O$$
$$CaO+MgO+4HNO_3 \rightarrow Ca(NO_3)_2 + Mg(NO_3)_2 + 2\,H_2O$$
$$Fe_2O_3+Al_2O_3+12HNO_3 \rightarrow 2Fe(NO_3)_3 + 2Al(NO_3)_3+6H_2O$$

Stage of admixture Precipitation pH=4-5;

$$2Fe(NO_3)_3+3MnO+3\,H_2O \rightarrow 2Fe(OH)_3+3Mn(NO_3)_2$$
$$2Al(NO_3)_3+3\,MnO+3\,H_2O \rightarrow 2Al(OH)_3+3Mn(NO_3)_2$$
$$H_3PO_4 + Fe(OH)_3 \rightarrow FePO_4 + 3H_2O$$

At the stage of obtaining of active manganese dioxide:

$$Mn(NO_3)_2 + O_3 + H_2O \rightarrow MnO_2\downarrow + 2HNO_3 + O_2$$

In the paper [3] oxidation of Mn (II) by ozone was studied where oxygene isotope O^{18} was used. It was ascertained that one oxygen atom passes from ozone to MnO_2 and the second one – from the solvent - H_2O.

It was established, that oxidation of Mn^{2+} to Mn^{3+} in acid medium proceeds by reactions:

1. $Mn^{2+}+2H^+ + O_3 \rightarrow Mn^{3+} + O_2 + H_2O$

$\underline{OH^- + Mn^{2+}+H^+ \rightarrow Mn^{3+} + H_2O}$

$$2Mn^{2+}+2H^+ + O_3 \rightarrow 2Mn^{3+} + O_2 + H_2O \qquad K = 6{,}4 \times 10^{10}$$

2. $Mn^{3+} + O_3 + H^+ \rightarrow Mn^{4+} + OH^{/} + O_2$

$\underline{Mn^{3+} + HO^{/} + H^+ \rightarrow Mn^{4+} + H_2O}$

$2Mn^{3+} + 2H^+ + O_3 \rightarrow 2Mn^{4+} + O_2 + H_2O \qquad K = 1{,}73 \times 10^8$

Overall reactions are of the form:

$Mn^{2+} + O_3 \rightarrow Mn^{3+} + O_2$

$O_3 + H_2O \rightarrow OH^- + HO^{/} + O_2$

$\underline{Mn^{3+} + OH^- \rightarrow Mn^{4+} + OH^-}$

$Mn^{2+} + O_3 + H_2O \rightarrow MnO_2 + 2H^{+-} + O_2$

To research the optimal conditions of this process, precipitation of MnO_2 was performed from manganese nitrate solutions. Ozone was produsedat laboratory ozonator ЛГО-15 with efficiency of 17-18 g O_3/hour, solution amount - 1 L.

Degree of ozone use was calculated in the terms of amount of obtained precipitate and its composition (table 1). Maximum degree of the use – 87%, and at acid addition (100g/l) reduces and comprises 52%, when the content of HNO_3 in the solution is equal to 320g/l.

From the table 2 it is evident, that in neutral solutions the precipitate is fine dispersed - $MnO_{1,70-1,91}$ and in acid medium – $MnO_{1,92-1,99}$.

Oxigen feeding rate – 300 l/hour; ozonator efficiency 15g O_3/hour; composition of 1-st solution: Mn - 56,6g/l, HNO_3 – 6,0g/l; composition of 1I solution: Mn – 53,3g/l; HNO_3 – 100g/l; solution volume – 1L.

At the begining the precipitation of manganese dioxide intensively proceeds, but after 40 minutes the process become slower. The manganese oxidation degree from the I-st as well as from the II-nd nitrate solutions after 2 hours composes 1,9398 and 1,9433 respectively.

Table 1. Obtaining of manganese dioxide from manganese nitrate solutions

№№	Initial solution, g/l		obtained solution, g/l		Precipitate amount, %			Precipitate weight, g	Degree of ozone use, %
	Mn	HNO_3	Mn	HNO_3	Mn	MnO_2	O:Mn		
1	51,6	6,0	40,1	56,8	59,82	89,06	1,9379	19,2	76,2
2	53,3	100,0	41,6	124,6	58,18	86,59	1,9377	20,3	77,5
3	97,3	0,0	80,7	33,3	58,11	87,29	1,9464	30,6	87,0
4	89,5	78,9	77,3	115,5	57,38	87,85	1,9645	30,0	85,8
5	92,5	155,0	78,7	180,2	57,20	88,10	1,9705	25,0	70,2
6	92,2	263,0	85,5	283,8	56,32	88,49	1,9895	24,0	66,3
7	92,8	320,0	82,2	335,0	55,2	87,0	1,9920	19,2	52,0

Table 2. The effect of the duration of the experiment on the oxidation degree of manganese

Experiment duration, min	I solution				II solution			
	Mn, g/l	HNO_3, g/l	ΔMn, g	MnO_x	Mn,g/l	HNO_3,g/l	ΔMn, g	MnO_x
0	51,6	6,0	0	-	53,3	100	0	-
10	50,6	12,3	1,0	1,906	50,0	98,7	3,3	1,9491
20	47,3	25,9	4,3	1,927	48,0	102,4	5,3	-
40	43,4	43,2	8,2	1,928	45,7	114,8	7,6	-
60	40,1	56,8	11,5	1,929	41,6	124,6	11,7	-
120	24,1	94,8	27,5	1,940	29,5	160,4	23,8	1,9430

ლიტერატურა - REFERENCES – ЛИТЕРАТУРА

1. *Kh. G. Purtseladze, T.V. Maslentsova, B. Kh. Purtseladze.* Obtaining of active manganese dioxide by ozone. Authors Certificate USSR, №569540. 02. 12 75.
2. *Dj. Burganadze, A. Khantadze, N. Razmadze, B. Purtseladze, G*. Soltan. A methode of producing ozone. Authors Certificate USSR, №4765805. 1990.
3. *Grinberg A. L. Shashukov E. A. et all.* Oxidation of manganese (II) by ozone in nitric acid solutions. Kinetics and katalysis, XII, 2, 1971. (Russian)

მანგანუმის ნიტრატული ხსნარების დაჟანგვა ოზონ - ჰაერის ნარევით

ბორის ფურცელაძე, მარინე ავალიანი, რუსუდან ჩაგელიშვილი, ლამზირა ბაღათურია,
ზურაბ სამხარაძე, ეთერი შოშიაშვილი, მაყვალა სვანიძე, ნანა ბარნოვი, მარინა გველესიანი
ივანე ჯავახიშვილის სახელობის თბილისის სახელმწიფო უნივერსიტეტის რ.აგლაძის არაორგანული ქიმიისა და ელექტროქიმიის ინსტიტუტი, 0186, მინდელის ქ.11, თბილისი, საქართველო

რეზიუმე

დამუშავებულია მანგანუმის დიოქსიდის მიღების ქიმიური მეთოდი: ოზონ - ჰაერის ნარევით მანგანუმშემცველი ხსნარების დაჟანგვა, რის შედეგად მიიღება γ-MnO_2. სიმარტივე, საიმედოობა, ეფექტურობა და უბალასტობა არის ის ძირითადი თვისებები, რაც ოზონურ მეთოდს საშუალებას აძლევს შეიქმნას უნარჩენო წარმოება.

ОКИСЛЕНИЕ НИТРАТНЫХ РАСТВОРОВ МАРГАНЦА С ПОМОЩЬЮ ОЗОНО-ВОЗДУШНОЙ СМЕСИ

Б.Х.Пурцеладзе, М.А.Авалиани, Р.Д.Чагелишвили, Л.В.Багатурия, З.В.Самхарадзе,
Э.Н.Шошиашвили, М.И.Сванидзе, Н.В.Барнова, М.К.Гвелесиани
Институт неорганической химии и электрохимии им. Р.И.Агладзе Тбилисского государственного университета им. И.Джавахишвили, 0186, ул. Миндели11, Тбилиси, Грузия

РЕЗЮМЕ

Разработан химический метод получения диоксида марганца, который состоит в окислении марганец-содержащих растворов смеси озон – воздух с образованием γ-MnO_2. Простота, надежность, эффективность и отсутствие балласта – это те основные характеристики, которые позволяют создать безотходное производство методом озона.

ADSORPTION OF TETRABUTYLAMMONIUM IODIDE AT THE MERCURY ELECTRODE / ETHYLENE GLYCOL SOLUTION INTERFACE

Shukri Japaridze, Irina Gurgenidze

R.Agladze Institute of Inorganic Chemistry and Electrochemistry of Ivane Javakhishvili Tbilisi State University, 0186, Mindeli st.11, Tbilisi, Georgia

The ionic liquids – melts of organic salts, being in the liquid state in a wide temperature range find extensive practical application at the present time. Ionic liquids are composed of bulky organic cations and inorganic anions [1]. The most important characteristics determining the prospects of the use of ionic liquids in electrochemistry shouldbethe ionic conductivity, the hydrophobicity and the width of the electrochemical "window". The width of electrochemical "window",the electrochemical stability of the ionic liquids (border "window" match the beginning and the end of the electrochemical decomposition of these ions) determine the potential range available for carrying out of electrochemical transitions thatdo not affect the solvent [2]. Ionic liquids have not only the catalytic activity but in some cases are able to maintain and enhance the biological activity of biosensor [3]. They are widely used in the field of electrochemical analysis in medicine, food industry, etc. [1,4]. All this make ionic liquids attractive to many areas of science and technology. Quaternary ammonium salts, in particular tetrabutylammonium iodide (TBA-I) also refer to ionic liquids. The data on adsorbability of TBA-I on mercury from ethylene glycol (EG) solutions is given in this paper. Tetrabutylammonium iodide - quaternary ammonium salt - $(C_4H_9)_4NI$ contains a volumetric organic cation of TBA-I and an inorganic iodide anion. TBA-I is slightly soluble in water (hydrophobic).TBA-I refers to ionic liquids by its structure and properties, right this causes the interest of studying ofitsadsorbability from the EG solutions.

EXPERIMENTAL

Adsorption was studied using a stationary Hg electrode by measuring the differential capacity (C) as a function of potential E by means of an a.c.bridge at 400 Hz [5]. The temperature of the solution was kept at 20^0C. Potentials were measured against a 0.2 M calomel electrode in EG whose potential differed by 6 *m*V from the potential of the saturated aqueous calomel electrode. The potential of zero charge of Hg in this solution was 0.35 V [6]. All chemicalswere purified according to methods given in the literature. EG was prepared as described in Refs.[5,7].

RESULTS AND DISCUSSION

Figure 1 shows the curves of the dependence of differential capacitance (C) from the electrode potential (E), C, E-curves were measured in 0.2M potassium iodide solution in EG (Fig.1, curve 1), and also with various additives TBA- I (Fig.1, curve 2÷7). As can be seen from the figure, C, E-curves have the shape characteristic for solutions containing small amounts of neutral organic compounds. Indeed, in minimum of C,E-curves, with increasing concentration of added TBA-I, capacitance decreases respectively reaching values 6 μF/cm^2, which indicates significant absorptivityof TBA-I from EG solutions.Cathode desorption peaks (Fig. 1, curve 4÷7)appear when increasing the negative electrode polarization.Because of considerable specific adsorption ofiodide ion of base electrolyte (KI) in EG [5, 6] anodic desorption peakcan'tbeobservedexperimentally. Comparing obtained results with the data of aqueous solutions [8, 9, 10] we conclude, that the adsorbability of TBA-I from the EG is less than from water.The adsorption effect of TBA-I begins to appear in the EG at concentration equal to 10^{-3}M, whereas in water solutions - at 10^{-6}M [8, 9, 10]. The reason for this fact is above mentioned hydrophobicity of ionic liquids, which include quaternary ammonium salts [1-3] and their relatively better solubility in the EG.Up to a concentration of organic substance c = 8.2 • 10^{-3} M cathode desorption peaks were not observed on C, E-curves (Fig. 1 curves 2÷4), although from capacitance depression one can see, that at such concentrations adsorption of these substances is appreciable. It can be assumed that, as in aqueous solutions [9],so in the EG TBA-I exists mainly in ionic and molecular forms. At low concentrations TBA-I is preferably in the ionic form, the retraction of these cations occurs in the double electric layer by specifically adsorbed anions of the base electrolyte. When the concentration of TBA-I c=8.2 • 10^{-3} M, while the value of the electrode potential E =

- 1.6 V (Fig.1, curve 5) there is an inflection in the C, E-curve, which transits into pronounced desorption peak, when the concentration of organic matter increases (Fig.1, curve 5).

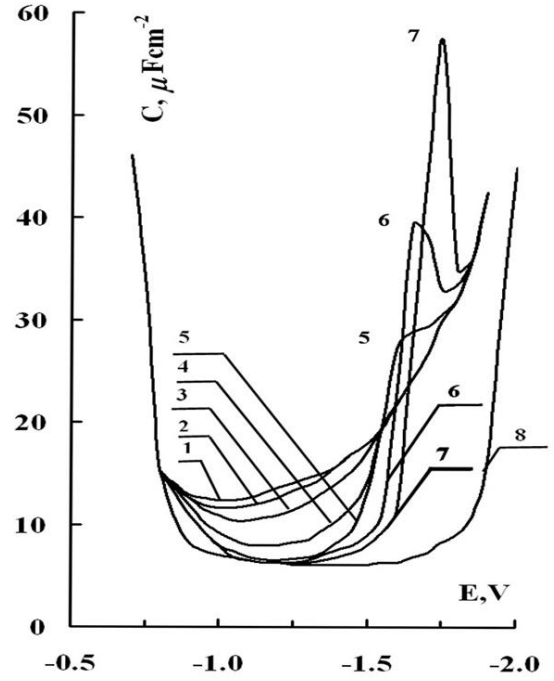

Fig. 1. Differential capacity curves of a Hg electrode in contact with a 0.2 M KI solution in EG containing tetrabutylammonium iodide (TBA-I) in the following concentration :
1 – 0; 2 – $1.1•10^{-3}$; 3 – $2.2•10^{-3}$; 4 – $4•10^{-3}$; 5 – $8.2•10^{-3}$; 6 – $1.4•10^{-2}$; 7 – $2.2•10^{-2}$ M; 8 – 0.2 M TBA-I (without a supporting electrolyte)

After certain TBA-I concentrations at considerable negative electrode potentials (-1.6V) (whichshift to the cathode side with increase of concentration of added substance) cathode desorption peaks characteristic for the adsorption of neutral organic substances appear on C, E-curves. Height of these peaks increases with the increase of concentration of organic substances (Fig.1, curve 6 and 7). Thus, in terms of the nature of the solvent and dissolved substance, i.e. taking into account property of EG - a low dielectric constant (D = 38), in comparison with water, and spatial isolation of charges, a high polarity and solvation ability of TBA-I [1], one may assume, that at high concentration of TBA-I (above $8 • 10^{-3}$ M) at accumulation in the solution of a large number of ions their mutual influencewill affect andthe conditions for the electrostatic interaction between the solvated ions of opposite signswill be created.In doing so they come close to each other and form an ion pair consisting of two oppositely charged ions, surrounded by EG molecules in which electric charges are mutually compensated, ie, are formed associates - uncharged, neutral molecules. Desorption of these formations is observed on Figure 1, curves 6 and 7. On the Fig. 1, curve 8 is presented C, E-curve corresponding to purely no-background TBA-I. This figure shows that the riseon C, E-curve from the EG solution occurs at much less negative potential, namely, when E = - 2.0 V, against E = - 2.5 V from aqueous solutions, i.e.width of electrochemical "window" in the EG is narrower than in water. Experimental data on the TBA-I adsorption on mercury from EG solutions were processed by the calculation methods developed by B.B.Damaskin [11] and is based on the Frumkin'sisotherm and model of two parallel-connected capacitors. The adsorption isotherm was determined at a potential of maximum adsorption E = - 1.2 V (Fig. 1 curves 2÷7), when regardless of particular isotherm's equation the capacity is transferred by the equation:

$$C = C_0 (1 - \Theta) + C'\Theta \quad (1)$$

where C_o is the electrode capacity for the coverage by organic substance$\Theta = 0$; C ' is theelectrode capacity at $\Theta = 1$, C is the capacity at $0 < \Theta < 1$. From this equation was calculated Θ for different concentrations of TBA-I by the formula

$$\Theta = (C_0 - C) / (C_0 - C') \quad (2)$$

and was constructed the concentration curve c for TBA-I (Fig. 2). The value C '= 6 μF cm^{-2} was obtained by the extrapolation of the curve $1 / C_K$ as a function of $1 / c \rightarrow 0$. As can be seen from Fig. 2, the isotherm has an S-shape, which is typical for attracting interaction of adsorbed molecules. S-shaped form of isotherm is steep in its middle part, as well as in case of isotherm of cations of quaternary ammonium salts constructed from data on their adsorption from aqueous solutions [9]. When the isotherm is S-shaped, most preferred to describe C, E- curves in the presence of organic substances is Frumkin isotherm, which is in good agreement with the experimental data. By the form of adsorption isotherm the value of attraction

constant has been determined at a potential of maximum adsorption E = - 1.2 V.For this, from the θ, c-curve, at first the TBA-I concentration was found equal to half the value of the coverage of the electrode by theadsorbate$C_{\theta = 0.5}$ = 2 • 10^{-3} M.There was thus calculated averaged value a = 1.62, which indicates a strong attractive value ofadsorbed molecules of TBA-I.If the adsorption of organic matter obeys the Frumkin isotherm, it should be observed by linear changeof function lg [Θ / (1 - Θ) c] to the degree of coverage θ, as revealed in the case of TBA-I adsorption in EG solution (Fig. 3). From Fig. 3 was calculated the value of a = 1.63. It was obtained entirely satisfactory agreement between the values calculated by the different methods. The value of the free energy of adsorption of TBA-I was calculated from linear dependence oflg [Θ / (1 - Θ) c] toΘ (Fig. 3) by the equation

$\Delta G = RT\ln (17.8\ B_0)$ (3),

where 17.8 - the number of moles in 1 l of ethylene glycol, and B_0 - adsorption equilibrium constant the value of which is determined by extrapolating the straight line on the y-axis (Fig. 3). Calculated from the equation (3), the value of ΔG = 17.6 kJ mol^{-1}.

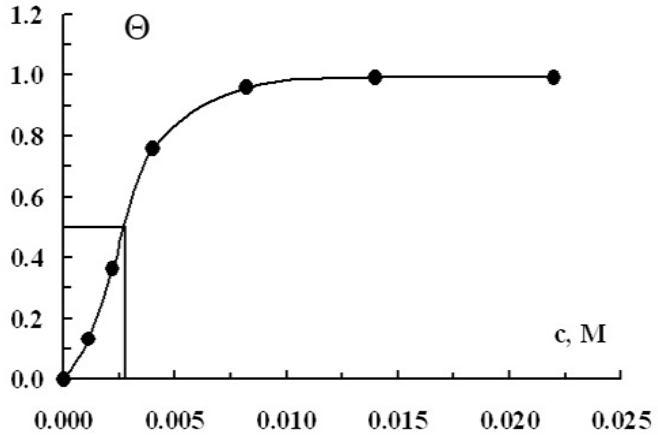

Fig. 2. Adsorption isotherm of tetrabutylammonium iodide on Hg from solution in ethylene glycol at E = - 1.2 V.

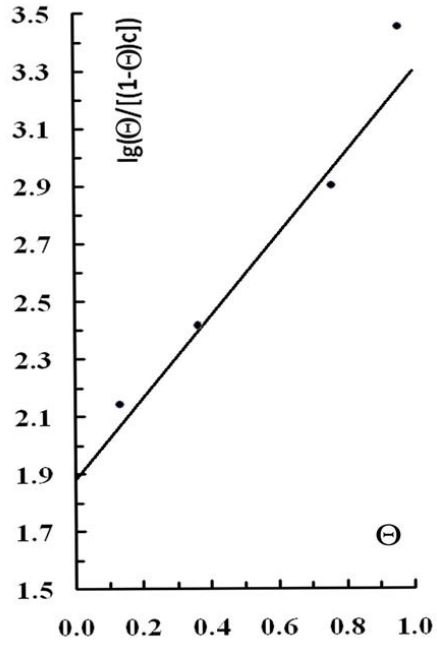

Fig. 3. Test of the Frumkin isotherm for adsorption of tetrabutylammonium iodide in ethylene glycol at E = -1.2 V

CONCLUSIONS

Thus, the shape and the analysis of the curves of the dependence of differential capacitance from the electrode potential, the adsorption isotherm at a potential values of maximum adsorption, values of calculated parameters: attraction constant, constant of adsorption equilibrium, the free energy of adsorption indicate a significant adsorption capacity of tetrabutylammonium iodide on mercury from ethylene glycol solutions.

ლიტერატურა - REFERENCES – ЛИТЕРАТУРА

1. Shvedene N.V., Chernishev D.V., Pletnev I.V. J.Ros.khim.obsh. im. D.I.Mendeleeva, 2008, V.52, #2, P. 80-91 (in rus.).
2. Wilkes J.S., Levicky J.A., Wilson R.A. Inorg. Chem., 1982, V.21,P.1262-1264.
3. Liu Y., Shi L., Liz ., Liu H., Li A. J.Creen. Chem., 2005, #7, P.655-658.
4. Zakharov A.M., Grinshtein I.A., Kaptsova A.A. Sorbtsionnie I khromatograficheskieprotsesi, 2014,V.14, #1, P.104-110.
5. Japaridze J.I., Tedoradze G.A., JaparidzeSh.S. Elektokhimiya, 1969, V.5, #8, P.955-957.
6. Japaridze J.I., JaparidzeSh.S., in : A.N.Frumkin, B.B.Damaskin (Eds.). Adsorptsia I dvoinoisloi v elektrokhimii (Adsorption and Double Layer in Electrochemistry), Nauka, Moskow, 1972, P.68-71.
7. Japaridze J.I.,Abuladze N.A.,Japaridze Sh.S., De Battisti A., Trasatti S. Electrochim. Acta, 1986,V.31,#6,P.621-628.
8. Frumkin A.N.,Damaskin B.B. DAN SSSR, 1959, V.129,P.862- 866.
9. Nikolaeva-Fedorovitch N.V., Damaskin B.B., Petriy O.A. Coll.Czech.Chem.Comm., 1960, V.25,P.2982-2992.
10. Gerovitch V.M.,Kaganovitch R.I.,DamaskinB.B. Elektrokhimiya, 1972,V.8,#3,P.420-422.
11. Damaskin B.B.,Petriy O.A.,Batrakov V.V. Adsorptsia organicheskikh soedineniy na elektrodakh. M., Nauka, 1969.

ტეტრაბუთილამონიუმის იოდიდის ადსორბცია ვერცხლისწყლზე ეთილენგლიკოლის ხსნარებიდან

შუქრი ჯაფარიძე, ირინე გურგენიძე

ივანე ჯავახიშვილის სახელობის თბილისის სახელმწიფო უნივერსიტეტის რ.აგლაძის არაორგანული ქიმიისა და ელექტროქიმიის ინსტიტუტი, 0186, მინდელის ქ.11, თბილისი, საქართველო

რეზიუმე

ტეტრაბუთილამონიუმის იოდიდის (TBA-I) ადსორბცია ეთილენგლიკოლის ხსნარებიდან შესწავლილ იქნა დიფერენციალური ტევადობის (C) დამოკიდებულებიდან ვერცხლისწყლის ელექტროდის პოტენციალზე (E), (C,E-მრუდები). ფრუმკინ-დამასკინის თეორიის გამოყენებით გათვლილი ექსპერიმენტული მონაცემების ანალიზი მიუთითებს იმაზე, რომ (TBA-I)-ის ადსორბცია აღიწერება ფრუმკინის იზოთერმით, რომელსაც შეესაბამება ადსორბირებული ნაწილაკების ურთიერთმიზიდულობა. ნაჩვენებია, რომ (TBA-I)-ის გარკვეული კონცენტრაციის შემდეგ ელექტროდის საკმაოდ უარყოფითი პოტენციალების დროს C,E-მრუდებზე ჩნდება ნეიტრალური ორგანული ნივთიერებისათვის დამახასიათებელი კათოდური დესორბციული პიკები, რომელთა სიმაღლე იზრდება ორგანული ნივთიერების კონცენტრაციის ზრდის შესაბამისად. გამხსნელის და გახსნილი ნივთიერების ბუნებიდან გამომდინარე (წყალთან შედარებით ეთილენგლიკოლის დიელექტრიკული მუდმივას დაბალი მნიშვნელობა, მუხტის სივრცობრივი იზოლირება, (TBA-I)-ის მაღალი პოლარობა და სოლვატაციის უნარი) შეიძლება ვივარაუდოთ, რომ (TBA-I)-ის მაღალი კონცენტრაციების დროს იქმნება იონური წყვილი, ანუ ასოციატები - დაუმუხტავი, ნეიტრალური მოლეკულები. C,E-მრუდების და ადსორბციის იზოთერმის ფორმა და ანალიზი, გათვლილი პარამეტრების (ატრაქციული მუდმივა, ადსორბციული წონასწორობის მუდმივა, ადსორბციის თავისუფალი ენერგია) მნიშვნელობები მიუთეთებენ ტეტრაბუთილამონიუმის იოდიდის დიდ ადსორბციულ უნარზე ეთილენგლიკოლის ხსნარებიდან.

АДСОРБЦИЯ ИОДИДА ТЕТРАБУТИЛАММОНИЯ НА РТУТИ ИЗ ЭТИЛКЕНГЛИКОЛЕВЫХ РАСТВОРОВ

Ш.С.Джапаридзе, И.А.Гургенидзе

Институт неорганической химии и электрохимии им. Р.И.Агладзе Тбилисского государственного университета им. И.Джавахишвили, 0186, ул. Миндели11, Тбилиси, Грузия

РЕЗЮМЕ

Адсорбция иодида тетрабутиламмония (TBA-I) из этиленгликолевых растворов изучалась измерением зависимости дифференциальной ёмкости (C) от потенциала ртутного электрода (E), (C,E-кривые). Анализ экспериментальных данных, проведенный с использованием теории Фрумкина-Дамаскина указывает на то, что адсорбция (TBA-I) описывается изотермой Фрумкина, соответствующей притягательному взаимодействию адсорбированных частиц. Показано, что после определенных концентраций TBA-I при значительных отрицательных потенциалах электрода на C,E-кривых появляются, характерные для адсорбции нейтральных органических веществ катодные десорбционные пики, высота которых растет с ростом концентрации органического вещества. Исходя из природы растворителя и растворенного вещества, т.е. учитывая низкую диэлектрическую проницаемость ЭГ, по сравнению с водой и пространственную изолированность зарядов, высокую полярность и сольватируемость TBA-I можно предположить, что при высокой концентрации TBA-I образуются ионные пары, т.е. ассоциаты – незаряженные, нейтральные молекулы. Форма и анализ кривых зависимости дифференциальной ёмкости от потенциала электрода, изотерма адсорбции при потенциале максимальной адсорбции, значения рассчитанных параметров: аттракционной постоянной, константы адсорбционного равновесия, свободной энергии адсорбции, указывают о значительной адсорбционной способности иодида тетрабутиламмония на ртути из этиленгликолевых растворов.

INVESTIGATION OF POLY-COMPONENT SYSTEMS IN AIMS FOR SYNTHESIS OF A NEW GROUPE OF INORGANIC POLYMERS – CONDENSED PHOSPHATES

Marina Avaliani, Marina Gvelesiani, Nana Barnovi, Boris Purtseladze,
Dali Dzanashvili, Eteri Shoshiashvili

R.Agladze Institute of Inorganic Chemistry and Electrochemistry of Ivane Javakhishvili Tbilisi State University, 0186, Mindeli st.11, Tbilisi, Georgia

The chemistry of inorganic compounds of phosphorous has developed intensively in the last few years. Very significant development of condensed crystal chemistry was due to the rapid progress of innovative methods of analysis, as well as to the achievements in this domain. Double condensed phosphates – in fact inorganic polymers of poly- and monovalent metals have a various interesting properties and numerous areas of application [1-7]. The offered data are the records of our studies – synthesis, analysis, examination of the experiments and their evaluation in correlation with achievements in inorganic polymer's chemistry. Condensed phosphates of polyvalent metals, containing monovalent metals are obtained by us during systematic investigation of M^{I}_2O-$M^{III}_2O_3$-P_2O_5-H_2O systems at temperature range 100℃ -550℃. (M^{III} are Ga, In, Sc, M^{I} – alkali metals and partially Ag). Compounds were wholly examined by chemical analysis and the structures are determined by X-ray structural techniques. During our fundamental researches numerous unknown condensed phosphates have been obtained. Dependency of composition VS temperature and molar ratio, reliance of structure from duration of synthesis are revealed.

In aim to search for new materials as well as to study the influence of trivalent and monovalent cations for the formation of anionic radical and the level of condensation, we have studied multicomponent systems containing monovalent and trivalent metals. Earlier we have done systematic study of systems M^{I}_2O-$M^{III}_2O_3$-P_2O_5-H_2O at 130^0 -550 ^{0}C, in which M^{I} are alkali metals and M ^{III} – Ga, In and Sc; Molar ratio P_2O_5 : M^{I}_2O:$M^{III}_2O_3$ = 15:2,5:1,5; 15:5:1,5; 15:7,5:1,5; 15:10:1,5.

Some double oligo-, poly- and and cyclophosphates are primarily synthesized and firstly examined by us [8-12, 14-15]. These recent achievements are examined and cited in significant monographs of Professor DURIF and Dr. Averbuch-Pouchot (France) [2, 4], Dr. I. Grunze and X. Grunze (Germany) [3, 6-7], I. V. Tananaev and N.N. Chudinova) [6, 8] etc. General dependency of structural composition and stability of double condensed phosphates from ion radius of M^{III} are also examined [8-11].

In extent of our previous exploration the present work is dedicated to the synthesis and studding of the system M^{I}_2O-$M^{III}_2O_3$-P_2O_5-H_2O at the temperature interval 120-160℃ where M^{I} are not any more alkali metals, but silver (Ag), M^{III}– Sc. In earlier studies we found that these and similar molar ratio of initial components help to obtain pure crystals, rather than the metastable phases or mixtures of compounds [9-11].

Thus, now we offer experimental data - the results of synthesis and investigation of compounds obtained by us at the variable molar ratio $P/M^{I}/M^{III}$ = 15/2,5/1; 15/3,5/1; 15/5,0/1; 15/6,0/1; 15/8,5/1; 15/10,0/1.

The most stable phase at relatively low temperatures from 130^0-150^0, and even to the 165^{0}C – is double acid diphosphate compounds $\boldsymbol{AgSc(H_2P_2O_7)_2}$, $\boldsymbol{Ag_2ScH_3(H_2P_2O_7)_2}$ and acid triphosphate $\boldsymbol{AgScHP_3O_{10}}$. For the first time the capacity of the synthesis of these compounds was mentioned by us in works [12-13], although there were not clearly defined nor optimal synthesis conditions neither the composition of the initial components. At that moment the reproducibility of the results was not entirely satisfactory, as well as were interfered with the impurity (due to crystallization of additional phases) or metastable phases.

We performed an analysis and comparison of analytical preparative data with literary publications available to date [16,17,7-12]. We did not find mention on these dual acid di- or triphosphate scandium-silver, although analytical chemistry is adequately and systematically described in the superb monograph [16]. It should be emphasized that $\boldsymbol{Ag_2ScH_3(H_2P_2O_7)_2}$ composition is similar to our earlier obtained crystals of $\boldsymbol{Cs_2GaH_3(H_2P_2O_7)_2}$. The heating conditions in molten mixtures of polyphosphoric acid at a temperature ranging from 130^0 to 165 -170^{0}C during about three to four days.

Detailed Information:

Double hydro-diphosphates are received by heating of mixtures at molar ratio $M^{I}_2O:M^{III}_2O_3$=5:1,5; 7,5:1,5; 10:1,5 (in the case of systems with Sc and Ag), and 5:1; 7,5:1; 10:1 (in the case of process of synthesis in systems with Ga and Cs). The heating conditions in molten mixtures of polyphosphoric acid (polyphosphoric acid melts) are: the temperature range from the 130^0 to 165 -170^0C during approximately three or four-five days. This phase is less or more metastable (the similar situation was in the system of gallium-caesium). If the heating will be pursued for more than 10-12 days and longer, it gradually becomes more stable double acidic diphosphate with formula $\boldsymbol{AgSc(H_2P_2O_7)_2}$ **(**at $M^{I}_2O:M^{III}_2O_3$=10:1,5 **),** and double hydro-triphosphate $\boldsymbol{AgScHP_3O_{10}}$ **(at** $M^{I}_2O:M^{III}_2O_3$=10:1,5 **),** The full finalization the phase transition demands 25-30 days…Obtained condensed compounds are insoluble in water, but they are able to dissolve in the acids. Similarly to the previously published works and the recent experiences referred in our articles [8-15], double hydro- triphosphate $\boldsymbol{AgScHP_3O_{10}}$ is a few soluble (more or less) in polyphosphoric acids. For removing obtained crystals from melts the synthesised mixture was cooled down and after in small doses was ported inside the glass vessel (volume 1-1,5 litres), quickly mixed with 500-700 ml distilled water.

Meanwhile, polyphosphoric acids have slowly dissolved with time undissolved part: $\boldsymbol{Ag_2ScH_3(H_2P_2O_7)_2}$ was filtrated, because the acidity of solution was not sufficient to dissolve synthesized $Ag_2ScH_3(H_2P_2O_7)_2$. Moreover it is also worth mentioning the problem consisting in the following fact: during parallel synthesis it is sedimentation of sufficient sludge - it's relatively problematic given the circumstance that this phase is not very stable.

Phase formation in system M^{I}_2O-$M^{III}_2O_3$-P_2O_5-H_2O and the microstructure of synthesized double condensed compounds $Ag_2ScH_3(H_2P_2O_7)_2$ and triphosphate $AgScHP_3O_{10}$ are investigated by X-Ray diffraction analyses (data summarized in table 1).

Table 1. XRD data for $AgScHP_3O_{10}$

$AgScHP_3O_{10}$		ASTM-11-642, $Ag_5P_3O_{10}$	
d_α/n, Å	I/I_0	d_α/n, Å	I/I_0
-	-	4.81	20
4.04	24	-	-
-	-	3.69	5
-	-	3.60	5
3.36	72	-	-
-	-	3.37	10
-	-	3.29	10
3.20	29	3.21	15
-	-	3.15	25
3.03	9	3.04	15
-	-	-	-
-	-	2.96	50
-	-	-	-
2.84	100	2.86	95
-	-	-	-
-	-	2.76	50
-	-	2.72	50
-		-	-
2.64	77	-	-
2.59	69	2.60	100
-	-	-	-
2.52	14	2.52	30
-	-	2.46	15
2.43	7	-	-
2.37	8	2.38	10
-	-	2.33	5
-	-	-	-
2.21	20	-	-
2.13	31	2.15	5
-	-	2.10	5
2.03	20	2.00	10
-	-	1.96	15
1.93	11	1.94	5
1.89	10	1.89	15
-	-	1.88	10
1.62	18	1.59	10

The powder diffraction data for cited compounds, intensity data collections are obtained on diffractometer DRON-3M, anodic Cu-Kα radiation, the range $2\theta=10^0$-60^0, detector's speed 2^0/min., lattice spacing d_α/n in Angströms Å, and I/I_0 – it is relative intensity (used model/ standard data – by American Society for Testing and Materials – ASTM).

Detailed comparison with our previously obtained XRD data for similar compounds of Gallium, Indium and Scandium are also carried out /performed.

On the assumption of the fact that combinations of cations (Ag-Sc) for di- and triphosphates have not been studied and hence are not given in the file index (typical XRD data), roentgenograms was compared to our standard data models, to similar compounds of Ag-P and our standard data prototypes for similar double condensed phosphates of Gallium, Indium, Scandium with alkali metals.

We perform, that any initial components: K_2CO_3, Sc_2O_3, $AgNO_3$ are already completely irreversibly interreacted during synthesis process. Based on the founded and published literary data [16-17, 8,9,1-2] also on our synthesis conditions, on experiences in this field, and to our standard data models, the structural composition of the compounds is set up. Phase's identification was given an accordance with standard data of International Center for Diffraction Data base of American Society for Testing and Materials – ASTM. The composition of the synthesised condensed compounds are $AgSc(H_2P_2O_7)_2$ and $AgScHP_3O_{10}$.

XRD data for Triphosphate $AgScHP_3O_{10}$ are presented in Table 1.

ლიტერატურა - REFERENCES – ЛИТЕРАТУРА

1. Less-Common Element Chemistry**.** Rare-Earth Element Chemistry. Silicates, Germinates, Phosphates, Arsenates, Vanadates. Monograph, Chief-editor Acad. I.V.Tananaev. International Union of pure and Applied Chemistry. 1988
2. A. Durif. Crystal Chemistry of Condensed Phosphates**.** Springer Sci & Business Media, 2013, 445 p.
3. I.V.Tananaev , Pure & Appl. Chem., Vol.52, Pergamon Press Ltd. (1980) p.1099-1115.
4. M.-Th.Averbuch-Pouchot, A. Durif. Topics in Phosphate Chemistry.World Scientific, 1996. 420p.
5. A. Durif, Solid State Sci. v.7 ; 2005, p. 760-766.
6. E.V. Murashova, N.N. Chudinova; J. Neorgan. Mater., v. 37, N12, 2001, pp. 1521-1524
7. I. Grunze, N.N. Chudinova, X. Grunze; J. Neorgan. Mater., v.25, N6, 1989,p. 886-899.
8. I. Grunze, K. Palkina, N. Chudinova, M. Avaliani; Energy Citations Database; Inorg. Mater. (Engl. Transl.); v. 23:4, p. 539-544; OSTI ID: 5847982. System Entry Date- 2009.
9. M. Avaliani, M. Gvelesiani. Proceeding of Georgian Academy of Sciences, Chemical Series, v. 32, N1-2, 2006, p. 52-58
10. M. Avaliani, M. Gvelesiani, V. Gaprindashvili; Proceeding of Georgian Academy of Sciences Macne, Chemical Series, v. 25, N1-2, 1999, pp. 9-15
11. M. A. Avaliani, I.V. Tananaev; Intern. Conf. on Phosphorus chemistry, Talinn. Abst., 39, 1989.
12. M. Avaliani, B. Purtseladze et all; Proceeding of Georgian Academy of Sciences Macne, Chemical Series, v. 41, N3, p. 227-231, 2015.
13. M. Avaliani; International Conference on Advanced Materials and Technologies; 2015, p. 240-245.
14. M. Avaliani; Synthesis and investigation of Condensed phosphates of Gallium and Indium, Doct. Thesis, Moscow, N. Kurnakof Inst., (1982), p.185.
15. M. Avaliani, I.Tananaev; M. Gvelesiani. Electronic Abstr. cheminform no: 1991 02 035 Copyright (C) FIZ CHEMIE Berlin, journal: Phosphorus, Sulfur Silicon Relat. Elem. 1990 51-52, p. 453; CODEN PSSLEC; ISSN 1042-6507 / imprint static data : © 2003 - 2011 FIZ CHEMIE Berlin.
16. L.M. Komissarova, Inorganic and analytical Chemistry of Scandium (Monograph in Russian), EDITORIAL URSS, 2001, 512 p.
17. N.P. Vassel, S.S. Vassel and all. Thermo-investigation of systems with metaphosphates of trivalent metals and silver (web-article in Russian, available from Sergei Vassel), May, 2015.

პოლიკომპონენტური სისტემების კვლევა ახალი ტიპის არაორგანული პოლიმერების– კონდენსირებული ფოსფატების სინთეზის მიზნით

მარინე ავალიანი, მარინა გველესიანი, ნანა ბარნოვი, ბორის ფურცელაძე,
დალი ძანაშვილი, ეთერი შოშიაშვილი

ივანე ჯავახიშვილის სახელობის თბილისის სახელმწიფო უნივერსიტეტის რ.აგლაძის არაორგანული ქიმიისა და ელექტროქიმიის ინსტიტუტი, 0186, მინდელის ქ.11, თბილისი, საქართველო

რეზიუმე

კონდენსირებული ფოსფატების ქიმიის სწრაფი განვითერება ბოლო წლებში განპირობებულია არაორგანული პოლიმერებისადმი, როგორც ნაერთთა ახალი კლასისადმი დიდი ინტერესით და კვლევის ახალი მეთოდების დანერგვით. ჩვენს მიერ მიღებულია დღემდე უცნობი, სამვალენტიანი და ერთვალენტიანი მეტალების ორმაგი კონდენსირებული ნაერთები, როგორიცაა გალიუმის, ინდიუმის და სკანდიუმის ორმაგი ტეტრა-ჰექსა-, ციკლოქტა-, ციკლოდოდეკაფოსფატები. წარმოდგენილი სამუშაო ეხება სკანდიუმისა და ვერცხლის ორმაგ კონდენსირებულ ფოსფატებს, რომლებიც მიღებულია სისტემების M_2^IO-$M_2^{III}O_3$-P_2O_5-H_2O კვლევისას ტემპერატურულ ინტერვალში 120-160(170)°C, სადაც M^I– Ag, M^{III}–Sc. პირველადაა სინთეზირებული სკანდიუმ-ვერცხლის ორმაგი სხვადასხვა

შედგენილობის მჟავა დიფოსფატები $AgSc(H_2P_2O_7)_2$, $Ag_2ScH_3(H_2P_2O_7)_2$ და მჟავა ტრიფოსფატი $AgScHP_3O_{10}$ ნაერთები შესწავლილია რენტგენოფაზური ანალიზის მეშვეობით. მოტანილია ინდიცირებული რენტგენოგრამის მონაცემები.

ИССЛЕДОВАНИЕ ПОЛИКОМПОНЕНТНЫХ СИСТЕМ С ЦЕЛЬЮ ПОЛУЧЕНИЯ НОВОГО ТИПА НЕОРГАНИЧЕСКИХ ПОЛИМЕРОВ – ДВОЙНЫХ КОНДЕНСИРОВАННЫХ ФОСФАТОВ

М.А.Авалиани, М.К.Гвелесиани, Н.В.Барнова, Б.Х.Пурцеладзе, Д.Д.Дзанашвили, Э.Н.Шошиашвили

Институт неорганической химии и электрохимии им. Р.И.Агладзе Тбилисского государственного университета им. И.Джавахишвили, 0186, ул. Миндели11, Тбилиси, Грузия

РЕЗЮМЕ

Быстрое развитие химии конденсированных фосфатов за последние десятилетия обусловлено возрастающим интересом к классу неорганических полимеров и внедрением прогрессивных методов анализа и синтеза новых соединений. Нами получены не известные ранее двойные конденсированные фосфаты трехвалентных металлов с щелочными металлами: олигофосфаты, полифосфаты и циклофосфаты, такие, как двойные тетра-, гекса-, окта или додекафосфаты галлия, индия и скандия. Данная работа посвящена синтезу и исследованию новых двойных конденсированных фосфатов скандия-серебра, полученным в системах M_2^IO-$M_2^{III}O_3$-P_2O_5-H_2O в интервале температур 120-160℃, где M^I – Ag, M^{III}– Sc. Синтезированы двойные кислые дифосфаты $AgSc(H_2P_2O_7)_2$, $Ag_2ScH_3(H_2P_2O_7)_2$ и кислый трифосфат $\boldsymbol{AgScHP_3O_{10}}$. Соединения были изучены также и рентгенофазовым анализом. Приведены данные индицирования рентгенограммы.

SOLVENT EFFECT ON COMPLEX FORMATION OF DIMETHYL SULFOXIDE

Nana Gegeshidze*,**, Lali Skhirtladaze*, Aivengo Mamulashvili**,
Tamar Edilashvili**, Neli Maisuradze**

*R.Agladze Institute of Inorganic Chemistry and Electrochemistry of Ivane Javakhishvili Tbilisi State University, 0186, Mindeli st.11, Tbilisi, Georgia
**Georgian Technichal University, 77 Merab Kostava St., Tbilisi, Georgia, 0175
nana.ge18@yahoo.com

Energetic, geometric and structural characteristics of Dimethyl sulfoxide are determined by quantum chemical method AM1. According to electronic structure, solvent effect on its complex formation ability with metals is established.

The goal of our research was to study properties of complex formation of Dimethyl sulfoxide in different solutions, manifestation of its donor properties and synthesis of new coordination compounds on the basis of obtained results, and also study of physical-chemical properties of synthesized compounds.

Based of the quantum-chemical metod AM1 [1, 2] calculated the power, geometrical and structural features of Dimethyl sulfoxide. According to electronic structure, solvent effect on its complex formation ability with metals is established. Water, acetone, methanol, ethanol, dimethyl sulfoxide, chloroform, hexane are selected as solvents.

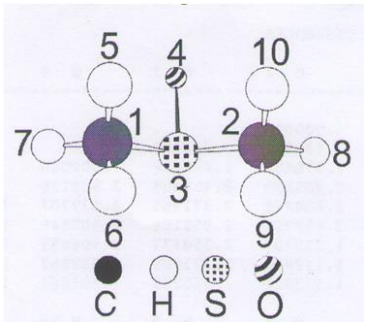

Picture 1. Molecul of of Dimethyl sulfoxside

Molecule formation heat, value of total energy, dipole moment, ionization potential, valence angles between atoms and bond lengths, effective charges, atomic orbitals filling with electrons etc. are calculated in all cases. These quantum-chemical calculations are shown in Table 1.

Table 1. Final heat of formation, net atomic charges and dipole contributions, atomic orbital electron populations in the molecul of dimethyl sulfoxside

№	Solvent, ε	ΔH, KJ	μ, Д	Atom	Charge, q	Electron density	Atomic orbital electron populations			
							2S	$2P_x$	$2P_y$	$2P_z$
1	Gas	-164.88	3.95	S(3)	1.393	4. 607	1.712	0.853	0.897	1.144
				O(4)	-0.778	6.778	1.946	1.844	1.649	1.338
2	Water, 78.5	-262.80	6.39	S(3)	1.581	4. 419	1.726	0.814	0.872	1.006
				O(4)	-1.025	7.025	1.939	1.907	1.793	1.386
3	Dimethyl sulfoxide, 49.0	-261.2	6.39	S(3)	1.579	4. 422	1.726	0.815	0.872	1.009
				O(4)	-1.021	7.021	1.939	1.905	1.791	1.385
4	Methanol, 32.6	-259.09	6.30	S(3)	1.574	4. 426	1.725	0.815	0.872	1.012
				O(4)	-1.016	7.016	1.940	1.904	1.788	1.384
5	Ethanol, 24.3	-257.13	6.25	S(3)	1.574	4. 426	1.725	0.816	0.872	1.015
				O(4)	-1.016	7.016	1.939	1.903	1.787	1.381
6	Acetone, 20.7	-255.77	6.21	S(3)	1.569	4.431	1.725	0.816	0.873	1.017
				O(4)	-1.008	7.008	1.940	1.903	1.786	1.370
7	Chloroform, 4.7	-228.84	5.50	S(3)	1.522	4.478	1.718	0.825	0.877	1.057
				O(4)	-0.943	6.941	1.941	1.887	1.748	1.367
8	Hexane, 1.9	-194.88	4.65	S(3)	1.456	4.544	1.714	0.839	0.885	1.106
				O(4)	-0.857	6.857	1.943	1.865	1.695	1.353

Table 2. Interatomic distances, bond orders and valencies in the molecule of dimethyl sulfoxside

	Solvent, ε	$R_{1,3}$	$P_{1.3}$	$R_{2,3}$	$P_{2.3}$	$R_{3,4}$	$P_{3.4}$
1	**Gas**	**1.739**	**0.796**	**1.739**	**0.796**	**1.491**	**1.336**
2	**Water**	**1.724**	**0.856**	**1.723**	**0.856**	**1.533**	**1.152**
3	**Dimethyl sulfoxide**	**1.725**	**0.855**	**1.724**	**0.855**	**1.532**	**1.155**
4	**Methanol**	**1.725**	**0.853**	**1.725**	**0.853**	**1.530**	**1.163**
5	**Ethanol**	**1.725**	**0.853**	**1.725**	**0.852**	**1.530**	**1.165**
6	**Acetone**	**1.725**	**0.853**	**1.725**	**0.852**	**1.530**	**1.165**
7	**Chlotofom**	**1.729**	**0.836**	**1.729**	**0.836**	**1.515**	**1.217**
9	**Hexane**	**1.734**	**0.815**	**1.734**	**0.815**	**1.50**	**1.280**

Table 3. Values of bond angles between the atoms in the molecule dimethyl sulfoxide

Angle	Solvent							
	Gas	**Water**	**DMSO**	**Methanol**	**Ethanol**	**Acetone**	**Chloroform**	**Hexane**
C_1-S_3-C_2	113.90	114.74	114.46	114.44	114.20	114.10	114.17	114.29

Analysis of the values of electron densities (formal population) and effective charges shows that the high values of the electron density is characterized by an Oxygen atom O (4), which is typical of any solvent. The Oxygen atom O (4) has a lone electron pair of δ-type. More precisely, he has a hybrid-type nuclear obrital sp^2 with s –component.

This circumstance determines the basic properties of the Oxygen atom O (4), i.e. its properties form the metal donor-acceptor bond.

Regarding Sulfur atom S (3), it can manifest electron-donor properties. Electron pair is on $3p_z$ orbitale, which is not capable of participating in bond formation with δ-type metal-complexing. The Sulfur atom S (3) can provide π-type bond and does not have possibility to provide δ-type bond with metal.

Compounds of copper(II), cobalt(II) and nichel(II) with Dimethyl sulfoxside are received. Copper(II), cobalt(II) and nichel(II) sulphates, chlorides and bromides have been taken as initial salts. Synthesis has been carried out in hot ethanol solutions.

New coordination compounds are received in solid state. Their composition is determined using elemental analysis, while individuality is defined via determination of melting temperature. Some physical-chemical properties are studies, namely: solubility in different inorganic and organic solvents. Synthesized compounds are studied using absorption infrared spectroscopy method.

ლიტერატურა - REFERENCES – ЛИТЕРАТУРА

1. Dewar M.I.S., Zoebich E.G., Rcoly E.F., Stewart I. AM1: A new purpose quantum mechanical molecular model. A.Amer. Chem. Soc. P. 3902-3909.
2. Химическая связь. Маррел Дж., Кент С., Тедер Дж. М.Мир 1980. 383 с.

გამხსნელის გავლენა დიმეთილსულფოქსიდის კომპლექსწარმოქმნის უნარზე

ნანა გეგეშიძე*,**, ლალი სხირტლაძე*, აივენგო მამულაშვილი**, თამარ ედილაშვილი**, ნელი მაისურაძე**

*რ.აგლაძის არაორგანული ქიმიისა და ელექტროქიმიის ინსტიტუტი

**საქართველოს ტექნიკური უნივერსიტეტი

რეზიუმე

ქვანტურ-ქიმიური მეთოდით AM1 გამოთვლილია დიმეთილსულფოქსიდის ენერგეტიკული, გეომეტრული და სტრუქტურული მახასიათებლები. ელექტრონული სტრუქტურის მიხედვით დადგენილია გამხსნელის გავლენა ლითონებთან მისი კომპლექსწარმოქმნის უნარზე.

ВЛИЯНИЕ РАСТВОРИТЕЛЯ НА КОМПЛЕКСООБРАЗУЮЩУЮ СПОСОБНОСТЬ ДИМЕТИЛСУЛЬФОКСИДА

Н. Гегешидзе*,**, Л.Схиртладзе*, А.Мамулашвили**, Т.Едилашвили**, Н.Маисурадзе**

*Иниститут неорганической химии и электрохимии им. Р.Агладзе

**Грузинский технический университет

РЕЗЮМЕ

Квантово-химическим методом AM1 вычислены энергетические, геометрические и структурные характеристики молекулы диметилсульфоксида. На основании электронной структуры определена зависимость способности комплексообразования молекулы с металлами от растворителей.

MIXED-LIGAND COORDINATION COMPOUNDS OF 3d-METALS WITH ORTO-AMINO-4,5-METHILPYRIDINE AND ISONYCOTINOILHIDRZONE OF PARA-DIMETHILAMINOBENZALDEHIDE

N.Kilasonia[*,**], M.Kereselidze[*], N.Tabuashvili[**], M.Mamiseishvili**, N.Endeladze[***]
**R.Agladze Institute Of Inorganic Chemistry and Electrochemistry*
***Georgian Technical University*
****Akaki Tsereteli State University, Kutaisi*

The goal of our research was the study of properties of complex formation of para-dimethylaminobenzaldehyde isonicotinoil-hydrazone, as well as methyl derivatives of aminopyridine, namely ortho-amino-4 and ortho-amino-5 methylpyridine molecules in different solutions, manifestaion of their donor properties and synthesis of new, different-ligand coordination compounds on the basis of obtained results, and also study of physical-chemical properties of synthesized compounds.

Calculation are made using quantum-chemical, semi-empirical AM1 method [1] in different solutions in order to study the property of complex formation of para-dimethylaminobenzaldehyde isonicotinoil-hydrazone, as well as ortho-amino-3,4,5 and 6-methylpyridine molecules and to study their electronic structure. Water, acetone, methanol, ethanol, dimethyl sulfoxide, chloroform, hexane are selected as solvents. Molecule formation heat, value of total energy, dipole moment, ionization potential, valence angles between atoms and bond lengths, effective charges, atomic orbitals filling with electrons etc. are calculated in all cases.

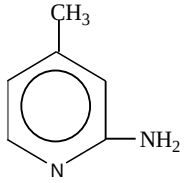

ortho-amino-5 methylpyridine

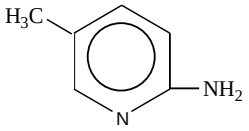

ortho-amino-4 methylpyridine

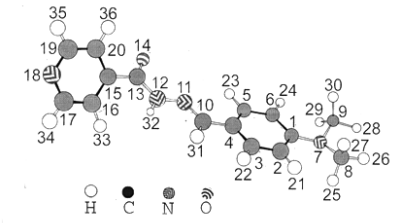

para-dimethylaminobenzaldehyde isonicotinoil-hydrazone

Calculation are made using quantum-chemical, semi-empirical AM1 method in different solutions in order to study the property of complex formation of para-dimethylaminobenzaldehyde isonicotinoil-hydrazone, as well as ortho-amino-3,4,5 and 6-methylpyridine molecules and to study their electronic structure. Water, acetone, methanol, ethanol, dimethyl sulfoxide, chloroform, hexane are selected as solvents. Molecule formation heat, value of total energy, dipole moment, ionization potential, valence angles between atoms and bond lengths, effective charges, atomic orbitals filling with electrons etc. are calculated in all cases. Oxygen atom of carbonyl group and nitrogen atom of azomethine group are manifested as donor atoms in hydrazone molecule. These atoms create σ-donor-acceptor bond with metal atoms. Besides, results of quantum-chemical calculations in different solutions show that coordination of hydrazone molecule with complex-former metal is possible both in cetonic and enol form, and as a result stable five-membered (pentatomic) metal cycles are forming.

As to molecules of methyl derivatives of aminopyridine, according to calculation results a nitrogen atom of heterocycle is manifested as donor atom.

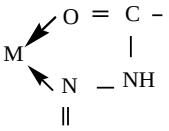
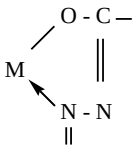

Manganese (II) cobalt (II), nickel (II) and copper (II) chlorides, nitrates and sulfates are taken as initial substances for synthesis of different-ligand coordination compounds with ortho-amino-4 and ortho-amino-5 methyl pyridines and with para-dimethylaminobenzaldehyde isonicotinoil- and nicotinoil hydrazones. Synthesis is carried out in hot ethanol solutions. Ratio of salt, hydrazone and methyl pyridine is 1:1:2. Cake (sediment) formation became visible directly as soon as hot ethanol solutions of salt and ligand were mixed. Obtained sediment has been filtrated, washed with cold ethanol and dried. Resulted substances have been cleaned by preliminary recrystallization from ethanol. 15 new coordination compounds are received in solid state. Their composition is determined using elemental analysis, while individuality is defined via determination of melting temperature. Some physical-chemical properties are studies, namely: solubility in different inorganic and organic solvents. Synthesized compounds are studied using X-ray diffraction method and absorption infrared spectroscopy method [2].

Infrared spectra (400-4000^{-1} cm range) of synthesized complex compounds' absorption are studied. Rule of organic ligands, water molecules and acido ligands coordination in synthesized compounds is established. Study of infrared spectra of coordination compounds' absorption shows that hydrazone coordinates with complex-former metal via oxygen atom of carbonyl group and nitrogen atom of azomethine group, while methyl pyridine molecules coordinate via nitrogen atoms of heterocycle that testifies the data of quantum-chemical calculations.

Presumable structure of synthesized complex compounds are offered on the basis of quantum-chemical, absorption infrared spectroscopy and X-ray diffraction data.

ლიტერატურა - REFERENCES – ЛИТЕРАТУРА

1. Dewar M.I.S., Zoebich E.G., Rcoly E.F., Stewart I. AM1: A new purpose quantum mechanical molecular model. A.Amer. Chem. Soc. P. 3902-3909.
2. Химическая связь. Маррел Дж., Кент С., Тедер Дж. М.Мир 1980. 383 с.

3d-მეტალების შერეულლიგანდიანი კოორდინაციული ნაერთების სინთეზი და ფიზიკურ-ქიმიური თვისებების კვლევა

ნ.კილასონია[*,**], მ.კერესელიძე[*], ნ.თაბუაშვილი**, მ.მამისეიშვილი**, ნ.ენდელაძე[***]

[*]რ.აგლაძის არაორგანული ქიმიის და ელექტროქიმიის ინსტიტუტი

[**]საქართველოს ტექნიკური უნივერსიტეტი

[***]აკაკი წერეთლის სახელმწიფო უნივერსიტეტი, ქუთაისი

რეზიუმე

პარა-დიმეთილამინობენზალდეჰიდის იზონიკოტინოილჰიდრაზონის და ორთო-ამინო 4,5-მეთილპირიდინების მოლეკულათა კომპლექსწარმოქმნის უნარის და ელექტრონული სტრუქტურის შესწავლის მიზნით ჩატარებულია გათვლები კვანტურ-ქიმიური ნახევრადემპირიული AM1 მეთოდით სხვადასხვა გამხსნელში (წყალი, აცეტონი, დიმეთილფორმამიდი, დიმეთილსულფოქსიდი, ქლოროფორმი, ჰექსანი).

СИНТЕЗ И ИССЛЕДОВАНИЕ ФИЗИКО-ХИМИЧЕСКИХ СВОЙСТВ СМЕШАННОЛИГАНДНЫХ КООРДИНАЦИОННЫХ СОЕДИНЕНИИ 3d-МЕТАЛЛОВ

Н.Киласония[*,**], М.Кереселидзе[*], Н.Табуашвили**, М.Мамисеишвили**, Н.Энделадзе[***]

**Институт неорганической химии и электрохимии им. Р.Агладзе*

***Грузинский технический университет*

****Государственный университет им.А.Церетели, Кутаиси*

РЕЗЮМЕ

С целью изучения комплексообразующей способности и электронной структуры молекул изоникотиноилгидразона, пара-диметиламинобензальдегида и орто-амино 4,5-метилпиридинов проведены расчеты квантово-химическим полуэмпирическим методом AM1 в различных растворителях (вода, ацетон, диметилформамид, диметилсульфоксид, хлороформ, гексан).

CHROMIUM CHELATES WITH BIOLOGICALLY ACTIVE LIGANDS

Spartak Urotadze, Iamze Beshkenadze, Nani Zhorzholiani, Maia Gogaladze, Nazibrola Klarjeishvili, Vladimer Tsitsishvili
Tbilisi State University, Petre Melikishvili Institute of Physical and Organic Chemistry
spartakurotadze@yahoo.com

Synthesis of trivalent chromium amorphous chelates $Cr(Mt)_3 \cdot 2H_2O$ (Mt – methionine anion) and $Cr \cdot Lig \cdot nH_2O$ (Lig – citrate ion (n=4), nitrilotriacetic acid anion (n=3)), as well as crystalline chelates of general formula $Cr_2 \cdot Lig_3 \cdot nH_2O$ (Lig – anions of succinic acid (n=0), tartaric acid (n=2), glutaminic acid (n=4), and cystine (n=5)) has been carried out for their further testing to define possibilities of their agricultural application as fertilizers, premixes, biologically active fodder additives. Experimentally defined elemental composition of synthesized compounds is in good accordance with corresponding calculated values; solubility of compounds in water and organic solvents is determined, and it is postulated, that chelates containing bivalent ligands are practically insoluble; said crystalline chelates are characterized by X-ray diffraction pattern parameters.

Introduction

Chromium (Cr) has been studied since the end of the 19th century, when carcinogenic effects of hexavalent Cr were discovered [1]. Essentiality of trivalent Cr was demonstrated in 1959; Cr^{3+} has been studied in humans and laboratory animals since the 1970-ies and it is only since the 1990-ies that Cr has been studied as an essential element in livestock animals with the same intensity. Trivalent chromium is essential to normal carbohydrate, lipid and protein metabolism, it is biologically active as a part of an oligopeptide – chromodulin – potentiating the effect of insulin by facilitating insulin binding to receptors at the cell surface. With chromium acting as a cofactor of insulin, Cr activity in the organism is parallel to insulin functions.

The demand for Cr has been growing as a result of factors commonly referred to as stressors, especially during different forms of nutritional, metabolic and physical strain. Absorbed Cr circulates in blood bound to the β-globulin plasma fraction and is transported to tissues bound to transferrin. Absorbed Cr is excreted primarily in urine, by glomerular filtration; a small amount is excreted through perspiration, bile and in milk. Review describing Cr metabolism, the different biological functions of Cr and symptoms od Cr deficiency was published in 2007 [2].

Cr absorption is low, ranging between 0.4 and 2.0% for inorganic compounds while the availability of organic Cr is more than 10 times higher [3]. There is information about the successful application of chromium coordination compounds in poultry and livestock [4-9], although published evidence [10] that chromium picolinate (Tris(picolinate)chromium(III), $Cr(C_6H_4NO_2)_3$) and nicotinate (Chromium(3+) tri(pyridine-3-carboxylate), $C_{18}H_{12}CrN_3O_6$) can be dangerous just because of organic parts (residues of picoline and nicotine acids) of said coordination compounds.

The aim of present study was to prepare chromium coordination compounds (chelates) with safe and nontoxic biologically active organic part (ligands) for their further testing to define possibilities of their agricultural application as premixes and fodder additives. Methionine ($HO_2CCH(NH_2)CH_2CH_2SCH_3$ = HMt), cystine ($C_6H_{12}N_2O_4S_2$ = H_2Cst), glutaminic acid ($C_5H_9NO_4$ = H_2Gl), as well as citrate acid ($H_3(C_6H_5O7)$), nitrilotriacetic acid (Trilon A, $N(CH_2COOH)_3$ = H_3NTA), succinic acid ($C_4H_6O_4$ = H_2SA) and tartaric acid ($C_4H_6O_6$ = H_2TA) have been used for construction of chelates.

Experimental

Trivalent chromium chelates $Cr(Mt)_3 \cdot 2H_2O$ (Mt – methionine anion ($O_2CCH(NH_2)CH_2CH_2SCH_3)^-$) and $Cr \cdot Lig \cdot nH_2O$ (Lig – citrate ion ($(C_6H_5O7)^{3-}$, n=4), nitrilotriacetic acid anion ($N(CH_2COO^-)_3$, n=3)) and chelates of general formula $Cr_2 \cdot Lig_3 \cdot nH_2O$ (Lig – anions of succinic acid ($(C_4H_4O_4)^{2-}$, n=0), tartaric acid ($(C_4H_4O_6)^{2-}$, n=2), glutaminic acid ($(C_5H_7NO_4)^{2-}$, n=4), and cystine ($(C_6H_{10}N_2O_4S_2)^{2-}$, n=5)) have been prepared from the Chromium(III)acetate ($C_6H_9CrO_6$) taking coordination compound and organic part in corresponding molar ratio. Optimal conditions (reactor vessel, solvent, temperature, duration, etc.) of reaction to be carried out, and tools for separating and cleaning targeted products have been chosen experimentally; chemical content of prepared compounds was testified by

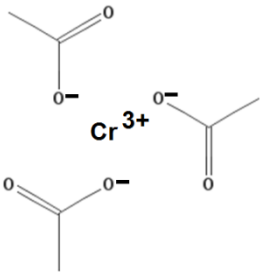

partial elemental analysis (CHN Analyser, Labertherm GmbH), X-ray diffraction patterns have been recorded on DRON-3M instrument, melting temperatures measured on Dynalon SMP10.

Results

Chemical content of prepared chelates is given in the Table 1, experimentally measured values are in a good agreement with calculated ones for the metal, carbon, hydrogen, and nitrogen content.

Table 1. Data of elemental analysis for prepared compounds

Formula	Molecular mass, mol/g	Measured, %				Calculated, %			
		Cr	C	H	N	Cr	C	H	N
$Cr(Mt)_3 \cdot 2H_2O$	532.69	9.53	34.21	5.98	7.56	9.76	33.82	6.39	7.89
$Cr \cdot L \cdot 4H_2O$	313.19	16.30	23.25	4.00	–	16.6	23.01	4.18	–
$Cr \cdot NTA \cdot 3H_2O$	291.45	17.66	24.54	4.35	4.78	17.84	24.73	4.15	4.8
$Cr_2 \cdot (SA)_3$	452.27	22.69	31.75	4.49	–	22.99	31.87	2.65	–
$Cr_2 \cdot (TA)_3 \cdot 2H_2O$	584.3	17.57	24.77	2.95	–	17.8	24.67	2.76	–
$Cr_2 \cdot (Gl)_3 \cdot 5H_2O$	629.465	16.76	28.02	4.68	6.47	16.52	28.62	4.48	6.67
$Cr_2 \cdot (Cst)_3 \cdot 4\ H_2O$	890.96	12.01	24.87	4.5	9.31	11.67	24.27	4.3	9.43

Several characteristics of synthesized compounds are given in Table 2, trivalent chromium chelates $Cr(Mt)_3 \cdot 2H_2O$ and $Cr \cdot L \cdot 4H_2O$ are amorphous compounds, and chelates of general formula $Cr_2 \cdot Lig_3 \cdot nH_2O$ (Lig = $(C_4H_4O_4)^{2-}$, n=0; $(C_4H_4O_6)^{2-}$, n=2; $(C_5H_7NO_4)^{2-}$, n=4; $(C_6H_{10}N_2O_4S_2)^{2-}$, n=5) are crystalline compounds with well-resolved X-ray diffraction patterns (see Table 3).

Table 2. Colour and solubility of synthesized compound

Chemical formula	Colour	Solubility			
		H_2O	C_2H_5OH	$(CH_3)_2CO$	C_3H_7NO
$Cr(Mt)_3 \cdot 2H_2O$	Violet	+	Low	–	Low
$Cr \cdot L \cdot 4H_2O$	Dark green	+t	–	–	–
$Cr \cdot NTA \cdot 3H_2O$	Gray green	+t	Low	Low	–
$Cr_2 \cdot (SA)_3$	Green	–	–	–	–
$Cr_2 \cdot (TA)_3 \cdot 2H_2O$	Green	Low	Low	–	–
$Cr_2 \cdot (Gl)_3 \cdot 5H_2O$	Gray violet	Low	–	–	–
$Cr_2 \cdot (Cst)_3 \cdot 4\ H_2O$	Gray	Low	Low	Low	Low

Table 3. X-ray diffraction characteristics of chromium (III) synthesized compounds

$Cr_2 \cdot (Gl)_3 \cdot 5H_2O$			$Cr_2 \cdot (SA)_3$			$Cr_2 \cdot (Cst)_3 \cdot 4H_2O$			$Cr_2 \cdot (TA)_3 \cdot 2H_2O$		
2θ	D	I/I_0	2θ	d	I/I_0	2θ	D	I/I_0	2θ	D	I/I_0
5.13	17.218	1.0892	5.19	17.027	0.7767	10.85	8.154	0.2144	10.80	8.192	0.3615
10.79	8.201	0,7321	7.74	11.422	0.9328	12.31	7.190	0.1566	11.01	8.036	0.8384
13.16	6.729	0.3714	9.03	9.793	0.3357	13.33	6.642	0.0955	13.22	6.697	0.4076
15.68	5.651	1	10.34	8.555	0.3728	15.80	5.609	1	13.40	6.607	0.700
16.22	5.465	0.1357	12.26	7.219	0.5271	17.11	5.182	0.1366	15.90	5.574	0.9384
17.10	5.185	0.2883	15.53	5.706	0.1614	18.35	4.835	0.1000	17.25	5.140	0.3923
18,29	4.849	0.3714	17.29	5.129	0.1557	19.35	4.587	0.0577	18.56	4.780	0.3923
19.82	4.480	0.1214	18.09	4.904	0.3642	19.82	4.479	0.1800	20.19	4.398	0.2846
20.21	4.393	0.0428	20.07	4.424	1	21.80	4.077	0.1211	20.77	4.277	0.5538
20.68	4.295	0.1642	20.34	4.366	0.3900	23.15	3.842	0.1422	21.83	4.071	0.6076
21.58	4.118	0.8428	20.74	4.283	0.6671	23.84	3.732	0.0377	22.02	4.036	0.3769
22.24	3.998	0.1750	21.60	4.114	0.3328	24.62	3.616	0.0566	23.05	3.858	0.1615
22.67	3.922	0.1000	22.00	4.040	0.0928	25.46	3.498	0.0977	23.92	3.720	0.400
23.60	3.769	0.3178	22.22	4.001	0.2114	26.41	3.375	0.1944	26.51	3.362	1
24.02	3.705	0.0571	23.34	3.811	0.0800	29.03	3.076	0.0722	29.15	3.063	0.2769

Table 3 –continueed

$Cr_2\cdot(Gl)_3\cdot5H_2O$			$Cr_2\cdot(SA)_3$			$Cr_2\cdot(Cst)_3\cdot4H_2O$			$Cr_2\cdot(TA)_3\cdot2H_2O$		
2θ	D	I/I_0	2θ	d	I/I_0	2θ	D	I/I_0	2θ	D	I/I_0
26.04	3.421	0.1321	24.43	3.643	0.3200	30.52	2.929	0.0600	30.23	2.956	0.2846
26.23	3.397	0.8464	25.86	3.445	0.1357	31.05	2.880	0.0933	31.11	2.875	0.9461
29.07	3.072	0.1142	26.38	3.378	0.0857	31.85	2.810	0.0788	32.02	2.795	0.1307
30.54	2.927	0.5714	26.84	3.322	0.0714	34.04	2.634	0.0854	33.92	2.643	0.2384
31.25	2.862	0.1964	27.59	3.233	0.0500	37.35	2.408	0.0755	34.42	2.605	0.1230
31.63	2.829	0.1607	28.47	3.135	0.0242	37.82	2.379	0.0688	35.37	2.538	0.1538
32.67	2.741	0.0750	28.84	3.096	0.2014	40.47	2.229	0.0711	35.82	2.507	0.4230
33.29	2.712	0.1464	29.88	2.990	0.0842	44.29	2.045	0.0488	37.74	2.384	0.3000
33.84	2.649	0.3571	30.05	2.974	0.1442	45.80	1.981	0.0233	37.88	2.375	0.3538
35.09	2.557	0.2357	30.17	2.962	0.0714	46.96	1.935	0.0488	40.33	2.228	0.3307
35.90	2.501	0.2250	30.55	2.926	0.0371	48.72	1.869	0.0944	40.71	2.216	0.3692
37.08	2.425	0.2034	31.40	2.849	0.2785	50.20	1.817	0.0366	44.26	2.046	0.4538
37.47	2.400	0.4301	32.48	2.757	0.3857				44.57	2.033	0.3538
38.25	2.353	0.3464	33.88	2.646	0.2585				47.02	1.932	0.2153
40.10	2.248	0.3254	34.91	2.570	0.0728				46.99	1.934	0.2230
40.15	2.246	0.1324	35.91	2.501	0.2385				48.71	1.869	0.2076
40.15	2.246	0.1324	35.91	2.501	0.2385				48.71	1.869	0.2076
42.39	2.132	0.0857	38.64	2.330	0.1100				48.87	1.864	0.2528
42.92	2.107	0.0392	38.91	2.315	0.0714				54.69	1.678	0.0923
43.86	2.064	0.2964	39.81	2.264	0.0814						
44.69	2.028	0.0678	40.64	2.220	0.1000						
46.62	1.948	0.1821	41.22	2.190	0.1442						
48.16	1.889	0.1392	43.16	2.096	0.1327						
48.61	1.873	0.0392	44.74	2.026	0.1800						
49.25	1.850	0.1142	46.34	1.959	0.0900						
50.57	1.805	0.0857	47.57	1.911	0.0600						
52.68	1.738	0.1107	48.26	1.886	0.0447						
53.07	1.704	0.1142	49.34	1.847	0.0300						
54.58	1.681	0.0642	50.34	1.813	0.0514						
57.92	1.592	0.0285									

X-ray diffraction pattern of chelate containing glutaminic acid residue is nearly similar to pattern of chelate coordinated by cysteine residue, that can display possibility for compounds $Cr_2\cdot(Gl)_3\cdot5H_2O$ and $Cr_2\cdot(Cst)_3\cdot4H_2O$ to have the isomorphous crystal structures, but it is impossible to solve such problem without X-ray structural study.

Chelates containing bivalent ligands are practically insoluble, which limits their applicability.

ლიტერატურა - REFERENCES – ЛИТЕРАТУРА

1. M.D.Cohen, B.Kargacin, C.B.Klein, M.Costa. Mechanisms of chromium carcinogenity and toxity. Critical Reviews in Toxicology, 1993, v. 23, p. 255-281.
2. A.Pechova, L.Pavlata. Chromium as an essential nutrient: a review. Veterinarni Medicina, 2007, v. 52, No 1, p. 1-18.
3. N.S.C.Chen, A.Tsai, I.A.Duer. Effects of chelating agents on chromium absorption in rats. Journal of Nutrition, 1973, v. 103, p. 1182-1186.
4. Mathison G.W., Engstrom D.F. Chromium and protein supplement for growing-finishing beef steers fed barley-based diets. Canadian J. Animal Sci., 1995, v. 75, p. 549-558.
5. Гогин А.Е. Взаимосвязь хрома с минеральными веществами и жирорастворимыми витаминами в организме мясных цыплят. Автореф. дис. канд: с.-х. наук. Сергиев-Посад, 2001. – 22 с.
6. Федаев А.Н., Кокорев В.А., Гибалкина Н.И. Теоретическое и практическое обоснование использования хрома в кормлении молодняка крупного скота. Саранск, 2003. – 224 с.
7. Pechova A., Pavlata L. Chromium as an essential nutrients: a review. Veterinarni Medicina (Czech Republic), 2007, v. 52, No 1, p. 1-18.
8. Лебедев С.В., Мирошников С.А., Суханова О.Н., Рахматуллин Ш.Г., Малюшин Е.Н., Сипайлова О.Ю., Кван О.В., Барабаш А.А., Нестеров Д.В. Способ повышения продуктив-

ности цыплят-бройлеров. Патент РФ на изобретение № 2370095 A23K 1/00, 20.10.2009, бюллетень № 29.
9. Кочеткова Н., Шапошников А., Симонов Г., Затеев В., Никульников В. Цитраты биометаллов в рационах цыплят-бройлеров. Птицеводство, 2010, www.webpticeprom.ru.
10. Vincent J.B. Chromium: Celebrating 50 years as an essential element? Dalton Transactions, 2010, v. 39, No 16, p. 3787-3794.

ქრომის ხელატები ბიოლოგიურად აქტიური ლიგანდებით

სპარტაკ უროტაძე, იამზე ბეშკენაძე, ნანი ჟორჟოლიანი, მაია გოგალაძე, ნაზიბროლა კლარჯეიშვილი, ვლადიმერ ციციშვილი
პეტრე მელიქიშვილის ფიზიკური და ორგანული ქიმიის ინსტიტუტი

რეზიუმე

ჩატარებულია სამვალენტიანი ქრომის (III) ამორფული ხელატური ნაერთების $Cr(Mt)_3 \cdot 2H_2O$ (I) და $Cr \cdot Lig \cdot nH_2O$ (Lig – ციტრატ-იონი (n=4), ნიტრილოტრიძმარმჟავას ანიონი (n=3)), აგრეთვე კრისტალური ხელატური ნაერთების $Cr_2 \cdot Lig_3 \cdot nH_2O$ (Lig – ქარვის მჟავის (n=0), ღვინის მჟავის (n=2), გლუტამინის მჟავისა (n=4) და ცისტეინის (n=5) ანიონები) სინთეზი სასოფლო-სამეურნეო დანიშნულებით მათი შემდგომი გამოყენების მიზნით. მიღებული ნაერთების ექსპერიმენტულად განსაზღვრული ელემენტური შემადგენლობა ემთხვევა გამოთვლილს, განსაზღვრულია მათი ხსნადობა წყალსა და ორგანულ გამხსნელებში. დადგენილია, რომ ორვალენტიანი ლიგანდების შემცველი ხელატები პრაქტიკულად უხსნადია, რაც ზღუდავს მათი გამოყენების სფეროს. კრისტალური ნაერთები დახასიათებულია რენტგენული დიფრაქტომეტრიის პარამეტრებით.

ХЕЛАТЫ ХРОМА С БИОЛОГИЧЕСКИ АКТИВНЫМИ ЛИГАНДАМИ

С.Уротадзе, И.Бешкенадзе, Н.Жоржолиани, М.Гогаладзе, Н.Кларджеишвили, В.Цицишвили
Институт физической и органической химии им. П.Г.Меликишвили
Тбилисский государственный университет им. Ив.Джавахишвили

РЕЗЮМЕ

Проведён синтез аморфных хелатов трёхвалентного хрома $Cr(Mt)_3 \cdot 2H_2O$ (Mt – анион метионина) и $Cr \cdot Lig \cdot nH_2O$ (Lig – цитрат-ион, n=4; анион нитрилотриуксусной кислоты, n=3), а также кристаллических хелатов хрома $Cr_2 \cdot Lig_3 \cdot nH_2O$ (Lig – анионы сукциновой (n=0), тартаровой (n=2), глютаминовой (n=4) кислот и цистина (n=5)) для их дальнейших испытаний с целью определить возможности сельскохозяйственного использования в качестве удобрений, премиксов, биологически активных пищевых добавок. Определённый экспериментально элементный состав синтезированных соединений совпадает с расчетным; определена их растворимость в воде и органических растворителях, и установлено, что содержащие двухвалентные лиганды хелаты практически нерастворимы, что ограничивает область их применения. Кристаллические хелаты охарактеризованы параметрами рентгеновской диффрактометрии.

SOLVENT EFFECT ON COMPLEX FORMATION OF DIMETHYLACETAMIDE AND N,N-DIMETHYLFORMAMIDE

G.Tsintsadze, D.Lochoshvili*, T.Giorgadze, E.Topuria, T.Tusiashvili
Georgian Technical University, Tbilisi, Georgia
**R.Agladze Institute of Inorganic Chemistry and Electrochemistry of the Iv.Javakhishvili Tbilisi State University, Tbilisi, Georgia, dimitri.lochoshvili@tsu.ge*

Various characteristics: formation heat, dipole moment, interatomic distances, bond orders, valence angle and electron population at atomic orbitals were calculated for dimethylacetamide and N,N-dimethylformamide by means of quantum-chemical semiempirical AM1 method in gaseous phase and in seven various solvents.The coordination ability of these molecules with organic ligands as well as with complex former metal was established.

It was expected, that dimethylacetamide and N,N-dimethylformamide (Fig. 1) as organic ligands will form a coordination bond with complex former metal by means of nitrogen as well as by oxygen. Actually x-ray structural analysis and infrared spectra of coordination compounds, obtained with above-mentioned ligands, have shown that the bond with complex former metal is formed only by oxygen atom. The aim was to ascertain the cause of coordination by oxygen atom instead of nitrogen one. For this purpose the use of semiempirical method – AM1 of modern computer quantum chemistry was decided which allows to calculate the structure and properties of interested molecules by means of relatively low power computer in rational time by experimentally closer [1-4].

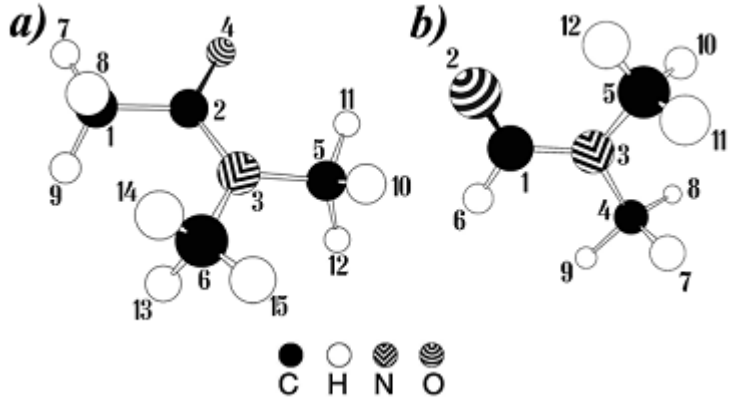

Fig. 1 ***a***–Dimethylacetamide and ***b***–N,N-dimethylformamide molecule

Energetic and structural characteristics of organic ligands – dimethylacetamide and N,N-dimethylformamide, were determined by calculation in gaseous phase as well as in various solvents, particularly, in water, dimethylsulfoxide, methanol, ethanol, acetone, chloroform and hexane.

Analysis of calculated formation heats and dipole moments (Tables 1-2) shows, that the stability of both molecules increases in the solvents in comparison with gaseous phase. The maximum value of this parameter is attained in water and minimum – in hexane. As to dipole moment, it also increases in solvents and maximum value is attained in water and dimethylsulfoxide. This fact may be explained by formation of dipole induction moment. From mentioned tables is also evident that in the case of both molecules oxygen s-orbitals and nitrogen p_z-orbitals are characterized by high electron density. Since it is well known that p_z-orbital may participate in the formation of π-bonds instead of σ-bond, it is apparent that nitrogen atom can not form σ-bond with complex former metal. Also an attention must be drawn to two methyl groups, associated with nitrogen atom, which form steric hindrances for bond with complex former metal.

All aforementioned explains the formation of monodentate bond with complex former metal only by oxygen atom instead of nitrogen atom. Analysis of the interatomic distances and bond orders value (Tables 3-4) shows, that respectively the maximum and minimum values of these parameters are is attained in water. Taking into consideration the fact, that an increase of bond length and order decrease causes an increase of reactivity, it may be suggested that for synthesis of coordination compound the use of water is reasonable.

It should be noted that calculated energetic and structural characteristics of the molecules of dimethylacetamide and N,N-dimethylformamide (Tables 3-6) are in close with X-ray structural data of $Ni(NCS)_2[CH_3CON(CH_3)_2]_4$ and $Me(NCS)_2[HCON(CH_3)_2]_4$, where *Me*=Mn(II); Co(II); Ni(II) [5-7].

Table 1. Solvent dielectric permeability (ε), heat of formation(ΔH), dipole moment (μ), charge on atom (q), atomic orbital electron population (s,p) of molecule dimethylacetamide.

N	Solvent,ε	ΔH, kJ/mole	μ, D	Atom	Q	Atomic orbital electron population			
						2s	$2p_x$	$2p_y$	$2p_z$
1	Gas	-173.39	3.59	C(2)	0.303	1.225	0.896	0.828	0.748
				N(3)	-0.343	1.470	1.067	1.055	1.752
				O(4)	-0.370	1.917	1.692	1.287	1.473
2	Water, 78.5	-222.67	5.99	C(2)	-0.348	1.227	0.905	0.818	0.702
				N(3)	-0.307	1.469	1.078	1.064	1.696
				O(4)	-0.575	1.915	1.731	1.322	1.607
3	Dimethylsulfoxide, 49.0	-221.79	5.95	C(2)	0.348	1.227	0.905	0.818	0.703
				N(3)	-0.308	1.469	1.078	1.636	1.698
				O(4)	-0.571	1.915	1.730	1.321	1.604
4	Methanol, 32.6	-220.57	5.90	C(2)	0.347	1.227	0.905	0.818	0.703
				N(3)	-0.309	1.469	1.078	1.063	1.699
				O(4)	-0.567	1.915	1.730	1.320	1.601
5	Ethanol, 24.3	-219.43	5.84	C(2)	0.346	1.227	0.904	0.819	0.704
				N(3)	-0.310	1.469	1.078	1.063	1.701
				O(4)	-0.562	1.915	1.729	1.319	1.598
6	Acetone, 20.7	-218.66	5.80	C(2)	0.346	1.227	0.904	0.818	0.705
				N(3)	-0.311	1.469	1.078	1.063	1.702
				O(4)	-0.558	1.915	1.727	1.320	1.596
7	Chloroform, 4.7	-204.08	5.13	C(2)	0.335	1.226	0.901	0.822	0.716
				N(3)	-0.326	1.469	1.074	1.061	1.722
				O(4)	-0.500	1.915	1.715	1.312	1.557
8	Hexane, 1.9	-186.13	4.34	C(2)	0.317	1.225	0.899	0.825	0.734
				N(3)	-0.340	1.468	1.070	1.058	1.743
				O(4)	-0.428	1.916	1.699	1.303	1.509

Table 2. Solvent dielectric permeability (ε), heat of formation(ΔH), dipole moment (μ), charge on atom (q), atomic orbital electron population (s,p) of molecule N,N-dimethylformamide.

N	Solvent,ε	ΔH, kJ/mole	μ, D	Atom	Q	Atomic orbital electron population			
						2s	$2p_x$	$2p_y$	$2p_z$
1	Gas	-154.60	3.55	C(1)	0.262	1.245	0.890	0.857	0.746
				O(2)	-0.365	1.915	1.110	1.873	1.466
				N(3)	-0.353	1.471	1.063	1.073	1.746
2	Water, 78.5	-208.52	5.85	C(1)	0.310	1.256	0.873	0.879	0.682
				O(2)	-0.588	1.914	1.156	1.907	1.610
				N(3)	-0.312	1.472	1.086	1.073	1.681
3	Dimethylsulfoxide, 49.0	-204.72	5.88	C(1)	0.307	1.254	0.873	0.882	0.684
				O(2)	-0.580	1.914	1.156	1.907	1.601
				N(3)	-0.314	1.472	1.082	1.073	1.685
4	Methanol, 32.6	-203.01	5.81	C(1)	0.305	1.255	0.874	0.881	0.685
				O(2)	-0.575	1.914	1.156	1.908	1.597
				N(3)	-0.315	1.474	1.082	1.073	1.686
5	Ethanol, 24.3	-205.02	5.69	C(1)	0.309	1.255	0.874	0.877	0.685
				O(2)	-0.574	1.914	1.154	1.905	1.601
				N(3)	-0.316	1.472	1.084	1.073	1.687
6	Acetone, 20.7	-204.23	5.67	C(1)	0.308	1.254	0.875	0.877	0.686
				O(2)	-0.571	1.915	1.153	1.905	1.599
				N(3)	-0.316	1.471	1.084	1.073	1.688
7	Chloroform, 4.7	-188.93	4.97	C(1)	0.297	1.251	0.880	0.870	0.701
				O(2)	-0.507	1.915	1.140	1.896	1.558
				N(3)	-0.331	1.471	1.077	1.073	1.710
8	Hexane, 1.9	-170.37	4.17	C(1)	0.280	1.248	0.886	0.863	0.724
				O(2)	-0.430	1.915	1.124	1.884	1.507
				N(3)	-0.345	1.471	1.070	1.073	1.732

Table 3. Interatomic distances (R) and bond orders (P) of molecule dimethylacetamide.

Bond		Solvent							
		Gas	Water	Dimethylsulfoxide	Methanol	Ethanol	Acetone	Cloroform	Hexane
C_1-C_2	R, Å	1.508	1.503	1.503	1.503	1.503	1.503	1.504	1.506
	P	0.941	0.954	0.954	0.953	0.953	0.954	0.950	0.945
C_2-N_3	R, Å	1.390	1.372	1.372	1.373	1.373	1.374	1.379	1.385
	P	1.066	1.194	1.192	1.189	1.185	1.183	1.144	1.101
C_2-O_4	R, Å	1.248	1.267	1.267	1.266	1.266	1.265	1.259	1.253
	P	1.755	1.568	1.572	1.576	1.581	1.585	1.640	1.704
N_3-C_5	R, Å	1.435	1.440	1.440	1.440	1.440	1.440	1.439	1.437
	P	0.941	0.931	0.931	0.931	0.931	0.932	0.933	0.935
N_3-C_6	R, Å	1.432	1.439	1.439	1.439	1.438	1.438	1.437	1.433
	P	0.951	0.932	0.932	0.933	0.933	0.934	0.939	0.945

Table 4. Interatomic distances (R) and bond orders (P) of molecule N,N-dimethylformamide.

Bond		Solvent							
		Gas	Water	Dimethylsulfoxide	Methanol	Ethanol	Acetone	Cloroform	Hexane
C_1-O_2	R, Å	1.243	1.264	1.262	1.262	1.262	1.262	1.255	1.248
	P	1.780	1.581	1.591	1.597	1.595	1.597	1.657	1.727
C_1-N_3	R, Å	1.380	1.362	1.364	1.365	1.364	1.363	1.369	1.375
	P	1.080	1.217	1.213	1.208	1.207	1.206	1.162	1.115
N_3-C_4	R, Å	1.433	1.441	1.441	1.441	1.440	1.440	1.438	1.435
	P	0.950	0.933	0.930	0.931	0.934	0.934	0.939	0.945
N_3-C_5	R, Å	1.435	1.439	1.440	1.439	1.439	1.439	1.438	1.436
	P	0.943	0.934	0.933	0.934	0.935	0.935	0.937	0.940

Table 5. Values of valence angles of molecule dimethylacetamide.

Angle	Solvent							
	Gas	Water	Dimethylsulfoxide	Methanol	Ethanol	Acetone	Cloroform	Hexane
C_1-C_2-N_3	118.56	120.20	120.18	120.19	120.14	120.00	119.69	119.15
C_1-C_2-O_4	120.92	120.31	120.32	120.31	120.34	120.48	120.72	121.10
C_2-N_3-C_5	120.90	119.78	119.76	119.79	119.77	119.60	119.47	119.19
C_2-N_3-C_6	120.94	120.42	120.42	120.39	120.40	120.54	120.53	120.70
C_2-C_1-H_7	108.58	109.23	109.22	109.17	109.16	109.27	108.96	108.77
C_2-C_1-H_8	110.11	110.22	110.22	110.24	110.24	110.05	110.34	110.38
C_2-C_1-H_9	110.97	110.31	110.32	110.32	110.32	110.51	110.36	110.47
N_3-C_5-H_{10}	109.67	110.47	110.47	110.47	110.47	110.51	110.54	110.59
N_3-C_5-H_{11}	110.11	109.73	109.73	109.67	109.67	109.76	109.68	110.67
N_3-C_5-H_{12}	110.37	109.91	109.91	109.94	109.94	109.99	109.97	109.96
N_3-C_6-H_{13}	111.07	110.27	110.27	110.30	110.31	110.36	110.44	110.55
N_3-C_6-H_{14}	110.36	110.09	110.10	110.07	110.08	110.14	110.18	110.30
N_3-C_6-H_{15}	109.83	110.30	110.31	110.29	110.30	110.40	110.38	110.45
O_4-C_2-N_3	120.51	119.49	119.49	119.51	119.52	119.51	119.59	119.75
C_5-N_3-C_6	117.64	119.78	119.80	119.77	119.78	119.81	119.95	120.06

Table 6. Values of valence angles of molecule N,N-dimethylformamide.

Angle	Solvent							
	Gas	Water	Dimethylsulfoxide	Methanol	Ethanol	Acetone	Cloroform	Hexane
O_2-C_1-N_3	122.92	121.88	122.20	121.76	121.86	122.00	122.24	122.61
C_1-N_3-C_4	121.26	120.80	119.75	119.48	120.80	120.87	121.01	121.15
C_1-N_3-C_5	121.81	122.36	120.81	120.76	122.48	122.51	122.33	122.08
O_2-C_1-H_6	122.68	121.60	121.52	121.63	121.80	121.66	121.99	122.36
N_3-C_4-H_7	110.24	109.71	110.57	110.53	109.64	109.63	109.79	109.99
N_3-C_4-H_8	109.94	109.52	110.01	110.24	109.54	109.64	109.82	109.91
N_3-C_4-H_9	110.88	110.83	110.44	110.03	110,87	110.83	110.82	110.88
N_3-C_5-H_{10}	110.02	109.62	110.41	110.66	109.61	109.66	109.81	109.94
N_3-C_5-H_{11}	110.13	110.12	110.36	110.28	110.08	110.02	110.01	110.03
N_3-C_5-H_{12}	109.89	110.08	109.75	109.54	110.15	110.13	110.10	110.00

ლიტერატურა – REFERENCES – ЛИТЕРАТУРА

1. Dewar M.J.S., Zoebisch E.G., Healy E.F., and Stewart J.J.P. AM1: A New General Purpose Quantum Mechanical Molecular Model // Journal of American Chemical Society, 1985, v. 107, pp. 3902- 3909.
2. Stewart J.J.P. Optimization of parameters for semiempirical methods // I. Method. Journal of Computational Chemistry, 1989, v 10, Issue 2, pp. 209–220.
3. MOPAC 6.0 for Windows 95 [electronic resource]: URL: http://www.ccl.net/cca/software/MS-WIN95-NT/mopac6/index.shtml (date accessed: 10.02.2013)
4. Marrel J., Kettl S., Tedder J. Chemical bond. M. Mir, 1980, 384 p. (in Russian).
5. Tsivtsivadze T.I. Candidate's dissertation, Tbilisi, (in Russian).
6. Turiashvili T.N. Candidate's dissertation, Tbilisi, (in Russian).
7. Tsintsadze G.V. X-ray structural research of the crystals of trans-diisoseleniumcyanato-tetradimethylformamide-nickel(II)-[$Ni(NCSe)_2(HCON(CH_3)_4$]. Publishing House of Georgian National Academy of Sciences. Tbilisi. 2014, 55 p. (in Russian).

გამხსნელის გავლენა დიმეთილაცეტამიდის და N,N-დიმეთილფორმამიდის კომპლექსწარმოქმნის უნარზე

გ.ცინცაძე, დ.ლოჩოშვილი*, თ.გიორგაძე, ე.თოფურია, თ.ტუსიაშვილი

საქართველოს ტექნიკური უნივერსიტეტი, თბილისი, საქართველო

**თსუ, რ.აგლაძის არაორგანული ქიმიისა და ელექტროქიმიის ინსტიტუტი, თბილისი, საქართველო, dimitri.lochoshvili@tsu.ge*

რეზიუმე

კვანტურ-ქიმიური ნახევრადემპირიული AM1 მეთოდით, აირად ფაზაში და შვიდ სხვადასხვა გამხსნელში გამოთვლილია დიმეთილაცეტამიდის და N,N-დიმეთილფორმამიდის მოლეკულების წარმოქმნის სითბო, დიპოლური მომენტი, ატომთაშორისი მანძილები, ბმის რიგები, ვალენტური კუთხეები და ელექტრონული სიმკვრივეები ატომურ ორბიტალებზე, დადგენილია ამ მოლეკულების, როგორც ორგანული ლიგანდების კოორდინირების უნარი ლითონ-კომპლექსწამომქმნელთან.

ВЛИЯНИЕ РАСТВОРИТЕЛЯ НА КОМПЛЕКСООБРАЗУЮЩУЮ СПОСОБНОСТЬ ДИМЕТИЛАЦЕТАМИДА И N,N-ДИМЕТИЛФОРМАМИДА

Г.В.Цинцадзе, Д.М.Лочошвили*, Т.З.Георгадзе, Е.С.Топурия, Т.Н.Тусиашвили

Грузинский Технический Университет, Тбилиси, Грузия

**ТГУ, Институт неорганической химии и электрохимии им. Р.И.Агладзе, Тбилиси, Грузия, dimitri.lochoshvili@tsu.ge*

РЕЗЮМЕ

Полуэмпирическим квантово-химическим методом AM1, в газовой фазе и семи разных расствoрителях вычислены теплота образования, дипольный момент, длины межатомных связей, порядки связей, ведичины межатомных углов, распределение электронов на атомных орбиталях диметилацетамида и N,N-диметилформамида. Установлена комплексообразующую способность этих молекул с металлами комплексообразователями.

SOLVENT EFFECT ON COMPLEX FORMATION OF UREA

Maia Tsintsadze*,**, Sofio Tchitchinadze*, Nona Bolqvadze**, Nino Imnadze**, Gulnara Manvelidze**
*R.Agladze Institute of Inorganic Chemistry and Electrochemistry of Ivane Javakhishvili Tbilisi State University, 0186, Mindeli st.11, Tbilisi, Georgia
**Georgian TechnichalUniversity, 77 MerabKostava St., Tbilisi, Georgia, 0175
m.tsintsadze@gtu.ge

Energetic, geometric and structural characteristics of Urea are determined by quantum chemical method AM1. According to electronic structure, solvent effect on its complex formation ability with metals is established.

The goal of our research was to study properties of complex formation of Urea in different solutions, manifestation of its donor properties and synthesis of new coordination compounds on the basis of obtained results, and also study of physical-chemical properties of synthesized compounds.

Based on the quantum-chemical metod AM1 [1-3] calculated the power, geometrical and structural features of Urea. According to electronic structure, solvent effect on its complex formation ability with metals is established. Water, acetone, methanol, ethanol, dimethyl sulfoxide, chloroform, hexane are selected as solvents.

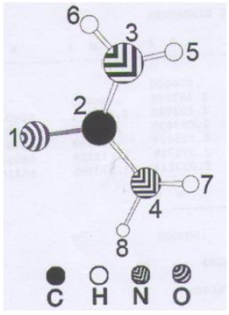

Picture 1.Molecul of of urea

Molecule formation heat, value of total energy, dipole moment, ionization potential, valence angles between atoms and bond lengths, effective charges, atomic orbitals filling with electrons etc. are calculated in all cases. These quantum-chemical calculations are shown in Table 1.

Table 1. Final heat of formation, net atomic charges and dipole contributions, atomic orbital electron populations in the molecul of Urea

№	Solvent, ε	ΔH, KJ	μ, D	Atom	Charge, q	Electron density	Atomic orbital electron populations			
							2S	$2P_x$	$2P_y$	$2P_z$
1	**Gas**	-186.27	3.83	O(1)	-0.407	6.407	1.921	1.072	1.872	1.542
				N(3)	-0.434	5.434	1.464	1.098	1.074	1.798
				N(4)	-0.405	5.405	1.501	1.106	1.067	1.731
2	**H_2O, Water, 78.5**	-275.16	6.45	O(1)	-0.650	6.650	1.920	1.122	1.913	1.695
				N(3)	-0.411	5.411	1.449	1.140	1.069	1.753
				N(4)	-0.400	5.400	1.520	1.136	1.059	1.684
3	**C_2H_6SO, Dimethyl sulfoxide, 49.0**	-273.72	6.41	O(1)	-0.647	6.647	1.920	1.121	1.912	1.693
				N(3)	-0.411	5.411	1.449	1.139	1.069	1.754
				N(4)	-0.400	5.400	1.520	1.136	1.059	1.685
4	**CH_3OH, Methanol, 32.6**	-271.64	6.31	O(1)	-0.639	6.639	1.920	1.120	1.911	1.688
				N(3)	-0.413	5.413	1.449	1.138	1.070	1.756
				N(4)	-0.399	5.399	1.523	1.136	1.060	1.681
5	**C_2H_5OH, Ethanol, 24.3**	-264.79	6.27	O(1)	-0.636	6.636	1.920	1.118	1.911	1.687
				N(3)	-0.414	5.414	1.448	1.137	1.069	1.759
				N(4)	-0.401	5.401	1.519	1.134	1.060	1.688
6	**$(CH_3)_2CO$, Acetone, 20.7**	-268.50	6.22	O(1)	-0.632	6.632	1.920	1.118	1.910	1.684
				N(3)	-0.415	5.415	1.449	1.137	1.070	1.760
				N(4)	-0.400	5.400	1.520	1.134	1.060	1.685
7	**$CHCl_3$, Chloroform, 4.7**	-244.70	5.25	O(1)	-0.554	6.554	1.920	1.105	1.898	1.631
				N(3)	-0.417	5.417	1.475	1.124	1.073	1.745
				N(4)	-0.398	5.398	1.519	1.124	1.068	1.687
8	**C_6H_{12}, 1.9 Hexane,**	-213.91	4.43	O(1)	-0.473	6.473	1.920	1.087	1.885	1.580
				N(3)	-0.426	5.426	1.473	1.111	1.074	1.768
				N(4)	-0.400	5.400	1.513	1.115	1.068	1.704

Analysis of the values of electron densities (formal population) and effective charges shows that the high values of the electron density is characterized by an oxygen atom O (1), which is typical of any solvent. The Oxygen atom O (1) has a lone electron pair of δ-type. More precisely, he has a hybrid-type nuclear obrital sp^2 with s –component. This circumstance determines the basic properties of the Oxygen atom O (1), i.e. its properties form the metal donor-acceptor bond.

Regard to the Nitrogen atoms N (3) and N(4), it can manifest electron-donor properties. Electron pair located on $3p_z$orbitali, which is not capable of participating in bond formation with δ-type metal-complexing. The Nitrogen atoms N (3) and N(4) have not possibility to provide π-type bond and they can provide δ -bond with metal - N (3) or N(4).

Molecule formation heat, value of total energy, dipole moment, ionization potential, valence angles between atoms and bond lengths, effective charges, atomic orbitals filling with electrons etc. are calculated in all cases. Thesequantum-chemicalcalculationsareshowninTable 1.

Compounds of copper(II), cobalt(II) and nichel(II) with Urea are received. Copper(II), cobalt(II) and nichel(II) sulphates, nitrates, chlorides and bromides have been taken as initial salts. Synthesis has been carried out in hot ethanol solutions.

Sediment formation became visible directly as soon as hot ethanol solutions of salt and ligand were mixed.Obtained sediments has been filtrated, washed with cold ethanol and dried. Resulted substances have been cleaned by preliminary recrystallization from ethanol.

New coordination compounds are received in solid state. Their composition is determined using elemental analysis, while individuality is defined via determination of melting temperature. Some physical-chemical properties are studies, namely: solubility in different inorganic and organic solvents. Synthesized compounds are studied using absorption infrared spectroscopy method.

ლიტერატურა - REFERENCES – ЛИТЕРАТУРА

1. Dewar M.I.S., Zoebich E.G., Rcoly E.F., Stewart I. AM1: A new purpose quantum mechanical molecular model. A.Amer. Chem. Soc. P. 3902-3909.
2. Химическая связь. Маррел Дж., Кент С., Тедер Дж. М.Мир 1980. 383 с.
3. Рентгеноструктурное исследование кристаллов транс-диизоселеноцианато-тетрадиметилформамид-никеля (II)-[$Ni(NCSe)_2(HCON(CH_3)_4$]. Г.В.Цинцадзе. Национальная Академия Наук Грузии. Тбилиси. 2014. 55 с.

გამხსნელის გავლენა კარბამიდის (შარდოვანას) კომპლექსწარმოქმნის უნარზე

მაია ცინცაძე*,**, ეკატერინე ჭიჭინაძე*, ნონა ბოლქვაძე**, ნინო იმნაძე**, გულნარა მანველიძე**

*ივ.ჯავახიშვილის სახელობის თბილისის სახელმწიფო უნივერსიტეტი
რ.აგლაძის არაორგანული ქიმიისა და ელექტროქიმიის ინსტიტუტი
**საქართველოს ტექნიკური უნივერსიტეტი

რეზიუმე

ქვანტურ-ქიმიური მეთოდით AM1 გამოთვლილია კარბამიდის (შარდოვანას) ენერგეტიკული, გეომეტრული და სტრუქტურული მახასიათებლები. ელექტრონული სტრუქტურის მიხედვით დადაგენილია გამხსნელის გავლენა ლითონებთან მისი კომპლექსწარმოქმნის უნარზე. სინთეზირებულია კობალტის(II), ნიკელის(II) და სპილენძის კოორდინაციული ნაერთები შარდოვანასთან. შესწავლილია სინთეზირებული ნაერთების ზოგიერთი ფიზიკურ-ქიმიური თვისება.

ВЛИЯНИЕ РАСТВОРИТЕЛЯ НА КОМПЛЕКСООБРАЗУЮЩУЮ СПОСОБНОСТЬ КАРБАМИДА (МОЧЕВИНЫ)

М.Цинцадзе*,**, Е.Чичинадзе*, Н.Болквадзе**, Н.Имнадзе**, Г.Манвелидзе**

*Иниститут неорганической химии и электрохимии им. Р.Агладзе
** Грузинский технический университет

РЕЗЮМЕ

Квантово-химическим методом AM1 расчитаны энергетические, геометрические и структурные характеристики молекулы диметилсульфоксида. На основании электронной структуры определена зависимость способности комплексообразования молекулы с металлами от растворителей. Синтезированы координационные соединения кобальта(II), никеля(II) и меди(II) с мочевиной. Изучены некоторые физико-химические свойства синтезированных соединений.

Li_2MnO_3 DEVELOPMENT AS A COMPONENT OF HIGH-VOLTAGE LITHIUM-RICH COMPOSITE $xLi_2MnO_3 \cdot (1-x)\ LiMnO_2$ CATHODE MATERIALS FOR Li-ION BATTERIES

Eteri Kachibaia, Ruth Imnadze, Tamar Paikidze, Dali Dzanashvili, Tengiz Machaladze

R.Agladze Institute of Inorganic Chemistry and Electrochemistry of Ivane Javakhishvili Tbilisi State University, 0186, Mindeli st.11, Tbilisi, Georgia
kachibaia@hotmail.com

Physical and chemical basis production of Li_2MnO_3 as a part of high-voltage lithium-rich composite $xLi_2MnO_3 \cdot (1-x)\ LiMnO_2$ cathode materials for Li-ion batteries has been developed. In this case, various methods of Li_2MnO_3 preparation have been tested. Among them, a method based on thermal decomposition of the eutectic mixtures of starting materials has been used. Phase-pure, nano-sized compounds with monoclinic structure have been obtained.

Nowadays batteries represent a very important technology. Electrodes (anode and cathode) and electrolyte are three major components of most batteries, including lead-acid batteries, used for startup of car engines, as well as compact lithium cells widely used in different applications (e-books, watch, etc.).For these new batteries all developed countries intensively search for above mentioned components that would be efficient in terms of price and operational performance. Lithium-ion batteries (LIB) are now ubiquitous. Recently they have been applied in electric and hybrid vehicles. There is an inevitable shift underway as the automotive industry transitions from traditional gasoline powered vehicles to more efficient, environmentally responsible modes of transport. Hybrid electric vehicles and electric vehicles are making inroads into the global marketplace, but the going is slow and the obstacles are many. As yet, these vehicles have not returned much profit for their manufacturers. However the problems can be solved with the improvement of batteries technology. There are opportunities to increase the energy of lithium batteries and reduce their prices by 30-40%. Currently new fuel sources are being developed. Meanwhile, lithium-ion power sources continue to be the most preferable in the next 20 years.

A class of cathode materials that emerged recently displays increasing reversible capacity upon oxygen release during the first charging. These compounds are referred to as ‘‘composite cathode materials” - layered-layered composites - $xLi_2MnO_3 \cdot (1-x)LiMO_2$ (M=Mn, Ni, Co, Cr).Initial charge to >4,5 V(Li^+/Li) removes lithium to the negative electrode with oxygen ions being removed from the initially inactive Li_2MnO_3 component activating it for subsequent electrochemical cycling. Today these materials are the subject of intense international research and development. It is considered that lithium-rich cathode materials can provide LIB with high electrochemical characteristics due to Li_2MnO_3 properties. Meanwhile, the preparation and characterization of nanoscale lithium rich cathode materials are still insufficiently studied. Particularly relevant is development of affordable and safe, modified, nanoscale materials based on $xLi_2MnO_3 \cdot (1-x)LiM_yMn_{1-y}O_2$ (M = Ni, Co, Cr), capable to replace commercially available $LiCoO_2$.It is assumed that maximum oxidation state of manganese in an octahedral oxygen environment cannot exceed +4. Subsequently, Mn^{+4} compounds, such as Li_2MnO_3 (having a layered structure - monoclinic structure), while rich with Li^+ ions, were considered electrochemically inert. Recently, it has been suggested that Li+ may be removed from Li-Mn^{+4} oxides. It was shown, that lithium extraction from these materials is possible, not by Mn^{+4}oxidation, but by the simultaneous removal (elimination) of oxygen in order to balance the charge and stabilize structure. In A. Robertson, et al., Chem.Mater., 15 (2003) 1984 paper, Li_2MnO_3 is presented as cheap component of Li_2MnO_3 - $LiMO_2$ (M = Cr, Co, Ni and Fe) solid solutions, since in the activation process they deliver high reversible capacity of 200mAh/g by removing oxygen during the initial charge. When all the lithium ions are utilized, theoretical capacity of Li_2MnO_3 is 458 $mAhg^{-1}$.

To obtain phase pure, nanosize Li_2MnO_3, with monoclinic structure, as a component of above mentioned $xLi_2MnO_3 \cdot (1-x)LiMO_2$ -type composite compounds, a number of methods have been tasted in the framework of presented study:1. Method, based on mechanochemical treatment of initial reagents during solid state reaction, followed with calcination. $MnCO_3$, LiOH, γ-MnO_2 (ЭДМ), Li_2CO_3 were used as initial reagents. Synthesis I step – preparation of the intermediate product: a) mechanochemical treatment of initial reagents mixture using spirit as dispersant; b) removal of the spirit at 60°C, τ=30 min; c) heat

treatment at T_1=350°C, τ_1=2h. Synthesis II step –treatment of the intermediate product at T_2=500°C, τ_1=2h.2. Malting-saturation method, where mixture of LiOH and MnO_2/Mn_3O_4 was pre-fired at 470 and 530°C on air, followed by heat treatment at different temperatures in the range of 1000°C.3. Method based on thermal decomposition of eutectic mixture of initial reagents – Li and Mn acetates, followed by heat treatment. Table 1 summarizes the results of X-ray diffraction patterns of Li_2MnO_3 samples, prepared by solid state method as a result of Li_2CO_3 and $MnCO_3$/ MnO_2 interaction.

Table 1.

Sample №	Heat treatment mode	Phase composition
Samp.№1 $MnCO_3$	T_1=350°C, τ_1=5h.	Main phase Li_2MnO_3, ASTM 27-1252 Sample contains an impurity of Li_2CO_3 (2.93, 2.83)
Samp.№2 $MnCO_3$	T_1=350°C, τ_1=5 h. T_2=500°C, τ_2=5h.	Li_2MnO_3-monoclinic structure, ASTM 27-1252
Samp.№3 γ-MnO_2	T_1=350°C, τ_1=5 h.	Main phase Li_2MnO_3, sample contains large amount of Li_2CO_3 (2.93, 2.83, 2.49, 3.03) impurity
Samp.№4 γ-MnO_2	T_1=350°C, τ_1=5 h. T_2=500°C, τ_2=5 h.	ASTM 27-1252, minor impurity of Li_2CO_3
Samp.№5 $MnCO_3$	T_1=350°C (samp.1) T_2=500°C (samp.2) T_3=1000°C, τ=5 h.	monoclinic structure, ASTM 27-1252

Tables 2-5 show the diffraction characteristics of the synthesized samples.

Table 2. Diffraction characteristics of Li_2MnO_3 samples, synthesized by different methods

Samp.№1 Li_2MnO_3, T_1=400°C T_2=600°C		Samp.№2 Li_2MnO_3, T_1=400°C T_2=600°C, (Li -2% excess)		Samp.№3 Li_2MnO_3, T_1=350°C		Samp.№4 Li_2MnO_3, T_1=350°C T_2=500°C		Samp.№5 Li_2MnO_3, T_1=180°C, T_2=600°C		Samp.№6 Li_2MnO_3, T_1=180°C, T_2=600°C, (Li -2% excess)		ASTM - 27-1252, Li_2MnO_3	
$d_{\alpha/n}$	I/I_0	$d_{\alpha/n}$	I/I_0	$d_{\alpha/n}$	I/I_0	$d_{\alpha/n}$	I/I_0	$d_{\alpha/n}$	I/I_0	$d_{\alpha/n}$	I/I_0	$d_{\alpha/n}$	I/I_0
4,69	95	4,71	62	4,74	50	4,76	39	4,67	48	4,73	41	4.74	100
		4,23	26	4,18	57	4,23	21	4,23	20	4,23	20	4.26	20
4,04	17	4,08	26	3,78	8	3,7	7	4,1	17	4,08	17	4.08	30
3,7	14	3,66	19	3,03	12	2,93	6	3,66	8	3,66	10	3.66	20
3,16	8			2,93	63			2,42	44	2,42	42	3.17	20
2,49	41	2,47	8	2,83	100	2,83	14	2,3	4	2,31	5	-	-
2,46	66	2,42	15	2,63	24			2,01	100	2,02	100	2.43	20
2,41	29			2,49	49			1,85	9	1,86	8	2.42	30
2,37	19	2,37	19	2,43	63	2,43	43	1,59	10			2.37	10
2,04	100	2,04	100	2,26	8	2,31	6	1,57	15	1,57	16	2.03	50
		2,02	71	2,03	57	2,02	100			1,43	28	2.02	90
1,86	15	1,88	19	1,83	12	1,86	7			1,42	28	1.86	10
1,58	23	1,6	26	1,57	21	1,57	14					1.58	10
1,54	33	1,57	32									1.56	30
1,44	50											1.44	30

Phase pure, nanosize (D=9.3÷11.3 nm) Li_2MnO_3 samples, obtained on the bases of lithium and manganese acetates are characterized by monoclinic structure

X-ray diffraction and X-ray structural analyses of the mixture's annealing products at 230-310-400-500°C confirm decomposition of double eutectic mixture and formation of Li_2MnO_3, with monoclinic structure and particle size about 9.3÷11.3 nm.

Table 3. Diffraction characteristic of Li_2MnO_3 (samples 1 and 2), obtained by the interaction of $LiOH \cdot H_2O$ and Mn_3O_4

Samp.№1 Li_2MnO_3, T_1=400°C, T_2=600°C		Samp.№2 Li_2MnO_3, T_1=400°C, T_2=600°C, (Li -2% excess)		ASTM - 27-1252, Li_2MnO_3		
$d_{\alpha/n}$	I/I_0	$d_{\alpha/n}$	I/I_0	$d_{\alpha/n}$	I/I_0	Hkl
4,69	95	4,71	62	4.74	100	002
-	-	4,23	26	4.26	20	020
4,04	17	4,08	26	4.08	30	111
3,7	14	3,66	19	3.66	20	111
3,16	8	-	-	3.17	20	022
2,49	41	-	-	-	-	-
2,46	66	2,47	8	2.43	20	200
2,41	29	2,42	15	2.42	30	131
2,37	19	2,37	19	2.37	10	113, 004
2,04	100	2,04	100	2.03	50	202
-	-	2,02	71	2.02	90	133
1,86	15	1,88	19	1.86	10	133
1,58	23	1,6	26	1.58	10	006
1,54	33	1,57	32	1.56	30	242, 135
1,44	50	-	-	1.44	30	-
1,42	34	-	-	1.42	40	-

In sample №1 impurity of $LiMn_2O_4$ (2.43, 2.37, 1.58, ASTM 18-736) is fixed.

Table 4. Diffraction characteristic of Li_2MnO_3 samples, obtained by the interaction of Li_2CO_3 and γ-MnO_2

Samp.№3 Li_2MnO_3, T_1=350°C		Samp.№4 Li_2MnO_3, T_1=350°C, T_2=500°C		ASTM - 27-1252, Li_2MnO_3	
$d_{\alpha/n}$	I/I_0	$d_{\alpha/n}$	I/I_0	$d_{\alpha/n}$	I/I_0
4,74	50	4,76	39	4.74	100
4,18	57	4,23	21	4.26	20
3,78	8	3,7	7	4.08	30
3,03	12	2,93	6	3.66	20
2,93	63	-	-	3.17	20
2,83	100	2,83	14	-	-
2,63	24	-	-	2.43	20
2,49	49	-	-	2.42	30
2,43	63	2,43	43	2.37	10
2,26	8	2,31	6	2.03	50
2,03	57	2,02	100	2.02	90
1,83	12	1,86	7	1.86	10
1,57	21	1,57	14	1.58	10
				1.56	30
				1.44	30
				1.42	40

The lithium-ion accumulators and batteries based on them have become part of people's daily lives. Cars and other devices operating on Li-ion batteries have been invented. The problem however is battery capacity fade during charging-discharging. This problem triggers development of Li-ion batteries.

Large amount of Li_2CO_3 (2.93, 2.83, 2.49, 3.03) impurity is fixed in sample №3. Li_2MnO_3 with monoclinic structure and minor impurity of Li_2Co_3 is fixed in sample №4.

Table 5. Diffraction characteristic of Li_2MnO_3 samples, obtained by the interaction of Li and Mn acetates

Samp.№5 Li_2MnO_3, T_1=180˚C, T_2=600˚C		Samp.№6 Li_2MnO_3, T_1=180^{0}C, T_2=600˚C, (Li-2% excess)		ASTM - 27-1252, Li_2MnO_3		
$d_{\alpha/n}$	I/I_0	$d_{\alpha/n}$	I/I_0	$d_{\alpha/n}$	I/I_0	Hkl
4,67	48	4,73	41	4.74	100	002
4,23	20	4,23	20	4.26	20	020
4,1	17	4,08	17	4.08	30	111
3,66	8	3,66	10	3.66	20	111
-	-	-	-	3.17	20	022
-	-	-	-	2.43	20	-
2,42	44	2,42	42	2.42	30	200
2,3	4	2,31	5	2.37	10	131
-	-	-	-	2.03	50	113, 004
2,01	100	2,02	100	2.02	90	202
1,85	9	1,86	8	1.86	10	133
1,59	10	-	-	1.58	10	133
1,57	15	1,57	16	1.56	30	006
		1,43	28	1.44	30	242, 135
		1,42	28	1.42	40	-
α sinβ = 0,4835 nm b = 0,8459 nm c sinβ = 0,935 α = 0,4909 ∠ β = 99°10' c = 0,9492 нм		α sinβ = 0,484 nm b = 0,8459 nm c sinβ = 0,946 α = 0,4914 ∠ β = 99°10' c = 0,9604 нм				

Physicochemical and electrochemical characteristics of cathode materials depend on their syntheses methods. Conventional solid-state reaction has several drawbacks, such as huge energy consumption due to prolonged high-temperature multi-stage process, heterogeneous composition and particles agglomeration. Low concentrations of starting materials are used to obtain the cathode material by soft chemistry methods (hydrothermal method, co-precipitation, etc.). Hence a small amount of the desired product is obtained. Therefore, these processes cannot be used for industrial production. Development of special synthesis methods suitable for creating nanosized cathode material can improve its kinetic performances. Reducing particle size to a nano-scale can lead to increased electrode/electrolyte interface area, decreased mechanical stress (tension) during lattice delithiation, and reduced lithium/ electron transport length in cathode material. Due to the small particles, lithium ions can diffuse through lattice from the particle's center towards its surface along the short path. This could ensure high electrochemical characteristics and good capacity stability. Well crystallized nanoparticles will provide for more rapid diffusion of lithium and hence provide high rate capability.

X-ray studies of samples were carried out using DRON-3 diffractometer in the focused CuKα radiation. The phase identification was carried out using diffractometric data for nonorganic compounds along with latest corresponding literature data. Evaluation of coherent scattering regions (d.nm) was carried out by the Debye-Scherer formula: $d=0{,}9\lambda/\beta\cdot\cos\theta$, where λ is wave length, β is line broadening at half the maximum intensity, θ - diffraction angle. Particle size of synthesized samples was calculated using

transmission electron microscope (TEM). Thermogravimetrical studies were carried out using Q-1000°C derivatograph with simultaneous recording of T, TG, DTA and DTG curves. Chemical analysis of the samples was determined by atomic absorption method, as well as by traditional methods of chemical analysis.

ლიტერატურა - REFERENCES – ЛИТЕРАТУРА

1. Tarascon J.M. and Armand M.//Nature, 2001.V.414, P.359
2. Chen Zao-Yong, et al.//Trans. Nonferrous Met. Soc. China.2010, P.614-618
3. Wang Li. et al.//Int.J.Electrochem.Sci.2011, V.6, P.2022-2030

Li-იონური ბატარეებისათვის მაღალვოლტიანი ლითიუმით მდიდარი $xLi_2MnO_3\cdot(1-x)LiMnO_2$ კომპოზიციური საკათოდე მასალებისათვის Li_2MnO_3-ის, როგორც შემადგენელი ნაწილის, შემუშავება

ეთერ ქაჩიბაია, რუფი იმნაძე, თამარ პაიკიძე, დალი ძანაშვილი, თენგიზ მაჩალაძე
ივანე ჯავახიშვილის სახელობის თბილისის სახელმწიფო უნივერსიტეტის რ.აგლაძის არაორგანული ქიმიისა და ელექტროქიმიის ინსტიტუტი, 0186, მინდელის ქ.11, თბილისი, საქართველო

რეზიუმე

ჩატარებულია Li-იონური ბატარეებისათვის მაღალვოლტიანი ლითიუმით მდიდარი $xLi_2MnO_3\cdot(1-x)LiMnO_2$ კომპოზიციური საკათოდე მასალებისათვის Li_2MnO_3, როგორც შემადგენელი ნაწილის, სტრუქტურული მახასიათებლებისა და ფაზური შედგენილობის კვლევები. ფაზურად-სუფთა, ნანოზომის მონოკლინური სტრუქტურის Li_2MnO_3-ის ნიმუშების მისაღებად გამოყენებული იყო სხვადასხვა მეთოდი, როგორიცაა გალღობა-გაჯერების მეთოდი; საწყისი რეაგენტების - ლითიუმისა და მანგანუმის აცეტატების ევთექტიკური ნარევის თერმულ დაშლაზე დაფუძნებული მეთოდი და სხვა.

РАЗРАБОТКА Li_2MnO_3 В КАЧЕСТВЕ СОСТАВЛЯЮЩЕЙ ЧАСТИ ВЫСОКОВОЛЬТНЫХ БОГАТЫХ ЛИТИЕМ КОМПОЗИЦИОННЫХ КАТОДНЫХ МАТЕРИАЛОВ $xLi_2MnO_3\cdot(1-x)LiMnO_2$ ДЛЯ Li-ИОННЫХ БАТАРЕЙ

Э.И.Качибая, Р.А.Имнадзе, Т.В.Паикидзе, Д.И.Дзанашвили, Т.Мачаладзе
Институт неорганической химии и электрохимии им. Р.И.Агладзе Тбилисского государственного университета им. И.Джавахишвили, 0186, ул. Миндели11, Тбилиси, Грузия

РЕЗЮМЕ

Приведены исследования структурных характеристик и фазового состава Li_2MnO_3 в качестве составляющей части высоковольтных богатых литием композиционных катодных материалов $xLi_2MnO_3\cdot(1-x)LiMnO_2$ для Li-ионных батарей. Для получения фазово-чистых, наноразмерных образцов Li_2MnO_3 с моноклинной структурой были опробованы различные методы, такие, как метод расплава-насыщения; метод, основанный на термическом разложении эвтектических смесей исходных реагентов -ацетатов лития и марганца и др.

ELECTROPLATING AND SURFACE ALLOYING OF METALS IN MOLTEN SYSTEMS

N.Gasviani, G.Kipiani, M.Khutsishvili, L.Abazadze, S.Gasviani, G.Imnadze
R.Agladze Institute of Inorganic Chemistry and Electrochemistry of Ivane Javakhishvili Tbilisi State University, 0186, Mindeli st.11, Tbilisi, Georgia
nodargasviani@mail.ru

The properties of metals are mainly determined by composition of surface layer. Therefore the variation of their surface composition is profitable in place of the variation of whole volume. This process is possible only in molten systems at (873-1173) K at preparation of metals electroplating. In parallel, the surface-diffusion alloying of the metals-bases takes place. In the paper the results of electroplating and surface alloying of metallic titanium and steels (CT-3, CT-40, X18H10T) by metallic molybdenum and intermetallides in oxy-halide melt at (873-1173) K are presented.

The preparation of electroplating of a number of metals, characterized by valuable properties, from aqueous solutions is impossible. From molten electrolytes the preparation of electronegative metals (Al, Ti, Zr, Hf, V, Nb, Ta, No, W and etc.) is possible. But in this case the difficulties appear which are excluded at the electrolysis of aqueous solutions. This is mainly caused by process high temperatures which occasionally exceed the temperatures of re-crystallization of plated metals. As a result, on one side, the macro-crystalline, loose, dendrite plating is formed, hindering the preparation of pure metal uniform plating at the cathode. On the other hand, the diffusion of separated metals into the cathode depth takes place by formation of alloys or intermetallides. This fact is very useful and profitable in many cases. Metals electrochemical deposition from molten electrolytes is associated with a process of alloy formation between separated metal and cathode. In this case, on one side, the regulation of the rate of metal plating appearance at the cathode is possible by variation of current density and, on the other hand, the regulation of the rate of diffusion of deposited metal is also possible by temperature variation independently of one another. In this case the diffusion (alloyed) layer of definite thickness is obtained in a base metal (for example, in the steel). Metal properties (hardness, corrosion-, heat- and thermal resistance) are determined by the composition of surface layers. For economy of alloying metals it is profitable to vary the composition of metal surface layer instead of the whole volume. Preparation of the plating in the metals and in their surface layers involve the compounds obtained by electrolysis. Explanation of alloyed layer in a solid metal only by diffusion is difficult to imagine. This well-known effect is referred to "electrochemical implantation" and may be explained by the fact that at the electrolysis the microscopic cracks are formed between the boundaries of cathode grains which determine a rapid diffusion of alloyed compound into the cathode depth. Therefore the surface electrochemical alloying in the melts proceeds relatively easier and is substantially profitable from economic viewpoint.

The investigations were carried out for the purpose of electrochemical plating and alloying of titanium and steels: CT-3, CT-40, X18H10T by molybdenum and intermetallides: $MoCo_3$ and $MoNi_3$.

Titanium plays a great role in the development of new technique because of many unique properties. Along with it, titanium is characterized by low anti-frictional properties, high braking factor, intense wear and etc. Plating and alloying by molybdenum enhances the surface strength of titanium hard ware, improves anti-frictional properties.

Equimolar mixture of KCl-NaCl was used as a background, molybdate: Na_2MoO_4 - as a depolarizer. Its electroreduction proceeds by the following scheme:

$$MoO^{2-}{}_{n/2+1} \leftrightarrow MoO_{n/2} + O^{2-} \quad (I)$$
$$MoO_{n/2} + ne \leftrightarrow Mo + n/2O^{2-} \quad (II)$$

O^{2-} - ions, formed by acid - base reaction (I), suppress the reaction (II) or the auto-inhibition of electrode process takes place. For neutralization of O^{2-} the scavenger of oxygen-ions is necessary. For this purpose $PO^{-}{}_3(NaPO_3)$ is added to the melt [1]. Therefore primarily in the practice metallic molybdenum was obtained from oxygen compound [2]. This is the most rational and short way in the technological cycle: "ore - finished products".

The most optimal is the following: electrolyte which involves (in mass %): eutectic K,Na/Cl (78-79) - Na_2MoO_4 (10-12) - NaP_3(1-2); cathode current density (0.01-0.025) A/cm^2. At the temperatures of (973-1173) K the smooth molybdenum plating of 80-120μm thickness are obtained with a good adhesion with titanium; current efficiency comprises 90-94%.

At the micro-section of titanium cathode lateral section the diffusion layer was determined. Micro-hardness of titanium comprises 209kg/mm^2. In diffusion layer the micro-hardness is gradually increased in surface direction and comprises 680kg/mm^2. The thickness of diffusion layer attains 80-110μm at 6 hour electrolysis. At the electrolysis process the surface electrochemical alloying of titanium takes place. As a result titanium micro-hardness increases by a factor of 3-4, the wear- and corrosion - resistances are also enhanced. The corrosion of alloyed titanium composes 0.2g/m^2.hour, whereas for usual titanium it comprises 0.82g/m^2.hour.

Research goal involves electroplating and diffusion alloying of the steels under study by molybdenum and molybdenum - cobalt (nickel) intermetallides in oxy-halide melts. Preliminary preparation of the surface of plated ware is of a great importance which was performed by thorough attention. The electrolysis was carried out in corundum glasses at the temperatures of (973-1073) K in air atmosphere. Steel plate of 10 cm^2 area was used as the cathode. Plating and alloying was performed in the following molten systems (mass %):

Eutectic: K,Na/Cl-89; $NaMoO_4$-10; $NaPO_3$-1 I
KCl-50; $BaCl_2$-25; $SrCl_2$-15; Na_2MoO_4-10; II
KCl-50; NaCl-25; $BaCl_2$-15; Na_2MoO_4-10; III

PO^-_3 wasn't added to II and III melts since the cations - Ba^{2+}, Ca^{2+}, Sr^{2+} are the strong scavengers of O^{2-}.

In the temperature range of (973-1073) K and at current densities: 0.01-0.2 A/cm^2 the shining plating of tight adhesion with a base are obtained. At 6 hour electrolysis the surface is plated by molybdenum layer of 30-50μm thickness. For example, a micro-hardness on the micro-section of the lateral section of molybdenum plated steel at a distance of 100μm from the edge comprises 310kg/m^2. Micro-hardness gradually reduces and at a distance of 160μm from the surface comprises 150 kg/mm^2.

By increase of electrolysis duration to 12-15 hours the thickness of alloyed layer increases to 450-550μm. The picture is similar for all steels and in the case of all three melts. X-ray structural analysis has shown that the alloyed layer consists of the solid solution of molybdenum in iron.

For all samples the micro-hardness of plating surface is equal to the micro-hardness of molybdenum - 1220 kg/mm^2.

Plating of steels (plates or cylinders) and alloying by intermetallides: $MoCo_3$ and $MoNi_3$ was carried out in the molten system:

$$K,Na/Cl - Na_2MoO_4 - CoCl_2(NiCl_2) - NaHPO_3$$

The optimal case takes place when the compounds are added to the background: KCl-NaCl by the following ratio:

$$[MoO^{2-}_4]:Co^{2+}\,(Ni^{2+}):PO_3=4:1:2.5$$

Their total amount in the melt mustn't exceed to 20-25 mass%. Working temperature comprises (973-1073) K, current density - (0.01-0.25)A/cm^2. The thickness of diffusion layer on the electrolysis duration. When electrolysis lasts 4-6 hours the silvery, smooth plating of (40-60) μm thickness are prepared with a good adhesion with a base. X-ray structural analysis confirms the presence of uniform plating - $MoCo_3$ ($MoNi_3$). The thickness of alloyed layer comprises (70-100) μm.

It is evident that in molten systems the metals (steels) gain a number of important properties by electrochemical plating and diffusion alloying

.

ლიტერატურა - REFERENCES – ЛИТЕРАТУРА

1. N.Gasviani, Ph.D.thesis, Tbilisi, 1975.
2. N.Gasviani, Doctoral thesis, Tbilisi, 2006.

ნალღობ სისტემებში ლითონთა გალვანური დაფარვა და ზედაპირული ლეგირება

ნ.გასვიანი, გ.ყიფიანი, მ.ხუციშვილი, ლ.აბაზაძე, ს.გასვიანი, გ.იმნაძე
ივ. ჯავახიშვილის სახელობის თბილისის სახელმწიფო უნივერსიტეტის რაფიელ აგლაძის
არაორგანული ქიმიისა და ელექტროქიმიის ინსტიტუტი, მინდელის 11, თბილისი, საქართველო

რეზიუმე

მეტალების თვისებებს ძირითადად განსაზღვრავს ზედაპირული ფენების შედგენილობა. ამიტომ მომგებიანია მათი ზედაპირული შედგენილობის შეცვლა და არა მთლიანად მოცულობითის. ეს შესაძლებელია მხოლოდ ლღობილ სისტემებში (873-1173) K ტემპერატურებზე მეტალთა გალვანური დანაფარების მიღების დროს. პარალელურად ადგილი აქვს სარჩული მეტალების ზედაპირულ - დიფუზიურ ლეგირებასაც. წარმოდგენილ ნაშრომში მოტანილია ოქსიჰალოგენიდურ ნალღობში მეტალური ტიტანის და ფოლადების (CT-3, CT-40, X18H10T) მეტალური მოლიბდენით და ინტერმეტალიდებით ($MoCo_3$ და $MoNi_3$) დაფარვის და ზედაპირული ლეგირების მონაცემები.

ГАЛЬВАНИЧЕСКОЕ ПОКРЫТИЕ И ПОВЕРХНОСТНО-ДИФФУЗИОННОЕ ЛЕГИРОВАНИЕ МЕТАЛЛОВ В РАСПЛАВЛЕННЫХ СИСТЕМАХ

Н.Гасвиани, Г.Кипиани, М.Хуцишвили, Л.Абазадзе, С.Гасвиани, Г.Имнадзе
Институт неорганической химии и электрохимии им. Р.И.Агладзе Тбилисского государственного университета им. И.Джавахишвили, 0186, ул. Миндели11, Тбилиси, Грузия

РЕЗЮМЕ

Состав поверхностного слоя металлов, в основном, определяет их свойства. Поэтому выгодно изменение их поверхнотного состава, а не целиком объемного. Это возможно только в расплавленных системах при температурах (873-1173) К во время получения гальванопокрытий металлов. Параллельно также происходит поверхностно-диффузионное легирование металлов-подложек. В работе приведены результаты гальванического покрытия и поверхностного легирования металлического титана и сталей (СТ-3, СТ-40, Х18Н10Т) металлическим молибденом и интерметаллидами – $MoCo_3$ и $MoNi_3$ в оксигалогенидном расплаве при (873-1173) К.

ELECTROCATALYTIC PROPERTIES AND PHOTOELECTROCHEMICAL CHARACTERISTICS OF NANOSIZED TITANIUM DIOXIDE FILMS MODIFIED BY La AND Nd

V.S.Vorobets, G.Ya.Kolbasov
V.I. Vernadsky Institute of General and Inorganic Chemistry of National Academy of Sciences of Ukraine, Kyiv, Ukraine
kolbasov@ionc.kiev.ua, vorobesvs@i.ua

Nanostructured TiO_2 films modified by La and Nd have been produced by sol-gel method and characterized by x-ray diffraction and ultraviolet-visible photocurrent spectra. The average size of nanoparticles was no more than 10 nm, the average thickness of the deposited layers was 800 – 1000 nm. The XRD results indicated that TiO_2, TiO_2/La and TiO_2/Nd electrodes calcined at 430°C consisted of anatase as the single phase. The photocurrent spectra of the TiO_2/La and TiO_2/Nd electrodes showed a stronger current in the UV range and a shift in the flat-band potential (E_{fb}) towards more negative values than that of TiO_2 electrodes. Electrocatalytic properties of TiO_2, TiO_2/La and TiO_2/Nd electrodes in the process of oxygen electroreduction have been investigated. Modifying of TiO_2 films by neodymium and lanthanum improves catalytic activity of TiO_2/Nd and TiO_2/La electrodes in the reaction of oxygen electroreduction. Improvement of electrocatalytic activity in comparison with unmodified TiO_2 has been observed for films with dopant concentrations up to 3 %. The correlation between electrocatalytic activity of electrodes and energy position of conduction band E_{fb}, is determined. Synthesized films can be used in electrochemical sensors for the determination of O_2 in biological liquids.

Introduction

Titanium dioxide is a promising material for application in environmental photocatalysis, for the generation of electricity in the solar and fuel cells, gas sensors, optical and protective coatings, electrochemical devices, as oxygen reduction catalyst etc. [1,2]. The catalytic activity of titanium dioxide increases greatly when nanoparticles are used. This paper presents results of studying the electrocatalytic properties and photoelectrochemical characteristics of electrodes based on nanosized titanium dioxide films modified by La and Nd. The prepared samples were characterized by using x-ray diffraction and ultraviolet-visible photocurrent spectra. Band gap energy and the position of flatband potentials were estimated by photoelectrochemical measurements.

Experimental

Synthesis of Materials. Electrocatalytic films based on nanosized titanium dioxide modified by La and Nd were produced by combined coprecipitation and sol-gel method on a Ti substrate from solutions containing titanium chloride, lanthanum nitrate and neodymium chloride according to the following procedure: at first aqueous $TiCl_4$ solution was prepared. A prescribed amount of lanthanide nitrate and neodymium chloride were dissolved in the aqueous $TiCl_4$ solution to form mixed ion solution. The transparent solution was added to aqueous ammonia solution slowly under vigorous stirring until the pH value of 10. After this, the reaction system was continuously stirred for 10 min at room temperature to obtain a homogeneous precipitate in composition, and then placed for separation. After that precipitate was rinsed by deionized distilled water to remove NH^{4+} and Cl^- ions. Then a prescribed amount of hydrogen peroxide solution was added to precipitate under vigorous stirring to form a clear yellowish sol, after that the reaction system was continuously stirred for 30 min at ~ 5^0 C. The sol was then dried at 100^0 C for 6 h to remove the water. The dip-coating technique was utilized for film deposition on titanum substrates. After that the electrodes were annealed in air at 430-500^0C.

To facilitate structural investigations by XRD powders have been prepared via gelation of the films' precursors, and their drying in air with following heat treatment to 450 or 500 °C. XRD analysis of crystalline phases was performed using a DRON-4-07 (Burevestnik, St. Petersburg) diffractometer (CuK_α radiation with Ni filter, λ=1.5418 Å) with Brag-Brentano registration geometry (2θ = 10–80°). The average size of crystallites was determined using Sherrer equation applied to the most intensive peak [3] at k=0.9. The degree of the powders crystallinity was estimated as the ratio of integrated intensities, such as for the (101) line of the studied and reference standard samples (reference standard: TiO_2, anatase 100%).

Photoelectrochemical investigations were carried out in the wavelength range 250 – 600 nm in a quartz electrochemical cell under irradiation of a high-pressure 500 W xenon lamp.The photoelectrochemical properties of the TiO_2, TiO_2/La and TiO_2/Nd electrodes were estimated using the spectral dependence of the photoelectrochemical current (i_{ph}), measured by commercial spectrometer KSVU-1 (LOMO, Russia) with spectral resolution 1 nm. The experiments were carried out at 22°C in the quartz cell. The i_{ph} spectra were measured with usage of the mechanical light chopper of 20 Hz frequencies and standard circuit synchronous detection. The i_{ph} spectra were expressed in units of quantum efficiency (electron/photon). Ag/AgCl electrode was used as the reference electrode on the pH value of the electrolyte.

Electrocatalytic properties of TiO_2, TiO_2/La and TiO_2/Nd electrodes in the processes of oxygen electroreduction was studied in potentiodynamic mode using electrochemical PC-based stand, having the following characteristics: measured currents - $2 \cdot 10^{-9} \div 10^{-1}$ A, potential sweep speed $v = 0{,}01 \div 50$ mV $\cdot$ s^{-1}, measurement range of working electrode potential -4 ÷ +4 V. Electrochemical measurements were carried out in a three electrode cell with separate anode and cathode space. Platinum electrode was used as the auxiliary electrode. Reference electrode was silver chloride electrode (Ag/AgCl). Measurements were carried out in physiological (0.9%) and isotonic (7.5%) solutions of NaCl.

Results and Discussion

Phase composition of TiO_2/Nd Films. The crystalline structures of TiO_2/Nd nanocomposites with dopant contents in the range 1 –10 mol. % were studied by XRD measurements of powders prepared from the precursors. Only anatase phase (JCPDS-ICDD, №21-1272) was identified in XRD patterns of TiO_2 and TiO_2/Nd powders [3]. XRD measurements of TiO_2/Nd powders in the range of Nd concentrations 5-10 mol.% did not reveal any peaks, typical for crystalline neodymium phase, or neodymium oxide [3]. Halo in the range of $2\theta < 20^o$ was observed on diffraction patterns of TiO_2/Nd samples with high neodymium content (> 5%) [3], caused probably by the presence of amorphous phase of TiO_2 and Nd compounds. The crystallinity of the samples was 80-85%.

The average crystallite size determined from the peak (101) broadening by Scherrer equation decreases with increasing content of neodymium (Table 1).

Table 1. Influence of Nd on structural characteristics of TiO_2 films. $T_{anl.}=430^0$C

№ п/п	Sample	2θ, º	Average crystallite size d, Å	a, Å	c, Å
1	**TiO_2**	**25.45**	**94.77**	**3.756**	**9.453**
2	**TiO_2:1 mol.% Nd**	**25.44**	**93.68**	**3.758**	**9.466**
3	**TiO_2:2 mol.% Nd**	**25.40**	**90.45**	**3.775**	**9.484**
4	**TiO_2:3 mol.% Nd**	**25.35**	**86.15**	**3.783**	**9.515**
5	**TiO_2:5 mol.% Nd**	**25.30**	**74.59**	**3.801**	**9.532**
6	**TiO_2:8 mol.% Nd**	**25.30**	**74.41**		
7	**TiO_2:10 mol.% Nd**	**25.44**	**66.56**		

These results indicate that in the TiO_2/Nd composites, crystallization of titanium oxide is suppressed when Nd content increases due to the neodymium retarding effect on anatase crystallites growth. Detailed analysis of XRD spectra of the TiO_2/Nd powders proved the formation of solid solution $Nd_xTi_{(1-x)}O_2$, with anatase structure as resulted from the anatase (101) crystal plane reflection shift into lower 2θ region (Table 1) due to the differences in the ionic radii of Nd^{3+} and Ti^{4+} and agree with data reported in [4.5]. The increase of lattice parameters a and c of solid solutions $Ti_{1-x}Zr_xO_2$ as function of neodymium content (x) up to mol. % 5 was observed (Table 1) and agrees with [4,5].

Photoelectrochemical Characteristics of TiO_2/La and TiO_2/Nd electrodes. Spectral dependences of photocurrent were measured for the TiO_2/La and TiO_2/Nd electrodes (films were coated on Ti substrate) to obtain the value of the band gap energy.

Quantum yield of photoelectrochemical current η in semiconductors can be expressed as [6]:

$$\eta = \frac{A}{h\nu}(h\nu - E_g)^m,$$

where *hv* is the photon energy, *m*=1/2 for the direct transition and *m*=2 for the indirect transition.

For the tested TiO_2/La and TiO_2/Nd electrodes, photocurrent spectra were presented as $(\eta \cdot hv)^{1/2} = f(hv)$ dependence which was linear in the wide range of wavelength. Band gap (E_g) values (Table 2) were calculated [7] by extrapolation of straight line of these dependences to the abscissa.

The position of the flatband potential (E_{fb}) of TiO_2/La and TiO_2/Nd electrodes was determined by the electrochemical measurements of photocurrent (i_{ph}) as a function of applied potential. Flatband potentials were estimated from i_{ph} changes measured at the photocurrency maximum for TiO_2, TiO_2/La and TiO_2/Nd electrodes plotted against applied potential by extrapolation straight line of these dependences to the abscissa.

Table 2. Influence of Nd and La on photoelectrochemical and electrocatalytic characteristics of TiO_2 films in 0,9 % solution of NaCl. $T_{anl.}=430^0C$

№ п/п	Sample	Flat-band potential, E_{fb}, V	Band-gap E_g, eV	Potential of oxygen electroreduction E_{O2}, V	Width of "electrochemical window" ΔE, V
1	**TiO_2**	**-0,30**	**3,20**	**-0.60**	**0.17**
2	**TiO_2/Nd**	**-0,54**	**3,10**	**-0.49**	**0.24**
3	**TiO_2/La**	**-0,60**	**3,20**	**-0.43**	**0.25**

The photocurrent spectra of the TiO_2/La and TiO_2/Nd electrodes showed a stronger current in the UV range (Figure 1) and a shift in the flat-band potential (E_{fb}) towards more negative values than that for undoped TiO_2 electrodes (Table 2). For TiO_2/La electrodes the photocurrent spectra showed a shift in photocurrent maximum toward longer wavelengths (Figure 1).

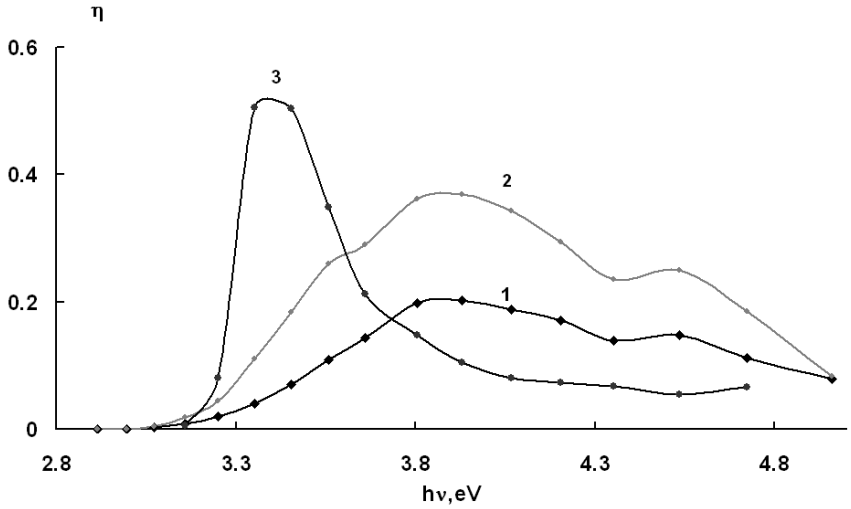

Fig. 1.Quantum yield of photocurrent for modified TiO_2 electrodes in 1 N KCl:
1 – TiO_2 ; 2 – TiO_2/Nd; 3 – TiO_2/La

The enhancement of photocurrent efficiency indicated that Nd^{3+} and La^{3+} ions addition is beneficial to promote charge separation within nanostructured TiO_2 film and to improve interfacial charge transfer process due to formation of impurity electron levels in the band gap of titanium dioxide [8], acting as traps of charge which retard the recombination process.

Electrocatalytic properties of TiO_2/La and TiO_2/Nd electrodes. Catalytic properties of TiO_2, TiO_2/La and TiO_2/Nd electrodes were investigated in the reaction of oxygen electroreduction in physiological (0,9 %) solution of NaCl. One current wave is observed on the current-voltage curves at potentials -0,45 ÷ -0,9 V (vs. Ag/AgCl electrode) (Figure 2). Important characteristic of electrodes for analysis of dissolved oxygen concentration is the oxygen electroreduction potential, or current half-wave reduction potential $E_{1/2}$ on the cathodic polarization curve, value of which should be minimum to avoid adverse electrochemical reactions when measuring the oxygen concentrationin.

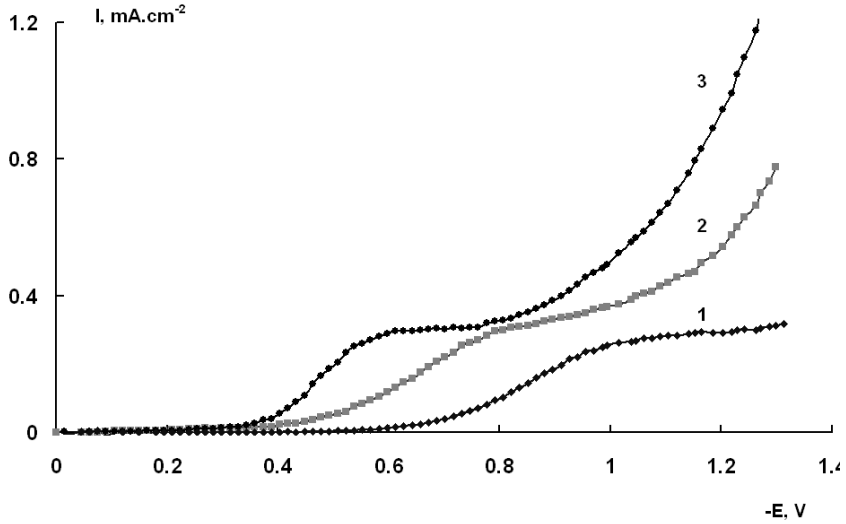

Fig.2 Current-voltage curves for oxygen reduction in solution of 0,9% NaCl at the electrodes:
1 – TiO_2 ; 2 – TiO_2/Nd; 3 – TiO_2/La. v = 10 mV • s^{-1}

It has been found by I-E curves measurements that the potential of oxygen electroreduction varies from the film composition (Table 2).

It is shown that modifying of TiO_2 films by neodymium and lanthanum improves catalytic activity of TiO_2/Nd and TiO_2/La electrodes in the reaction of oxygen electroreduction, which is manifested in decreasing of oxygen reduction potential E_{O2} and increasing of dynamic range of O_2 electroreduction potentials ("electrochemical window") (Table 2). As shown in [9], the high catalytic activity of TiO_2 electrodes in the electrochemical reduction of oxygen due to the existence at the TiO_2 surface nonstoichiometric titanium oxide $TiO_{1.91}\cdot(OH)_{0.09}$ and its hydroxide phase. Introduction into the crystal lattice of TiO_2 Nd or La, probably leads to the formation of additional catalytic centers, which also participate in this reaction.

The mechanism of oxygen reduction at the investigated electrodes is determined by mixed kinetics. We have shown that limiting current of oxygen electroreduction for studied semiconductor electrodes (Figure 2) is the limiting diffusion current.To prove this, the dependence of limiting current maximum from the potential sweep velocity v has been investigated. We have obtained that this dependence was straight in coordinates $i_d=f(v)^{0.5}$ and cut the x-axis at $i_d=0$, which due the diffusion control of oxygen reduction in this area [9]. In this case the dependence of density limiting current on the concentration of dissolved oxygen in NaCl solution for electrodes based on nanosized TiO_2 films is, as a rule, linear [9].

The correlation between electrocatalytic activity of electrodes and energy position of conduction band E_{fb}, is found. Overvoltage oxygen reduction E_{ov} on TiO_2, TiO_2/La and TiO_2/Nd electrodes significantly depends on the flat-band potential value E_{fb} (Table 2). Modification of TiO_2 electrodes by Nd and La nanoparticles leads to increasing of E_c into the region of more negative values and increase the energy of conduction band electrons, which are involved in the process of oxygen electroreduction. Thus, the decrease of half-wave potential of O_2 electroreduction for investigated electrodes associated with the shift of conduction band bottom toward more negative values.

The modified TiO_2 electrodes characterized by a high sensitivity to dissolved oxygen ($(4\text{-}5)\cdot10^{-6}$ g/l) and high reproducibility of characteristics in long-time cycling. These electrodes are promising for use in electrochemical sensors for the determination of oxygen in biological liquids.

ლიტერატურა - REFERENCES – ЛИТЕРАТУРА

1. A. Mills, R. H. Davies, and D. Worsley. Water purification by semiconductor photocatalysis. *Chemical Society Reviews.* 1993, 6(22), 417-425.
2. N.Smirnova, V.S. Vorobets, O.Linnik, E.Manuilov, G.Kolbasov, A.Eremenko. Photoelectrochemical and photocatalytical properties of mesoporous TIO_2 films modified with silver and gold nanoparticles. *Surf. And Interface Analysis*, 2010, 42, 1205-1208.
3. V.S. Vorobets, I.G. Kolbasova, O.V. Linucheva, S.V. Karpenko, V.I. Alontseva. Synthesis and electrocatalytic properties of nanostructured films based on TiO_2-Nd. *Chemistry, physics and technology of surface*. 2016, 1(7), 59-64.(in Russian).

4. V. Štengl, S. Bakardjieva, N. Murafa. Preparation and photocatalytic activity of rare earth doped TiO_2 nanoparticles. *Mater. Chem. and Physics*. 2009, 114, 217-226.
5. *Y. Xie, Ch. Yuan.* Photocatalytic and photoelecttrochemical performance of crystallized titanium dioxide sol with neodymium ion modification. *J. Chem. Technol. Biotechnol*. 2005, 80, 954-963.
6. *Gurevich Yu., Pleskon Yu.* Photoelectrochemistry of the semiconductors , M.: Nauka, 1983. – 312 p. in Russian).
7. *Hamilton J.W.J., Byrne J.A., McCullagh C., Dunlop P.S.M.* Electrochemical Investigation of Doped Titanium Dioxide. Hindawi Publishing Corporation. International // J. of Photoenergy. 2008, 2008, Article ID 631597, 1–8.
8. *Linsebigler A.L., Lu G.Q., Yates J.T.* Photocatalysis on TiO_2 surfaces: principles, mechanism and selected results. *Chem. Rev.* 1995, 95, 735–758.
9. G.Ya. Kolbasov, V.S. Vorobets, A.M. Korduban et al. Electrodes based on nanodispersed titanium and tungsten oxides for sensor of dissolved oxygen**.** *Russian Journal of Applied Chemistry*. 2006, 4(79), 596-601.

La და Nd მოდიფიცირებული ტიტანის დიოქსიდის ნანოზომის ფირების ელექტროკატალიზური და ფოტოელექტროქიმიური თვისებები

ვ. ს. ვორობეცი, გ. ი. კოლბასოვი

უკრაინის ეროვნული სამეცნიერო აკადემიის ვ.ი. ვერნაცკის ზოგადი და არაორგანული ქიმიის ინსტიტუტი, კიევი, უკრაინა *kolbasov@ionc.kiev.ua, vorobesvs@i.ua*

რეზიუმე

La და Nd -ით მოდიფიცირებული ტიტანის დიოქსიდის ნანოზომის ფირები მიღებულია ზოლ-გელ მეთოდით და დახასიათებულია რენტგენოდიფრაქციული და ულტრა ხილული ფოტოდენის სპექტრით. ნაწილაკების საშუალო ზომა იყო არაუმეტეს 10ნმ; ფირების საშუალო სისქე იყო 800-1000 ნმ. რენდგენოდიფრაქციის შედეგების მიხედვით TiO_2, TiO_2/La და TiO_2/Nd ელექტროდები გამომწვარი 430°C - ზე შედგებოდა ერთი ფაზური ანატაზისაგან. TiO_2/La და TiO_2/Nd ფოტოდენის სპექტრმა უჩვენა უფრო ძლიერი დენი ულტრაიისფერ დიაპაზონში და ბრტყელი ზონის პოტენციალის გადახრა (E_{fb}) უფრო უარყოფითი მნიშვნელობებისკენ TiO_2 -ის ელექტროდთან შედარებით. შესწავლილი იქნა ჟანგბადის აღდგენის პროცესისთვის TiO_2, TiO_2/La დაTiO_2/Nd ელექტროდების ელექტროკატალიზური თვისებები. ნიობიუმით და ლანთანით TiO_2 -ის ფირების მოდიფიცირება აუმჯობესებს TiO_2/La დაTiO_2/Nd აქტივობას ჟანგბადის აღდგენის რეაქციაში. გაუმჯობესება იქნა შემჩნეული TiO_2 -თან შეფარდებით 3% -მდე დოპირებულ ელექტროდებში. ელექტროდის ელექტროკატალიზურ აქტიურობასა და გამტარი ზონის ენერგიას (E_{fb}) შორის კორელაცია იქნა დადგენილი. სინთეზირებული ფირები შეიძლება გამოყენებული იქნას ბიოლოგიურ ხსნარებში ელექტროქიმიურ სენსორებში O_2 -ის დეტექციისათვის.

ЭЛЕКТРОКАТАЛИТИЧЕСКИЕ СВОЙСТВА И ФОТОЭЛЕКТРОХИМИЧЕСКИЕ ХАРАКТЕРИСТИКИ ПЛЕНОК НАНОРАЗМЕРНОГО ДИОКСИДА ТИТАНА, МОДИФИЦИРОВАННОГО La И Nd

В.С.Воробец, Г.Я.Колбасов

Институт общей и неорганической химии им. В.И.Вернадского НАН Украины, Киев, Украина

РЕЗЮМЕ

Наноструктурные пленки TiO_2, модифицированного La и Nd, полученные золь-гель методом, охарактеризованы методами рентгеновской дифракции и спектров фототока в УФ и видимом диапазонах. В спектрах фототока TiO_2/La и TiO_2/Nd электродов наблюдалось повышение фототока в УФ-диапазоне и сдвиг потенциала плоских зон (E_{fb}) в сторону более отрицательных значений по сравнению с TiO_2 электродами. Установлено, что модифицирование TiO_2 пленок неодимом и лантаном повышает каталитическую активность TiO_2/La и TiO_2/Nd электродов в реакции электровосстановления кислорода. Установлена корреляция между электрокаталитической активностью электродов и энергетическим положением зоны проводимости. Синтезированные пленки могут быть использованы в электрохимических сенсорах для определения содержания кислорода в биологических жидкостях.

VOLTAMMETRIC STUDIES OF Ca DOPED Y-114 LAYERED COBALT PEROVSKITE ELECTRODES WITH CATALYTIC EFFECT FOR ETHANOL ELECTROOXIDATION IN ALKALINE SOLUTIONS

Dan Mircea Laurentiu, Duca Delia Andrada, Vaszilcsin Nicolae, Craia-Joldes Victor-Daniel
University Politehnica Timişoara, Faculty of Industrial Chemistry and Environmental Engineering, 300223, Parvan 6, Timisoara, Romania
mircea.dan@upt.ro

In this paper, ethanol anodic oxidation reaction on $Y_{0.5}Ca_{0.5}BaCo_4O_7$ electrode in aqueous alkaline solution was investigated using voltammetric studies. The catalytic activity on ethanol anodic oxidation becomes a serious issue, mainly in order to use layered cobalt perovskite as anode in fuel cells. The research is necessary to understand the ethanol oxidation reaction (EOR) mechanism on the surface of these type of compound electrodes. Electrochemical behavior has been studied by cyclic voltammetry and linear polarization. Obtained results have shown that layered cobalt perovskites are appropriate as anodes in high temperature fuel cells.
Keywords: *$Y_{0.5}Ca_{0.5}BaCo_4O_7$, cobalt layered perovskite, ethanol electrooxidation, voltammetric studies*

Introduction

During the last period fuel cells have been found as an energy source for various applications in fields such as telecommunications, transport, medicine, and others [1]. The alkaline fuel cells (AFCs) were developed between 1950 and 1980, and are the oldest fuel cells that combine hydrogen with oxygen to produce electricity and water in alkaline media (potassium hydroxide) [2]. The most known AFC are Direct alcohol fuel cells (DAFCs). The increased interest and rapid development are due to the possibility of their use as alternative power sources for automobile and portable consumer electronics [3]. Their principal advantage consists in using of liquid fuels (alcohols) with low-molecular weight which can be easy handled, stored and transported [3]. Primary alcohols such as methanol and ethanol have relatively high mass energy density, comparable to that of gasoline. The utilization of alcohols as fuel would reduce the requirements of establishing totally new infrastructure as required for hydrogen initially used in fuel cells [4]. Most of the liquid electrolyte based DAFC research has concentrated on methanol or ethanol mixed with alkaline electrolyte media [4].

Methanol was considered the most promising liquid fuel for use in DAFC because it has the simplest molecular structure without carbon bonds and it is easily oxidized [5]. Methanol toxicity is its major disadvantage, which makes the fuel unsustainable and unsafe for many applications [4,5].

In contrast, ethanol is not toxic and has an approximate 30% higher energy density than methanol [5]. Also, it can be produced in big quantity from biomass using a fermentation process from renewable resources [3-5].

In acid media, platinum is the only known active and stable noble metal, the best known material for the dissociative adsorption of small organic molecules and the most effective catalyst for ethanol oxidation reaction (EOR) [5,6] Unfortunately the Pt catalyst do not show good tolerance to the CO containing intermediates obtained in EOR [5]. Generally, palladium is used as a catalyst-base for EOR in alkaline media [1]. The oxides of V, Fe, Ni, In, Sn, La and Pb were earlier used as anode materials [7]. In recent years, studies on various transition metal mixed oxides have shown that the perovskite oxides can be used as fuel cell electrodes [7]. Perovskite can be use in oxygen electrochemical evolution/reduction, alcohols oxidation, nitrogen oxides reduction and CO and hydrocarbons oxidation [7].

In the last period, layered cobalt perovskites type 114 were most investigated due to their structural, magnetic and electrochemical properties. Based on these properties cobalt perovskites can be used as membranes with high oxygen permeability, oxygen sensors and fuel cells electrodes. $Y_{0.5}Ca_{0.5}BaCo_4O_7$, was first synthesized by M. Valldor by half substitution of Y^{3+} with low valence Ca^{2+} cations in $YBaCo_4O_7$ structure [8]. A correlation between the compound structure and its properties was presented in previous studies. Especially due to the variable cobalt ions valence it was found that oxygen adsorption properties can be modified greatly by Y^{3+} ions substitution. [8].

In this paper, new aspects of the electrocatalytic oxidation of ethanol on $Y_{0.5}Ca_{0.5}BaCo_4O_7$ electrode have been studied using cyclic and linear voltammetry. Also, a mechanism was proposed for the electrochemical reaction. The results are expected to provide basic information in order to understand the mechanism of EOR on cobalt layered perovskites catalysts.

Experimental

$Y_{0.5}Ca_{0.5}BaCo_4O_7$ perovskite was obtained using solid state reaction, mixing Y_2O_3 (Aldrich 99,99%), $CaCO_3$ (Aldrich 99,99%), $BaCO_3$ (Aldrich 99,99%) and $CoO_{1.38}$ (99,99% Normapur) precursors according to the stoichiometric cations ratio. Electrodes preparation consisted of the following steps: decarbonation at 600°C, fired in air for 48 h at 1100°C and then rapid removing from furnace and set ambient temperature. After reground, the mixture was pressed into discs (1 cm^2) and sintered at 1100°C for 24 h in air.

Electrochemical tests were performed at room temperature using a SP-150 potentiostat/galvanostat (Bio-Logic, SAS, France). A 100 mL typical glass cell was equipped with three electrodes: working electrodes consisting of perovkites samples, Ag/AgCl reference electrode and two graphite rods used as counter electrodes. For performed experiments, the exposed surface of working electrode was 0.2 cm^2. All potentials are given versus the reference electrode (E_{ref} = 0.197 V vs NHE).

Cyclic voltammograms (CVs) were recorded at different scan rate, between 5 and 500 mV s^{-1}. Linear polarization curves were registered potentiostatically with 1 mV s^{-1} scan rate. 1 M KOH solution (prepared using Merck KOH, p.a.) ensured the alkaline media used in all experimental studies. Different concentrations of ethanol were added: 0.06, 0.12, 0.25, 0.5, 1 and 2 M, prepared from Sigma-Aldrich reagent p.a. min 99.8%.

Results and discussions

In a direct ethanol fuel cell (DEFC), with ethanol mixed in an alkaline electrolyte, EOR occurs according the reaction:

$$C_2H_5OH + 12OH^- \rightarrow 2CO_2 + 9H_2O + 12e^- \quad (1)$$

In EOR, different intermediate chemisorbed species are produced, including carbon monoxide, acetaldehyde and acetate ions. EOR mechanism involves the water molecules or its adsorption species, so that a adequate anodic electrocatalyst should activate both ethanol and water chemisorption. Finally, EOR to CO_2 requires C-C bond breaking. The complexity of the process mechanism make EOR more difficult than that of methanol (MOR).

In Figure 1 linear voltammograms (LVs) recorded with 1 mV s^{-1} scan rate are shown, in absence and presence of ethanol different concentrations used in the alkaline electrolyte. LVs shape analysis indicates only one oxidation process on perovskite electrode surface.

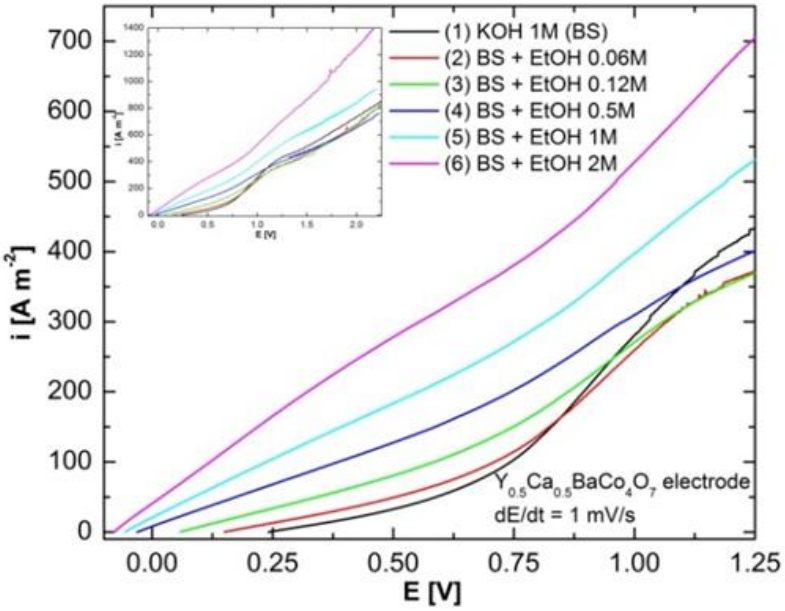

Figure 1. LVs recorded on $Y_{0.5}Ca_{0.5}BaCo_4O_7$ electrode in 1 M KOH solution with different ethanol concentration, at 1 mV s^{-1}

In 1M KOH solution, without ethanol the anodic behavior of perovskite electrode can be described by the following reaction (2) in a potential range between open circuit potential (OCP) and +1.50 V [9]:

$$Y_{0.5}Ca_{0.5}BaCo_4O_7 + 2\delta HO^- \leftrightarrow Y_{0.5}Ca_{0.5}BaCo_4O_{7+\delta} + \delta H_2O + 2\delta e^- \quad (2)$$

After overcomint the potential of +1.50 V anodic oxygen evolution occur (3):

$$4HO^- \rightarrow O_2 + 2H_2O + 4e^- \quad (3)$$

In this circumstances, the anodic oxidation of perovskite becomes prosible. This consists in oxygen insertion in oxide structure, assigned by the equation (4):

$Co(II) \rightarrow Co(III) + e^-$ (4)

In alkaline solution with ethanol, EOR on $Y_{0.5}Ca_{0.5}BaCo_4O_7$ perovskite occurs with similar mechanism as on $La_{2-x}Sr_xNiO_4$ in KOH solutions and it involves the following steps [10]:

$Co(II) \rightarrow Co(III) + e^-$ (5)

$Co(III) + OH^- \leftrightarrow Co(III)\cdot OH + e^-$ (6)

$Co(III) + CH_3CH_2OH \leftrightarrow Co(III)\cdot CH_3CH_2OH$ (7)

$Co(III)\cdot CH_3CH_2OH + Co(III)\cdot OH + OH^- \rightarrow Co(III)\cdot CH_3CHO + Co(II) + 2H_2O$ (8)

$Co(III)\cdot CH_3CHO + Co(III)\cdot OH + OH^- \rightarrow$ products (9)

EOR seems to be mediated by the Co(III)/Co(II) redox couple from inside of perovskite electrode. As well, the ethanol dehydrogenation is catalyzed by the same couple. *Reactions (5) and (9) take place rapidly [10].*

On LVs from figure 1 it can be observed the potential domain specific for EOR, between +0.25 and +1.50 V, including Co(II) to Co(III) oxidation potential. This behavior is somehow specific for layered perovskites in alkaline media [10].

Besides, EOR limiting current density increase along with the increasing of ethanol concentration in alkaline electrolyte.

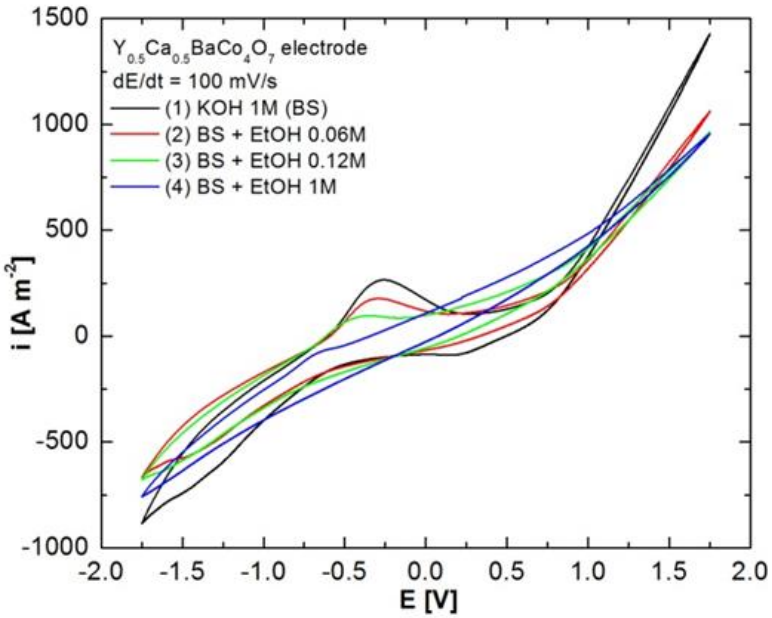

Figure 2. CVs recorded on $Y_{0.5}Ca_{0.5}BaCo_4O_7$ in BS without and with different ethanol concentrations

In figure 2 are depicted CVs recorded at 100 mV s^{-1} in alkaline solutions, in the absence and presence of ethanol, in a wide range of the potential (+1.75 and -1.75 V). It can be observed a pronounced anodic peak between -0.50 and 0.00 V and a cathodic current plateau at -1.40 and -1.70 V potential range. *These are associated with* acetaldehyde/acetate redox couple in alkaline medium for ethanol solution and Co(II) to Co reduction/oxidation for blank solution. In alkaline electrolyte with ethanol concentrations higher than 1 M characteristic peaks which may be attributed to EOR are not distinguished. At higher potentials, over +1.50 V, the increase of the current was associated with the oxygen evolution reaction (OER). At more negative electrode potentials than -1.70V hydrogen evolution reaction (HER) occurs.

Cyclic voltammetric studies have shown that it is possible to separate the peaks associated with the electrochemical processes occurring at the interface $Y_{0.5}Ca_{0.5}BaCo_4O_7$ – 1 M KOH without (figure 3) and with 0.12 M ethanol (figure 4) only if the potential scan rate is around 5 mV s^{-1}. *According to possible processes at the interface electrode/electrolyte, CVs can be divided in four potential domains for both perovskite oxidation and EOR: I - HER domain, II* - redox couple domain - *Co/Co(II) and* acetaldehyde/acetate, *II - oxidation domain - EOR and Co(II)/Co(III) and IV - OER on electrode surface domain.*

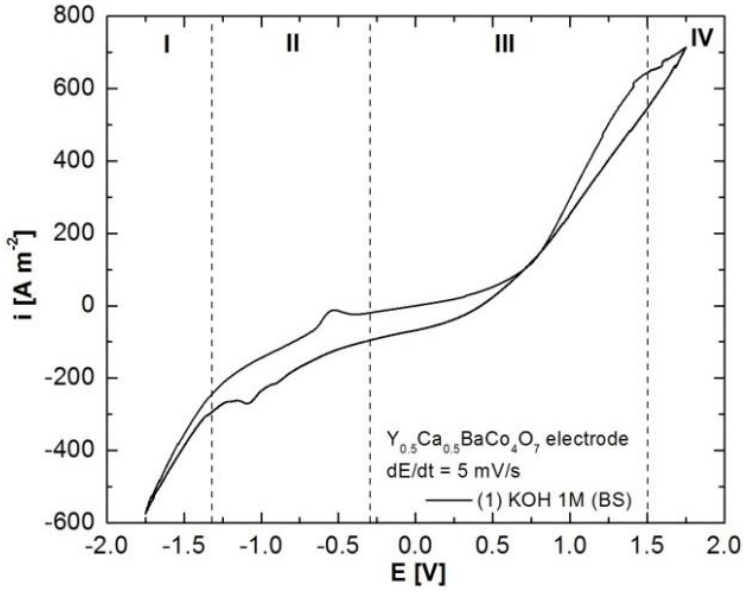

Figure 3. CV recorded on $Y_{0.5}Ca_{0.5}BaCo_4O_7$ electrode in 1 M KOH (BS) solution

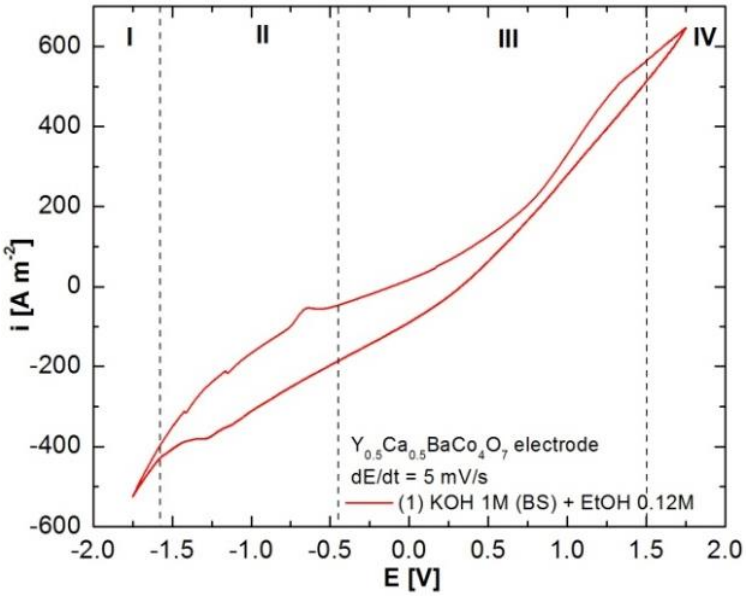

Figure 4. CV recorded on $Y_{0.5}Ca_{0.5}BaCo_4O_7$ electrode in BS with 0.12 M ethanol

Conclusions

Experimental data presented have confirmed the possibility to oxidize ethanol in alkaline media on an electrode based on cobalt layer perovskite type 114.

From the perspective of using cobalt layered perovskite as potential electrode materials in alkaline direct ethanol fuel cells, the possibility to oxidize ethanol on their surface provides a good reason for continuing studies presented in this paper. A deepening of the research is necessary both for complete characterization of processes occurring at the interface by electrochemical impedance spectroscopy. Furthermore, optimum characteristic parameters will be accessible.

Acknowledgement

This work was partially supported by University Politehnica Timisoara in the frame of PhD studies.

ლიტერატურა - REFERENCES – ЛИТЕРАТУРА

8. Sheikh A.M., Abd-Alftah K.A., Malfatti C.F. On reviewing the catalyst materials for direct alcohol fuel cells (DAFCs), *JMEST*. 2014, 1(3), 1-10.
9. Sahu O.P., Basu S. Direct Alcohol Alkaline Fuel Cell as Future Prospectus, *AEIJ*. 2014, 1(1), 43-52.
10. Antolini E., Gonzalez E.R. Alkaline direct alcohol fuel cells, *J.Power Sources*. 2010, 195, 3431–3450.
11. Badwal S.P.S., Giddey S., Kulkarni A., Goel J., Basu S. Direct ethanol fuel cells for transport and stationary applications – A comprehensive review, *Appl. Energy*. 2015, 145, 80–103.

12. Zhao T.S., Li Y.S., Shen S.Y. Anion-exchange membrane direct ethanol fuel cells: Status and perspective, *Front. Energy Power Eng. China*, 2010, 4(4), 443–458.
13. Lan A., Mukasyan A.S. Perovskite-based Catalysts for Direct Ethanol Fuel Cells, *ECS Trans.* 2007, 2 (24), 1-10.
14. Ekrami-Kakhki M.S, Yavari Z., Saffari J.,Ekrami-Kakhki S.A. Perovskite-Type LaFeO3 and LaFeO3-CNTs Nanocrystals as Active Anode for Methanol Oxidation in Alkaline Solutions, *JEE*. 2016, 4, 88-99.
15. Valldor M. Remnant magnetization above room temperature in the semiconductor $Y_{0.5}Ca_{0.5}BaCo_4O_7$, *Solid State Sci.* 8, 2006, 1272-1280.
16. Dan M., Pralong V., Vaszilcsin N., Kellenberger A., Duteanu N., Electrochemical behaviour of $YBaCo_4O_7$ in alkaline aqueous solution, *J. Solid State Electrochem.* 2011, 15(6), 1227-1233.
17. Singh R.N., Sharma T., Singh A., Anindita, Mishra D., Tiwari S.K. Perovskite-type $La_{2-x}Sr_xNiO_4$ ($0 \le x \le 1$) as active anode materials for methanol oxidation in alkaline solutions, *Electrochim. Acta*. 2008, 53, 2322-2330.

Ca-ით ლეგირებულიY-114 ტიპის შრეებრივი კობალტის პეროვსკიტის ელექტროდების ვოლტამპერული შესწავლა ტუტე ხსნარებში ეთანოლის ელექტროდაჟანგვისათვის კატალიზური ეფექტით

დან მირკეა ლაურენტი, დუკა დელია-ანდრადა, ვასზილცინ ნიკოლაე, კრაია-იოლდეს ვიქტორ-დანიელ
ტიმიშოარას პოლიტექნიკური უნივერსიტეტი, ინდუსტრიული ქიმიის და გარემოს დაცვის ფაკულტეტი

რეზიუმე

ამ სტატიაში მოცემულია ეთანოლის ანოდური დაჟანგვის რეაქციის შესწავლა $Y_{0.5}Ca_{0.5}BaCo_4O_7$ ელექტროდზე ტუტე წყალხსნარებში ვოლტამპერული კვლევების გამოყენებით. ეთანოლის ანოდური დაჟანგვის კატალიზური აქტივობა წარმოადგენს სერიოზულ საკითხს, განსაკუთრებით დაფენილი კობალტის პეროვსკაიტის გამოყენების თვალსაზრისით ანოდის სახით თბურ ელემენტებში. ეს კვლევა აუცილებელია ეთანოლის დაჟანგვის რეაქციის (ედრ) მექანიზმის გასარკვევად ამ ტიპის შედგენილი ელექტროდების ზედაპირზე. ელექტროქიმიური თვისებები შესწავლილ იქნა ციკლური ვოლტამპერმეტრიისა და წრფივი პოლარიზაციის საშუალებით. მიღებულმა შედეგებმა აჩვენეს, რომ დაფენილი კობალტის პეროვსკაიტები გამოსადეგია ანოდების სახით მაღალტემპერატურულ თბურ ელემენტებში.

საკვანძოსიტყვები: $Y_{0.5}Ca_{0.5}BaCo_4O_7$, შრეებრივი კობალტის პეროვსკიტი, ეთანოლის ელექტროდაჯანგვა, ვოლტამპერული შესწავლა

ВОЛЬТАМПЕРОМЕТРИЧЕСКИЕ ИССЛЕДОВАНИЯ ЛЕГИРОВАННОГО Ca СЛОИСТОГО КОБАЛЬТОВОГО ПЕРОВСКИТА ТИПА Y-114 В ЩЕЛОЧНЫХ РАСТВОРАХ С КАТАЛИТИЧЕСКИМ ЭФФЕКТОМ ДЛЯ ЭЛЕКТРООКИСЛЕНИЯ ЭТАНОЛА

Дан Миркея Лауренти, Дука Делия Андрада, Васзилцин Николаэ, Края-Ёлдес Виктор-Даниэл
Политехнический Университет Тимишоары, Факультет индустриальной химии и охраны окружающей среды

РЕЗЮМЕ

В этой работе изучалась реакция анодного окисления этанола на электроде $Y_{0.5}Ca_{0.5}BaCo_4O_7$в щелочных растворах с использованием вольтамперометрических исследований. Каталитическая активность при анодном окислении этанола является серьезной проблемой, особенно в вопросеиспользования слоистого кобальтовогоперовскита как анода в топливном элементе. Это исследование необходимо для понимания механизма реакции окисления этанола (РОЭ) на поверхности составных электродовтаково типа. Электрохимическое поведение изучалось с помощью циклической вольтамперометрии и линейной поляризации. Полученные результаты показали, что слоистые кобальтовыеперовскиты приемлемы в виде анодов для высокотемпературных топливных элементов.

Ключевые слова: $Y_{0.5}Ca_{0.5}BaCo_4O_7$, слоистый кобальтовый перовскит, электроокисление этанола, вольтамперометрические исследования

VOLTAMMETRIC STUDIES ON ANODIC OXIDATION OF SULPHITE IN ALKALINE SOLUTIONS ON SMOOTH NICKEL BASED 3 LAYERS PLATINUM NANOPARTICLES ELECTRODE

Enache Andreea Floriana, Dan Mircea Laurentiu, Vaszilcsin Nicolae
University Politehnica Timişoara, Faculty of Industrial Chemistry and Environmental Engineering, 300223, Parvan 6, Timisoara, Romania
andreea.enache13@yahoo.com

In this paper, anodic oxidation of sulphite ions on smooth nickel electrode based 3 layers platinum nanoparticles (Ni–Pt) in aqueous alkaline solutions has been investigated by electrochemical techniques in order to find optimum parameters of the process. Electrochemical behavior of sulphite ions has been studied by cyclic voltammetry and linear polarization on Ni-Pt electrode as a function of sulphite concentration at different polarization rate. The research is necessary to establish the oxidation mechanism on the surface of this kind of electrodes, taking into account both chemical and electrochemical reactions.
Keywords: smooth nickel, platinum nanoparticles, sulphite electrochemical oxidation

Introduction

Nanoparticles are the key elements in the energy technology development. The range of nanomaterials applications in catalysis is growing rapidly, as a result of using these materials in a large variety of catalytic reactions. Therefore, new strategies are required in order to achieve nanoparticles in large volume through techniques that are advantageous in terms of cost. Thus, nanoparticles of metals, semiconductors, oxides and other compounds have been widely used in important chemical reactions such as for hydrogen production from solid material, liquid or gaseous energy carriers [1], in electronics and optics [2], enzyme immobilization [3], for industrial synthesis of nitric acid [4], reduction of exhaust gases from vehicles [5] and as catalytic nucleating agents for synthesis of magnetic nanoparticles [6].

The basic role of the catalyst layer in a fuel cell is to provide a conductive environment for electrochemical reactions. The main processes that occur in the catalyst layer include mass transport, interfacial reactions at electrochemically active sites, proton transport in the electrolyte phase, and electron conduction in the electronic phase.

Platinum is still the dominant catalyst both as anode and cathode in almost all types of fuel cells, due to the high catalytic activity and long-term stability of operation [7]. Among the most important challenges for the commercialization of fuel cells achieving of catalysts with high activity, robust and low cost is included. The number of researches relevant for fundamentals of fuel cells with nano-catalysts is steadily increasing [8-12].

In a fuel cell, the electrolyte is essential for a proper work. Therefore, the electrochemical oxidation of sulphite ions has been a subject of great researches regarding the possibility to use SO_3^{2-} as electrolyte in alkaline fuel cells [13]. Sulphite ions oxidation can lead to a variety of sulphur compounds as elemental sulphur, polysulfide, thiosulphates and sulphates. The properties of sulphur dioxide, and more specifically its oxidation to sulphur trioxide, have been extensively investigated [14]. Electrochemical oxidation of SO_2 has been studied since 1930s, usually on noble metals electrodes and their oxides [15]. The mechanism of the electrochemical oxidation of sulphur dioxide was investigated on platinum, gold and graphite electrodes. On platinum electrode were revealed two possible oxidation mechanisms: first, a direct electron transfer at low anodic polarization and second, oxidation of the sulphur dioxide by the surface metal oxides at higher anodic polarization [14].

Sulphite oxidation under alkaline conditions has been studied in order to find new electrode materials with high catalytic activity. The research started from the premise that the electrodes must have catalytic properties also for oxygen reaction evolution (OER). In this case, nickel is commonly used to obtain anodes for OER. The issue associated with long-term electrochemical application is the fact that the anodic potential is unstable over time, which has as result an increase of power consumption [16].

The main purpose of this study is to obtain a catalyst that can be used in a fuel cell SO_3^{2-} / O_2. It is desirable to obtaine a catalyst with increased selectivity and activity, low energy consumption and long lifetime. As well, it aims to reduce the amount of noble metal by obtaining nanometric particles, thus improving chemical reactivity and reducing process costs.

Experimental

Electrode preparation

Chloroplatinic acid hexahydrate ($H_2PtCl_6 \cdot 6H_2O$) and isopropanol (Sigma-Aldrich, 99.7%) were used to obtain platinum salt precursor solution.

Platinum nanoparticles were deposited on smooth nickel substrate by spray-pyrolysis technique using an ultrasonic nebulizer SONO-TEK Corporation Exacta Coat. After the deposition process, electrodes were heated at 350°C for 30 minutes to evaporate the solvent and obtain Pt nanoparticles on smooth nickel substrate [17].

Electrochemical measurements

Experimental data were obtained with a SP 150 Bio-Logic potentiostat/galvanostat in a three-electrode electrochemical cell consisting of Ni – $Pt_{3layers}$ electrode as working electrode with a surface area exposed of 0.8 cm^2. Two graphite roads were used as counter electrodes and placed symmetrically to the working electrode. All potential values are presented versus the reference electrode Ag/AgCl ($E_{Ag/AgCl}$ = 0.197 V vs. SHE; SHE represents the standard hydrogen electrode).

Electrochemical experiments were carried out in 1 mol L^{-1} NaOH solution (Merck NaOH, p.a.) in which different concentrations of Na_2SO_3 (Merk, p.a. min. 98%) were added: 10^{-3}, 10^{-2} and 10^{-1} mol L^{-1}.

Cyclic voltammograms were recorded at different scan rate between 5 and 500 mV s^{-1}. Linear polarization curves were registered with 1 mV s^{-1} scan rate.

Results and disscusion

Figure 1 illustrates the comparative cyclic curves obtained in 1 mol L^{-1} NaOH solution in the absence of SO_3^{2-} ions and presence of 10^{-3}, 10^{-2}, respectively 10^{-1} mol L^{-1} SO_3^{2-}.

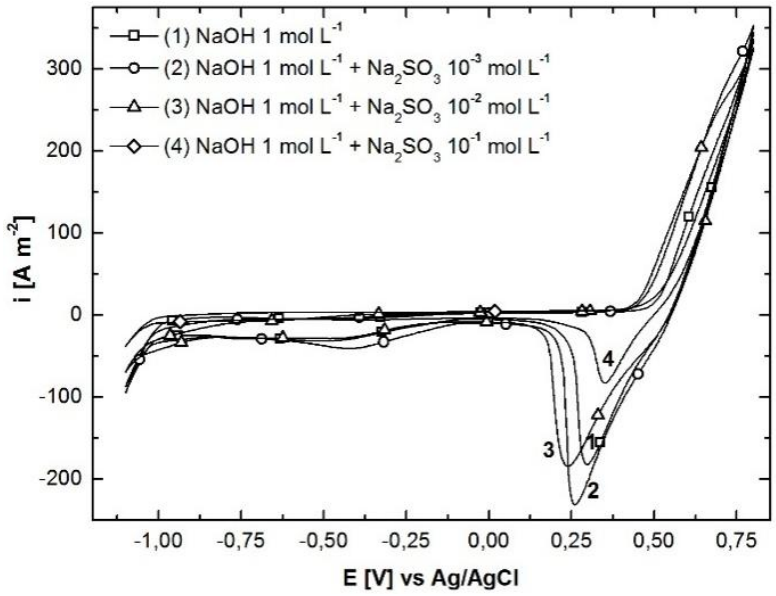

Figure 1. Cyclic voltamograms recorded on Ni – $Pt_{3layers}$ electrode in 1 mol L^{-1} NaOH wihout/with different concentration of Na_2SO_3 at 500 mV s^{-1}

Based on these curves it can be seen that the only electrode process on the cathodic scan is the hydrogen evolution reaction (HER). When the potential is shifted towards anodic values in the absence of sulphite ions, in 0.5 - 0.75 V potential range, it can be seen the wave associated with OER. In the presence of 10^{-3} mol L^{-1} sulphite, the process is shifted to more negative potential values, starting at 0.4 V. Analysing the obtained curves it can be considered that at this potential, sulphite oxidation begins, process in which additionally dissolved oxygen from electrolyte solution is involved, contributing to the unfolding of sulphite oxidation.

In figure 2a, on the curve corresponding to the electrolyte solution containing 10^{-3} mol L^{-1} SO_3^{2-}, a limited current plateau around 0.70 V potential value, associated with OER, is observed. This plateau cannot be observed when a concentration of 10^{-1} mol L^{-1} sulphite is used, as it is shown in figure 2b. Based on these results, it can be stated that the corresponding potential for sulphite oxidation increases with increasing concentration of sulphite ions.

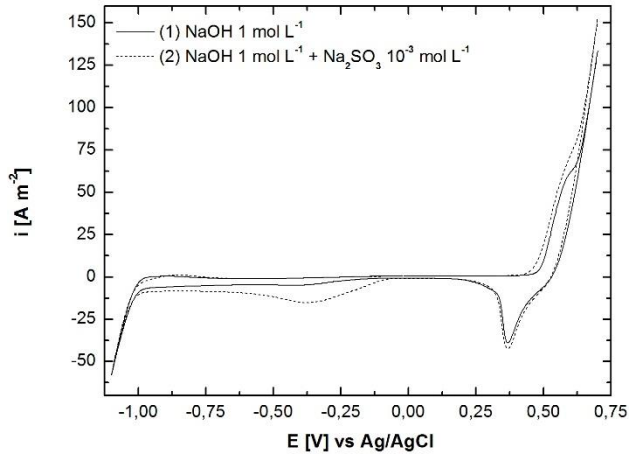

Figure 2a. Cyclic voltamograms recorded on Ni – $Pt_{3layers}$ electrode in 1 mol L^{-1} NaOH wihout/with 10^{-3} mol L^{-1} Na_2SO_3 at 50 mV s^{-1}.

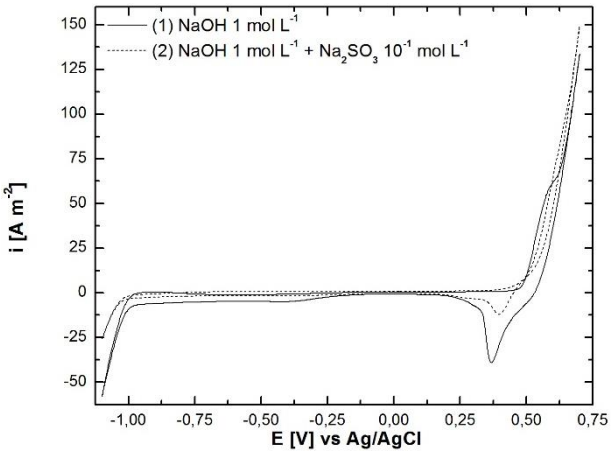

Figure 2b. Cyclic voltamograms recorded on Ni – $Pt_{3layers}$ electrode in 1 mol L^{-1} NaOH wihout/with 10^{-1} mol L^{-1} Na_2SO_3 at 50 mV s^{-1}.

Under alkaline conditions, the generally mechanism accepted for OER on different electrode materials is described by steps (1) - (4). Reaction (2) is the rate-determining step at lower potentials while reaction 1 is rate-determining at higher potentials [18-20]:

$OH^- = OH_{ads} + e^-$ (1)

$OH_{ads} + OH^- = O_{ads}^- + H_2O$ (2)

$O_{ads}^- = Oads + e^-$ (3)

$O_{ads} + O_{ads} = O_2$ (4)

Linear voltammetry technique was applied to confirm the above presented results. The curves obtained at 5 mV s^{-1} in alkaline media with SO_3^{2-} ions are shown in figure 3.

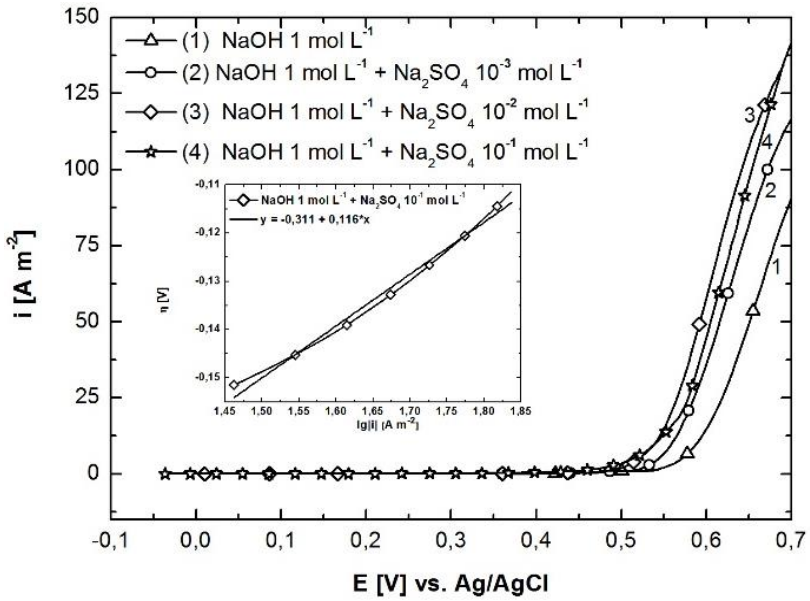

Figure 3. Linear voltammograms recorded on Ni – $Pt_{3layers}$ electrode in 1 mol L^{-1} NaOH with/without Na_2SO_3 at 5 mV s^{-1}; Tafel slope for electrochemical oxidation of SO_3^{2-} in alkaline media inserted.

The two possible mechanisms which can describe the electrochemical oxidation of sulphite to sulphate ions in alkaline media presented by Skavas comprise the reactions (5) - (9) [21]. According to the first mechanism, SO_3^{2-} is oxidized to SO_4^{2-} in two successive steps, each implying one electron transfer:

$$SO_3^{2-} \rightarrow SO_3^{\bullet-} + e^- \quad (5)$$

$$SO_3^{\bullet-} + 2OH^- \rightarrow SO_4^{2-} + H_2O + e^- \quad (6)$$

$$2SO_3^{\bullet-} \rightarrow S_2O_6^{2-} \quad (7)$$

$$S_2O_6^{2-} + 2OH^- \rightarrow SO_3^{2-} + SO_4^{2-} + H_2O \quad (8)$$

$$2SO_3^{2-} + O_2 \rightarrow 2SO_4^{2-} \quad (9)$$

In the second mechanism, sulphite anion is oxidized to sulphite radical (5) followed by the interaction between two sulphite radicals forming dithionate ions (7). Finally, these ions consecutively cleave in SO_4^{2-} and SO_3^{2-} ions (8).

OER mechanism on Ni – Pt electrode takes place according to reactions (1) - (4) and SO_3^{2-} ions oxidation is conducted directly in alkaline electrolyte by a chemical irreversible process (9) in which the molecular oxygen was produced on electrode active surface in OER.

Based on Tafel plots $\eta = f(\log i)$ inserted in figure 3, kinetic parameters (transfer coefficient α and exchange current density i_o) for electrochemical oxidation of sulphite ions in alkaline solution on Ni – Pt electrode have been calculated (Table 1).

Table 1. Kinetic parameters for sulphite oxidation in alkaline solutions:

Na_2SO_3 concentration [mol L^{-1}]	b [mV dec^{-1}]	α	i_o [A m^{-2}]
10^{-1}	116	0.51	14.6

Conclusions

Smooth nickel based platinum nanoparticles (3 layers) electrode prepared by spray-pyrolysis technique has been characterized by cyclic voltammery technique according with its applicability as electrocatalytic material in fuel cells for sulphite ions oxidation in alkaline solution. The insertion of Pt nanoparticles has significantly increased the activity of studied reaction and the presented results confirmed the possibility of oxidizing electrochemically SO_3^{2-} to SO_4^{2-} on smooth nickel based platinum nanoparticles electrode.

Acknowledgement

This work was partially supported by University Politehnica Timisoara in the frame of PhD studies.

ლიტერატურა - REFERENCES – ЛИТЕРАТУРА

1. Giancaterini L, Cantalini C, Cittadini M, Sturaro M, Guglielmi M, Martucci A, Resmini A, Anselmi-Tamburini U. Au and Pt nanoparticles effects on the optical and electrical gas sensing properties of sol–gel-based ZnO thin-film sensors. IEEE Sens. J. 2015, 15, 1068-1076.
2. Chauhan N, Narang J, Sunny, Pundir CS. Immobilization of lysine oxidase on a gold–platinum nanoparticles modified Au electrode for detection of lysine. Enzyme Microb Technol. 2013, 52, 265-271.
3. Sanap KK, Varma S, Waghmode SB, Bharadwaj SR, Supported Pt nanoparticles for the hydrogen mitigation application. Int. J. Hydrogen Energy. 2014, 39, 15142-55 .
4. Reddington E, Sapienza A, Gurau B, Viswanathan R, Sarangapani S, Smotkin ES, Mallouk TE, Combinatorial electrochemistry: A highly parallel, optical screening method for discovery of better electrocatalysts. Science. 1998, 280, 1735-1737.
5. Williams KR, Burstein GT. Aspects of the anodic oxidation of methanol. Catal. Today, 1997, 38, 425-437.
6. Bell AT. The impact of nanoscience on heterogeneous catalysis. Science. 2003, 299, 1688–1691.
7. Yan Qiao, Chang Ming Li. Nanostructured catalysts in fuel cells. J. Mater. Chem. 2011, 21, 4027–4036.
8. Zhong CJ, Luo J, Fang B, Wanjala BN, Njoki PN, Loukrakpam R, Yin J. Nanostructured catalysts in fuel cells. Nanotechnology. 2010, 21, 062001.
9. Qiao Y, Li CM. Nanostructured catalysts in fuel cells. J. Mater. Chem. 2011, 21, 4027–4036.
10. Basri S, Kamarudin SK, Daud WRW, Yaakub Z. Nanocatalyst for direct methanol fuel cell (DMFC). Int. J. Hydrogen Energy. 2010, 35 (15), 7957–7970.
11. Liu H, Song C, Zhang L, Zhang J, Wang H, Wilkinson DP. A review of anode catalysis in the direct methanol fuel cell. J. Power Sources. 2006, 155 (2), 95–110.

12. Antolini E. Carbon supports for low-temperature fuel cell catalysts. Appl. Catal. B: Environ. 2009, 88, 1–24.
13. Bagotsky V.S., Fuel cells: Problems and Solution, 2nd Edition, Ed. John Wiley & Sons, 2012.
14. Nikolov I, Petrov K, Vitanov T. Low temperature electrochemical oxidation of sulfur dioxide. J. Appl. Electrochem. 1996, 26, 703-709.
15. Seo ET, Sawyer DT. Electrochemical oxidation of dissolved sulphur dioxide at platinum and gold electrodes. Electrochim. Acta. 1965, 10 (3), 239-252.
16. Miao HJ, Piron DL. Electrodeposition of Ni-transition alloys for the oxygen evolution reaction. J. Appl. Electrochem. 1991, 21, 55-59.
17. Iacob A, Dan ML, Vaszilcsin N. Enhancement of hydrogen evolution reaction on nickel based electrodes modified with platinum nanoparticles, Annals of University of Oradea, Fascicle of Environmental Protection, 2015, 25, 193-200.
18. Iwakura C, Fukuda K, Tamura H. The anodic evolution of oxygen on platinum oxide electrode in alkaline solutions. Electrochim. Acta. 1976, 21, 501-508.
19. Damjanovica A, Dey A, Bockris JO'M. Kinetics of oxygen evolution and dissolution on platinum electrodes. Electrochim. Acta. 1966, 11, 791-814.
20. Akano UG. Oxygen evolution reactions on nickel, nickel oxide electrodes using galvanostatic methods, Doctoral Thesis, 1980, McMaster University, Department of Engineering Physics, Hamilton, Ontario.
21. Skavas E, Hemmingsen T. Kinetics and mechanism of sulphite oxidation on a rotating platinum disc electrode in an alkaline solution. Electrochim. Acta. 2007, 52, 3510-3517.

სულფიტის ანოდური დაჟანგვის ვოლტამპერული შესწავლა ტუტე ხსნარებში ერთგვაროვან ნიკელზე დაფუძნებულ პლატინის ნანონაწილაკების 3 შრიან ელექტროდზე

ენახ ანდრეა ფლორიანა, დან მირკეა ლაურენტი, ვასზილცინ ნიკოლაე
ტიმიშოარას პოლიტექნიკური უნივერსიტეტი, ინდუსტრიული ქიმიისა და გარემოს ინჟინერიის ფაკულტეტი

რეზიუმე

პროცესის ოპტიმალური პარამეტრების დადგენის მიზნით ელექტროქიმიური ტექნილოგიის საშუალებით, შესწავლილ იქნა სულფიტის იონების ანოდური დაჟანგვა, ერთგვაროვან ნიკელის ფუძეზე პლატინის ნანონაწილაკების 3 შრიან ელექტროდზე (Ni–Pt) ტუტე ხსნარებში. სულფიტის იონების ელექტროქიმიური ქცევა შესწავლილ იქნა ციკლური ვოლტამპერომეტრიისა და Ni–Pt-ის ელექტროდზე წრფივი პოლარიზაციის საშუალებით, როგორც სულფიტის კონცენტრაციის ფუნქციისა პოლარიზაციის სხვადასხვა სიჩქარეზე. ეს კვლევა მნიშვნელოვანია ქიმიური და ელექტროქიმიური რეაქციების გათვალისწინებით ამ ტიპის ელექტროდების ზედაპირზე დაჟანგვის მექანიზმის დასადგენად.

საკვანძო სიტყვები: ერთგვაროვანი ნიკელი, პლატინის ნანონაწილაკები, სულფიტის ელექტროქიმიური დაჯანგვა.

ВОЛЬТАМПЕРОМЕТРИЧЕСКИЕ ИССЛЕДОВАНИЯ АНОДНОГО ОКИСЛЕНИЯ СУЛЬФИТА В ЩЕЛОЧНЫХ РАСТВОРАХ НА ТРЁХСЛОЙНОМ ЭЛЕКТРОДЕ ПЛАТИНОВЫХ НАНОЧАСТИЦ,ОСНОВАННОМ НА ОДНОРОДНОМ НИКЕЛЕ

Энах Андрэа Флориана, Дан Миркея Лауренти, Васзилцин Николаэ
Политехнический Университет Тимишоары, Факультет индустриальной химии и охраны окружающей *среды*

РЕЗЮМЕ

В этой работе проведено исследование анодного окисления ионов сульфита в водных щелочных растворах на основанном на однородном никеле 3-слойном электроде платиновых наночастиц(Ni–Pt),электрохимических методом, для определения оптимальных параметров процесса. Электрохимическое поведение ионов сульфита было изучено с помощью циклической вольтамперометрии и линейной поляризации на Ni-Pt электроде как функции концентрации сульфита при различных скоростях поляризации. Это исследование необходимо для установления механизма окисления на поверхности такого типа электродов, с учетом как химических, так и электрохимических реакций.

Ключевые слова: однородный никель, платиновые наночастицы, электрохимическое окисление сульфита.

VOLTAMMETRIC STUDIES OF METHANOL ELECTROOXIDATION IN ALKALINE SOLUTIONS ON SKELETAL NICKEL BASED 6 LAYERS PLATINUM NANOPARTICLES ELECTRODE

Duca Delia-Andrada, Dan Mircea Laurențiu, Vaszilcsin Nicolae
University Politehnica Timişoara, Faculty of Industrial Chemistry and Environmental Engineering, 300223, Parvan 6, Timisoara, Romania
duca.delia@gmail.com

In this paper, new aspects of methanol electrocatalytic oxidation on skeletal nickel based 6 layers platinum nanoparticles electrode in aqueous alkaline solution were investigated. Pt and its alloys are the most commonly used catalytic materials as anode of direct alcohol fuel cells, taking into account their excellent adsorptive properties and easy methanol dissociation. New electrodes have been prepared by spray pyrolysis technique and are propose for methanol oxidation reaction (MOR). The electrochemical activity for MOR was investigated by cyclic voltammetry and linear polarization techniques. The present study concerns the preparation of several Ni based platinum electrode materials and evaluation of their electrocatalytic properties toward MOR.
Keywords: skeletal nickel electrode, platinum nanoparticles, methanol electrooxidation

Introduction

Currently, an attractive alternative for fossil fuels combustion is the fuel cell, the most efficient and ecological energy source [1]. Among different types of fuel cells, alkaline fuel cells (AFCs) are the most developed. AFCs have numerous advantages over proton exchange membrane fuel cells (PMFC) of which the best known is the less corrosive nature of an alkaline environment which ensures a greater longevity [2]. As well, AFCs consist in a low cost technology compared to PEMFCs, which are equipped mainly with platinum catalysts [2].

Direct alcohol fuel cells (DAFCs) are electrochemical energy supplies that continuously remain the focus of research, especially in terms of finding new electrode materials with high efficiency for alcohols oxidation. Liquid fuels, such as alcohols with low molecular weight, have several advantages compared to pure hydrogen. Methanol is the most commonly alcohol used in DAFCs because it is a renewable energy source, available in big quantities, and easily stored and handled [3].

A large part of researches on direct methanol fuel cells (DMFC) were conducted in order to elucidate aspects of methanol oxidation mechanism on the anode surface [4]. Literature data emphasizes a complex reaction mechanism, underlining that methanol oxidation electrocatalysis is the most difficult task in a DMFC achieving [4]. It was proved that platinum has the best catalytic activity for MOR in both alkaline and acid media [2-4]. Alkaline media open the possibility of using non-noble, less expensive metal catalysts. MOR on other metal electrodes such as: gold, palladium, nickel or their alloys has been the aim of numerous studies, mainly due to the possibility of using them as anode in fuel cells.

In MOR, one of the intermediate product is CO. It is also the most harmful product for anode metal materials. Searching for efficient electrocatalysts that offset CO poisoning of Pt-based anode, binary or ternary alloys have shown considerable alternative for MOR [5-7]. Among these catalysts, PtNi alloy has received attention [7,8]. Nickel and nickel oxy-hydroxide are good materials for organic compounds oxidation in alkaline media [9]. From the alloys anode material point of view, the MOR rate depends on factors such as: amount of second metal content, degree of its alloying with Pt, electrode pretreatment, and supporting substrate material [7].

Formaldehyde, formate and CO are considered reaction intermediates in alkaline media. MOR mechanism involves a reaction of adsorbed intermediates and adsorbed OH^- on anode surface. So far, the final product of MOR in alkaline media is not clearly defined.

In this paper, skeletal nickel based 6 layers platinum nanoparticles electrode electocatalytic activity was evaluated performing MOR in alkaline medium using cyclic and linear voltammetry.

Experimental

Skeletal nickel electrode was prepared in two steps. For skeletal Ni electrodes preparation, Ni (Fluka, 99.2%) and Al (Fluka, 99.5%) have been used as anode, respectively as cathode. In first step, using thermal arc spraying technique, the arc current and voltage were set to 200 A and 30 V. In order to remove Al from

the coating, the electrodes were submitted into alkaline solution 1 M NaOH for 2 h at about 80°C [10]. Finally, the electrodes were cleaned for 15 minutes in distilled water using an ultrasonic bath.

In a second step, chloroplatinic acid hexahydrate ($H_2PtCl_6 \cdot 6H_2O$, Sigma-Aldrich) and isopropanol (Sigma-Aldrich, 99.7%) were used for preparation of Pt salt precursor solution. A smooth nickel disk with a diameter of 10 mm was used as electrode substrate. A fixed quantity of mixture was then sprayed, using an ultrasonic nebulizer SONO-TEK Corporation Exacta Coat, onto the top surface of the nickel plate to prepare the electrode. After deposition, the electrode was heated at 350°C for 30 minutes, achieving the solvent evaporation and obtaining the Pt nanoparticles. The process was repeated 6 times [11].

Cyclic and linear voltammetric measurements were performed using a SP 150 Bio-Logic potentiostat/galvanostat. Electrochemical experiments were performed in a three-electrode typical glass electrochemical cell. The three-electrode system consisted of a working electrode skeletal Ni based 6 Pt nanoparticles), embedded in a Teflon holder, exposing a geometric surface area of 0.5 cm^2, two graphite roads as counter electrodes, and a Ag/AgCl as reference electrode. Potentials are given versus the reference electrode (E_{ref} = 0.197 V vs NHE). All experiments were carried out in 1 M KOH (prepared using Merck KOH, p.a.) supporting alkaline electrolyte solution. Different methanol concentrations were added: 0.125, 0.25, 0.5, 1 and 2 mol L^{-1}, all prepared from Sigma-Aldrich reagent p.a. min 99.8%.

Cyclic voltammograms (CVs) were recorded at different scan rate, between 5 and 100 mV s^{-1}. Linear polarization curves (LVs) were registered potentiostatically with 1 mV s^{-1} scan rate.

Results and discussion

CVs recorded in alkaline solutions, in the absence and presence of methanol, in a wide range of potential (from -1.20 to +0.70 V), at 100 and 5 mV s^{-1} are depicted in Figure 1a and b. Starting from open circuit potential (OCP) towards anodic polarisation it is observed an anodic plateau (especially at methanol low concentrations) associated with MOR and with $Ni(OH)_2$ to NiOOH oxidation for blank solution. When the electrode potential is over +0.60 V, oxygen evolution reaction (OER) on electrode surface can be noticed. On the backward scan, a reduction peak (with high intensity on CVs recorded at 100 mV s^{-1}), associated with adsorbed oxygen reduction, was recorded. When the electrode potential becomes more negative than -1.10 V, hydrogen evolution reaction (HER) occurs. Further, when the potential is scanned in anodic direction, up to OCP, an oxidation peak is observed at approximately -0.25 V due to the formaldehyde oxidation to formate ions or other products. This anodic peak is inserted in both figures.

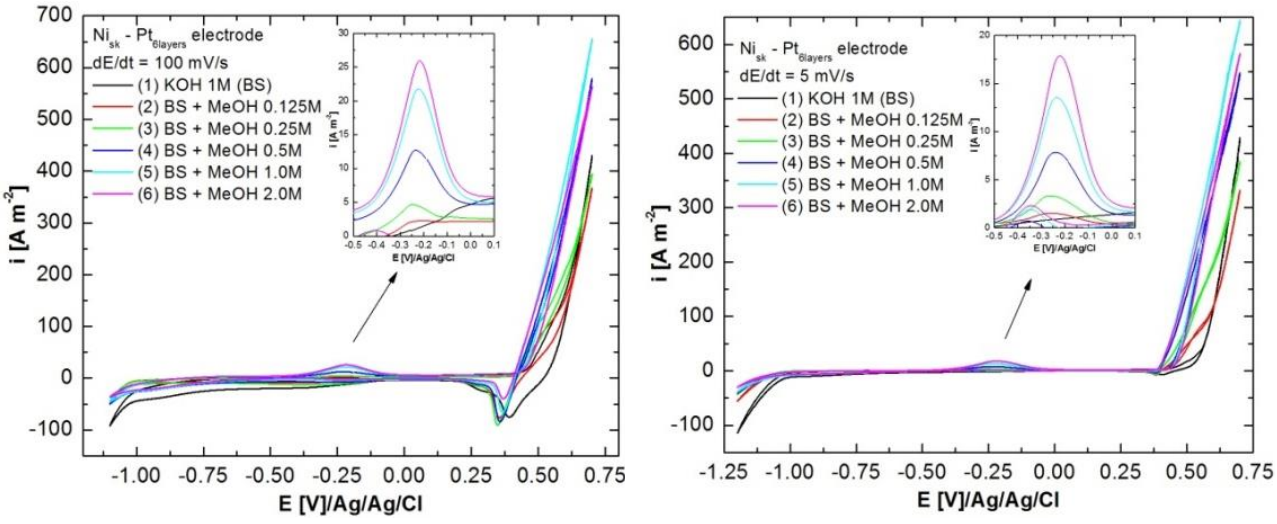

Figure 1. Cyclic voltammograms in 1M KOH without and with methanol different concentration, scan rate 100 mV s^{-1}(a) and 5 mV s^{-1}. Inserted anodic peak for formaldehyde to formate oxidation

In order to identify how methanol concentration in alkaline media influences the MOR, polarization curves were recorded separately at higher sensitivity in anodic domain, as shown in Figure 2.

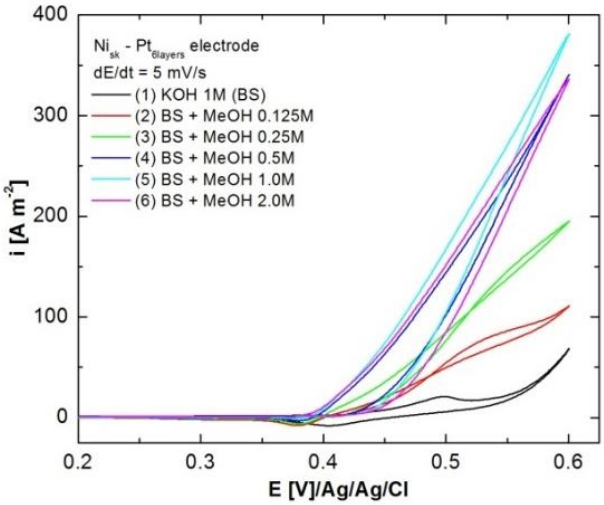

Figure 2. Cyclic voltammograms (anodic domain) in 1M KOH without and with methanol different concentration, scan rate 5 mV s^{-1}

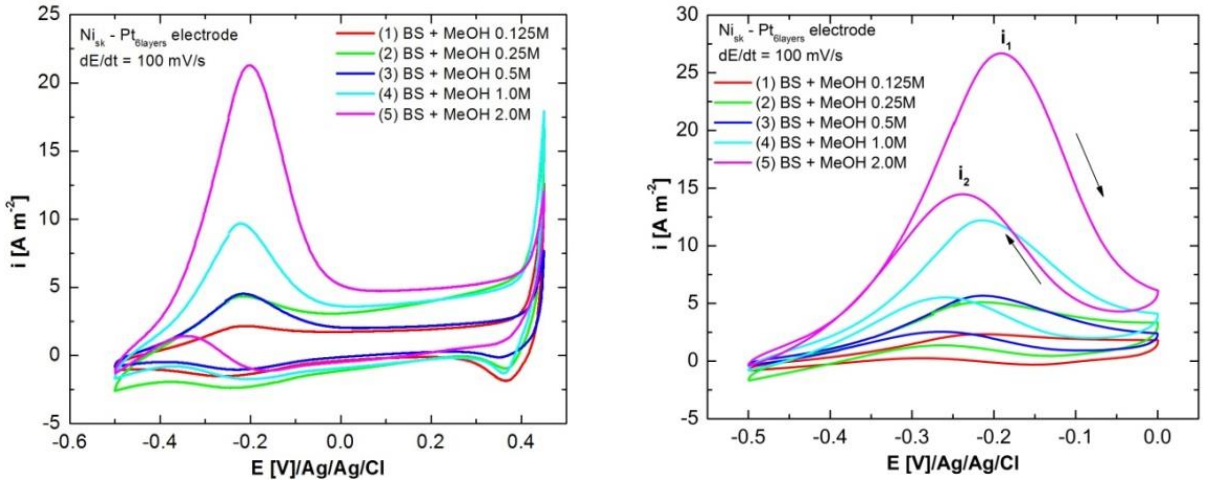

a) b)

Figure 3. Cyclic voltammograms (formaldehyde/formate redox couple domain) in 1M KOH without and with methanol different concentration, scan rate 5 mV s^{-1}

In Figure 3a and b CVs recorded for formaldehyde/formate redox couple in two potential ranges are presented. Only if CVs are recorded up to MOR potential value, a peak characteristic for formate reduction to formaldehyde appears on the backward scan. Electrochemical parameters from CVs (peaks current density) are shown in Table 1.

Table 1. Electrochemical parameters from CVs (Formaldehyde/Formate redox couple) and LVs (MOR):

Electrolyte	**CVs Formaldehyde/Formate redox couple**		**LVs MOR**	
	i_1 **[A m^{-2}]**	i_2 **[A m^{-2}]**	E_{ox} **range [V]**	$i_{lim.ox}$ **[A m^{-2}]**
BS + MeOH 0.125 M	2.34	0.31	0.45 ÷ 0.56	91.3
BS + MeOH 0.25 M	4.96	1.46	0.44 ÷ 0.60	201
BS + MeOH 0.5 M	5.84	2.63	0.43 ÷ 0.62	402
BS + MeOH 1 M	12.25	5.64	0.43 ÷ 0.64	407
BS + MeOH 2 M	26.71	14.58	0.42 ÷ 0.66	446

The relationship between oxidation current (i_1 and i_2 - current density for forward and backward scan) characteristic for formaldehyde/formate redox couple and methanol concentration is linear and can be described by the following equations, obtained by linear regression:

$i_1 = 0.51 + 12.7\ C_{methanol}$ (1)

$i_2 = -0.89 + 7.5\ C_{methanol}$ (2)

where: 12.7 and 7.5 are scan rate constants depending and $C_{methanol}$ is methanol concentration in alkaline electrolyte.

LVs plotted at low scan rate (1 mV s^{-1}) in alkaline media with different concentrations of methanol are shown in Figure 4. The curves shape indicates only one oxidation process on electrode surface. Specific parameters (oxidation range potential and limiting current density) for MOR on skeletal nickel based 6 layer platinum nanoparticles are presented in Table1.

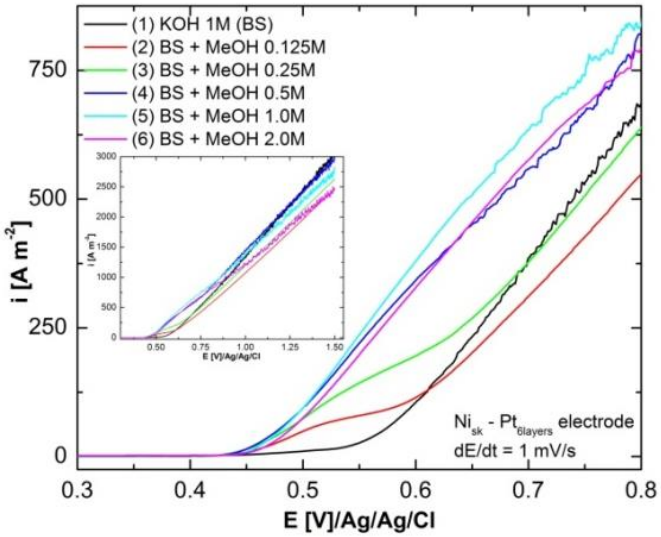

Figure 4. Linear voltammograms (anodic domain) in 1M KOH without and with methanol different concentration, scan rate 1 mV s^{-1}

Anodic methanol oxidation process is really complex, involving 6 electron transfers and forming several intermediate organic species. MOR overall equation in alkaline medium is given by equation (3):

$CH_3OH + 6OH^- \rightarrow CO_2 + 5H_2O + 6e^-$ (3)

MOR in alkaline medium on Pt or Pt-alloys electrode was described by S. S. Mahapatra and J. Datta and proceeds through the following steps [12]:

$Pt + (CH_3OH)_{sol} \rightarrow Pt - (CH_3OH)_{ads}$ (4)

$Pt - (CH_3OH)_{ads} + OH^- \rightarrow Pt - (CH_3O)_{ads} + H_2O + e^-$ (5)

$Pt - (CH_3O)_{ads} + OH^- \rightarrow Pt - (CH_2O)_{ads} + H_2O + e^-$ (6)

$Pt - (CH_2O)_{ads} + OH^- \rightarrow Pt - (CHO)_{ads} + H_2O + e^-$ (7)

$Pt - (CHO)_{ads} + OH^- \rightarrow Pt - (CO)_{ads} + H_2O + e^-$ (8)

$Pt - (CO)_{ads} + OH^- \rightarrow Pt - (COOH)_{ads} + e^-$ (9)

$Pt - (COOH)_{ads} + OH^- \rightarrow Pt + CO_2 + H_2O + e^-$ (10)

Reactions (8) and (9) can proceed directly to CO_2 production [12]:

$Pt - (CHO)_{ads} + 3OH^- \rightarrow Pt + CO_2 + 2H_2O + 3e^-$ (11)

$Pt - (CO)_{ads} + 2OH^- \rightarrow Pt + CO_2 + H_2O + 2e^-$ (12)

Conclusions

In this study, 6 layers Pt nanoparticles with an electroless method were deposited on the skeletal nickel electrode. The electrodes prepared using this method has a high surface area and increased catalytic activity for MOR in alkaline media. Due to ease way of preparation, high performance in MOR, and good adherence of Pt nanoparticles, the proposed electrode is suitable as anode in DMFC.

Acknowledgement

This work was partially supported by University Politehnica Timisoara in the frame of PhD studies.

ლიტერატურა - REFERENCES – ЛИТЕРАТУРА

1. Skowroński J. M., Ważny A. Electrooxidation of methanol in alkaline solution on composite electrodes. Mater. Sci.-Poland. 2006, 24(1), 291-297.
2. Antolini E., Gonzalez E.R. Alkaline direct alcohol fuel cells. J. Power Sources. 2010, 195, 3431–3450.
3. Verma L. K. Studies on methanol fuel cell. J. Power Sources. 2000, 86(1), 464–468.
4. Iwasita T. Methanol and CO electrooxidation. Handbook of Fuel Cells – Fundamentals, Technology and Applications, Edited by Vielstich W., Gasteiger H.A., Lamm A., Volume 2, Electrocatalysis, 2003 John Wiley & Sons, Ltd., ISBN 0-471-49926-9.
5. Holt-Hindle P., Yi Q.F., Wu, G.S., Koczkur K., Chen A.C. Electrocatalytic activity of nanoporous Pt–Ir materials toward methanol oxidation and oxygen reduction. J. Electrochem. Soc.2008, 155, K5–K9.
6. Hsieh C.T., Lin J.Y. Fabrication of bimetallic Pt–M (M = Fe, Co, and Ni) nanoparticle/carbon nanotube electrocatalysts for direct methanol fuel cells. J. Power Sources. 2009, 188, 347–352.
7. Kang J., Wang R, Wang H., Liao S., Key J., Linkov V., Ji S. Effect of Ni Core Structure on the Electrocatalytic Activity of Pt-Ni/C in Methanol Oxidation. Materials. 2013, 6, 2689-2700.
8. Deivaraj T.C., Chen W., Lee J.Y. Preparation of PtNi nanoparticles for the electrocatalytic oxidation of methanol. J. Mater. Chem. 2003, 13, 2555–2560.
9. El-Shafei, A.A. Electrocatalytic oxidation of methanol at a nickel hydroxide/glassy carbon modified electrode in alkaline medium. J. Electroanal. Chem. 1999, 471, 89–95.
10. Kellenberger A., Vaszilcsin N., Brandl W., Duteanu N. Kinetics of hydrogen evolution reaction on skeleton nickel and nickel–titanium electrodes obtained by thermal arc spraying technique. Int. J. Hydrogen Energy. 2007, 32 (15), 3258–3265.
11. Iacob A., Dan M.L., Kellenberger A., Vaszilcsin N. Hydrogen Evolution Reaction on Nickel-Based Platinum Electrodes. Chem. Bull. "POLITEHNICA" Univ. (Timisoara). 2014, 59(73), 2, 42-45.
12. Mahapatra S. S., Datta J. Characterization of Pt-Pd/C Electrocatalyst for Methanol Oxidation in Alkaline Medium. Int. J. Electrochem. 2011, 1-17.

მეთანოლის ელექტრო დაჟანგვის ვოლტამპერული შესწავლა ტუტე ხსნარებში ნიკელის კარკასზე დაფენილი პლატინის ნანონაწილაკების 6 შრიან ელექტროდზე

დუკა დელია-ანდრადა, დანმირკეალაურენტი, ვასზილცინ ნიკოლაე

ტიმიშოარას პოლიტექნიკური უნივერსიტეტი, ინდუსტრიული ქიმიის და გარემოს ინჟინერიის ფაკულტეტი

რეზიუმე

ამ სამუშაოში შესწავლილ იქნა ნიკელის კარკასის ფუძეზე პლატინის ნანონაწილაკების 6 შრიან ელექტროდზე ტუტე წყალხსნარებში მეთანოლის ელექტროკატალიზური დაჟანგვის ახალი ასპექტები. პლატინა და მისი შენადნობები მათი შესანიშნავი ადსორბციული თვისებებისა და მეთანოლის ადვილი დისოციაციის გათვალისწინებით, ყველაზე ხშირად გამოყენებადი კატალიზური მასალებია როგორც პირდაპირი ალკოჰოლური თბური ელემენტების ანოდები. ახალი ელექტროდები დამზადდა ჭავლური პიროლიზური ტექნიკის საშუალებით და შემოთავაზებულ იქნა მეთანოლის დაჟანგვის რეაქციისთვის (მდრ). მდრ-ის ელექტროქიმიური აქტივობა შესწავლილ იქნა ციკლური ვოლტამპერმეტრიისა და წრფივი პოლარიზაციის ტექნოლოგიების საშუალებით. წარმოდგენილი კვლევა მოიცავს ნიკელზე დაფუძნებული პლატინის რამოდენიმე საელექტროდე მასალის დამზადებას და მათი ელექტროკატალიზური თვისებების შეფასებას მდრ-ის მიმართ.

საკვანძო სიტყვები: ნიკელის ელექტროდი,პლატინის ნანონაწილაკები, მეთანოლის ელექტროდაჯანგვა.

ВОЛЬТАМПЕРОМЕТРИЧЕСКИЕ ИССЛЕДОВАНИЯ ЭЛЕКТРООКИСЛЕНИЯ МЕТАНОЛА В ЩЕЛОЧНЫХ РАСТВОРАХ НА ШЕСТИСЛОЙНОМ ЭЛЕКТРОДЕ ПЛАТИНОВЫХ НАНОЧАСТИЦ, ОСНОВАННОМ НА СКЕЛЕТНОМ НИКЕЛЕ

Дука Делия Андрада, Дан Миркея Лауренти, Васзилцин Николаэ

Политехнический Университет Тимишоары, Факультет индустриальной химии и охраны окружающей среды

РЕЗЮМЕ

В этой работе проведено исследование новых аспектов электрокаталитического окисленияметанола в водных щелочных растворах на основанном на скелетном никеле 6-слойном электроде платиновых наночастиц. Pt и её сплавы являются широко применяемыми каталитическими материалами для анодов прямых алкогольных топливных элементов, с учетом их отличных адсорбционных свойств и легкой диссоциации метанола. Новые электроды приготовлялись методомструйного пиролиза и предлагаются для реакции окисления метанола (РОМ). Электрохимическая активность РОМ была исследована метом циклической вольтамперометрии и линейной поляризации. Данная работа касается приготовления нескольких основанных на никеле платиновых электродных материалов и оценки их электрокаталитических свойств относительно РОМ.

Ключевые слова: скелетный никелевый электрод, платиновые наночастицы, электроокисление метанола.

INHIBITORY EFFECT OF RESVERATROL ON ALUMINUM CORROSION IN ALCOHOLIC SOLUTIONS

Cristian George Vaszilcsin, Mircea Laurentiu Dan*, Delia-Andrada Duca*, Mihaela Labosel*
National Institute of Electrochemistry, Dr. A. Paunescu Podeanu 144, 300569,Timisoara, Romania,
**University Politehnica Timişoara, Faculty of Industrial Chemistry and Environmental Engineering, 300223, Parvan 6, Timisoara, Romania, cristi_vasz@yahoo.com*

This paper presents results obtained using resveratrol as corrosion inhibitor for aluminum in ethanol solutions. Inhibitory properties of resveratrol were studied in 12% ethanol + 0.25 M Na_2SO_4 solutions in the presence of different concentrations of inhibitor, between 10^{-6} and 10^{-3} M. Electrochemical tests have been performed on two materials types: polished and brushed aluminum. Resveratrol electrochemical behavior in ethanol solutions was examined by cyclic voltammetry on platinum electrode. The inhibitory effect was studied by linear polarization (Tafel method) in order to determine the kinetic parameters, providing thus information about the inhibitory effect mechanism.
Keywords: resveratrol, corrosion inhibitor, aluminum corrosion

Introduction

Corrosion resistance is the main property to be considered in the materials choice for food industry, but the final selection must be a compromise between technological and economic factors [1,2].

Aluminum is present in food naturally, as a food additive, and also is used in food preparation and storage. The use of aluminum in cookware has begun around 1900 due to its thermal conductivity. The aluminum surface oxidizes forming a few nm thick layer of aluminum oxide, which is corrosion resistant in a wide pH range [1]. Aluminum as substrate for food packaging has become increasingly popular due to its durability, low transportation cost and recyclability. As packing, aluminum cans are also widely used as containers for pressured beverages which are designed to have the strength required for operation with a minimum material consumption [2]. Aluminum is used in the wine industry as material component for cans and screw cap [3]. It has been demonstrated that aluminum affects the human brain; patients with Alzheimer or Parkinson disease have elevated levels of aluminum traces in their brain [4].

Resveratrol (3,5,4′-trihydroxy-trans-stilbene) is a stilbenoid, a type of natural phenol, and at the same time, a phytoalexin produced naturally by several plants as response to the injuries or attacks of pathogens, such as bacteria or fungi [5]. As a chemical entity, it is known since 1940, when it was first isolated from the roots of white hellebore (*Veratrum grandiflorum*) and later from *Polygonum cupsidatum*, a medical plant [6]. Food sources of resveratrol include the skin of grapes, blueberries, raspberries and mulberries. As well, it can be found in wines [7].

Resveratrol exists in two isomeric forms, as trans- and cis-resveratrol, whereas the trans-form is the most abundant one [8-9]. Both isomeric forms have been detected in wines. The chemical structures of resveratrol ($C_{14}H_{12}O_3$) are presented in Figure 1 [10]. However, trans-resveratrol can be easily converted into its cis-isomer under the influence of heat and UV-light [9].

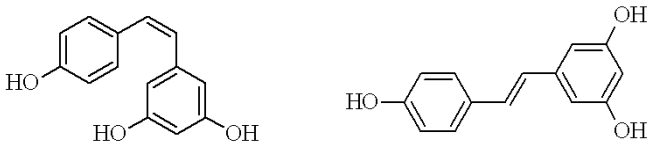

Figure 1. Chemical structures of *cis*- and *trans*-resveratrol [10]

The aim of this study is to investigate the inhibitory effect of resveratrol in 12% ethanol solution using linear polarization and cyclic voltammetry methods. The results are expected to provide basic information about the inhibitory effect of resveratrol from wines on aluminum corrosion process.

Experimental

Two types of aluminum, polished and brushed, were used as working electrodes in corrosion tests. To determine the inhibitory effect of resveratrol on the corrosion rate of aluminum in alcoholic solution,

different concentrations of the natural extract, between 10^{-6} and 10^{-3} M, have been used. The 12% ethanol (prepared from 96% ethanol Merck, 99.9%) corrosive media in witch was added 0.25 M Na_2SO_4 (prepared from Sigma-Aldrich reagent p.a. min 99.8%) for increase the electrolyte conductivity was used in tests.

The cyclic voltammetry and linear polarization (Tafel polarization method) were used in order to notice the inhibitive properties of resveratrol on aluminum corrosion process.

The electrochemical studies were recorded using a SP150 BioLogic potentiostat/galvanostat in a typical corrosion flat glass cell consisting of aluminum specimen with 1 cm^2 exposed area as working electrode (WE), platinum counter electrode (CE), and Ag/AgCl reference electrode. All potentials are referred to the saturated Ag/AgCl reference electrode. The polished aluminum electrode has been cleaned in ultrasonic bath, washed with distilled water and finally dried. The brushed aluminum electrode was pickled 5 minutes in 15% NaOH solution, than cleaned, washed and dried. Before each experiment, the test solutions were deaerated bubbling high purity nitrogen. The electrode potential was stabilized 60 min before starting the measurements.

Results and discussions

In order to obtain information about resveratrol oxidation/reduction resistance, as well as about its influence on cathodic and/or anodic processes, voltammetric measurements were carried out on platinum electrode. In figure 2 are shown the cyclic voltammograms recorded on platinum in 12% ethanol + 0.25 M Na_2SO_4 solutions in the absence and presence of different resveratrol concentrations, at 100 mV s^{-1}.

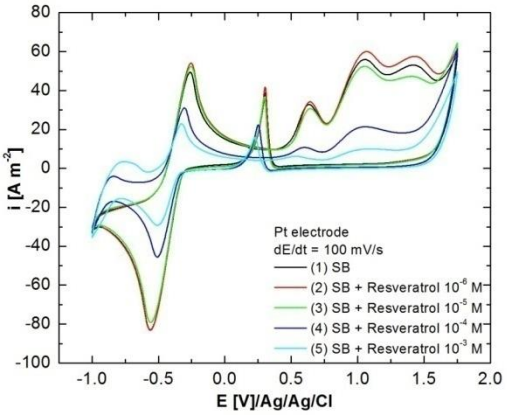

Figure 2. Cyclic voltammograms in 12% ethanol + 0.25 M Na_2SO_4 (SB) in absence and presence of resveratrol different concentrations, scan rate: 100 mV s^{-1}.

The base curve obtained in blank solution (12% ethanol + 0.25 M Na_2SO_4) presents the characteristic polarization curve drawn in ethanol solutions. Starting from open circuit potential (OCP), on the anodic branch of the voltammogram, after +0.50 V, three peaks corresponding to ethanol oxidation reaction on platinum electrode can be distinguished, as well as the characteristic plateau for oxygen release. On the backward scan, can be observed an anodic peak around +0.25 V, associated with ethanol oxidation on cleaned platinum surface, uncovered with platinum oxides, and a cathodic peak at approximately -0.60 V, corresponding to acetate ions reduction to acetaldehyde. Further, at more negative potentials then -1.0 V, the increasing current can be associated with hydrogen evolution reaction. Scanning the potential back to OCP, two anodic peaks are recorded, first at -0.80 V, associated with adsorbed hydrogen oxidation and second, at -0.25 V, characteristic to acetaldehyde oxidation.

The addition of resveratrol in the electrolyte leads to decrease of characteristic peaks intensity for all electrochemical reactions in platinum - ethanol system. According to Figure 2, both hydrogen and oxygen evolution reactions in the presence of resveratrol in test solutions are inhibited due to the organic compound adsorption onto platinum surface. The effect is more obvious at 10^{-3} M resveratrol concentration in alcoholic media.

Resveratrol effect on aluminum corrosion was studied in 12% ethanol + 0.25 M Na_2SO_4 corrosive environment by linear polarization method. Studies were carried out after about 1 hour, enough time to establish an electrode equilibrium or a quasi-equilibrium state. Potential values (E_{OCP}) are presented in Table 1 for both polished and brushed aluminum electrodes.

Table 1. Aluminum open circuit potential values (E_{OCP}) after 1 hour:

Electrolyte	E_{OCP} [mV]	
	Polished Al	**Brushed Al**
12% ethanol + 0.25M Na_2SO_4 (BS)	-506	-411
BS + 10^{-6} M resveratrol	-546	-423
BS + 10^{-5} M resveratrol	-554	-438
BS + 10^{-4} M resveratrol	-564	-459
BS + 10^{-3} M resveratrol	-576	-484

In solutions with different concentrations of inhibitor, aluminum electrode equilibrium potential is shifted to more negative values, phenomenon that can be attributed to adsorption of resveratrol molecules or deposition of corrosion products on the electrode surface.

The manner resveratrol acts as corrosion inhibitor for aluminum in test solutions and its effect on the corrosion rate can be estimated by different procedures, one of the most used being Tafel polarization method. The potentiodynamic polarization curves recorded without and with various concentrations of resveratrol are shown in Figure 3 for polished aluminum and in Figure 4 for brushed aluminum electrode.

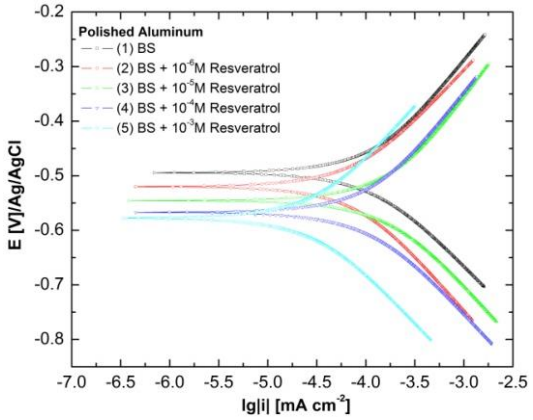

Figure 3. Linear polarization curves on polished aluminum electrode in test solutions in the absence/presence of resveratrol, scan rate: 1 mV s^{-1}.

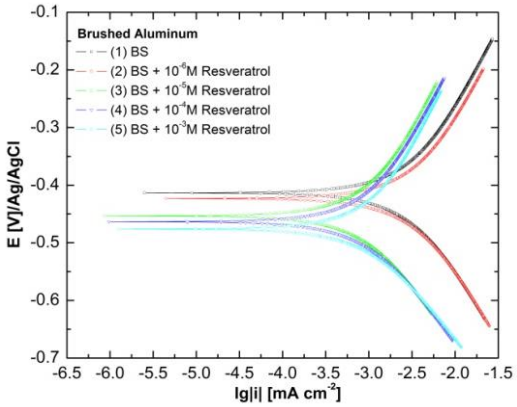

Figure 4. Linear polarization curves on brushed aluminum electrode in test solutions in the absence/presence of resveratrol, scan rate: 1 mV s^{-1}.

Polarization parameters for the corrosion of aluminum, *i.e.*, corrosion potential (E_{cor}), corrosion current density (i_{cor}), cathodic and anodic Tafel slopes (b_c and b_a), polarization resistance (R_p) and corrosion rate (v_{cor}) were determined extrapolating potentiodynamic curves. The inhibition efficiency *IE(%)* and has been calculated with equation (1) and the results are gathered in Table 2 for polished aluminum and in Table 3 for brushed aluminum electrode.

$$IE(\%) = ((i^0_{corr} - i^{inh}_{corr})/i^0_{corr})\times 100 \quad (1)$$

where $i^0_{corr}, i^{inh}_{corr}$ are the uninhibited and inhibited corrosion current densities, respectively.

Table 2. Polarization parameters for polished aluminum corrosion process in test solutions at 25°C.

Inh.conc. [M]	i_{cor}, [μA cm^{-2}]	E_{cor}, [mV]	$-b_c$, [mV dec^{-1}]	b_a, [mV dec^{-1}]	R_p, [kΩ]	v_{cor}, [mm an^{-1}] · 10^3	IE, %
BS	0.162	-494	205	242	223	4.5	-
10^{-6}	0.087	-520	204	241	488	2.5	46.30
10^{-5}	0.067	-545	201	236	654	1.8	58.64
10^{-4}	0.044	-567	193	226	867	0.9	72.84
10^{-3}	0.012	-578	189	201	1210	0.1	92.59

Table 3. Polarization parameters for brushed aluminum corrosion process in test solutions at 25°C.

Inh.conc. [M]	i_{cor}, [μA cm^{-2}]	E_{cor}, [mV]	$-b_c$, [mV dec^{-1}]	b_a, [mV dec^{-1}]	R_p, [kΩ]	v_{cor}, [mm an^{-1}] ·10^3	IE, %
BS	1.112	-413	259	288	22	37	-
10^{-6}	1.034	-423	262	291	26	34	7.01
10^{-5}	0.404	-453	229	298	50	16	63.67
10^{-4}	0.293	-493	214	287	86	11	73.65
10^{-3}	0.109	-477	207	284	96	7	90.20

From the results presented in Table 2 and 3, it can be stated that increasing the inhibitor concentration in test solutions, corrosion rate is diminished and the inhibition efficiency is elevated. Also, can be concluded the inhibitor do not cause significant changes in the anodic and cathodic Tafel slopes. This suggests that resveratrol behaves as a mixed-type inhibitor and can be classified as adsorptive-type.

Conclusions

The diminution of corrosion rate of aluminum in the presence of resveratrol can be attributed to the adsorbtion of organic compound onto the metal surface, blocking the active sites, or depositing corrosion products on the aluminum surface. Resveratrol act as an efficient corrosion inhibitor in alcoholic test solutions and it exhibits a maximum inhibition efficiency of 93% for polished aluminum and 90% for brushed aluminum.

The inhibitory properties of resveratrol on aluminum corrosion process offers considerable prospects for wines or other alcohols industry, also defining it as a natural or eco-friendly corrosion inhibitor in alcoholic media.

.

Acknowledgement

This work was partially supported by University Politehnica Timisoara in the frame of PhD studies.

ლიტერატურა - REFERENCES – ЛИТЕРАТУРА

1. Yokel R.A. Aluminum in Food – The Nature and Contribution of Food Additives, Food Additive, Prof. Yehia El-Samragy (Ed.), ISBN: 978-953-51-0067-6, InTech, 2012, 212.
2. Salas B.V., Wiener M.S., Stoytcheva M., Zlatev R., Beltran M.C. Corrosion in the Food Industry and Its Control, Food Industrial Processes - Methods and Equipment, Dr. Benjamin Valdez (Ed.), ISBN: 978-953-307-905-9, InTech, 2012, 374.
3. Ramos M., Valdés A., Mellinas A.C., Garrigós M.C., New Trends in Beverage Packaging Systems: A Review. *Beverages*. 2015, 1, 248-272.
4. Kawahara M., Kato-Negishi M. Link between Aluminum and the Pathogenesis of Alzheimer's Disease: The Integration of the Aluminum and Amyloid Cascade Hypotheses. *Int J Alzheimers Dis.* 2011, 276393, 1-17.
5. Fremont L. Biological effects of resveratrol, *Life Sci.* 2000, 66, 663-673.
6. Nemcova L., Barek J., Zima J. Determination of Trans-Resveratrol Using Voltammetric and Amperometric methods at Carbon Fiber Rod Electrode and Carbon Paste Electrode. *Int. J. Electrochem. Sci.* 2012, 7, 9221-9231.
7. Jasiński M., Jasińska L., Ogrodowczyk M. Resveratrol in prostate diseases - a short review. *Cent. European J. Urol.* 2013, 66 (2), 144-149.

8. Goldberg D.M., Ngb E., Karumanchiri A., Yan J., Diamandis E.P., Soleas G.J. Assay of Resveratrol Glucosides and Isomers in Wine by Direct-Injection HighPerformance Liquid Chromatography. *J. Chromatogr. A.* 1995, 708, 89-98.
9. Pekec B., Oberreiter A., Hauser S., Kalcher K., Ortner A .Electrochemical Sensor Based on a Cyclodextrin Modified Carbon Paste Electrode for Trans-Resveratrol Analysis. *Int. J. Electrochem. Sc.* 2012, 7, 4089-4098.
10. https://en.wikipedia.org/wiki/Resveratrol.

რესვერატროლის ინჰიბიტორული გავლენა ალუმინის კოროზიაზე სპირტხსნარებში

კ.გ.ვასზილცინ, მ.ლ.დან*,. დ.-ა.-დუკა*, მ.ლაბოსელ*
ელექტროქიმიის ეროვნული ინსტიტუტი, დოქტორ ა. პაუნესკუ პოდეანუ 144, 300569, ტიმისოარა, რუმინეთი
[2]უნივერსიტეტი პოლიტექნიკა ტიმისუარა, ინდუსტრიული ქიმიისა და გარემოს ინჯინირინგის ფაკულტეტი, 300223, პარვან 6, ტიმისუარა, რუმინეთი
cristi_vasz@yahoo.com

რეზიუმე

ეს სტატია წარმოადგენს რესვერატროლის, როგორც ალუმინის კოროზიის ინჰიბიტორად ეთანოლის ხსნარში გამოყენების შედეგებს. რესვერატროლის ინჰიბიტორული მახასიათებლები შესწავლილი იქნა 12%-იან ეთანოლში +0.25M Na_2SO_4 ხსნარში ინჰიბიტორის სხვადასხვა კონცენტრაციის (10^{-6} – 10^{-3}M) შემთხვევაში. ელექტროქიმიური ტესტები შესრულდა ორ მასალაზე: პოლირებულ და გასუსფთავებულ ალუმინზე. რესვერატროლის ელექტროქიმიური ქცევა ეთანოლის ხსნარში გამოცდილი იყო ციკლური ვოლტამპერომეტრიით პლატინის ელექტროდზე. ინჰიბიტორული ეფექტი შესწავლილი იქნა ხაზობრივი პოლარიზაციით (ტაფელის მეთოდით) რათა განგვესაზღვრა კინეტიკური პარამეტრები და ამგვარად მიგვეღო ინფორმაცია ინჰიბიტორული ეფექტის შესახებ.

საკვანძო სიტყვები: რესვერატროლი, კოროზიის ინჰიბიტორი, ალუმინის კოროზია

ИНГИБИТОРНЫЙ ЭФФЕКТ РЕСВЕРАТРОЛА НА КОРРОЗИЮ АЛЮМИНИЯ В СПИРТОВЫХ РАСТВОРАХ

К.Г.Васзилцин, М.Л.Дан*, Д.А.Дука*, М.Лабосел*
Национальный институт электрохимии, Румыния
Политехнический Университет Тимишоары, Факультет индустриальной химии и охраны окружающей среды, Румыния
cristi_vasz@yahoo.com

РЕЗЮМЕ

В данной работе представлены результаты, полученные с использованием ресвератрола как ингибитора коррозии алюминия в спиртовых растворах. Ингибиторные свойства ресвератрола изучались в 12% этаноле + 0.25M Na_2SO_4 в присутствии различных концентраций ингибитора, от 10^{-6} до 10^{-3}. Электрохимические опыты были выполнены на материалах двух типов: полированном и очищенном алюминии. Электрохимическое поведение ресвератрола в растворах этилового спирта было исследовано методом циклической вольтамперометрии на платиновом электроде. Эффект ингибитора был изучен методом линейной поляризации (метод Тафеля) для определения кинетических параметров.

Ключевые слова: резвератрол, ингибитор коррозии, коррозия алюминия.

THE SEQUENCE OF THE PREPARING PROCESS OF OPTIMAL COMPOSITION OF ANTISUBLIMATION COATINGS FOR SEMICONDUCTING BRANCHES OF THERMOELEMENTS

Fridon Basaria, Guram Bokuchava, Iasha Tabatadze, Meri Rekhviashvili
Ilia Vekua Sukhumi Institute of Physics and Technology,Tbilisi,Georgia,sip@sipt.org.ge

The sequence of the technological process for preparing optimal chemical composition of electroinsulatingantisublimation coatings based on inorganic vitreous enamels have been developed for protecting all types semiconducting branches of thermoelements against sublimation. Proposed method gives possibilities to create antisublimationcoatings in a short time with using the minimum amount of materials, which perfectly satisfy requirements.

It is know, that the most effective thermoelectric materials and alloys based on them at hot junction temperature of thermobatteries350-1100^{0}Carecharacterized by noticeable volatility [1], therefore during fabricating branches of thermoelements based on them beforehand is required creation of electroinsulatingantisublimation coatings on their surfaces.

Based on formerly conducted works were established, that the best antisublimation material for medium temperature branches of thermoelements (p-GeTe, n-PbTe, junction temperature below 550 ^{0}C) is coating based on inorganic vitreous enamels [2]. Analogous results were obtained for lowtemperature(junction temperature below 350 ^{0}C) branches of thermoelements based on alloys of p-$Bi_2(TeSe)_3$, n-$(BiSb)_2Te_3$and hightemperature(junction temperature below 1100 ^{0}C) branches of thermoelements based on alloys of p-and n-SiGe.

Based on the temperature characteristics and properties of the branches of thermoelement, development of specific optimal composition of antisublimation coatings should be carried out in compliance with the following sequence of execution of mentioned works:

1. Drawing up the technical tasks;
2. Drawing up the technical requirements, which must be satisfied by materials for antisublimation coatings.
3. Analyzing the relevant literature [3] and revealing materials and their compounds suitable for branches of thermoelements;
4. Mixing selected metal oxides,substances and compoundswith powder of given semiconducting alloys and annealing on air at temperatures (400-500˚C)for formation of antisublimation coatings for revealing process of chemical interaction of contacting materials. Annealing duration of 25-30 minutes.
5. Observing (visually or by optical microscope)annealed samples and separation of metal oxides (substances or compounds) into strongly, weakly and not interacting, i.e. inert materials.

Taking into account the received results we choose suitable metal oxides for these branches of thermoelementsand create systems of glasses and based on them vitreous enamels with specific compositions (at least 5 compositions from each selected system) for investigation. We consider the sequence of preparing process of electroinsulating–antisublimation coatings for lowtemperaturebranches of thermoelements based on semiconducting alloys ofn- type $Bi_2(TeSe)_3$and p-type $(BiSb)_2Te_3$.

On the basis of the technical requirements to the newly createdcoatings, taking into account physical and chemical properties of metal oxides and obtained results, liquid glass (LG) as the liquid phase of vitreous enamels slips and PbO, B_2O_3,Bi_2O_3, TeO_2, SiO_2 and Na_2O as solid fillers were chosen [3].

Experimental results of branches of thermoelements without coatings, and also with the known and proposed coatings are presented in table 1.

It's clear that antisublimation properties of vitreous enamels are much better and more stable, thanorganosilicate material used in practice.

Table 1 shows, that vitreous enamel especially based on Na2O-B2O3–Bi2O3-TeO2-PbO-SiO2 is the best material for application as electroinsulatingantisublimation coating of lowtemperature branches of thermoelements of n- and p-types.

It follows from the foregoing that the proposed sequence of theoretical and experimental works, in order to reveal optimal chemical composition of inorganic vitreous enamel coating for lowtemperature(temperature of the hot junction below 350 ^{0}C) branches of thermoelements, is the fastest and most optimal way to solve this task. This method was successfully applied for solution similar

problems for medium temperature - (temperature of the hot junction below 550 ^{0}C) [2] and hightemperature(temperature of the hot junction - 1150 ^{0}C)branches of thermoelements [4].

Table 1. Antisublimation properties of coatings at 300 ^{0}C

Type of branches	Materials for coating	Amount of the evaporated Te, Se,mg/cm^{2}hrs (the average of 5 tests)	
		In vacuum 10^{-1}-10^{-2}Torr.,during 20 hrs.	In helium atmosphere, during 500 hrs.
N BiTeSe	Without coating	O,20	0,25
	Organosilicate KO-89	0,08	0,10
	Vitreous enamelbased on**Na_2O-B_2O_3 – Bi_2O_3-TeO_2 PbO - SiO_2**	0,005	0,01
P BiSbTe	Without coating	0,36	0,26
	Organosilicate KO-89	0,10	0,09
	Vitreous enamelbased on **Na_2O-B_2O_3 – Bi_2O_3-TeO_2 PbO - SiO_2**	0,01	0,01

Therefore it recommended to carry out the development of electroinsulatingantisublimation coatings based on inorganic vitreous enamels for protection of semiconducting branches of thermoelements from sublimation, taking into account the physical-chemical properties of metal oxides and chemical interactions of the selected oxides with the respective thermoelectric materials.

ლიტერატურა - REFERENCES – ЛИТЕРАТУРА

1. Пахоловская Н.С., Челнокова Л.М., Мархолия *Т.П. ППТЭЭ и ТЭ,* 1977, 3(77), 113.
2. Басария Ф.П., Кобяков В.П. *Авт.св. СССР №56063*от 20.04.1971.
3. Басария Ф.П.,Гугушвили Г.М. *ППРВЭЭ,* 1984, 1 (117), 93.
4. Basaria F.P., Bokuchava G.V and etc. Antisublimationprotection for branches of thrmoelements based on PbTealloyC. *Georgian Engineering News*, 2006, #3, 92.

თერმოელემენტების ნახევარგამტარული შტოების ანტისუბლიმაციური დანაფარების ოპტიმალური შედგენილობის შედგენის პროცესის თანმიმდევრობა

ფრიდონ ბასარია, გურამ ბოკუჩავა, იაშა ტაბატაძე, მერი რეხვიაშვილი
სოხუმის ილია ვეკუას ფიზიკა-ტექნიკის ინსტიტუტი, *თბილისი, საქართველო, sipt@sipt.org.ge*

რეზიუმე

შემოთავაზებულია ყველა სახის თერმოელექტრული ბატარეების შტოებისათვის არაორგანული მინის სისტემის ფუძეზე ანტისუბლიმაციური ელექტროსაიზოლაციო მასალების შემუშავების ოპტიმალური თანმიმდევრული ტექნოლოგიური პროცესი, რომელიც იძლევა მოკლე დროში მინიმალური რაოდენობის მასალების გამოყენებით კონკრეტული ქიმიური შედგენილობის არაორგანული მინა-მინანქრის შექმნა-შემუშავების საშუალებას.

ПОСЛЕДОВАТЕЛЬНОСТЬ ПРОЦЕССА СОСТАВЛЕНИЯ ОПТИМАЛЬНОГО СОСТАВА АНТИСУБЛИМАЦИОННЫХ ПОКРЫТИЙ ДЛЯ ПОЛУПРОВОДНИКОВЫХ ВЕТВЕЙ ТЕРМОЭЛЕМЕНТОВ

Ф.П.Басария, Г.В.Бокучава, Я.М.Табатадзе, М.Г.Рехвиашвили
Сухумский Физико-Технический Институт им. И. Векуа, Тбилиси, Грузия,sipt@sipt.org.ge

РЕЗЮМЕ

Разработана последовательность технологического процесса создания оптимального химического состава электроизоляцинно-антисублимационного покрытия на основе неорганических стекло-эмалей для защиты от сублимации всех видов полупроводниковых ветвей термоэлементов.

THE LIQUID SORBENT CONDITIONAL SYSTEMS ON GEOTHERMAL WATER BASE

K.Vezirishvili-Nozadze, I.Zhordania, N.Mirianashvili, T.Nozadze,
Z.Lomsadze, T.Tsotsonava-Durglishvili

The Technical University of Georgia, The Centre Studying Productive Forces and Natural Resources of Georgia. 69, M. Kostava 3 str. 0175 Georgia. Ketivezirishvili@mail. com

The World energetic crisis forces the countries to look for new alternative energy sources. Such sources can be clear, non-traditional energy resources, like: solar, wind, bio and geothermal. Our object of research in this article concerns the geothermal energy resources. Geothermal energy provides a huge, reliable, renewable resource, unaffected by changing weather conditions. It reduces reliance on fossil fuels and their inherent price unpredictability and when managed with sensitivity to the site capacity, it is sustainable. Geothermal energy is relatively environmentally friendly. The use of conventional polluting fuels such as oil and coal can be reduced if geothermal and other alternative energy forms be used (reducing pollution).

Georgia is rich by geothermal resources, but today they are not used effectively. One of the ways of effective use of geothermal water resources suggested by us is their use in refrigerating equipment of fruit and vegetable store-houses. Besides, the scheme is already developed for using geothermal water for drying and cooling cereals in grain-elevators. For cooling atmospheric air the special air-cooling units are developed.

Key Words: non-traditional energy, geothermal water, liquid sorbents, conditional systems

In different branches of agriculture the acceleration of refrigerating equipment development is possible only with inculcation of cheap cool supplying systems on native non-traditional energy resources with minimal expenditure. Such systems are: absorbing water-ammoniac refrigerating aggregates and liquid sorbent units on geothermal water base.

For optimum maintenance of temperature-moist conditions (t=2-4ºC, φ=85-95%) in fruit and vegetable cool chamber we have suggested for the first time air cooling system with liquid sorbent which uses prior utilized thermal water (fig. 1). The air processing principle is based on the different salts(sorbents) and chemical solutions′ feature of moisture absorption.

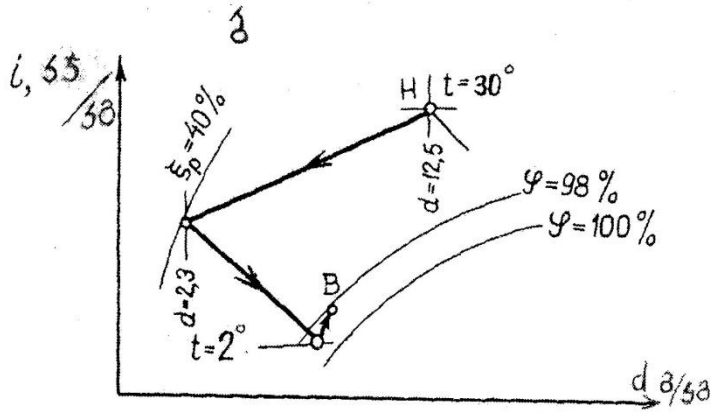

Fig. 1. The process on id-diagram.

The preliminary air drying process with liquid sorbents allow the conditional air to be reduced to the necessary parameters cooling exactly in the evaporator(adiabatic moistening). It is very perspective in fruit and vegetable store-houses for technological air conditioning, when along with low temperature(4ºC), high relative humidity(95-98%) is necessary.

Our research confirms the high efficiency of air conditioning units on liquid sorbents. They allow us at the equal energetic expenditures to get cold 3- times more, than with Freon, or steam-rejecting refrigerating machines and on 30% more, than with ammonia refrigerating machines.

On fig.2 is presented the principle scheme of air technological conditioning with liquid sorbent on different objects suggested by us. The processing air passing in apparatus- 1 is contacting with liquid sorbent. At first ,the air is drying and cooling somehow, then it passes injecting chamber -2 , contacting

with constantly circulating water, cooling and moistening up to technologically needed parameters and by 3 ventilators is passing to the premises. The part of impoverished solution after chamber 1 is pumping over to the solution regenerating chamber-4. The regenerated solution is warming by used thermal water in warm-exchanging chamber-5. Therefore in chamber-4 evaporation of absorbed moisture and restoration of sorbent concentration takes place. The restored solution is passing to the drying chamber-1 again and the cycle is repeated.

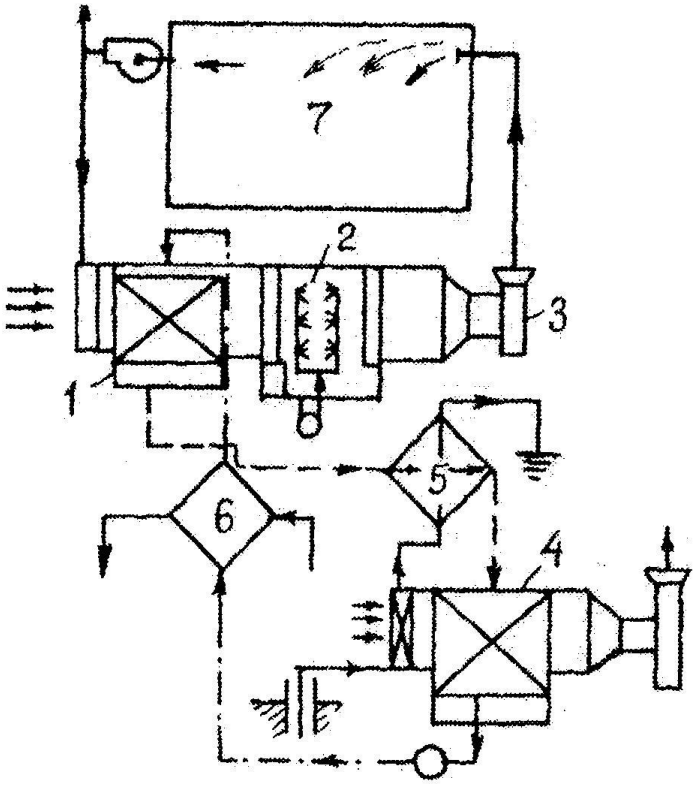

Fig.2. Fruit-vegetable store-houses' cool-supplying scheme on geothermal base.
1-contacting apparatus 2-sparkling chamber 3- ventilator 4- liquid sorbent refrigerating apparatus 5-6 heat exchangers 7- fruit-vegetable store-house

Apparatus 1 and 4 can be with sparklers, as well as, with membranes. For determination of heat-technical efficiency between air and sorbent solution and getting characteristics of heat and mass-exchanging processes we have made special experimental research of liquid sorbent air conditioning system on geothermal water base.

As we have already noted the air cooling system on liquid sorbent can be successfully used for technological and comforting purposes in all branches of the national economy. For example, it is already developed the scheme of using geothermal water for drying and cooling cereals in grain-elevators. For atmospheric air cooling are specially developed air-cooling units where for heat-exchanging are used membrane spray-coolers of 40-50 type and ,,KTC-3'' type central conditioners.

The suggested air processing system can be principally developed in climatic conditions of Georgia and its cooling and moistening be ensured by cooling water of 17-18^{o}C temperature. Sorbent solution regeneration can be ensured at water temperature of 60-65^{o}C.

As the geothermal springs of Georgia have enough high temperature potential the suggested system can be successfully used for supplying fruit-vegetable store-houses in the zones of geothermal wells. It will annually save more than one million kilowatt .electric power on each fruit-vegetable store-house of 1000ton capacity and that is very important for country's economic development.

ლიტერატურა - REFERENCES – ЛИТЕРАТУРА

1. Geothermal resources. European geothermal conference. 2010.384pp.
2. World geothermal congress. Japan. 2000. vol. 2.348pp.
3. K.Vezirishvili-Nozadze. The prospects of rational use of geothermal energy in Georgia “Energy” №3(35), 2005, 69-71pp.
4. K.Vezirishvili-Nozadze. The geothermal demonstrating project in Tbilisi “Science and technologies”, № 10-12, 2005, 29-31pp.

გეოთერმული წყლების ბაზაზე თხევადი სორბენტების გამოყენებით ჰაერის კონდიცირების სისტემების შექმნა

ქ.ვეზირიშვილი-ნოზაძე, ირ.ჟორდანია, თ.ნოზაძე, ნ.მირიანაშვილი,
ზ.ლომსაძე, თ.დურგლიშვილი-წოწონავა

რეზიუმე

სტატიაში წარმოდგენილია ჩვენს მიერ პირველად შემოთავაზებული ჰაერის გაცივების სისტემა სორბენტების ხსნარის მეშვეობით თერმული წყლების ბაზაზე.

ჰაერის დამუშავების პრინციპი ემყარება სხვადასხვა მარილების (სორბენტების) მიერ ტენის შთანთქმის თვისებას. ჰაერის წინასწარი შრობის პროცესები თხევადი სორბენტებით საშუალებას იძლევა კონდიცირებული ჰაერი დაყვანილ იქნეს საჭირო პარამეტრებამდე: (t=2-4°C, ფარდობითი ტენიანობა φ=85-98%). ეს ძალზე მნიშვნელოვანია ხილ-ბოსტნეულის საცავებსა და აგროსამრეწველო კომპლექსის ობიექტებზე ჰაერის ტექნოლოგიური კონდიცირების განხორციელებისათვის.

ჩვენს მიერ ჩატარებული ექსპერიმენტული გამოკვლევები მოწმობენ თხევადი სორბენტებით ჰაერის კონდიცირების დანადგარების გამოყენების მაღალ ეფექტურობას; ეს შესაძლებელს ხდის ერთიანი ენერგეტიკული დანახარჯების დროს მიღებულ იქნეს 3-ჯერ მეტი სიცივე, ვიდრე ფრეონის გამოყენებით და 30%-ით მეტი, ვიდრე ამიაკურ სამაცივრო დანადგარებში.

СОЗДАНИЕ СИСТЕМ КОНДИЦИРОВАНИЯ ВОЗДУХА С ИСПОЛЬЗОВАНИЕМ ЖИДКИХ СОРБЕНТОВ НА БАЗЕ ГЕОТЕРМАЛЬНЫХ ВОД

К.Везиришвили-Нозадзе, Ир.Жордания, Т.Нозадзе, З.Ломсадзе,
Н.Мирианашвили, Т.Дурглишвили-Цоцонава

РЕЗЮМЕ

В статье рассмотрены нами впервые предложенные системы охлаждения воздуха сорбентами на базе термальных вод.

Принцип подготовки воздуха основан на свойства различных солей (сорбентов) активно поглащать влагу. Предварительная подготовка воздуха с жидкими сорбентами дает возможность, чтобы кондиционирование довести к потребляемым параметрам воздуха, а именно: (t=2-4°C, относительная влажность φ=85-98%). Что очень важно для фрукто-овощнохранилищ и для других объектов агропромышленного комплекса.

Нами впервые были проведены экспериментальные опыты с жидкими сорбентами для кондиционирования воздуха, чтобы доказать высокую эффективность этой системы.

При одинаковые энергетические затраты нашим методом был получен в 3 раза больше холода, чем при использовании фреона и аммиака.

TECHNOLOGY FOR PREPARATION OF ECO-FRIENDLY HIGH-TEMPERATURE HEAT-INSULATING MATERIALS ON THE BASIS OF LIQUID GLASS AND SWOLLEN PERLITE

D.Gventsadze, B.Mazanishvili, L.Robakidze
LEPL RafielDvali Institute of Machine Mechanics, Mindeli str. 10, 0186, Tbilisi, Georgia
david.gven@gmail.com

In the paper the technology is presented for preparation of eco-friendly high-temperature heat-insulating materials on the basis of liquid glass and Georgian swollen perlite by the use of modifiers of various nature as clinoptilolite, plastic clay and carbon black. It was established that the indroduction of the modifiers in materials' composition improves their compression hardness by a factor of 1.8 – 2.3. The density of materials is in the range between 250kg/m3 to 450 kg/m2 and the coefficient of the heat conductivity comprises 0.06-0.08 W/m·°C.
Key words: liquid glass, swollen perlite, heat-insulating materials

At present there is a large demand on high-temperature and power-consuming materials in mechanical engineering, food industry and in other fields. They are used in cabinet driers of various function, in thermostats, in the furnaces of technological and domestic function. In all above-listed devices the use of high heat-resistant, low heat-conducting and relatively cheap heat-insulating materials is desirable. Nowadays the heat-insulating materials of such type aren't produced in Georgia and foreign ones are relatively costly. The price of the devices, manufactured on their basis, comprises several thousands of dollars.

By our opinion the particular emphasis must be placed upon the search of the technologies for preparation of new, eco-friendly, high-temperature heat-insulating materials and the creation of new materials.

At present the materials prepared on the basis of swollen perliteare of significant importance among existing high-temperature, heat-insulating materials.

They are widely used in various fields of mechanical engineering as well as in constructions. They are characterized by good heat-insulating properties, by lightness and cheapness. Their indroduction in mineral binders allows to prepare the incombustible materials, characterized by high rigidity and good thermal-physical properties. As it is well-known, glass-perlite or perlite goods on basis of liquid glass are manufactured in various versions such as perlitephosphogenic, perlite-burnt, light and etc [1-6].

Preparation of high-temperature, heat-insulating materials by our technology involves the following main technological operations: mixing, compressing, drying and thermal treatment. Research objects involve: liquid glass of 1300kg/m3 density and of silicate modulus 2.8, swollen perlite of middle fraction (production of Ltd "PARAVANPERLITE") of grain size 2.5mm. Modifiers were: clinoptilolite powderof grain size: 5-10 μm, plastic clay of grain size: 0.5-5 μm and carbon black (ПМ-803) of grain size 30-250 nm. For preparation of small size samples the mixing was carried out manually and for large samples the mixer of "drunk barrel" type was used. After mixing of the ingredients compression of the samples was performed by 0.3, 0.5, 0.8 and 1.0 MPa pressure in three moulds of various size which comprised 40×40mm, 50×50mm and 400×300mm, respectively. By means of first two moulds the compressing of thesamples was carried out at universal stretching machine by means of special devices. Large samples were compressed in the mould of our elaboration at technological press of 63 ton power.After cold pressing of the samples their thermal treatment was carried out at 350°C overb3-3.5 hours.

The results of the research of physical-mechanical properties are presented in table 1 and on the graphs in fig.1.

From the table 1 it is evident that the indroduction of corresponding modifiers in the composition of heat-insulating material causes the increase of the density of all obtained compositions. It is obvious that this process in large extent depends on the pressure of samples preparation. Plastic clay causes the minimum increase of weight of samplesand in the case of clinoptilolite the weight increase is maximum, hardness of materials is also increased at indroduction of the modifiers. Compression hardness increase is maximal in the case of the compositions modified by clinoptilolite and plastic clay.

At preparation of the compositions at low pressures (0.3-0.5MPa) the hardness is increased by a factor of 1.5-1.8. At high pressures (0.8-1.0 MPa) the hardness is enhanced by a factor of 1.8-2.3 and the best index is fixed in the case of modification by plastic clay. At compressing by pressure of 1.0 MPa the hardness value comprises 2.81 MPa. It may be suggested that, probably, in mentioned composition the clay

acts as an additional binder in spite of the fact that the temperature of the thermal treatment (350°C) is low in order for perfect revelation of the properties of the clay as a binder.

Table 1. Physical-mechanical properties of obtained materials

Modifier	Physical-mechanical properties	Pressure of sample production, Mpa			
		0,3	0,5	0,8	1,0
Without modifier	Density, kg/m3	220	270	325	360
Carbon black		260	350	410	435
Clinoptilolite		310	368	420	485
Plastic clay		250	310	400	450
Without modifier	Limit of compression hardness, Mpa	0,46	0,65	1,16	1,24
Carbon black		0,48	0,88	1,20	1,30
Clinoptilolite		0,68	1,12	1,46	2,42
Plastic clay		0,85	1,15	2,09	2,81

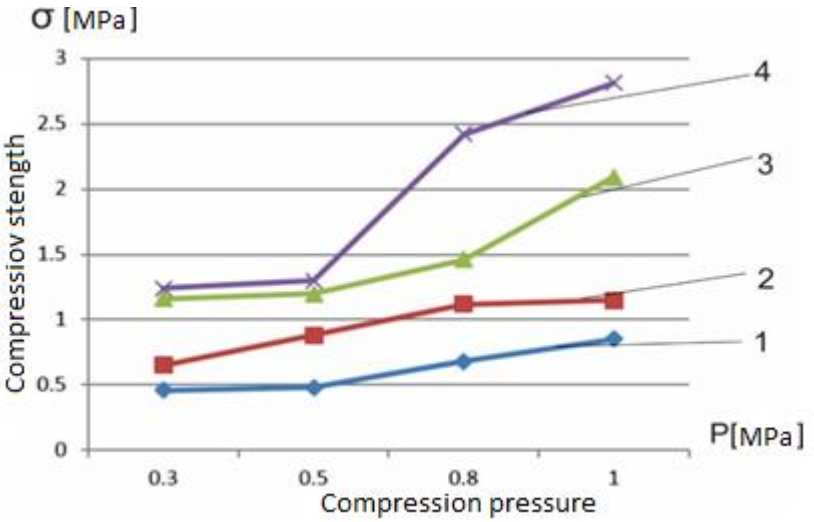

Fig. 1. Effects of modifiers and compression pressure on materials hardness:
1 – without modifiers, 2 – carbon black, 3 – clinoptilolite, 4 – plastic clay.

The measurements by means of express Lambda Meter have shown that the coefficient of heat conductivity of elaborated materials varies in the range from 0.06 W/m ·°C to 0.08 W/m ·°C which is in accordance with the indexes of international standards.

ლიტერატურა - REFERENCES – ЛИТЕРАТУРА

1. Korneev V., Production and use of soluble glass. Liquid glass. L.: Stroiizdat. 1991 – p.176(Russian)
2. Budnikov P.P. et all. Technology of ceramics and refractory materials. Ganatleba, Tbilisi, 1975, p.360 (Georgian)
3. Borodai F. Ya., Ceramic materials on the basic of quartz glass. “Glass and ceramics”, №4, p.p.24-26, 1992 (Russian)
4. Demin E.N., Andreev V.P. Efficiency of Heat-insulating materials at high temperatures. – “New refractory materials”, NG, 2004 (Russian).
5. http://spetsogneupor.ru/stati/stati_09-new-materiali.htm
6. http://spetsogneupor.ru/products/teplo-odeyalo-bio.htm

მაღალტემპერატურული თბოსაიზოლაციო მასალების მიღების ტექნოლოგია თხევადი მინისა და აფუებული პერლიტის ბაზაზე

დ. გვენცაძე, ბ. მაზანიშვილი, ლ. რობაქიძე
სსიპ რაფიელ დვალის მანქანათა მექანიკის ინსტიტუტი, თბილისი, მინდელის ქ.10, 0186, საქართველო
david.gven@gmail.com

რეზიუმე

სტატიაში აღწერილია თხევადი მინისა და საქართველოში წარმოებული აფუებული პერლიტის ბაზაზე ეკოლოგიურად უსაფრთხო მაღალტემპერატურული თბოსაიზოლაციო მასალების ტექნოლოგია სხვადასხვა ბუნების მქონე მოდიფიკატორების გამოყენებით, როგორიცაა კლინოპტილოლიტი, პლასტიკური თიხა და ტექნიკური ნახშირბადი. დადგენილი იქნა, რომ მასალების კომპოზიციებში მოდიფიკატორების შეყვანამ გაუმჯობესა მათი სიმტკიცე კუმშვაზე 1.8–2.3-ჯერ. მასალების სიმკვრივის დიაპაზონი 250-450 კგ/მ^3, ხოლო სითბოგამტარებლობის კოეფიციენტი 0.06-0.08 ვტ/მ·°C ფარგლებშია.

საკვანძო სიტყვები: თხევადი მინა, აფუებული პერლიტი, თბოსაიზოლაციო მასალები

ТЕХНОЛОГИЯ ПОЛУЧЕНИЯ ЭКОЛОГИЧЕСКИ БЕЗОПАСНЫХ ВЫСОКОТЕМПЕРАТУРНЫХ ТЕПЛОИЗОЛЯЦИОННЫХ МАТЕРИАЛОВ НА ОСНОВЕ ЖИДКОГО СТЕКЛА И ВСПУЧЕННОГО ПЕРЛИТА

Д.Гвенцадзе, Б.Мазанишвили, Л.Робакидзе
Институт Механики Машин им. Р.Двали, Тбилиси, 0186, Миндели 10, Грузия
david.gven@gmail.com

РЕЗЮМЕ

В статье описана технология получения экологически безопасных высокотемпературных теплоизоляционных материалов на основе жидкого стекла и вспученного перлита Грузинского производства с применением модификаторов различной природы, таких как клиноптилолит, пластичная глина и технический углерод. Установлено,что введение модификаторов в композицию материалов улучшает их прочность на сжатие в 1.8-2.3 раза.Удельный вес материалов находится в пределах 250-450 кг/м^3,а коэффициент теплопроводности в пределах 0.06-0.08 вт/м·°C.

Ключевые слова: жидкое стекло, вспученный перлит, теплоизоляционные материалы

ELECTRIC CONDUCTIVITY OF LASER DOPED POLYMER SURFACES

Jimsher Aneli, Nana Bakradze*, Teimuraz Dumbadze*

R. Dvali Institute of Machine Mechanics, 10, Mindeli str., 0186, Tbilisi, Georgia
jimaneli@yahoo.com
** Georgian Technical University 77, M. Kostava str., 0175, Tbilisi, Georgia*

Physical-chemical processes in the polymer surfaces initiated by laser irradiation with use of modern physical experimental methods are studied. It is established the regularities of the dependences between laser beam parameters and polymer structures and physical-chemical transformations in laser irradiated polymer materials. It is established that the transition of type dielectric - conductor is due to formation of the conjugated double bonds in the polymer macromolecules having semiconducting character of p-type (at moderate laser beam energy) and n-type (at more high energies). Temperature dependence of electric conductivity of laser irradiated polymers is described by the Mott formulas.
Keywords: CO_2 laser; irradiation; phenol-formaldehyde resin; electrical conductivity; conjugated bonds; paramagnetic centers.

Introduction

The studies of chemical modifications of polymer materials under influence of laser radiation have sufficiently spread character [1]. It is known the initiation of photo-polymerization after absorption of the light by sensitive molecule [2] or directly –by monomer [3]. The quant output strongly depends on the used photo-sensitive material. It must be existed a possibility of monitoring of the polymer molecular weight by change of the laser irradiated conditions. The substances under conditions of laser irradiation undergo to double influences of laser beam – effect of electromagnetic waves and thermal heating at rather high temperatures. It is known that high temperature (higher 500-600^{o}C) treatment (pyrolysis) of polymers in vacuum or in the inert atmosphere leads to deep structural transformations of these materials [4]. First of all these changes are expressed in excitation of macromolecules with consequent formation of free radicals and the systems of conjugated double bonds with linear or cyclic structures. In the presented work some local physical and chemical transformations on the surfaces of polymer plates due to laser irradiation at normal physical conditions have been studied.

Experimental

The composites were prepared using the well known technological method (mixing of components with planned ratio of ones and following heating of mixture up to 240^{o}C under pressure and cooling).The experiments were carried out on the plates with thickness of 4 mm. The irradiation was proceeded at using of CO_2 laser generator of type LGI-702 (λ = 10.6 mcm, power 800 W). The scheme of irradiation is given on the Fig.1. The laser beam generated from source 1 reflected on the reflector 2, passes through the lens 3 with focus distant 300mm and falls on the sample 4, which is placed on the table 5 automatically movable in three coordinate directions. The diameter of light spot on the polymer plate surface was changed in the interval 1-8mm. Laser irradiation doses were changed in the interval 20-40 J.

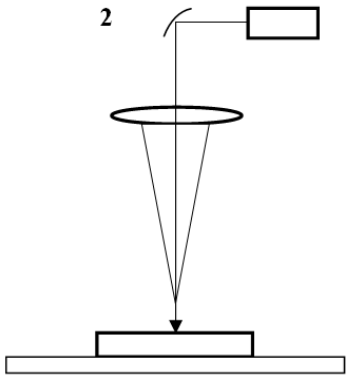

Fig. 1. Scheme of irradiation of samples:
1 – laser source; 2 – reflector; 3 – lens; 4 – sample; 5 – moving table

By means of displacement of the table with sample on it at regulated rate there were formed the black paths with different width and configuration. These paths are characterized with electrical conductivity and ESR spectra depending on irradiated energy. Irradiated samples were tested by polarization microscopy technique, electric conductivity – by two-contact method. Paramagnetic properties of the probes took from path materials were measured using of ESR spectrometer. The type and mobility of

charge carriers investigated were measured by the Hall effect technique. The structure changes in the macromolecular system was established by infrared spectra.

Results and Discussion

On the Fig.2 the electrical conducting channels with different shapes on the surface of polymer material plate on the basis of phenolformaldehide resin, polymethylsilsesqwioxane and fiber glass are shown. The channels were formed after laser irradiation at energy up to 40 J by means of straight line moving of plate with different rate under focused laser beam.

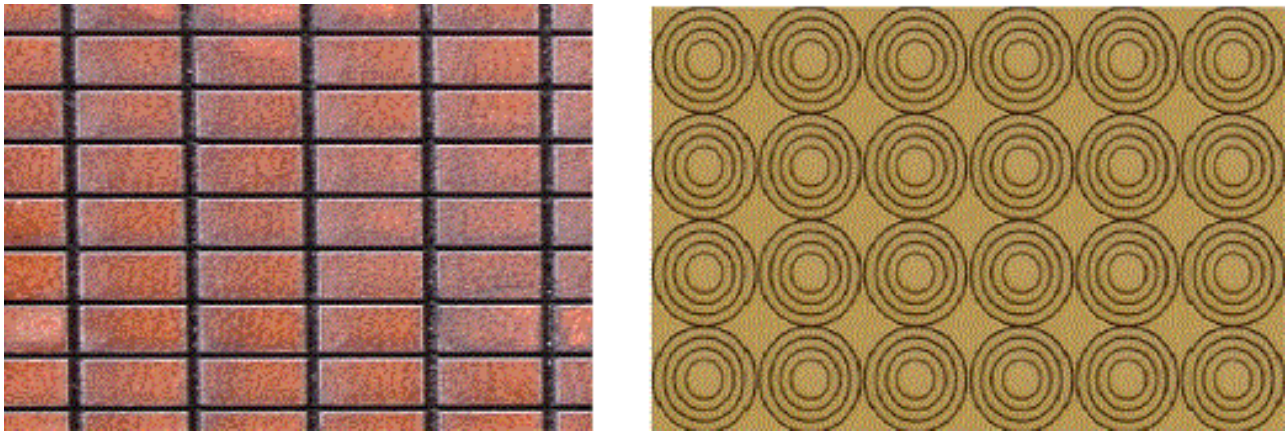

Fig. 2. Electrical conducting channels with different shapes formed on the surface of sample plates after focused laser beam irradiation

Infrared spectra of the alloys of the black material took from path shown the existence of definite amount of conjugated double bonds with linear structure of carbon chain of type ~CH = CH –CH =CH ~. It was established that the concentration of such bonds depends on type of irradiated material, the laser source power, beam intensity, the rate of table displacement of spot diameter of light on the sample surface [5].

Electric conductivity of the channels on the surface of polymer materials on the laser beam energy grows monotonously. This dependence points out a constant accumulation of poly-conjugation systems due to initiated by electromagnetic waves and high temperature photo- and thermo-chemical complex reactions. As to our point of view formation of poly-conjugated systems is rather probable at laserolysis of a compound containing phenoloformaldehyde resin and of polymethylsilsesqwioxane at the glass surface. These conjugated systems are covalently linked to Si-O groups on the glass surface by the skeleton of polymethylsilsesqwuoxane (‘a cube’). The electrically conducting system of the materials can be considered as a heterogeneous composite material, consisted of highly conducting spheres of poly-conjugation and barrier interlayers between them [6,7]. Volumetric part of the poly-conjugation spheres is determined by the pyrolysate production technique. It increases gradually with temperature of pyrolysis and the conductivity of composites increases.

The most apparently true model of electric conductivity in materials with the system of double conjugated bonds seems to be the change transfer in the ranges of polyconjugation possessing metal conductivity and jump conductivity between polyconjugation spheres. Such systems are known as the organic semiconductors, conductivity of which is described with formula (1) [8,9]:

$$\gamma = \gamma_0 \exp(-\Delta E/kT), \qquad (1)$$

or with formula (2) proposed by N. Mott (Nobel laureate) [9]:

$$\gamma = \gamma_0 \exp\left[-\left(\frac{T_0}{T}\right)^{1/4}\right], \qquad (2)$$

where T_0 and γ_0 are parameters of the present model.

Fig. 3 shows that the temperature dependence of conductivity of the polymer composite irradiated by three energy of the laser beam satisfactorily well described by the Mott formula (2) in the coordinates lgγ - $T^{-1/4}$ while preliminarily proceeded analogical measurements elucidate essential deviations from data calculated with using formula (1). However, the difference in temperature dependences of conductivity, composed in both coordinates, become so smooth with beam energy rises that they are nearly drawn together for the sample with laser beam energy higher 40 J. On the other hand, the same dependences show that the activation energies (according to the curve slope) decrease with laser beam energy increase. It is explained by intensification of processes promoting increase of the polyconjugation regions (clusters) and their drawing together, which result in continuous decrease of the potential barrier height, and conductivity approximates to the metal type. Evidently, at very high energies electric conductivity dependences on temperature cannot be described by equations noted above.

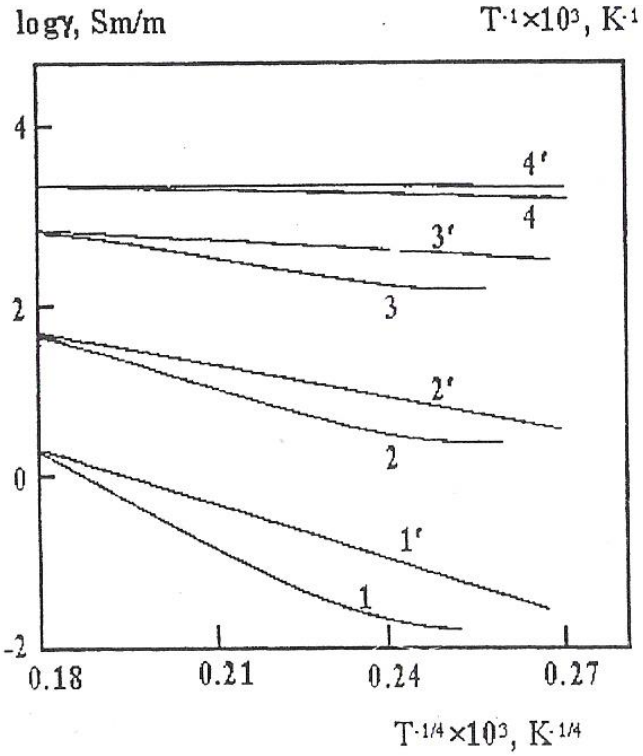

Fig. 3. Temperature dependence of γ for composite materials based on ED-20 + PFS + KO-812 + FG, pyrolized at 873 (1, 1'), 1173 (2, 2'), 1373 (3, 3') and 1573 K (4, 4') in the lgγ - T^{-1} (1 - 3) and lgγ - $T^{-1/4}$ (1' - 3') coordinates, respectively

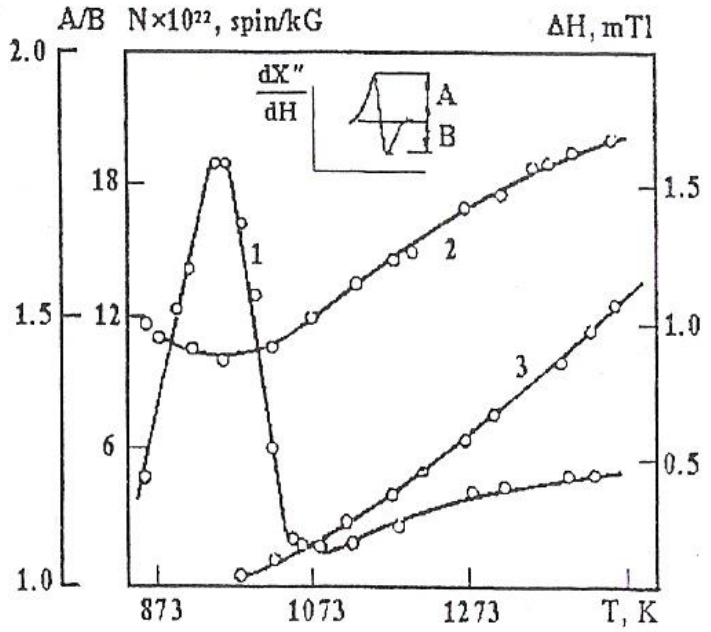

Fig. 4. Temperature dependence of paramagnetic centers N (1), ESR line width (2) and ESR line assimetry parameter A/B (3) on the pyrolysis temperature for the ED-20 + PFS + KO-812 + FG composites

Pyrolysis of the investigated surfaces leads to formation of the paramagnetic centers, dependence of concentration of which on the energy of laser beam has an extreme character (Fig. 4). Curve of the present dependence possesses maximum, which is corresponded to 600 - 700°C range. Change of the ESR absorption line intensity is accompanied by a definite change of its width. In this case, the form and width of the ESR line changes (at constancy of the g-factor) - lines are broadened, and asymmetry of singlet occurs. These changes are more effective for composites, pyrolized at rather high temperatures.

Maximum on the concentration dependence for paramagnetic centers on pyrolysis temperature is corresponded to the temperature range, in which volatile products of pyrolysis are released and poly-conjugated systems occur (possessing linear or cyclic structure). Decrease of concentration of the centers above 700°C proceeds due to coupling of a definite amount of unpaired electrons. According to this coupling new chemical structures occur (for example, polyconjugation responsible for electric conductivity increase). Some authors [6] think that this is bound to graphitization of the carbonic skeleton. However, according to X-ray analysis absence of the lines, characteristic for graphite, makes doubtful the occurrence of graphite spheres in pyrolysates.

At more high temperatures of pyrolysis the ESR line width and the asymmetry parameter increase due to the following phenomena. Deepening of thermo-chemical reactions in composites leads to formation of local paramagnetic centers due to thermal decomposition of organic chains of polymer substrates of composites with further localization of an unpaired electron in oxygen atoms, possessing increased affinity to electron. Due to occurrence of the spin-orbital interaction contribution into the spin-Hamiltonian the time of spin-spin relaxation, responsible for ESR line broadening, decreases. On the other hand, it is probable to increase the contribution of free charges-current carriers into ESR signal, the line of which is characterized by asymmetry (so called Dayson form [10]).

Conclusions

1. The irradiation of surfaces of some plate of the glass textolyte containing of carbon chain and polyorganosiloxane polymers with focused laser beam leads to formation of electrical conducting channels, the sizes of which depend on the energy of irradiation.

2. Irradiation of the polymer materials by laser radiation stimulates the processes of formation of the polyconjugated systems, in the frames of which the transport of the electric charges proceeds with a very low activation energy (it has semimetal character).

3. Charge transfer between polyconjugation systems is ruled by the jump conductivity mechanism with variable jump length. In this case, its temperature dependence is described by the Mott formulas.

4. Irradiation of the polymer materials by laser radiation stimulates the processes of formation of paramagnetic centers, dependence concentration of which on pyrolysis temperature has an extreme character and possesses both to localized in defects centers and free (conducting) electrons.

Presence of a glassy fiber and polymethylsilsesquioxane in composites promote formation of covalent bonds between organic and inorganic parts of the composite, at laserolysis of which good contacts between glass surface and conducting clusters is ensured.

ლიტერატურა - REFERENCES – ЛИТЕРАТУРА

1. Duley W.W.: Laser processing and analysis of materials, New-York, Plenum Press, (1983).
2. Grunwald E., Diver D., Kin F.: Infrared laser chemistry, New-York, Plenum Press, (1981).
3. Letokhov V.S.: Uspekhi fizicheskikh nauk (Advances of physical sciences), Vol.125 (1978), p.104.
4. Aneli J.N., Khananashvili L.M., and Zaikov G.E.: Structuring and conductivity of polymer composites, New-York, Nova Sci.Publishers, 1998, 326 pp.
5. Kajiwara T., Inokuchi H., Minomura S., Jap.Plast.Age, 1974,12(1),17-24.
6. Enzel P.,Bein T.//Chem.Materials,1992, 4, 819-824.
7. Shklovskii B.I., Efros A.L., Electronic properties of alloyed semiconductors, Moscow, Nauka, 1979,416.
8. Aviles M.A., Gines J.M., Del Rio J.C., Pascual J.. Perez J.L., Sanchez-Soto P.J. // J.Thermal Analysis and Calorimetry, 2002, V.67,177- 188.
9. Mott N.F., Davis E., Electron Processes in noncrystalline materials, 2nd Ed., oxford, Clarendon Press,1979.
10. Dyson F.J., Phys.Rev.,1955,98,349-358.

ლაზერული გამოსხივებით დოპირებული პოლიმერული მასალების ზედაპირების ელექტროგამტარობა

ჯიმშერ ანელი, ნანა ბაქრაძე, თეიმურაზ დუმბაძე
რ.დვალის მანქანათა მანქანათა მექანიკის ინსტიტუტი, თბილისი, საქართველო,
ელ.ფოსტა: jimaneli@yahoo.com

რეზიუმე

შესწავლილია ფენოლფორმალდეჰიდური და ეპოქსიდური ფისების, პოლიმეთილსილსეს-ქვიოქსანისა და მინაბოჭკოს ბაზაზე მიღებული კომპოზიტების ზედაპირებზე CO_2 ლაზერის ზემოქმედებით ჰაერის გარემოცვაში ინდუცირებული ელექტროგამტარი არხების თვისებები. ნაჩვენებია, რომ წარმოქმნილი ნივთიერებების ელექტროგამტარობის სიდიდე და პარამაგნიტური ცენტრების კონცენტრაცია დამოკიდებულია პოლიმერის ტიპზე და სხივთა კონის ენერგიაზე. ელექტროგამტარი არხების წარმოქმნა მიეწერება პოლიმერულ მასალაში ლაზერის სხივთა ზემოქმედებით შეუღლებული ორმაგი ბმების წარმოქმნას. ამ სტრუქტურების წარმოქმნას ადგილი აქვს აგრეთვე იგივე კომპოზიტების მაღალტემპერატურული პიროლიზის დროს, თუმცა პიროლიზის ტექნოლოგიით შეუძლებელია სასურველი კონფიგურაციისა და ელექტროგამტარობის მქონე არხების მიღება მაღალი ვაკუუმის გარეშე.

ЭЛЕКТРОПРОВОДНОСТЬ ПОЛИМЕРНЫХ ПОВЕРХНОСТЕЙ, ДОПИРОВАННЫХ ЛАЗЕРНЫМ ИЗЛУЧЕНИЕМ

Дж.Н.Анели, Н.Г.Бакрадзе, Т.Н.Думбадзе
Р.Двали Институте Механики Машин, Тбилиси, Грузия

РЕЗЮМЕ

Изучены свойства электропроводящих каналов, образованных в результате CO_2 лазерного облучения полимерных композитов на основе фенолформальдегидной и эпоксидной смол, а также полиметилсилсесквиоксана и углеволокна в присутствии воздуха. Показано, что электропроводность и концентрация парамагнитных центров образованных на поверхности композитов зависят от типа полимеров и энергии лазерного луча. Появление электропроводящих сойств веществ в каналах приписывается образованию в полимерном материале двойных сопряженных связей под действием лазерного облучения. Образование аналогичных веществ в тех же материалах имеет место в процессе высокотемпературного пиролиза, однако известная методика пиролиза не позволяет получить каналы с желательной конфигурацией и электропроводности без применения высокого вакуума.

COMPOSITES BASED ON POLYESTER LACQUER AND MINERAL FILLERS

L.G.Shamanauri, J.N.Aneli
R.Dvali Institute of Machine Mechanics, 10 Mindeli Str.Tbilisi 0186 Georgia
lana-shamanauri@mail.ru

The work is devoted to the obtaining and investigation of some properties of composites based on polyester with such fillers, as quartz sand, andesite, trachite and clay. The average size of these powders particles was lower than 50 microns. The physical-mechanical and hydrophobic properties of the composites have been investigated. It is experimentally shown that the dependence of mechanical strengthening of the composites on the fillers concentration has an extreme character- it is characterized with maximums at definite concentrations of fillers. For its part location of these peaks depends on the type of filler. So for example, for composites containing andesite and quartz sand, strength maxima occur at concentrations of fillers near 50 weight % and the largest substantially exceed those for composites containing clay and trachyte. The effect of the type and concentration of the filler is also reflected in the degree of hydrophobicity of composites. Composites water absorption decreases until the keeping of the wettability of all filler particles, which is achieved at relatively low polymer filling. With the deterioration of wetting that occurs at high filler content increases the probability of their associates and creation of microvoids in the polymer matrix. The experimental results are explained by the peculiarities of the microstructure of materials. Mainly it is due to the nature of interfacial interaction, what significantly affects on the distribution of the filler particles in the polymer matrix.

Introduction

At recent time polymer materials are used in the construction industry widely. Such consumption of the polymer materials in the construction industry is due to their high chemical stability to atmospheric phenomena, simple technology, decorative, etc.

Progress in polymer chemistry gives lot of means for obtaining of polymer materials with desirable properties [1]. It must be noted that now the polymer materials, in general, are yet deficit and expensive. Therefore in the practice the polymer materials containing silicate fillers as polymer-silicate materials are used often [2]. Polymer-silicate composition materials are new effective ones, in which the amount of the mineral filler reaches to 90 -95wt % (for example, in polymer-concrete) [3]. Such composition materials are characterized with high mechanical strengthening, chemical stability in the aggressive media in the wide temperature range [4]. The selection of polymers and fillers gives a possibility of obtaining of polymer-silicate composites with high dielectric properties, or vice versa, the polymer-silicates with good electric conducting properties [5].

At the recent time in many foreign countries more than 10 widely spread polymers (both thermoplastics and thermosetting polymers) are used in the industry of polymer-silicate composites. Among them the polymer-silicate composites based on polyester and epoxy resin are used more often [6].

Main goal of our work is development of different type of polymer-silicate composites on the basis of polyester lacquer for elaboration of the hydrophobic and decorative coatings on the ceramic plate and brick surfaces.

Results and discussion

In the experiment there were used the polyester lacquer and several mineral (silicate) fillers (clay, trachite, andesite, quartz sand, drywall) with different proportion. 2 -5wt% of hyperiz as hardener was added initially to the mixture of polyester lacquer and silicate powders (average diameter of the particles was lower than 50 mcm) and sometimes later the reaction accelerator – cobalt naftenate was added with the same concentration. After this the mixture is hardened in the special forms in accordance with the standard. 12 h later the form is opened and the sample is ready for the thermal treatment, which proceeds in the thermostat at 150^{o}C during 3 h. After such treatment the samples surfaces acquire smoothness and the material become stiff (the surface not scratched).

Testify was proceeded for determination of the following parameters: ultimate strength at compression, water absorption and specific weight. The numerical values of these characteristics are presented in the table 1.

Table 1. Ultimate strength at compression, water absorption and specific weight of composites

#	Filler type and content (wt %)	Density, g/cm3	Ultimate strength, MPa	Water absorption, %
1	Trachite (50)	2.4	158	2.5
2	“ (80)	2.3	125	5.3
3	“ (120)	2.1	100	4.2
4	Andezite (50)	2.5	174	1.8
5	“ (80)	2.3	160	3.9
6	“ (120)	2.15	147	3.1
7	Clay (50)	2.3	95	4.8
8	“ (80)	2.6	74	8.1
9	“ (120)	2.4	45	7.3
10	Quartz sand (50)	2.7	169	2.7
11	“ (80)	3,4	162	3.4
12	“ (120)	2.9	128	2.9
13	Drywall (50)	2.4	124	2.1
14	“ (80)	2.8	77	3.7
15	“ (120)	2.2	68	2.4

The table data show that the technical characteristics of the composites essentially depend on both the type and concentrations of the fillers. The character of such dependences it must be found in the peculiarities of the microstructure of composites.

It is well known that the mineral fillers are characterized with different morphology and microscopic empties. From the other side these minerals differ one from another by different values of the interaction energies between two phases [7]. Besides of it must be took into account the degree of dispersity of the filler particles. On the basis of this suggest the increasing of densities of composites containing clay, drywall and quartz send (from 50 up to 80 wt %) may be due to low degree of homogeneity of distribution of these fillers particles in the polymer matrix (it is probability of formation of the associates-clusters of these particles). Although at relatively high content of these fillers increasing of the degree of composite structural inhomogeneity enhances, which is connected with formation of microscopic empties in the polymer matrix. This process is promoted also by relatively low energy of inter-phase interactions. This situation is well reflected on the value of the composite mechanical strengthening – it decreases at increasing of the filler concentration. Such dependence of the ultimate strength on the filler concentration is the general phenomenon for all composites. It is well known also that in general the dependence of the ultimatum strength of the composites on the filler concentration is extreme – maximum corresponds to filler concentration, when the filler particles of last maximally form the contacts with macromolecules. At increasing of filler concentration when the formation of associates will be started or by other words when not all particles will be coated with macromolecules and others will be stay without organic molecular surrounding and will be not take participation in the hetero-phase interactions. At following increasing of the filler concentration the composite strengthening decreases. This phenomenon is known in the scientific literature as Rebinder effect.

The maximal ultimatum strength among investigated composites corresponds to composites containing 50 wt% of filler. Relatively high significances of strengthening of the composites containing andezite and quartz sand show that there are inter-phase interactions higher in comparison with other composites.

The water absorption of investigated composites is in good correlation with the significances of density. From the table data it is seen that both density and ultimate strength for composites containing 80wt % of the filler are higher to some extent in comparison with other composites. In this case there are two processes acting in one and same time, but one against to other: increasing

of the density (because of increasing of more tight phase) and formation of the mineral particles associates, which leads to increasing of water absorption because of increasing of diffusion of water molecules between filler particles.

In the composites containing 120 wt% of the fillers the decreasing of density is observed to some extent (in comparison with composites containing 80wt% of the filler). The reason of this fact may be the capsulation of the filler particles by macromolecules. The decreasing of penetration of the water trough composites with high filler concentration may be described by same reason.

Conclusions

1. The properties of composites based on polyester lacquer generally depend both on filler type and it concentration.
2. With high strengthening are characterized the composites containing andezite and quartz sand with amount 50wt% because of high inter-phase interactions.
3. With low strengthening are characterized the composites containing clay, which show on the low inter-phase interactions.

The gradation of the composite properties is the result of simultaneously action of several physical factors, which are due to inter-phase interactions, formation of micro-empties and filler particles association and capsulation.

ლიტერატურა - REFERENCES – ЛИТЕРАТУРА

1. Khananashvili L.M., Andrianov K.A. Technology of the elementorganic monomers. M.Khimia,1983.-416 p.
2. Ivanchev S.S., Dmitrenko A.V.Uspekhi Khimii, v.51,N7, 1178-1800.
3. Berlin Al.Al., Volfson S.A.,Enikolopov N.S. Principles of creation of the polymer composite materials. M.Khimia, 1990, -240.
4. Lipatov Y.S. Physical chemistry of the filled polymers. M.Khimia, 1977,-304.
5. Gul E.V., Shenfil L.Z. Electric conducting polymer composites. M.Khimia, 1984,-340.
6. Sukhareva L.A. Polyester coatings (Structure and properties). M.Khimia, 1987,-190.
7. Mambish S.E. Mineral fillers in the industry. M.Plastmassi, 2006.-105.

კომპოზიციური მასალები პოლიმერული ლაქისა და მინერალური შემავსებლების საფუძველზე

ლანა შამანაური, ჯიმშერ ანელი

რ.დვალის მანქანათა მანქანათა მექანიკის ინსტიტუტი, თბილისი, საქართველო

რეზიუმე

პოლიმერული ლაქის საფუძველზე მიღებულია პოლიმერული კომპოზიტები საქართველოში გავრცელებული მინერალების ტრაქიტის, კვარცის ქვიშის, გაჯის, თიხისა და ანდეზიტის შემცველობით. შესწავლილია კომპოზიტების ფიზიკურ-მექანიკური თვისებები (სიმკვრივე, სიმტკიცის ზღვარი) და წყალშთანთქმის სიდიდე. ნაჩვენებია, რომ მიღებული კომპოზიციური მასალების სიმტკიცის ზღვარი მნიშვნელოვნად არის დამოკიდებული შემვსების კონცენტრაციაზე, კერძოდ, აღნიშნული პარამეტრის სიდიდე მაქსიმალურ მნიშვნელობას აღწევს მინერალების 50%-იანი შემცველობისას. მიღებული შედეგები ახსნილია კომპოზიტების მიკროსტრუქტურის თავისებურებებით.

КОМПОЗИЦИОННЫЕ МАТЕРИАЛЫ НА ОСНОВЕ ПОЛИЭФИРНОГО ЛАКА И МИНЕРАЛЬНЫХ НАПОЛНИТЕЛЕЙ

Л.Г.Шаманаури, Дж.Н.Анели

Р.Двали Институте Механики Машин, Тбилиси, Грузия

РЕЗЮМЕ

Получены полимерные композиты на основе полиэфирного лака и распространенных в Грузии минералов трахита, андезита, кварцевого песка, гажи и глины. Показано, что предел прочности исследованных композитов существенно зависит от содержания и типа наполнителя. В часности, максимальные значения данного параметра соответствуют 50%-ому содержанию наполнителей. Полученные результаты обьяснены в терминах особеностей микроструктуры композитов.

UTILIZATION OF AGRO-INDUSTRIAL WASTE MATERIALS BY USING SEQUENTIAL SUPERCRITICAL FLUID AND ULTRASOUND EXTRACTION METHODS

Mzia Tsitsagi, Mariam Chkhaidze, Manana Buzariashvili, Miranda Khachidze, Vladimer Tsitsishvili
Petre Melikishvili Institute of Physical and Organic Chemistry of Ivane Javakhishvili Tbilisi State University, 0186, 31 A.Politkovskaia str., Tbilisi, Georgia

Extraction of biologically active compounds from agro-industrial waste materials of most common fruits and vegetables in Georgia by sequential supercritical fluid and ultrasound methods is described. These method provide high quality targeted products, both options have their advantages. The method you choose depends on the class of targeted product, as well as on provided depth of extraction and release of compounds.

In recent years, there has been a growing interest in the so-called functional food additives. These ingredients are preferred by consumers to have a natural origin, being commonly extracted from natural sources such as plants or food by-product. Grape seeds and skin, orange and tangerine peel, tomato paste waste are the most abundant agro-industrial waste materials in Georgia. Extraction of natural food colorants and small scale high cost bioactive compounds from above mentioned waste materials is the main goal of our research.

The choice of the suitable technique for extraction of bioactive compounds from botanic matrix depends on: the desired class of compounds to be extracted, quality and yield required for extract; the process conditions and economic feasibility for scaling up the process.

Sequential supercritical Fluid extraction and ultrasound assisted extraction, the environmentally friendly separation techniques has been used for extraction of target products.

Supercritical fluid extraction is an advanced separation technique based on the enhanced solvating power of gases above their critical point. One of the most frequently used supercritical fluids is carbon dioxide. Besides the advantages of having a low critical temperature and being neither toxic nor flammable, carbon dioxide is also available at low cost and high purity; On account of these characteristics, the fluid is an ideal solvent for in the food dye, pharmaceutical and cosmetic industries, where it is essential to obtain final products of a high degree of purity.

Another modern technique we use is ultrasound-assisted extraction method. The application of ultrasound disrupts the cell wall structure and accelerates diffusion through membranes, allows cellular material release and improves mass transfer as well. Ultrasound-assisted extraction is an upcoming extraction technique that can offer high reproducibility in shorter time, higher yields of bioactive compounds, simplified manipulation, decreased temperature during processing, reduced solvent consumption, and lower energy input.

Figure 1. Ultrasound extractor

Sequential, stepwise supercritical and ultrasound extraction methods makes available selective and quantitative extraction of oils, phenolics, carotenoids, lycopene, pentacyclic triterpenes and pectins from different botanic matrixes.

Selectivity, reproducibility was main challenge of our research. Thus, large range of pressure, temperature, extraction time and different solvent for sequential extraction of different class of compounds has been studded.

Essential oil, carotenoids, hesperidin and pectin has been extracted from tangerine and orange peel; quercetin and natural dyes from onion skin; lycopene and carotenoids from tomato peel, anthocyanins from “Saperavi” skin, phenolics and pentacyclic triterpenes from apple peel. Optimal extraction parameters and suitable extraction techniques have been selected for each target products. Main requirements were selectivity, reproducibility and feasibility for industrial means.

Black grape skin contains a great number of polyphenolic compounds, the concentration of which varies greatly according to the variety of grapevine and is influenced by cultivator, season and environmental factors. Red grape skin is the waste of winemaking. All red grape sorts are good source of

anticianins, colored natural compounds. They have bright attractive colors. High solubility in water of these compounds allows their easy incorporation into aqueous food systems. Moreover, the proved antioxidant activity of antocyanins, related to the prevention of a number of degenerative diseases. Provides added benefits to food dyed with these natural substances. Anthocianins give rise to the plue-purple- red-orange color of flowers and fruits. Antocyanins are chemically phenolic compounds belonging to the flavonoid family. Antocyanins are glycosides of antocyanidins and sugar. Antocyanidins are almost always glycosylated in the 3-possition. Color Changes with pH. At low pH3 the antocyanins are most strongly colored, exhibits their well-known purple-red color, around pH5 it twins almost colorless and at neutral and alkaline pH the color goes from blue to green. The use of antocyanins as natural dyes has been studied for many years due to their ready availability. The recovery of antocyanins from wine industry by- products is also of great importance because it could exploit a large amount of the wine industry waste, which is mainly used today as cattle feed or for soil conditioning or it is tucked away to disposal sites, reducing consequently their environmental impact.

Figure 2. "Saperavi" grapes and extracts from grape skin

Ultrasound extraction of anthocyanins from "Saperavi" skin, byproduct of winemaking by using different ratio of ethanol/water mixture, gives very good recovery of target products at $25C^0$. Method is fast, cheap and highly reproducible.

Figure 3. Grape seed and grape seed oil

The grape seed is another by product of winemaking. Valuable by- product of grape seed is grape seed oil. The grape seed oil is a vegetable oil, abundant by product of wine making. This oil is high in nutrients, being rich in vitamin E, single and polyunsaturated fatty acids of which linolenic acid an essential fatty acid 70%. The oil is primarily used for cooking and in salads, marinades, deep frying, flavored oils, baking, massage oil, sunburn repair lotion, hair product, body hygiene creams, lip balm and hand creams. In all products grape seed oil is a preferred cosmetic ingredient for damaged and stressed tissues possessing regenerative and restricting qualities which allow a better control of skin moisturizations. It can help skin refine the normal structure of epithelium cells and nerve cells via supporting the cell membranes. It has a relatively high smoke point approximately 216 C so it can be safely used to cook at high temperature. The metabolic energy density of the grape seed oil is comparable to of other oil: about 120Kcal per tablespoon (34Kj/ml) however because less oil is needed for cooking it can be used within low-fat diet. The grape seed oil is reputed to contain plentiful antioxidant as well as to lower cholesterol levels. In a study presented in 1993 at the American College of Cardiology Scientific Session Nagh and collegues showed in 56 men and

women using up 43 g per day, an amount that one can cook with, that grape seed oil raised HDL levels by 13% and reduced LDL levels by 7% in three weeks. The total cholesterol/HDL ratio fell 15.6 % and the total LDL/HDL ratio fell 15.3% which could be significant for these at risk of heart attack.

One of the main aspects that should be considered in SFE of oil is the extraction optimization. The use of the optimum values for the different variables influencing the SFE extractions could significantly enhance the recovery of extraction yield of a target compound. On the one hand, the increasing of temperature results in the decrease of solvent density thus decreases the solubility and yield of oil. Increase of pressure increases density of CO_2, which induce complex extraction and difficult analysis. The ultrasound technique is based on the formation of ultrasonic waves of high frequency, which are capable of causing cavitations due to expansion and contraction cycles undergone by the material. Such cycles disrupt the cell walls of the vegetable matrix, favoring the penetration of the solvent and mass transfer, thus increasing the extract yield.

Influence of ultrasound on subcritical fluid extractions of the grape seed oil has been studied. While ultrasound was applied as in USFE, the following parameters were preferred: *T* at 25 °C, *P* at 100 atm. The results show that subcritical fluid extraction with the assistance of ultrasound could reduce the temperature and pressure used in the process. Compared with SFE, USFE could give a 5% increase in the yield in case of the grape seed oil.

As it was mentioned above tangerine peel is one of the most abundant agroindustrial waste materials in Georgia. Sequential supercritical fluid extraction method were used for extraction of essential oil, carotinoids and bioflavanoids from tangerine (Citrus Unshiu) peel. First step of this process is supercritical CO_2 extraction of oil. Major constituent of tangerine oven dried peel oil is d-limonene (> 90%). Second step is 7% V/V acetone modified supercritical CO_2 extraction of β-carotene. Third step is 5% methanol modified supercritical CO_2 extraction of hesperidin. Studied and determined optimal parameters provide efficient, fast and selective extraction of target products. Method can be used for utilization of any other citrus peel.

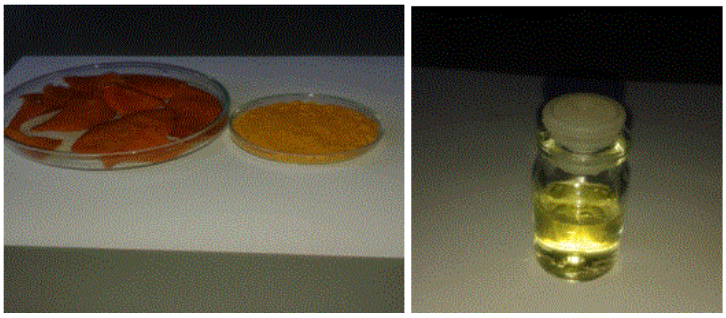

Figure 4. Tangerine peel and tangerine peel oil

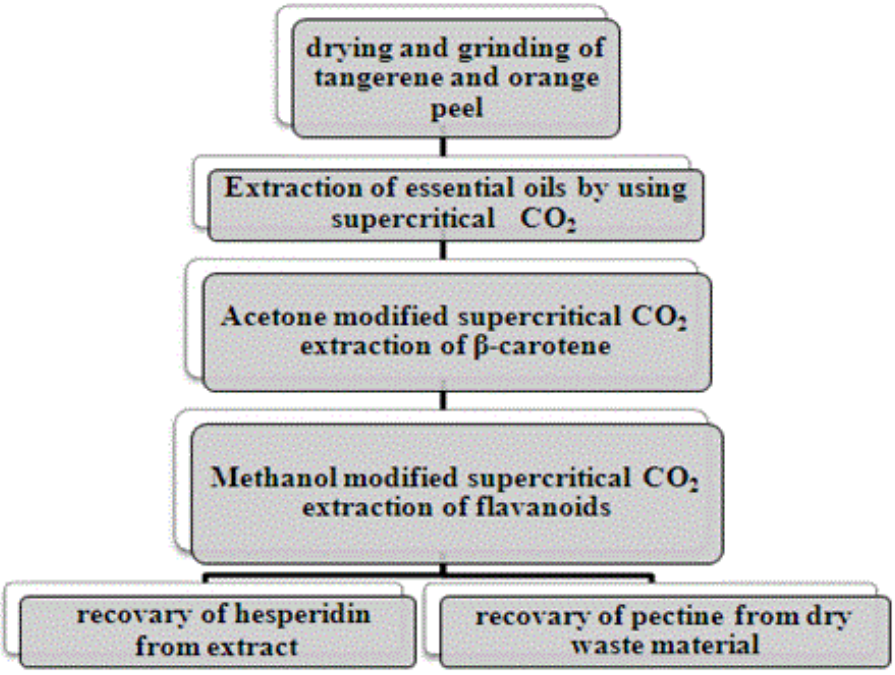

Figure 5. Scheme of tangerine and orange peel processing

Limonene is a chemical found in the peels of citrus fruits and in other plants. It is used to make medicine. d-Limonene is used to promote weight loss, prevent cancer, treat cancer, and treat bronchitis. In foods, beverages, and chewing gum, limonene is used as a flavoring. In pharmaceuticals, limonene is added to help medicinal ointments and creams penetrate the skin. In manufacturing, limonene is used as a fragrance, cleaner (solvent), and as an ingredient in water-free hand cleansers.

Hesperidin is a plant chemical that is classified as a "bioflavonoid." It is found primarily in citrus fruits.People use it as medicine. Hesperidin alone, or in combination with other citrus bioflavonoids (diosmin, for example), is most often used for blood vessel conditions such as hemorrhoids, varicose veins, and poor circulation (venous stasis). It is also used to treat lymphedema, a condition involving fluid retention that can be a complication of breast cancer surgery.

Beta-carotene is one of a group of red, orange, and yellow pigments called carotenoids. Beta-carotene and other carotenoids provide approximately 50% of the vitamin A needed in the American diet. Beta-carotene can be found in fruits, vegetables, and whole grains. It can also be made in a laboratory. Beta-carotene is used to decrease asthma symptoms caused by exercise; to prevent certain cancers, heart disease, cataracts, and age related macular degeneration (AMD); and to treat AIDS, alcoholism, Alzheimer's disease, depression, epilepsy, headache, heartburn, high blood pressure, infertility, Parkinson's disease, rheumatoid arthritis, schizophrenia, and skin disorders including psoriasis and vitiligo.

Figure 6. Hesperidin crude and after purification

The last step of this process is recovery of pectin from dry waste material. Our study was focused on the potential of tangerine peel as a source of pectin. Pectin was extracted from tangerine peel powder remained after supercritical fluid extraction of essential oil, β-carotene and hesperidin using H form of clinoptilolite. Extraction conditions are T= 80C^0, pH= 1,5-2, extraction time= 1h. The percentage yield is 69.3%, equivalent weight of extracted pectin was 760, methoxyl content 6.5 %, total anhyrouronic acid content 78%, degree of esterification 47.3%. From the result obtained, tangerine peel can be considered in commercial production of pectin alongside with other citrus sources.

Figure 7. Dry waste material after extraction of oil, β-carotene and hesperidine.

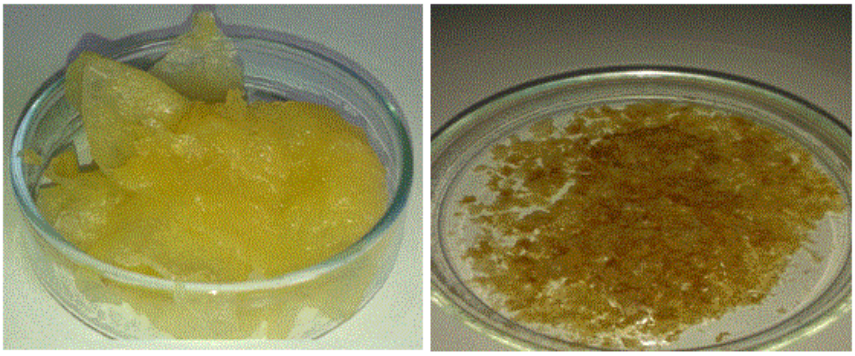

Figure 8. Pectin extracted from dry material

Red onion (Allium cepa) is the most common and richest natural source of flavonoids and anthocyanins.

Our study was focused on the influence of some operative parameters and co-solvents on sequential supercritical fluid extraction employed for the extraction of quercetin and colorants from red onion outer skin. Supercritical CO_2 modified with acetone was used for the extraction of quercetin and supercritical CO_2 modified with ethanol/ acetic acid (80:1) was used for extraction of colorants.

Figure 9. Red onion and extracted material

Extraction of quercetin and colorants from onion skin also has been done by using sequential ultrasound extraction method. Method is simple, rapid and provides high yield of target products.

The carotenoids are natural pigments that provide the natural yellow, orange and red colors of fruits. According to epidemiological studies carotenoids play an important role in prevention of cancer, cataracts, and aging diseases. Besides some applications of carotinoids for provitamin A activity, they are widely used as colorants in food.

Supercritical fluid extraction method was used for extraction of lycopene and β-carotene from the skins of ripe tomato. Optimal operative conditions are 65-70^{0}C temperature, 250-300 atm pressure, 5% acetone as a co-solvent, static extraction time 1h, dynamic- 2h.

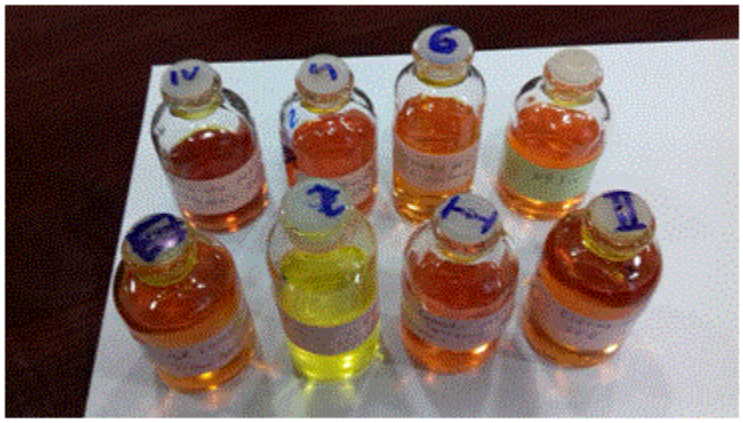

Figure 10. Extracts from tomato skin

Uninspected result gave ultrasound extraction of lycopene and carotene from tomato skin. First step of extraction by using acetone as a solvent obtains complicated mixture of different compounds with low content of target products. The second step is highly selective and major components are lycopene and beta carotene. Method is fast and selective.

ლიტერატურა - REFERENCES – ЛИТЕРАТУРА

1. G. Kvartskhava, M. Tsitsagi, M. Chkhaidze, M. Khachidze, I. Jinikashvili Utilization of winery wastes by using supercritical CO_2 Proceedings of the Georgian national academy of science 2010 vol 36 № 2 149-152
2. M. Tsitsagi, M. Chkhaidze, M. Khachidze, M. Buzariashvili, K. Ebralidze.Sequential supercritical fluid extraction of quercetin and colorants from red onion (*allium cera)* Proceedings of the Georgian national academy of science 2014 vol 40 № 4 264-266
3. M. Chkhaidze M. Tsitsagi, , K. Ebralidze M. Khachidze, N. Chaganava. Supercritical fluid extraction of natural colorants from tomato skin. Proceedings of the Georgian national academy of science 2012 vol 38 № 2-3 262-264

4. M. Tsitsagi, M. Chkhaidze, M. Khachidze, M. Buzariashvili, K. Ebralidze, Ts.Ramishvili, V.Tsitsishvili Sequential supercritical fluid extraction of essential oil, carotinoids and bioflavanoids from tangerine (Citrus Unshiu) peel Proceedings of the Georgian national academy of science, 2015 vol 41 № 3 248-250
5. Mzia Tsitsagi, Mariam Ckhaidze, Gulnara Balarjishvili, Miranda Khachidze, Manana Buzariashvili, Ketevan Ebralidze Extraction of pectin from tangerine peel Proceedings of the Georgian national academy of science 2015 vol 41, № 3, 86-88.

აგროინდუსტრიული ნარჩენების უტილიზაცია საფეხურებრივი სუპერკრიტიკული და ულტრაბგერითი ექსტრაჰირების მეთოდების გამოყენებით

მზია ციცაგი, მარიამ ჩხაიძე, მანანა ბუზარიაშვილი, მირანდა ხაჩიძე, ვლადიმერ ციციშვილი
ივანე ჯავახიშვილის სახელობის თბილისის სახელმწიფო უნივერსიტეტის პეტრე მელიქიშვილის ფიზიკური და ორგანული ქიმიის ინსტიტუტი, 0186, ა.პოლიტკოვსკაიას ქ. 31, თბილისი, საქართველო

რეზიუმე

სტატია ეხება საქართველოში ყველაზე ფართოდ გავრცელებული ხილისა და ბოსტნეულის გადამუშავების შედეგად დარჩენილი აგროინდუსტრიული ნარჩენის სუპერკრიტიკული და ულტრაბგერითი საფეხურებრივი ექსტრაქციის მეთოდით სხვადასხვა ბიოლოგიურად აქტიური ნივთიერებების მიღებას. აღნიშნული მეთოდები საშუალებას იძლევა მიღებული იქნას მაღალი ხარისხის მიზნობრივი პროდუქტები. ზემოთ აღნიშნულ ორივე მეთოდს აქვს თავისი უპირატესობები. შესაფერისი ტექნიკის შერჩევა დამოკიდებულია: მიზნობრივი საექსტრაქციო ნივთიერებების კლასსზე, პროცესის პირობებზე, ექსტრაქციიის ხარისხსა და გამოსავალზე.

УТИЛИЗАЦИЯ АГРОПРОМЫШЛЕННЫХ ОТХОДОВ МЕТОДОМ СТУПЕНЧАТОЙ ЭКСТРАКЦИИ СУПЕРКРИТИЧЕСКИМИ ФЛЮИДАМИ И УЛЬТРАЗВУКОМ

М.Цицаги, М.Чхаидзе, М.Бузариашвили, М.Хачидзе, В.Цицишвили
Институт физической и органической химии им. П.Г.Меликишвили Тбилисского государственного университета им. И.Джавахишвили, 0186, ул. А.Политковской 31, Тбилиси, Грузия

РЕЗЮМЕ

В статье описан метод ступенчатой экстракции суперкритическими флюидами и ультразвуком биологически активных соединениий из агропромышленных остатков переработки самых распространенных в Грузии фруктов и овощей. Данные методы обеспечивают высокое качество целевых продуктов, у обоих методов есть свои преймущества. Выбор метода зависит от класса целевых продуктов, условии процесса, глубины экстракции и выхода соединений.

CREATION OF CELLULOSE ACETATE MEMBRANE ON THE BASIS OF DIFFERENT COMPOSITIONS

G.Bibileishvili, N.Gogesashvili
Engineering Institute of Membrane Technology, Georgian Technical University, Godziashvili second-side street 19, 0159, Tbilisi, Georgia
bibileishvili@hotmail.com nanagogesashvili@gmail.com

Today polymer membranes are widely used to filter solutions. Theyconstitute 80 % of the world production of membranes. The usage of polymers is due to their physical structure and their chemical properties. The Goal of polymermodification is to obtain the membrane with a structure desired for the particular process of filtering. Properties of polymer membrane in exploitation depends on polymer, its concentration, composition of the polymer solution, solvent type and the concentration of nonsolvent. Cellulose Acetate areoften used for preparation of membranes [1]. Their properties are moderate hydrophilic, inertto filtering components of the solution and relatively cheap raw materials. The research was conducted on solutions with different concentration of cellulose Diacetate (5-7%) in DMAc/LiCl for creation of Cellulose Acetate membranes in the Engineering Institute of Membrane Technology [2].The study of the process of phase inversion ofobtained solutions in different correlation conditions ofsolvent and nonsolvent revealed that the range of this correlation for Coagulation bath is 0-20%. The research was conducted on the automated laboratory instrument created in the Institute. The instrument allowed to control the membrane precipitation process by regulating bath temperature and the speed and angle of immersing of the polymer solution in the bath. The morphology of the obtained samples is studied by the microscope which is equiped with a digital camera (x5000). The structures of obtained membranes differ. The pore size of some microfiltration membrane is 0, 3-0, 45mkm.

To study creation and properties of Cellulose Acetate membranes the scientific research was conducted in the Engineering Institute of Membrane Technology. For preparation of membrane cellulose diacetate was used. The degree of esterification is γ =250-270, while the degree of substitution is 2,5-2,8.

Using Mark-Kuhn-Houwink's equitation $[\eta] = K \times M^{a}$ the average viscous molecular weight was calculated; K and a was determined according to the known method , $K=0{,}8 \times 10^{-4}$, $a = 0{,}78$.

Properties of polymer membrane in exploitation depends on polymer, its concentration, composition of the polymer solution, solvent type and the concentration of nonsolvent, also temperature and composition of coagulation bath.

The change of each of these parameters can alter the properties of the received membrane. Taken into consideration of these factors the research was conducted with a variety of polymeric composition and precipitation in different conditions.

For dissolution of cellulose diacetate aprotic substance dimethylacetamide was used. It is known that by using this solvent highly porousmembrane can be received. Lithium chloride was solved in dimethylacetamide in advance. Lithium chloride aids dissolution and is the pore-forming agent for Cellulose Acetate. It also causes change of the structure of polymer solvent [2]. Solvents of different concentration were prepared. Data of the received solvents is given in table 1.

Table 1.

Cellulose diacetate concentration, mass %	5	6	7	8	9	10
Dimethylacetamide concentration, mass %	94	92	90	88	86	84
Lithium chloride concentration, mass %	1	2	3	4	5	6

The process of phase inversion was conducted on the automated laboratory instrument created in the Institute (picture 1).

Laboratory instrument controls the process of membrane precipitation. Particularly: a) regulation of bath temperature; b) regulation of speed of immersing sample in the bath; c) regulation of angle change while immersing in bath.

Picture 1. Instrument of phase inversion

Thickness of all sample was 0.1 mm. Precipitation was conducted in the water bath.

The conditions of phase inversion process of some of the samples and permeabilityof obtained membrane is given in table 2.

Table 2.

N	Concentration of cellulose diacetate, mass%	Bath immersing angle,^{0}	Bath immersing speed mm/min	Bath temperature ℃	Permeability l/m^2.h
1	5	10	300	20	70
2	5	45	200	30	160
3	5	80	200	40	100
4	7	10	300	20	50
5	7	45	200	30	80
6	7	80	200	30	40

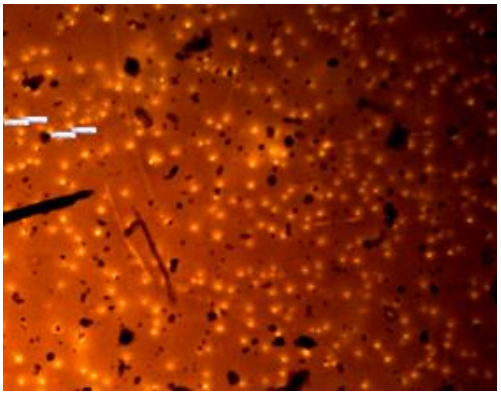

Table shows that increase of polymer concentration and coagulation bath temperature causes the decrease of membrane permeability.The optimal conditions of phase inversion process is established- the angle of bath immersing 45^0, bath immersing speed 200 mm/min, bath temperature 30℃.

The pore size of the membrane was determined on the bubble-point test apparatus created in the Institute. The size of some of the membrane is 0,3-0,45mkm. The sample of one of the membranes is given in picture 2.

Picture 2. Membrane of Celluloce Acetate (X 5000)

ლიტერატურა - REFERENCES – ЛИТЕРАТУРА

1. Sedelkin V.M., Potekhina L.N., Chirkova O.A., Mashkova D.A., Oleynikova E.V., Structure And Properties of Cellulose Acetate Solutions for Moulding Nanostructured Filtration Membranes,*Vestnik*, 2013, 2, 98.
2. Mulder M., Basic Principles of Membrane Technology, Springer Netherlands, 1996, 95.

აცეტატცელულოზური პოლიმერული მემბრანების შექმნა სხვადასხვა კომპოზიციის ბაზაზე

გ.ბიბილეიშვილი, ნ.გოგესაშვილი

საქართველოს ტექნიკური უნივერსიტეტის მემბრანული ტექნოლოგიების საინჟინრო ინსტიტუტი, თბილისი, გოძიაშვილის ქ. 19, 0159, საქართველო

რეზიუმე

მემბრანული ტექნოლოგიების საინჟინრო ინსტიტუტში შექმნილ ლაბორატორიულ დანადგარზე შესწავლილია დიაცეტატცელულოზას სხვადასხვა კონცენტრაციის ხსნარების ფაზურ იინვერსიის პროცესი. დადგენილია ფაზური ინვერსიის ჩატარების პირობების დამოკიდებულება მიღებული მემბრანების ხვედრით წარმადობებთან. ინსტიტუტში შექმნილ ბუშტულაკის წერტილის წარმოქმნის განმსაზღვრელ ხელსაწყოზე დადგენილია მიღებული მემბრანების ფორის ზომები. ზოგიერთი მემბრანის ფორის ზომა შეადგენს 0,3-0,45 მკმ.

СОЗДАНИЕ АЦЕТАТЦЕЛЛЮЛОЗНЫХ МЕМБРАН НА БАЗЕ РАЗНЫХ КОМПОЗИЦИЙ

Г.В.Бибилеишвили, Н.Н.Гогесашвили

Инженерный институт мембранной технологии Грузинского Технического Университета

РЕЗЮМЕ

На автоматизированном лабораторном приборе, созданном в Инженерном институте мембранной технологии, был изучен процесс фазовой инверсии растворов различной концентрации диацетатацеллюлозы. Установлена взаимосвязь с условиями проведения процесса фазовой инверсии и производительностью полученных мембран. Размер пор мембраны определяли на лабораторном приборе, созданном в Институте, в основе которого лежит метод точки пузырка. Размер пор некоторых мембран составляет 0,3-0,45 мкм.

INFLUENCE STRUCTURE MATRIX TO ACTIVITY OF NANOCATALYSTS ON ACTIVATED CARBON FIBERS

Tokhir Kh. Rakhimov, Mukhtor Ganievich Mukhamediev

Department of Chemistry, National University of Uzbekistan named after M.Ulughbek, Tashkent, 100174, Uzbekistan

The aim of investigation is to reveal there is or not influence thin differences of structure matrix-bearer on border dimension of active nanoparticles bearing on fiber polymeric materials. In experiments activated carbon fibers with similar physico-chemical characteristics and differences determined by nature of precursors have been used as matrixes. Nanoparticles have presented themself an active component by composition of palladium-containing nanocatalysts which have been tested in reaction of low-temperature of CO oxidation. By bordering dimensions were supposed minimal and maximal dimensions of particles in limits of which they retained special properties of nanoparticles-in this case responding for unusually high catalytic activity. Boundary dimensions were calculated by methods of mathematical statistics on the base of model "coloring bolls". Investigations have shown that activity is inherent only to particles of determined diameter which is limits not only from above but also from bellow. Interval of boundary dimensions in dependence on of nature of carbon fiber and degree of reduction treatment can be both sufficiently wide and also maximum by narrow. In case of using more homogeneous by composition precursors the calculated diapason of dimensions of active particles was in considerable degree narrow. Thus the determined role of polymeric matrix on properties nanostructures has been proved what has opened way to purposeful obtain functional nanomaterials with high effectiveness.

Keywords: nanocatalyst, catalysis, oxidation, carbon oxide (II), palladium, carbon fibers, dimensions of nanoparticles, phase transition.

Introduction

Before last quarter of last century the fallowing ideas about dispersion state of substance have been prevailed: the more surface the stronger are properties connected with area of surface; as fares at decreasing of particles dimensions the area of surface smoothly has increased and correspondently all processes surface effects including catalytical processes must also smoothly increase with decreasing of particles dimensions. Additional increasing of surface are a can be carried out at distortion of particles form.

Sometime this station is confirmed. However it has determined that as some different substances in dimensions of particles there anamalical changings properties what at present time is object of investigations of such science as nanotechnology. In connection with this, following consequences are appeared: 1) There are borders of dimensions in limits of which anomaly has preserved but behind there- it has disappeared; 2) Particles with dimensions which are more them dimension from which anomaly has disappeared mast be carry away to massive state.

To present time numerous investigations have shown that upper borders of particles are in limits 2-1000 nm but usually-50 nm and by this reason they were named conditionally "nanoparticles". Therefore dispersion systems with particles dimensions on nanometre level (from 1 nm to 1 μm) which haven't anomaly can not by attributed to nano objects. If there are particles dimensions of which are behind levels of manifestation of anomaly then their contribution in common surface of particles of sample must not tack into account (if there dimensions are less than 1 nm)-this position is essence of nano objects. At this particles, with dimensions exceeding dimensions of the anomaly borders can to contain greater part of dispersion phase by mass. By this reason it is incorrect to find correlation between dimensions and properties without determination of these levels. However before appearance of model "coloured balls" have been absent methods of estimation values of above mentioned levels. And what is more such estimation is estimated as main question at investigation of nanocrystalline state formulated as!" there is or no some critical dimension of particle bellow of which there are properties characteristic for nanocrystall

and above which-for massive substance? That is question is raised-from the point of thermodynamics: transition from massive substance to nanocrystallical is or not a phase transition of first order [1].

If there is phase transition than it will inevitably wash away owing of dispersion of particles by their dimensions. For determination of dependence any property from dimensions of particles that is dependence is continuous or not it is necessary to except influence of dispersion of particles by their dimensions. However experiments on series of materials of the same chemical composition but different granulometric composition when each from these materials must to consist from particles only the same dimension it is impossible to carry out at present time.

The main scope of investigations of the nanocrystalline state is to answer the following questions: … Is there some critical grain (particle) size below which the characteristic properties of nanocrystals become observable, and above which the material behaves as a bulk one? In other words, is the transition from the bulk to the nanocrystalline state the phase transformation of the first order from the thermodynamic viewpoint?» [i].

For decision of this problem model "of colouring bolls" using mathematical statistics was applied [1]. This model is based on experiments with polydispers particles without carrying out above described experiment. This model was investigated on samples of palladium-containing nanocatalysts at low-temperature oxidation of CO. Catalysis in the presence nanocomponents which are noble metals or their salts are very sensible to surface structure. By this reason using of this model in one case is proved and calculation on it's base are in good consent with experimental data.

This is signified, that in limits of above-mentioned anomaly there is smooth dependence between catalytic activity and value of active surface. For minimal dimensions of border of phase transition it was determined that physical and catalytic properties are changed at achievement of particles with dimensions 2-8 nm. Experiments have shown however that some time the catalytic activity has raised with increasing of particles dimensions in particular for oxidation of CO by oxygen on platinum nanocatalyst [3]. Thus model "colouring balls" has proved that from the point of view of thermodynamics that transition of massive compound to nanocrystallic can be a phase transition of first type and has opened some new perspectives for metabolically right carrying out experimental investigations on the nano-level and right understanding of obtained results.

The following step is an investigation of characteristics of nanocatalysts from matrix structure because this fact has important significance both theory and for practical application.

In accordance with above-stated the aim of this work was concluded in revealing of influence of thin exchanging of structure of matrix on border dimensions of active nanoparticles.

Experimental

Materials

In the present work are used:

Carbonated polymeric fibers of two marks: activated carbon fibrous mats (CFM) of mark "Mtilon-M" of production MTI (Moscow); activated thick felt " Karbopon – Active" on the base of grafting copolymer of hydrate cellulose and poly acrylic nitryl fabric from viscous thread (further "Mtilon") of production PUP JPI "Chimfiber", Svetlogorsk, Beylorussia.

Helium gaseous of high purity of mark A,TC 0271-135-312323949-2005; 99,95%. Hydrogen gaseous pure, 1 sort, GOST P 51673-2000; 99,99%.

Measurements

Average-square diameter of nanoparticles and coefficient of poly dispersion were used as and quantitative statistical characteristics reflected average relative values of active surface of nanomaterials. Values of these characteristics were determined from experimental data-microphotography.

Dimensions of particles were determined by data of electronic microscopy JEOLIT 300, JEOL, Japan). Structural data were obtained with using atom-power microscope "Nano-Observe AFM" (CS Instrument, Switzerland).

Catalytic activity was determined by method [1] by decreasing of CO contend in gas-air mixture at initial it's content 2 vol.%.

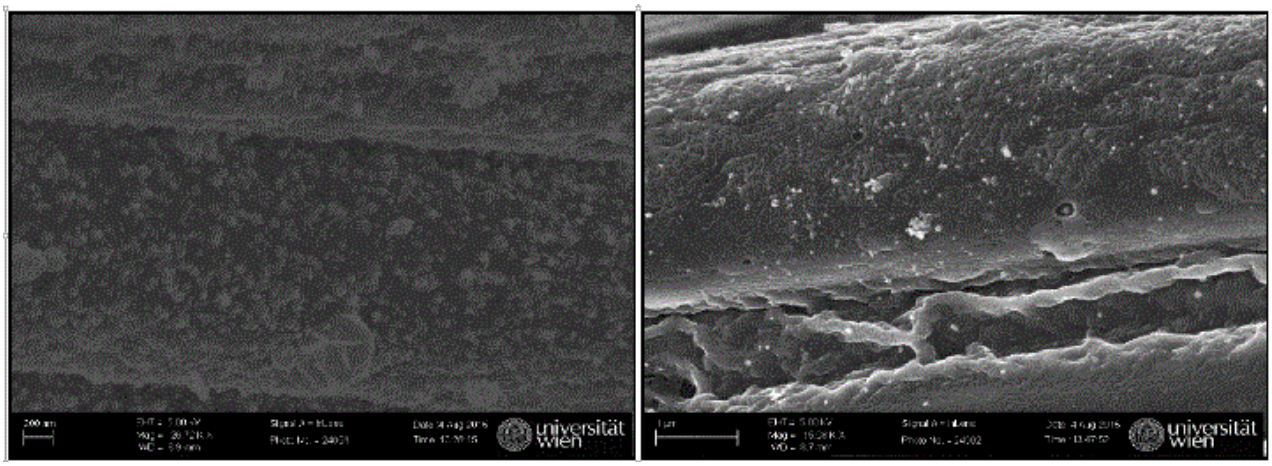

Figure 1. Microphotography carbon fibers with palladium-containing nanoparticles with different middle dimension and dispersion of distribution by dimension (from left-karbopon; from right-Mtilon).

Synthesis

Palladium-containing nanocompesitional catalysts were obtained by drawing of it's salts on activated carbon fibrous mates (CFM) with regulation of drying parameters by method [4]. The obtained samples have contained 1,0 mas % of Pd in calculation on metal.

Reduction of palladium-containing nanocomposits was carried out by action of dosed amount of hydrogen dissolved in helium. For this sample of palladium containing fibre was placed in hermetic glass vessel filled by helium. Mixing in vessel was caused by micro ventilation. Then calculation amount of hydrogen dissolved in helium was added and mixture was contained in there conditions no less than twenty-four hours. Than the catalytic activity was determined in impulse regime.

Calculation of border dimensions

The middle dimensions of nanoparticles and dispersion have been calculated by small excerpt no less than 40 treating obtained results by means MS Excel 2013. The main approach for carrying out of calculation of border dimensions was model of "colouring balls" colouring[5], corresponding calculations were carried out by method [1].

Results and Discussion

For achievement of aim in this work calculation of border dimensions of active nanoparticles of palladium-containing nan catalysts bearing on CFM obtained from precursors of two types was carried out marked nan catalysts with different middle dimensions and dispersion by dimensions were obtained by regulation of parameters of synthesis.

The very important question consists in the following-in influenced whether the nature of bearer on the dimensions of active fractions or else active particles are particles with the same dimensions independently from nature of bearer. The last assumption is more probable if inert materials such as carbon fibers are used.

For elucidation of this question series of samples for which CEM differing by middle dimensions of particles and their dispersion. Then samples from each series were subjected to reduction treatment by hydrogen with different degree: such were obtained about 100 samples differing by middle dimensions of particles, dispersion of distribution of them by diameters and depth of reduction by hydrogen. Each sample was tested on catalytic activity in impulse regime [6] in reaction of carbon oxide (CO) with oxygen of air at room temperature (298K).

Obtained results are presented in Table 1. Take into account that reaction has autocatalytic character than it's rate and catalytic activity of samples are function of reaction duration; by this reason lower the initial rate and initial vales of activity are presented. From these data it is shown that in spite of wailings the nature of bearing has an essential in influence on the bordering dimensions of fractions.

For nanoparticles nan catalysts on the Carbon not only displacement of activity in side of particles with smaller diameter but also essential narrowing of interval of diameters (in limits of which nanoparticles have retained activity) have observed (Figure 2).

Table 1. Catalytic activity palladium-containing nanoparticles bearing on different carbon fibers in oxidation of CO by oxygen of air (T=298; content of Pd-1,0%; initial concentration of CO vol.%.

Bearing - Karbopon

Middle diameter, nm	2,9	6,4	12,5	33,2	63,6	143	187	222
Dispersion	2,8	5,0	10,6	27,3	54,3	119	142	187
H_2/Pd, %	Activity A*10^5 mole/kg							
0	0,10	0,12	0,14	0,00	0,00	0,00	0,00	0,00
5	0,10	0,40	0,28	0,00	0,00	0,00	0,00	0,00
10	2,00	2,30	4,20	0,44	0,08	0,04	0,01	0,00
15	0,20	0,94	7,30	4,70	1,10	0,22	0,08	0,00
20	0,91	1,10	4,20	11,40	17,40	11,00	3,90	1,18
25	0,92	1,08	1,10	2,10	9,00	9,00	0,20	0,18
50	0,01	0,08	0,11	0,21	2,00	1,40	1,00	0,18
75	0,00	0,00	0,00	0,04	0,16	0,27	0,00	0,00
100	0,00	0,00	0,01	0,01	0,10	0,08	0,11	0,07
200	0,00	0,00	0,04	0,10	0,10	0,10	0,10	0,10

Bearing - Mtilon

Middle diameter, nm	9,4	34,3	60,4	91,6	136	250	308	350
Dispersion	3,6	13,8	14,1	30,0	33,6	109,3	150,1	176,2
H_2/Pd, %	Activity A*10^5 mole/kg							
0	0,0	0,0	0,0	0,0	0,0	0,0	0,0	0,00
5	0,0	0,0	0,0	0,0	0,0	0,0	0,0	0,00
10	0,9	1,2	0,2	0,1	0,0	0,0	0,0	0,00
15	0,9	1,3	8,2	7,4	3,2	0,9	0,1	0,00
20	1,1	4,2	11,4	27,2	18,2	3,9	1,2	1,18
25	1,1	1,1	2,1	11,6	9,0	0,2	0,2	0,18
50	0,1	0,1	0,2	1,6	1,9	1,2	0,2	0,18
75	0,0	0,0	0,0	0,2	0,3	0,1	0,1	0,00
100	0,0	0,0	0,0	0,1	0,1	0,1	0,1	0,07
200	0,0	0,0	0,1	0,1	0,1	0,1	0,1	0,10

Reduction has carried out to continuous narrowing of above-mentioned interval and by this reason summary activity has lowered with increasing content of reduced phase. That is for increasing of activity of nan catalysts on Karbopon it is necessary to use methods of synthesis allowing to obtain nanoparticles with narrow distribution by dimensions. Mtilon has allowed to obtain marked catalysts with wide distribution by dimensions but at this only exceptionally large particles (dimensions of which have approached to micron dimensions) have displayed activity.

The observed phenomenon has waited of it's explanation. Obviously it is necessary to remember that initial fibres by carbonization and activation of which have obtained an activated carbon-fibrous materials possessing by different degree of chemical homogeneity. Mtilon-M is obtained on the base of grafting copolymer acrylonitrile (50%)-viscousestople fiber [7], but Karbopon is obtained on the base of viscous technical thread that is it is more chemically homogeneity.

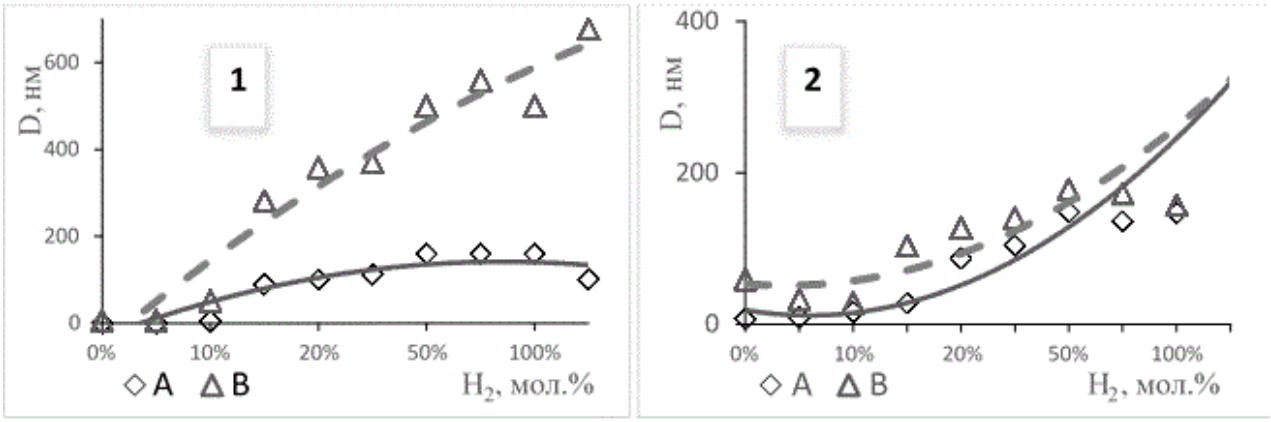

Figure 2. Low (A) and upper (B) values of border dimensions of particles displaying catalytic activity in reaction of low-temperature oxidation of CO: 1-nanocatalysts on the Mtilon; 2-on the Karbopon

Conclusions

Calculation by methods of mathematical statistic of border dimensions of existence of nanoproperticles at dispersion systems has allowed to make conclude about influence of matrix on properties of nanosystems. Investigation of border limits of dimensions of particles displayed activity in composition palladium-containing catalysts of low-temperature oxidation of CO on carbon fibrous materials has shown that only particles of definite diameter (limited not only from above but also from below) have possessed by activity. Interval of border dimensions in dependence from nature of carbon fibre and degree of reduction treatment can be both enough wide and also maximally narrow. Calculation of the activity borders has open way to purposeful increasing of affectivity of low-temperature catalysis construction of deco rational materials with functional activity for their using for purification of atmosphere of habitable compartments in industry, transport hermetically-reserved objects of special purpose.

Acknowledgement

Authors have expressed sincere thankfulness to prof. M.A.Abramov (MTI, Moscow) and Mr. A.Kovalchuk (“M-Karbo”,Svetlogorsk, Byelorussia) for amiably placing samples of carbon fibers.

ლიტერატურა - REFERENCES – ЛИТЕРАТУРА

1. Gusev A. I., Rempel A. A. Nanocrystalline materials. – Cambridge Int Science Publishing, 2004. – p. 21.
2. Gusev A. I., Rempel A. A., Magerl A. J. Disorder and order in strongly nonstoichiometric compounds: transition metal carbides, nitrides and oxides. – Springer Science & Business Media, 2013. – T. 47.
3. Briot P., Auronx A., Jones D., Primet M. Effect of particle size on the reactivity of oxygen-absorbed platinum supported on alumina. // Appl. Catalysis. 1990. V.59. Afel. P. 141-152.
   Lundwall M. J. et al. The Structure–Sensitivity of n-Heptane Dehydrocyclization on Pt/SiO2 Model Catalysts //The Journal of Physical Chemistry C. – 2012. – T. 116. – №. 34. – C. 18155-18159.
   Goodman D. W. Catalysis: from single crystals to the “real world”. // Surface Sci. 1994. V.299/300. P.837-848.
   Kalamaras C. M., Dionysiou D. D., Efstathiou A. M. Mechanistic Studies of the Water–Gas Shift Reaction over Pt/Ce x Zr1–x O2 Catalysts: The Effect of Pt Particle Size and Zr Dopant //ACS Catalysis. – 2012. – T. 2. – №. 12. – C. 2729-2742.
4. АС СССР № 1524767, C01B31/18. Способ получения катализатора для низкотемпературного окисления окиси углерода / Рахимов Т.Х., Мусаев У.Н., Хакимджанов Б.Ш. - № 4664024, заявл. 20.03.1989 г, опубл. 01.10.1990 г.

5. Вычисление размеров активных фракций нанесенных нанокристаллов // Computational nanotechnology, 2015, №2. – С. 6-16.
6. Рахимов Т.Х., Мухамедиев М.Г. Доступные методы биофизического анализа газовоздушной среды // Узб. Биол. журнал. – 2014, № 5. – С. 6-9.
7. Масленников К.Н. Химические волокна. – М.: Химия, 1973. – С. 72.

მატრიცის სტრუქტურის ზეგავლენა აქტივირებული ნახშირბადის ბოჭკოებზე მდებარე ნანაკატალიზატორების აქტივობაზე

ტ.რახიმოვი, მ.მუხამედიევი
ქიმიის დეპარტამენტი, მ. ულუგბეკის სახელობის უზბეკეთის ეროვნული უნივერსიტეტი, ტაშკენტი, 100174, უზბეკეთი

რეზიუმე

კვლევის მიზანია გაირკვეს არის თუ არა მატრიცა-მატარებლის სტრუქტურის გავლენა პოლიმერულ მასალებზე დაფენილი აქტიური ნანონაწილაკების სასაზღვრო განზომილებაზე. მსგავსი ფიზიკო-ქიმიური მახასიათებლების მქონე აქტივირებული ნახშირბადის ბოჭკოები და პრეკურსორის ბუნებით განსაზღვრული განსხვავებები ექსპერიმენტებში გამოყენებული იყო როგორც მატრიცა. პალადიუმ შემცველი ნანოკატალიზატორები, რომლებიც გამოცდილი იყო CO-ს დაჟანგვაზე დაბალ ტემპერატურაზე წარმოადგენს აქტიურ კომპონენტს. განზომილების საზღვრით იყო ნავარაუდევი ნაწილაკების მინიმალური და მაქსიმალური ზღვარი რომლებშიც ნანონაწილაკები ავლენენ უჩვეულოდ მაღალ აქტიურობას. სასაზღვრო განზომილებები გამოთვლილი იყო მათმატიკური სტატიკის მეთოდით „შეფერილი სათესლე კაფსულის“ მოდელის საფუძველზე.
კვლევებმა აჩვენა, რომ აქტიურობა არის მხოლოდ განსაზღვრული დიამეტრის ნაწილაკების მახასიათებელი თვისება. უფრო მეტად ჰომოგენური შემადგენლობის პრეკურსორის გამოყენებისას აქტიური ნაწილაეკბის განზომილების გაანგარიშებული დიაპაზონი იყო საგრძნობლად ვიწრო. ამგვარად განსაზღვრული პოლიმერული მატრიცის როლი ნანოსტრუქტურის მახასიათებლებზე იყო დამტკიცებული, რამაც გზა გაუხსნა მაღალი აქტივობის მქონე ფუნქციონალური ნანონაწილაკების წარმოებას.

ВЛИЯНИЕ СТРУКТУРЫ МАТРИЦЫ НА АКТИВНОСТЬ НАНОКАТАЛИЗАТОРОВ НА ВОЛОКНАХ АКТИВИРОВАННОГО УГЛЯ

Тохир Х. Рахимов, Мухтор Г. Мухамедиев
Химический факультет Национального университета Узбекистана им. М.Улугбека, Ташкент 100174, Узбекистан

РЕЗЮМЕ

Целью исследования является показ влияния тонких различий структуры матрицы-носителя на граничные размеры активных частиц на волокнах полимерных материалов. В экспериментах в качестве матрицы использовались волокна активированного угля с аналогичными физико-химическими характеристиками и с различиями, определенными природой прекурсоров. Наночастицы представляют собой активный компонент с палладий-содержащими нанокатализаторами, которые были проверены в низкотемпературной реакции окисления CO. С ограничением размеров предполагались минимальные и максимальные размеры частиц, в пределах которых они сохраняли специальные свойства наночастиц (в этом случае, высокую каталитическую активность). Граничные размеры рассчитывались методами математической статистики на основе модели “окраска семенных коробочек”.
Исследования показали, что активность свойственна лишь частицам с определенным диаметром. В случае использования более гомогенного состава прекурсоров рассчитанный диапазон размеров активных частиц был достаточно узок. Таким образом, была доказана определенная роль полимерной матрицы на свойства наноструктур, что дало возможность целеустремленно получать функциональные наноматериалы с высокой эффективностью.

SEMICONDUCTOR OPTICAL AMPLIFIER IN COMMUNICATION

David Lapherashvili
Georgian Technical University, Tbilisi, Georgia

As the optical signal is translated by fiber waveguide for a long distance, it attenuated and it can become very weak and photo detector of receiver would not detect signal. Optical amplifiers are key devices that reconstitute the attenuated optical signal, thus expanding the effective fiber span between data source and destination. For fiber optical communication needs amplifiers at electromagnetic wavelength at 1300-1550 nm. III-V semiconductors (InP, InGaAsP) are suitable for such devices. The method fabrication and optical properties of semiconductor optical amplifiers are studied in this work.

Introduction

The needs of communication often were a driving force of rapid increasing in studies of the physical chemical sciences and technology, and nowadays requirements increasing enhancement in speed of information translation cause development of new directions of nano science and nanotechnoloqy. Because secure and safe communication is one of the key technologies to support our present society, quantum information and communication is guaranteed of its safety with quantum mechanical principle and is expected to be the way to realize secure information networks in near future.

The optical communication link comprises a transmitter, a receiver and optical fiber cable connecting them. Optical signals are attenuated during propagation in optical fiber. In Fig.1. The variation of attenuation with wavelength of a typical modern silica fiber, absorption peaks and low-los windows are shown. As the optical signal is translated by fiber waveguide for a long distance, it attenuate and it can become very weak and there is a limit of about 100 km on the distance the signals can travel before becoming too noisy to be detected [1].

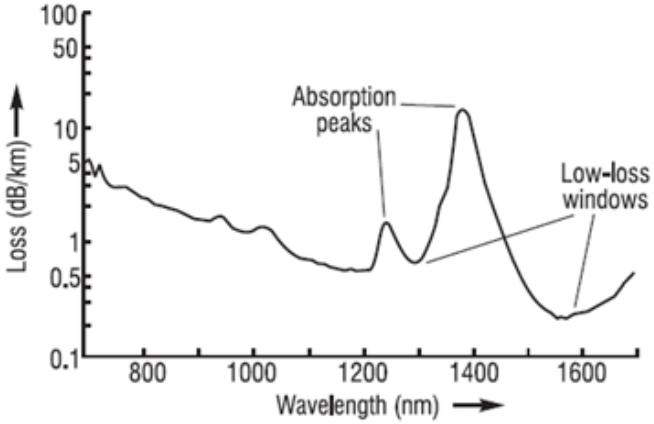

Fig.1. Attenuation Spectrum of Silica Fibers.[1]

Optical amplifiers are devices that reconstitute the attenuated optical signal. There are three most important types of optical amplifiers: the erbium-doped fiber amplifier, the semiconductor optical amplifier (SOA), and the fiber Raman amplifier. Semiconductor optical amplifiers SOA have shown great promise for use in evolving optical communication networks, especially long-reach passive optical networks (LR-PONs). These networks can be beneficial in reducing the number of required optical line termination sites (i.e., to a few major central offices) [2].

As can be seen from Fig.1, fiber optical communication system needs amplifiers electromagnetic waves at wavelength 1.30 and 1.55 μm, but there are no single elements or binary semiconductor compounds compatible with commercial substrates and emitting light at 1.3 μm or 1.55 μm. The most suitable materials for amplifier are complex alloys of III-V semiconductors. The principles of SOA, method fabrication and optical properties of III-V semiconductor based devices are studied in this work.

.

Semiconductor Optical Amplifier

A semiconductor optical amplifier is essentially like a laser diode where the end mirrors have been replaced with anti-reflection coatings. Input and output faces of the amplifier are antireflection coated in order to prevent optical feedback to the gain medium and lasing. A semiconductor optical amplifier (SOA) is pumped with electrical current. The injection current creates a certain carrier density in the conduction band, allowing for optical transitions from the conduction band to the valence band. The gain maximum occurs for photon energies slightly above the bandgap energy. SOAs are noisier than the erbium-doped fiber amplifier and generally handle less power, however, SOAs are less expensive and are therefore suitable for use in local area networks where best performance is not required but cost is an important factor.

In literature is reviewed recent progress in development of quantum-dot semiconductor optical amplifiers (QD SOA) as ultra-wide band polarization-insensitive high-power amplifiers, high-speed signal regenerators, which gives perspectives on optical amplifiers in the next-generation communication systems [2-5]. The fundamental requirements imposed on the material and structure of QDs for broadband amplification are, emission wavelengths covering 1.3 - 1.6 μm. The most extensively investigated QD system is Indium Arsenide (InAs) embedded in a Gallium Arsenide (GaAs) matrix. The 1.3 μm lasers and amplifiers were fabricated using this system [3].

Quantum-dot semiconductor optical amplifiers **(QDSOA)** have been extensively investigated during the last years. Both theoretical and experimental studies have proven the unique capabilities of these devices. The Full Service Access Network and the International Telecommunication Union's Telecommunication Standardization Sector have recently defined the next-generation passive optical network (NGPON) wavelength window. Within this window, an initial future time and wavelength division multiplexed passive optical network (TWDM-PON) has been identified. And was shown, that it is necessary for SOAs to have a 3dB bandwidth of at least 80nm to fully cover both the upstream (US) and downstream (DS) operation wavelengths [4].

For this purpose, QD SOAs are quite suitable because they not only have freedom of wavelength choice like other SOAs, but also have capability to drastically expand the operating wavelength range. QD SOAs have already realized and operating wavelength range drastically exceeding any other existing optical amplifiers. The key feature of QD SOAs which provides unusual amplification characteristics is ultrafast gain response of QDs. Semiconductor optical amplifiers (QD SOAs) offer unique features, the most important being the inhomogeneous gain broadening due to the dot size and strain distribution of self organized QDs. This broadening caused complex carrier and gain dynamics. The important practical characteristics are ultra-fast response, large saturation power, pattern effect free amplification of fast signals under saturated conditions and amplification of multi channel high bit rate signals with no cross talk [3, 4].

QD SOA properties benefit from their discrete electronic structure consisting of a ground (GS) and excited states (ES). Complex carrier dynamics governs the coupling between the confined states and high energy states through which carriers are fed to the QD. A novel theoretical time-domain model for a quantum dot semiconductor optical amplifier, which allows simulating sub picoseconds pulse propagation including power-based and phase-based effects, is elaborated in [5].

Fabrication of III-V Semiconductor Based Semiconductor Nanomaterial

As was mentioned above, semiconductor alloys of III-V elements are the best materials for optical amplifier. The object of our study are semiconductors GaAs, GaP and InP. The electro deposition method and electron less were used for fabrication of III-V based semiconductor devices, such as high-frequency detector on GaAs [6] and infrared photodiode based on In/GaP [7]. The Technology electrodeposition of different metals on the semiconductor surface, and the results of investigation of photo spectral characteristics of structures obtained by annealing contacts metal-semiconductor in hydrogen environment show interesting features of spectral characteristic [8].

For measurement of the photospectral characteristics was developed and used an equipment the principal scheme of which is shown in Fig.5., where 1 and 2 are light sources; 3, 4 and 8 are lenses; 5 is mechanics for converting of incident light into impulses; 6 is photodiode, 7 is monochromator of type DMR-2; 9 and 10 are selective amplifiers; 11 is detector; 12 is recorder; 13 is resistance; 14 is an object for measurement; 15 is capacitor and 16 is switch. The high measurement sensitivity is achieved using synchronous detection system embedded in the equipment.

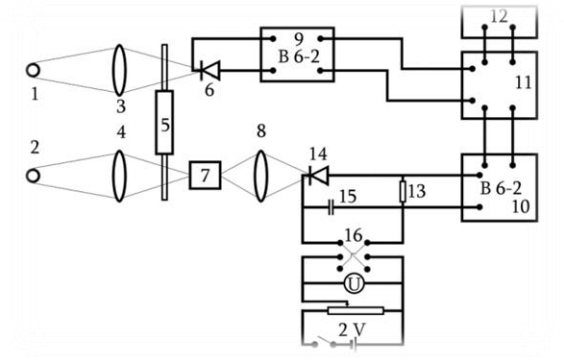

Fig.2. The principal scheme of photoresponce measurement device

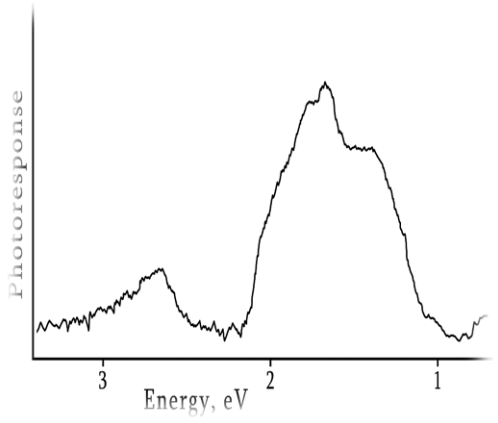

Fig.3. Photo response spectra of In/GaP after annealing at 290°C during 3 minutes, with the 0.2 V reverse bias

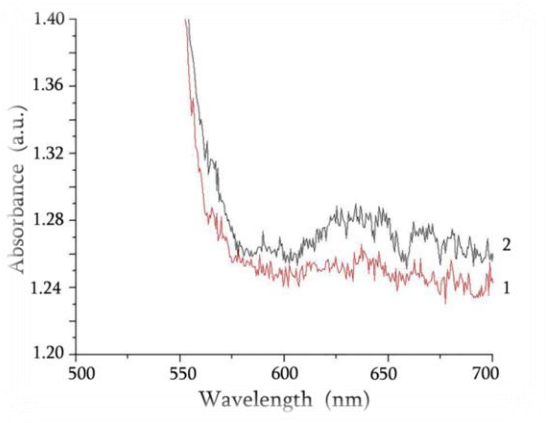

Fig.4. The Photo absorption of In/GaP before annealing (1) and after annealing at 270 ^{0}C (2)

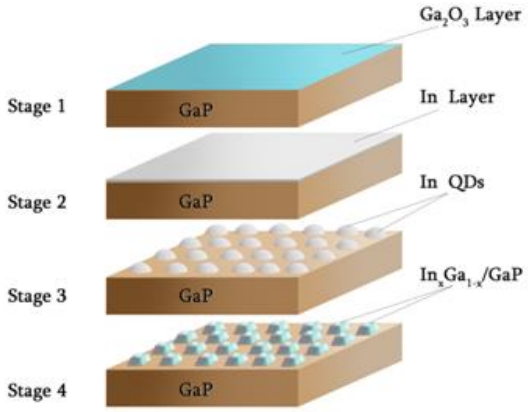

Fig.5. Illustration of InP nanoclasters formation on the GaP surface

Spectral studies of In/GaP structures show, that after annealing at 250 - 350 0C the photoelectric characteristic consists of two separated from each other regions of photosensitivity (1-2.2) eV and (2.6-3) eV. Photoresponce of In/GaP afther annealing at 290 0C during 3 min. at 0.2 V reverse bias is shown in Fig.3, and tail of absorption spectera of In/GaP after annealing at 270 0C (1) and without annealing, measured on the AvaSpec-2048 Fiber Optic Spectrometer is shown in Fig.5.

It is known, that GaP has a number of unique aspects because its surface is unstable against loss of phosphorous. It is interesting to study the influence of annealing on the properties of GaP based devices [6]

After deposition of metal, semiconductor wafer were annealed in hydrogen atmosphere during various time at the various temperature and photo spectral characteristics of annealed structures have been investigated. At first time was found, that after annealing of In/GaP exhibits the region of the strong photosensitivity[7], that was related with the formation of a new material (InP or InGaP nanocrystals) on the surface of GaP via interaction between metal (In) and semiconductor (GaP) during annealing of the In/GaP. We have no technical possibilities to approve this assumption directly, but the mechanism of formation of the InP NCs on the GaP surface is discussed taking into account the publications [9], according of which PL from InP/GaP QDs have peak between 1.9 and 2 eV.

So, mechanism of nanoclasters formatting process are not clear yet. But in [10] is presented phenomenological model formation of the InGaP nanocrystals on GaP surface., according which the

technology of formation of the InP nano crystals on the GaP surface (see Fig.5), consists of four main stages: Electrochemical etching of semiconductor surface; Electro deposition of the thin metallic film on the freshly cleaned semiconductor; Heating of metal-semiconductor contact for generation of metal droplets on the surface, and Annealing of samples in hydrogen. At the last step, crystallization takes place. Under phosphorous pressure, In droplets on GaP surface transforms into crystalline nanostructures via phosphorous diffusion from GaP substrate to metallic droplet during heath treatment. The size and distribution of the nano crystals depend on the thickness of deposited metallic film and on further annealing regime, which is characterized by time, temperature, type of substrate etc. Fig.5. shows the proposed steps of crystallization process.

Conclusion

Both theoretical and experimental studies have proven the unique capabilities of SOAs especially QD SOAs For next generation communication. It was shown, that the excellent materials for fabrication QD SOAs are complex alloys of the III-V semiconductor. Nowadays are realized and operate optical amplifiers based on such materials, already.

From investigation photoelectric characteristics of the devices based on III-V semiconductor was found, that after annealing of contacts In/GaP exhibits the region of the strong photosensitivity, which was related with formation of a new nanostructuredmaterial InP or InxGa1-xP (0,x,1) nanocrystals on the surface of GaP via interaction between metal (In) and semiconductor (GaP) during annealing of the In/GaP in hydrogen environment. Proposed simple technology of electrochemical deposition of thin metallic films of Indium and low temperature annealing may be in principle used for fabrication nano materials based on III-V based semiconductors suitable for communication application.

ლიტერატურა - REFERENCES – ЛИТЕРАТУРА

1. M.J. Adams, I.D. Henning Optical Fibres and Sources for Communications Electron. Letts, Vol 15, 106, 1979
2. Xiao Sun, Qingjiang Chang, Zhensen Gao and Chenhui Ye.,A novel dual-active-layer structure broadens the gain spectrum and can be used as a single bidirectional device for multi-wavelength channel amplification. *Ultra-broadband semiconductor optical amplifier for long-reach optical access networks Optoelectronics & Communications.* 21 April 2016, SPIE Newsroom
3. Christian Meuer, Jungho Kim, Matthias Laemmlin, Sven Liebich, Amir Capua, Gadi Eisenstein, Alexey R. Kovsh, Sergey S. Mikhrin, Igor L. Krestnikov, and Dieter Bimberg. *Static gain saturation in quantum dot semiconductor optical amplifiers. optics express* 8270,2008 / Vol. 16, No. 11
4. D. Puris, C. Schmidt-Langhorst, K. Lüdge, N. Majer, E. Schöll, and K. Petermann Time-domain model of quantum-dot semiconductor optical amplifiers for wideband optical signals. *Optics Express*, Vol. 20,Issue 24,, pp. 27265-27282, (2012)
5. K. Abedi and H. Taleb. Sub-Nanosecond Phase Recovery in Quantum-DotSemiconductor Optical Amplifiers, *acta physica polonoca a* No2, vol:123, (407-410), (2013)
6. Laperashvili T., Kvitsiani O., Imerlishvili I., Laperashvili D., Terahertz pulse detection by the GaAs Schottky diodes; *Proceedings of SPIE* 7728, 77281K doi:10.1117/12.8540 , 2010
7. Laperaschvili T,. Immerlischvili I., Khachidze M, Laperaschvili D. Photoelectric characteristics of contacts In-Semiconductor $A^3B^{5.}$ *Proc. SPIE* Vol.5118, p.502, Nanotechnology 2003
8. T. Laperashvili, O. Kvitsiani, D. Laperashvili, M. Elizbarashvili, A. Chanishvili Nanotechnology and Semiconductor Devices, *Journal " Nano Studies"*, N 10, pp.83-88, 2014
9. Fariba Hatami, Dissertation "Indium Phosphide Quantum Dots in GaP and in In 0.48Ga0.52P" Humboldt-Universitatzu Berlin, 2002
10. Laperashvili D., Laperashvili T. and Chanishvili A. InP Based Nanomaterials for Telecommunication, in press.

ნახევარგამტარული ოპტიკური გამაძლიერებლები კავშირგაბმულობაში

დ. ლ. ლაფერაშვილი
საქართველოს ტექნიკური უნივერსიტეტი, თბილისი, საქართველო
dlaferashvili@mia.gov.ge

რეზიუმე

ოპტიკური სიგნალის გადაიცემისას ოპტიკურ-ბოჭკოვანი ტალღგამტარით გრძელ მანძილზე, ხდება მისი მილევაისე, რომ მიმღებზე ფოტოდეტექტორმა შეიძლება ვერ აღმოაჩინოს სიგნალი. ოპტიკური გამაძლიერებელი არის მოწყობილობება, რომელიც აღადგენს აღდგეს მილეულ (შესუსტებულ) ოპტიკურ სიგნალს. ოპტიკურ-ბოჭკოვანი საკომუნიკაციო სისტემას სჭირდება გამაძლიერებლები ელექტრომაგნიტური ტალღის სიგრძის 1.30-1.55 მიკრონის არეში. ასე რომ საჭირო გახდა მაღალი ტექნოლოგიების დამუშავება ახალი ნანო მასალების მისაღებად. კვანტურ-განზომილებიანი სტრუქტურები III-V ნახევარგამტარების (GaAs, Inas, INP, InGaAsP, GaInNAs, etch.) ბაზაზე წარმოადგენენ სესაფერის ნანომასალებს ასეთი დანიშნულებისათვის. წარმოდგენილ შრომაში შესწავლილია, ნახევარგამტარული ოპტიკური გამაძლიერებლების თვისებები და მათი წარმოების მეთოდები.

ПОЛУПРОВОДНИКОВЫЕ ОПТИЧЕСКИЕ УСИЛИТЕЛИ В СВЯЗИ

Д.Л.Лаперашвили
Грузинский технический университет, 77 Костава ул. 0175, Тбилиси, Грузия
dlaferashvili@mia.gov.ge

РЕЗЮМЕ

По мере того, как оптический сигнал транслируется на волоконный световод на дальние расстояния, он затухает и фотодетектор не сможет обнаружить сигнал. Оптические усилители являются ключевыми устройствами, которые восстанавливают ослабленный оптический сигнал, расширяя тем самым эффективный участок волокна между источником данных и пунктом назначения. Для волоконно-оптической связи нужны усилители электромагнитной волны в области длин волн 1,30-1,55 мкм. Таким образом возникла нужда в развитии высоких технологий для формирования новых нано материалов. Квантово- размерные структуры на основе III-V полупроводников (GaAs, InAs, InP, InGaAsP, GaInNAs, etch.) являются подходящими нано-материалами для такого применения. В данной работе исследуются свойства полупроводниковых оптических усилителей и способы их изготовления.

POPs MANAGEMENT ISSUES IN GEORGIA

A.M.Berejiani
Ministry of Environment and Natural Resources Protection of Georgia, 6 Gulua str, 0114, Tbilisi, Georgia, falestras@gmail.com

Georgia has signed and ratified the Association Agreement with the EU. According to this Agreement, the parties shall develop and strengthen their cooperation on environmental issues, thereby contributing to the long-term objective of sustainable development. Policy objectives concerning management of chemicals, are included in the 2014 Association Agreement with the EU. Also, Georgia is a party to the Multilateral Environmental Agreements (MEAs) in the field of chemicals management.

Georgia has signed and ratified the Association (Agreement with the EU Association Agreement between the European Union and the European Atomic Energy Community and their Member States, of the one part, and Georgia, of the other part and Association Agenda Between the European Union and Georgia). According to this Agreement, the parties shall develop and strengthen their cooperation on environmental issues, thereby contributing to the long-term objective of sustainable development. Policy objectives concerning management of chemicals, are included in the 2014 Association Agreement with the EU. [6] Also, Georgia is a party to the Multilateral Environmental Agreements (MEAs) in the field of chemicals management.

The Stockholm Convention on Persistent Organic Pollutants is a global treaty to protect human health and the environment from chemicals that remain intact in the environment for long periods, become widely distributed geographically, accumulate in the fatty tissue of humans and wildlife, and have harmful impacts on human health or on the environment. Exposure to Persistent Organic Pollutants (POPs) can lead to serious health effects including certain cancers, birth defects, dysfunctional immune and reproductive systems, greater susceptibility to disease and damages to the central and peripheral nervous systems. [8]

The Rotterdam Convention (formally, the Rotterdam Convention on the Prior Informed Consent Procedure for Certain Hazardous Chemicals and Pesticides in International Trade) is a multilateral treaty to promote shared responsibilities in relation to importation of hazardous chemicals. The convention promotes open exchange of information and calls on exporters of hazardous chemicals to use proper labeling, include directions on safe handling, and inform purchasers of any known restrictions or bans. Signatory nations can decide whether to allow or ban the importation of chemicals listed in the treaty, and exporting countries are obliged to make sure that producers within their jurisdiction comply. [9]

In order to translate the EU Association Agreement into more specific actions, the Government adopted the 2014 National Action Plan for the Implementation of the Association Agreement. The National Action Plan for the Implementation of the Association Agreement presents a road map for development of legislation that is necessary for the implementation of EU directives that are relevant for chemicals management. [7]

The Ministry of Environment and Natural Resources Protection is responsible for the chemicals management planning. [4] The responsibilities of the ministry include general chemicals management planning and elaboration of legislation. The Ministry of Environment and Natural Resources Protection is responsible to implement international obligations, mainly control and management of chemicals according to the Rotterdam Convention on the Prior Informed Consent Procedure for Certain Hazardous Chemicals and Pesticides in International Trade and Stockholm Convention on Persistent Organic Pollutants. [3] Also, Georgia has signed The Minamata Convention on Mercury on October 10, 2013, but not yet ratified it. [2]

Environmental pollution is one of the major issues in Georgia. Among the problems POPs Pesticide is one of the important as character of those chemicals is dangerous and cause acute risk on Environment and human health. In 1970 use of DDT was banned and to avoid further use of the chemicals Soviet time government of Georgia decided to build a toxic waste polygon where was taken DDT, but later all other chlor-organic chemicals which was banned later period. According the dates from Ministry of Agriculture who was the owner of the Polygon in that time there amount of the chemicals buried in Tranches and concrete pits where 2700t. Problem comes from the mismanagement and stile of soviet planning system. After the collapse of the USSR the supplies of the agrochemicals stopped. To compensate a shortfall in agrochemicals farmers/people took out the useful agrochemicals from the trenches and sarcophagi. In the

period 1998-2000 and later outdated pesticides and other agrochemicals were dumped in trenches In 2001 Georgia was one of the country who signed the Stockholm convention on "Persistent Organic Pollutant" (POPs) and in 2007 it was ratified by Georgian Government. [4]

In 2003-2007 the Government of Georgia with assistance of GEF/UNDP developed draft National Implementation Plan (NIP) on Stockholm convention on "Persistent Organic Pollutant" (POPs). In 2011 NIP was adopted by the Order of Government of Georgia. According to the inventory data of UNDP/GEF project "Initial Inventory and preparation National Implementation plan" there were 46 warehouses in Georgia with POPs and Obsolete pesticides and Polygon with 2700t of banned and centralised in Iagluja polygon. Inventory was not carried out according FAO standard and no PSMS data. FAO Inventory forms were use during the project supported by Dutch government and NGO Milieukontakt International in 2005-2006. In 2009-2012 - FAO/GEF/IHPA/GC/MKI – EECCA project trained the representatives from governmental organizations and initiated the mini-grant where food agency (MoA with collaboration of MoE) was leading the activities. [5]

One of the top priorities of NIP is reduction of releases of POPs pesticides. The Inventory of POPs pesticides was defined as first activity of the action plan under this target. Moreover this issue is in line with draft NEAP 2 document (Target 2: Reducing environmental pollution from accumulated waste). Situation was that total amount of POPs and obsolete Pesticides were 2700t banned pesticides + 600t contaminated soil + 230t OP from different region of Georgia collected and taken to sarcophagus in the above mentioned polygon. There were still some of the sites in the regions of Georgia and total amount known sites are 15 with up to 5 t of OP. So if we summarise the situation there was - 3 530t OP centralised in Iagluja Polygon and 35 t of OP in 16 sites in different regions of Georgia.

In 2007 state project "Inventory, repackaging and safety store the outdated and obsolete pesticides in Georgia" was carried out and 50t of OP from 12 top priority sites were repacked, transported and stored in central storage. 200t of contaminated soil was disposed in Iagluja Polygon. [4]

In 2009 second state project "Inventory, repackaging and safety store the outdated and obsolete pesticides in Georgia" was carried out and 60t of OP from 7 sites identified by MoE by claims coming from local population - were repacked, transported and stored in central storage. [4]

In 2009 - After complains rising from local population related to the unwillingness to have central storage in their village - all repacked 230 t of pesticides were taken to the Iagluja polygon.

The ongoing Global Environmental Facility (GEF) funded project "Review and update of the national implementation plan for the Stockholm Convention on Persistent Organic Pollutants (POPs) in Georgia" is implemented by United Nations Environment Programme (UNEP) in cooperation with the MENRP. Project envisages the new POPs inventory, assessment of the existing plan and development and adoption of the new plan, as well as public awareness raising regarding POPs. [2]

Within the UNDP project "Disposal of POPs Pesticides and Initial Steps for Containment of Dumped POPs Pesticides in Georgia" 230 tones of POPs Pesticides were collected, packed and exported to Belgium and France for disposal in 2014. The territory of Iagluja Dumpsite was fenced and the warning signs has been installed, Iagludja chemicals landfill remediation action plan is elaborated (for site remediation and environmental improvement three conceptual scenarios). Also, POPs inventory and Awareness raising activities has been carried out. [1]

Additional 208 tones of POPs Pesticides were collected, packed and sent to France for disposal in April 2016 within the FAO/EU project "Improving capacities to eliminate and prevent recurrence of obsolete pesticides as model for tackling unused hazardous chemicals in the former Soviet Union".

Furthermore, it is agreed that UNIDO will implement in Georgia project on PCB management (inventory, collection, packaging, disposal, public awareness raising).

In the scope of the GEF/UNDP project "Demonstrating and Scaling up Sustainable Alternatives to DDT for the Control of Vector Borne Diseases in Southern Caucasus and Central Asia" the demonstration of viability and cost-effectiveness of the use of sustainable alternatives of DDT was held on the selected sites and DDT was replaced by pyrethroids.

Additionally, to meet the the requirements and procedures of Rotterdam and Stockholm Conventions, the Decree of the Government "on Rule of Import and Export of Certain Hazardous Chemicals and Pesticides and Implementation of Prior Informed Consent Procedure" was Adopted on 13.06.2016 (Governmental decree N263).

ლიტერატურა - REFERENCES – ЛИТЕРАТУРА

1. 2013-2015 years Report of the Ministry of Environment and Natural Resources Protection of Georgia. Tbilisi, 2016, pp. 8-14.
2. 2015 annual Report of the Ministry of Environment and Natural Resources Protection of Georgia. Tbilisi, 2016, pp. 7-13.
3. Second National Environmental Action Plan of Georgia (2012-2016). Tbilisi, 2012. pp. 32-35.
4. Georgian National Report on the State of the Environment, 2007-2009, Tbilisi, 2011, pp. 135-147.
5. Environment Education for Sustainable Development - The National Strategy and Action Plan of Georgia, Tbilisi, 2012, pp. 4-7.
6. Agreement with the EU Association Agreement between the European Union and the European Atomic Energy Community and their Member States, of the one part, and Georgia, of the other part and Association Agenda Between the European Union and Georgia. Official Journal of the European Union, 2014. pp. 112-113; pp. 261-262
7. 2015 National Action Plan for the Implementation of the Association Agreement between Georgia, of the one part and the European Union and the European Atomic Energy Community and their Member States, of the other part and the Association Agenda between Georgia and the European Union. Approved by the Decree №59 of the Government of Georgia 26 January 2015. p.90
8. The Stockholm Convention on Persistent Organic Pollutants. pp. 2-12
9. The Rotterdam Convention on the Prior Informed Consent Procedure for Certain Hazardous Chemicals and Pesticides in International Trade. pp. 3-6

მდგრადი ორგანული დამბინძურებლების (მოდ-ების) მართვის საკითხები საქართველოში

ანა ბერეჟიანი

გარემოსა და ბუნებრივი რესურსების დაცვის სამინისტრო, თბილისი, საქართველო, falestras@gmail.com

რეზიუმე

საქართველომ ხელი მოაწერა და მოახდინა ევროკავშირთან ასოცირების შესახებ ხელშეკრულების რატიფიცირება. ამ ხელშეკრულების თანახმად, მხარეები განავითარებენ და განამტკიცებენ თანამშრომლობას გარემოს დაცვის საკითხებში, რითაც ხელი შეეწყობა გრძელვადიან მდგრადი განვითარების მიზნებს. 2014 წელს ევროკავშირთან დადებულ ასოცირების შესახებ ხელშეკრულებაში ასევე გათვალისწინებულია ქიმიური ნივთიერებების მართვის საკითხები. გარდა ამისა, არის საქართველო წარმოადგენს მრავალი მრავალმხრივი გარემოსდაცვითი შეთანხმების (MEAs) მხარე ქვეყანას ქიმიური ნივთიერებების მართვის სფეროში.

ВОПРОСЫ УПРАВЛЕНИЯ СТОЙКИМИ ОРГАНИЧЕСКИМИ ЗАГРЯЗНИТЕЛЯМИ (СОЗ) В ГРУЗИИ

А.М.Бережиани

Министерство По Охране Окружающей Среды и Природных Ресурсов, Тбилиси, Грузия, falestras@gmail.com

РЕЗЮМЕ

Грузия подписала и ратифицировала Соглашение об ассоциации с ЕС. В соответствии с этим Соглашением, стороны должны разработать и расширить свое сотрудничество по вопросам охраны окружающей среды, тем самым способствуя долгосрочной цели устойчивого развития. Цели политики в отношении регулирования химических веществ также включены в Соглашение 2014 года об ассоциации с ЕС. Кроме того, Грузия является стороной многосторонних природоохранных соглашений (МПС) в области регулирования химических веществ.

QUANTITATIVE DETERMINATION OF TOTAL MANGANESE IN ZESTAFONI SOIL AND DRINKING WATER AND ABNORMALITIES CAUSED BY ITS ABUNDANCE

I.Lomsianidze, L.Khvichia, B.Chkheidze
Akaki Tsereteli State University, Kutaisi
izoldalomsianidze@yahoo.com

According to the statistical indicators of the non-commercial legal entity "Municipal Public Health Center" Zestafoni residents are plagued by nervous system diseases including the so called “manganese-induced parkinsonism” and musculoskeletal disorders.The total amount of manganese in the soil ranges between2100 mg/kg and 3045 mg/kg, and in the drinking water it is between 1.25 mg/l and 3.05 mg/l.Such amount of manganese endangers human health.

The Zestafoni ferroalloy plant was founded in 1933 on the base of Chiatura manganese ore _ pyrolusite MnO_2.

Over time, due to the growth of the capacity of electric furnaces and the use of low-grade manganese ore the plant has become one of the sources of environmental pollution. In 1975-1989 a gas cleaning system was installed in the plant. It had to ensure the collection of toxic dust in the atmosphere. [3]

Today the shareholders of the plant claim that new filters have been installed. However, according to statistical data provided by the non-commercial legal entity "Municipal Public Health Center" diseases of the nervous system are common among the residents of the city of Zestafoni, including the so-called "manganese-induced parkinsonism" and musculoskeletal disorders.

The excessive amounts of manganese compounds are potent poisons thatdamage CNS, the cardiovascular system and parenchymal organs. [2,3].

In the early stages of poisoning extreme tiredness, weakness, dizziness, memory impairment, dull pain in the temples and the forehead area are observed. Hindered processes prevail in nervous system, liver is enlarged and bilirubinemia is observed in blood. [2,3]

The second stage – slowed movements, distorted walking, paraesthesia, sexual weakness, insomnia, stiffness in movements, interstitial lung disease. [2,3]

The third stage – “manganese-induced parkinsonism”, serious disorders of CNS; face looks like a mask without any emotions; movements are very slow.

Table 1. Manganese norms in 24 hours

Age	Manganese daily norm in mg.
adolescent	from 2,5mg to 9mg
1-15 years	2 mg
1 year	1 mg

Intake of 40 mg manganese causes poisoning. Poisoning may be caused by the following: air, soil, water, plant. [2]

Therefore, we aimedat determining the content of manganese in arable soils and drinking waters (springs, wells) of the city of Zestafoni. Research was carried out in chemistry research laboratory of Ak. Tsereteli State University and in laboratory of physico-chemical analysis of R. Agladze Institute of Inorganic Chemistry and Electrochemistry.

Soil and water samples were obtained within 15 km away from the Zestafoni ferroalloy plant in full compliance with the methodology. 4 samples _ 3 km; 6 km; 10 km; 15 km; (Village of Zeda Sakara).

Methods: Folgard’s and Potentiometric methods formeasuring total manganese content in the soil were used. [4]

The persulphate-photocolorimetric method for measuring total manganese content in drinking waters was used. [1,5,6]

The soils taken for research are podzolic soils with low acidity pH=6. Themaximum permissible concentration (MPC) of total manganese content for such type of soils is 500 mg/kg [1, 4]and 0.4 mg/l in drinking waters.

The results obtained are presented in Tables 2,3.

Table 2. Total manganese in the soil

№	Distance from the ferroalloy plant	Folgard's Method g/l	Potentio-metric method g/l	The final resultmg/kg
1	3 km	3,145	3,045	3045
2	6 km	2,320	2,30	2300
3	10 km	2,010	2,10	2100
4	15 km	2,560	2,400	2400

Table 3. Total manganese in the drinking waters

№	Distance from the ferroalloy plant	Total manganese mg/l
1Sample (spring)	3 km	1,25
2Sample(spring)	6 km	2,3
3 Sample (well)	10 km	1,25
4 Sample(well)	15 km	3,05

As the survey shows, the total amount of manganese in the soil and drinking water is much higher than the standards adopted by our country (Order №297/NApproval of environmental quality standards. Valid_ 20.09.2006 №70 _15 January,2014, Tbilisi).

The total amount of manganese in the soil ranges between2100 mg/kg and 3045 mg/kg, and in the drinking waters it is between 1.25 mg/l and 3.05 mg/l.

Such number of manganese endangers human health. To get a full picture it is necessary to conduct the second phase of researchand determine total manganese content in leaves and fruits of plants.

ლიტერატურა - REFERENCES – ЛИТЕРАТУРА

1. Turkadze Ts. Khukhianidze M. (in Georgian) _ Complex Methodological Guidance for Laboratory Works, Kutaisi, 2015.
2. Avtsyn A. P. and others. (in Russian) _ Mikroelementoses in Humans, Moscow, Medicine, 1991.
3. Volodina. G. B. Yakushina I. V. (in Russian) _ General Ecology. Tambov, TSTU Press, 2005.
4. Mineeva V. G. (in Russian) _ Workshop on Agricultural Chemistry, Moscow, Moscow State University Press, 2001.
5. Reznikov A. A. and others. (in Russain) _ Methods of Analysis of the Natural Waters, Moscow, Nedra, 1970.
6. Semenov A. D. (in Russian) _ Guide on Chemical Analysis of Continental Surface Waters, Leningrad, Gidrometeoizdat, 1977.

ქ. ზესტაფონის ნიადაგებსა და სასმელ წყლებში საერთო მანგანუმის რაოდენობრივი განსაზღვრა და მისი სიჭარბით გამოწვეული პათოლოგიები

ი. ლომსიანიძე, ლ.ხვიჩია, ბ. ჩხეიძე

აკაკი წერეთლის სახელმწიფო უნივერსიტეტი, ქუთაისი

რეზიუმე

შესწავლილი იქნა ქალაქ ზესტაფონში ფეროშენადნობების ქარხნის ირგვლივ 15 კმ–ის არეალში, ნიადაგებსა დ ასასმელ წყლებში საერთო მანგანუმის რაოდენობა. ვსაზღვრავდით საერთო მანგანუმის რაოდენობას ფოლგარდისა და პოტენციომეტრული მეთოდებით, წყალში პერსულფატური მეთოდით ფოტოელექტროკოლორიმეტრზე. საკვლევი ნიადაგი ეწერია, დაბალი მჟავიანობით. მისთვის მანგანუმის ზდკ ტოლია 500 მგ/კგ. საერთოდ კი – 1000 მგ/კგ. სასმელ წყალში მანგანუმის ზდკ ტოლია 0,4 მგ/ლ. კვლევის შედეგები ასეთია: ნიადაგში საერთო მანგანუმის რაოდენობა 2100 მგ/კგ–3045 მგ/კგ–ია. წყალში 1,25 მგ/ლ–3,05 მგ/ლ. მანგანუმის ასეთი რაოდენობა საშიშროებას წარმოადგენს აღნიშნულ ტერიტორიაზე მცხოვრები მოსახლეობის ჯანმრთელობისათვის.

ОБЩЕЕ КОЛИЧЕСТВО МАРГАНЦА В ПИТЬЕВЫХ ВОДАХ И ПОЧВЕ Г. ЗЕСТАФОНИ И ВЫЗВАННЫЕ ЕГО ИЗБЫТКОМ ПАТОЛОГИИ

И.Ломсианидзе, Л.Хвичия, Б.Чхеидзе

Государственый университет им. Ак. Церетели г. Кутаиси

РЕЗЮМЕ

Изучено количество общего марганца в водах и в почве г. Зестафони, вокруг завода ферросплавов завода в ареале 15 км. В почве общий марганец определялся потенциометрическим методом и методом Фольгарда, а в питьевой воде персульфатным методом на ФЭК-е. Полученные данные общего марганца превышают ПДК Грузии, для подзолистых почв ПДК = 500 мг/кг, для питьевой воды ПДК = 0,4 мг/л. Получены следующие данные: в почве количество общего марганца колеблется от 2100 мг/кг до 3045 мг/кг., в питьевой воде от 1,25 до 3,05 мг/л. Такое количество марганца опасно для здоровья жителей этого города.

OXIDE-MANGANESE CATALYSTS FOR SOLVING OF ECOLOGICAL PROBLEMS

V.Sh.Bakhtadze, V.P.Mosidze, R.V.Janjgava, N.D.Kharabadze, M.V.Pajishvili, N.M.Chochishvili

R.Agladze Institute of Inorganic Chemistry and Electrochemistry of Ivane Javakhishvili Tbilisi State University, 0186, Mindeli st.11, Tbilisi, Georgia, Vbakhtkat@yahoo.com

The brief review of the works on elaboration and study of manganese catalysts for solving of ecological problems is given. The data are presented on improvement of the technology of coating of manganese oxides and palladium on the fragments of alumosilicate blocks on the stainless steel: " 20X23H18". It wass hown that CO oxidation degree on Mn-Pd catalyst , coated on the steel, attains 90-98 % at $W= 30 . 10^3$ hour $^{-1}$ and at (130 – 160) ºC. Dispersity of manganese oxides on the plates of alumosilicate blocks comprises nearly 100 nm.

In the laboratory of catalysis of R. Agladzwe Institute of Inorganic Chemistry and Electro chemistry the systematic researches from the date of its foundation (1961 year) are carried out for elaboration and study of physical-chemical processes of manganese catalysts for gas purification as well as for realization of other chemical-technological processes [1]. For example, for methane conversion by water steam the cobalt-manganese catalyst on the basis of alumocalcium was elaborated. The catalyst is characterized by enhanced activity, by thermal and chemical stability. Manganese oxides increase the catalyst stability toward to carburizing [2]. On the basis of the concentrates of manganese natural ores the manganese catalyst- adsorbents were elaborated for purification of technological gases from H_2S . By activity, adsorbtivity and by operation regime they are highly competitive with industrial zink absorbers of some marks and by mechanical strength and thermal stability surprass them [3].

The technology for modification of the carrier from γ - χ - Al_2O_3 by calcium oxide was elaboratied. Processing methods, realized in this case, allow to activate the solid- phase reaction for formation of calcium aluminates at lower temperatures, to stabilize the surface structural characteristics, to enhance the thermal stability and mechanical strength of the carrier [4]. On the basis of modified carrier $CaO\cdot 2\ Al_2O_3$ a number of catalysts Mn - Pd (МПК-1), Pd (НПК) and Pt (ПЛК-1 or ПЛК-2) were elaborated with a low content (from 0. 05 to 0. 2 mass.%) of noble metal (Pt, Pd), which is mainly concentrated in near surface layers of carrier granule . Proportional dependence between the amount of introduced palladium and the value of active surface was shown at constant value of particles dispersity: 29 – 34 Å [5] .

Pilot batches of elaborated catalysts were promoted in some enterprises of chemical and metallurgical industry as well as in auto transport entities. Activity and some physical- chemical characteristics of elaborated catalyst are presented in Table 1. As evident, the low-percentage palladium catalyst (up to 0.2 mass. % of Pd) surprasses other samples by activity. The experience of operative testing of the catalyst НПК – 2 in the systems of purification of spent gases as well as of diesel engines has shown that they may compete with a well- known industrial catalysts .

Table 1. Catalyst activity in the reaction of CO oxidation ($W = 10\cdot10^3$ hour $^{-1}$, $G_{cat.} =1$ g, reaction mixture: 1% CO + air, whole granule 4.0 mm)

Catalyst mark	**Temperatures of attainment of CO transformation degree, ºC**				Specific surface, m^2/ gr	Strength th, kg/cm^2	Packed density, g/ cm^3	Total volume of pores, cm^3 / g
	25%	**50%**	**75%**	**85%**				
МПК-1	**151**	**156**	**159**	**161**	**98,0**	**114,0**	**0,88**	**0,27**
НПК-2	**112**	**113**	**114**	**115**	**93,0**	**120,0**	**0,86**	**0,32**
ПЛК-2	**151**	**153**	**154**	**156**	**116,0**	**125,0**	**0,85**	**0,35**
ПЛК-2	**136**	**138**	**143**	**152**	**118,0**	**115,0**	**0,86**	**0,.33**

Mn – Pd catalyst МПК-1, containing a minimum amount of palladium (up to 0. 05 mass. %) is perspective for the use in the systems of gas purification [6] . By means of the method of

electron scanning microscopy it was shown that in Mn-Pd catalyst (МПК-1) the increase of palladium concentration from 0. 023 to 0.06 mass.% causes a nearly total overlapping of the surface by palladium particles. In this case Pd covers exactly the surface, occupied by manganese oxide, without penetration in the pores depth, which are plugged by the particles of manganese oxide [7] . The characteristic property of oxide (MnO_x , CoOx , CuO) catalysts is a synergistic result which is revealed at the addition of noble metal (Pt, Pd or Ag). Such combined system is more active in some processes than individual components separately.

At present the granulated and monolithic systems: metallic and alumosilicate blocks have received wide acceptance. For improvement of the catalysts of cellular structure the researches are carried out for coating of active component on the surface of block catalyst- secondary coating by its further fixing.Coating technology on ceramic and metallic carriers are as yet elaborated. Below the results of the research for creation of secondary coating on the surface of standard ceramic blocks-cellular structure and on metallic plates of stainless steel are presented.Manganese oxides are selected as a secondary coating and palladium - as a promotor component.

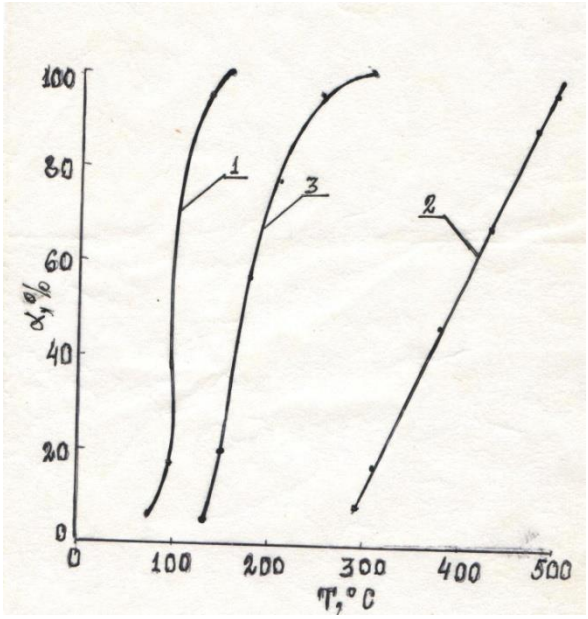

Figure 1. Dependence of CO conversion degree on temperature at the catalysts:
1 – Mn-Pd/ stainless steel; 2 – stainless steel; 3 – Mn-Pd - alumosilicate

For elaboration of competitive oxide-manganese catalysts for CO oxidation the works were performed to improve the technology of coating of manganese and palladium oxides on the fragments of alumosilicate block and on stainless steel of "20 X 23H 18" mark. Activity of the samples of Mn - Pd catalysts in the reaction of CO oxidation was studied in the flowing quartz reactor of 15 mm diameter; catalyst volume – 1cm^3 , granule size 2.0 – 2.5 mm, volume rate of gaseous mixture (1.0 vol. % of CO + air), W = 30 . 10^3 hour $^{-1}$.Oxidation degree of CO in the case of Mn - Pd catalyst, deposited on a steel, attains 90 – 98 % in the temperature range from 130 ºC to `160 ºC (Fig.1) . X-ray phase and thermal analyses of elaborated catalysts were performed. On the carriers surface the phase of manganese oxide - Mn_2O_3 appears in the course of the formation of Mn - Pd catalyst. By means of scanning electron microscope JSM - 65 10 LV the samples morphology, surface distribution of active components (Mn and Pd) in the layer depth (no more than 1 μm) were studied. Manganese oxides are most uniformly deposited on the plates of alumosilicate blocks. Dispersity of manganese oxides comprises nearly 100 nm.

ლიტერატურა - REFERENCES – ЛИТЕРАТУРА

1. Ioseliani D.K., Bakhtadze V.Sh., Georgian Academy of sciences, Chemistry and Chemical Technology. Proceedings., Tbilisi, "Metsniereba", 2001, 120-133.

2. Mosidze V. P., Bakhtadze V.Sh., Andguladze Sh.N., Janjgava R. V., Kartvelishvili D. G., Kharabadze N. D., Chochishvili N. M., Pajishvili M.V. Georgia Chemical Journal, 2011 , vol.11 , №4 , 363-365.
3. Bakhtadze V.Sh., Mosidze V. P., Janjgava R. V., Chochishvili N. M., Dzanashvili D.I., Kharabadze N. D., Pajishvili M.V. European Chemical Bulletin . 2014, 3 (1), 46-49
4. Bakhtadze V.Sh., Mosidze V. P., Kartvelishvili D. G. , Janjgava R. V., Kharabadze N. D., Journal, "Catalysis in the Industry," Moscow , 2012 , №2, 62-64.
5. Bakhtadze V.Sh., Mosidze V. P., Kharabadze N. D., Dzanashvili D.I., Janjgava R. V., Pajishvili M.V., Chochishvili N. M. Georgia Chemical Journal, 2015 , vol. 15 , №1 , 66 – 68.
6. Bakhtadze V.Sh., Kharabadze N. D., Moroz E. M., Journal "Catalysis in the industry". Moscow, 2007,№3. 115-118.
7. Bakhtadze V.Sh., Mosidze V. P., Kharabadze N. D., Dzanashvili D.I., Janjgava R. V., Pajishvili M.V. Chochishvili N. M., Georgia Chemical Journal, 2014 , vol. 14 , №1 , 100-103

ეკოლოგიური ამოცანების გადაწყვეტის ოქსიდურ- მანგანუმიანი კატალიზატორები

ვ.ბახტაძე, ვ.მოსიძე, რ.ჯანჯღავა, ნ.ხარაბაძე, მ.ფაჭიშვილი, ნ.ჩოჩიშვილი
ივანე ჯავახიშვილის სახელობის თბილისის სახელმწიფო უნივერსიტეტის რ.აგლაძის არაორგანული ქიმიისა და ელექტროქიმიის ინსტიტუტი, 0186, მინდელის ქ.11, თბილისი, საქართველო

რეზიუმე

სტატიაში მოცემულია ეკოლოგიური ამოცანების გადაჭრის მანგანუმიანი კატალიზატორების დამუშავებისა და შესწავლის სამუშაოების მოკლე ანალიზი. წარმოდგენილია ალუმოსილაკატური ბლოკის ფრაგმენტებსა და "20X23H18" მარკის უჟანგავ ფოლადზე - მანგანუმის ოქსიდებისა და პალადიუმის დაფენის ტექნოლოგიის სრულყოფის მონაცემები. ნაჩვენებია, რომ ფოლადზე დაფენილ Mn-Pd კატალიზატორზე 130 – 160 °C ტემპერატურულ ინტერვალში და სარეაქციო აირის W= $30 \cdot 10^3$ სთ$^{-1}$ მოცულობით სიჩქარეზე CO-ს დაჟანგვის ხარისხი აღწევს 90–98%-ს. ალუმოსილიკატური ბლოკის ფირფიტაზე დაფენილი მანგანუმის ოქსიდების დისპერსულობა 100 ნმ-მდეა.

ОКСИДНО-МАРГАНЦЕВЫЕ КАТАЛИЗАТОРЫ В РЕШЕНИИ ЭКОЛОГИЧЕСКИХ ЗАДАЧ

В.Ш.Бахтадзе, В.П.Мосидзе, Р.В.Джанджгава, Н.Д.Харабадзе, М.В.Паджишвили, Н.М.Чочишвили
Институт неорганической химии и электрохимии им. Р.И.Агладзе Тбилисского государственного университета им. И.Джавахишвили, 0186, ул. Миндели11, Тбилиси, Грузия

РЕЗЮМЕ

В статье дан краткий обзор работ по разработке и изучению марганцевых катализаторов для решения экологических задач. Представлены данные по усовершенствованию технологии нанесения оксидов марганца и палладия на фрагментах алюмосиликатных блоков и на нержавеюшей стали марки "20X23H18". Показано, что степень окисления CO на Mn-Pd катализаторе, нанесенном на сталь при объемной скорости реакционной смеси W= $30 \cdot 10^3$ час$^{-1}$ достигает 90–98 % в интервале температур 130 – 160 °C . Дисперсность оксидов марганца на пластинках алюмосиликатных блоков составляет около 100 нм.

CLEARING-TREATMENT OF QUARRY WATERS OF COPPER-PYRITE DEPOSITS

Rusudan Dundua, Nana Butliashvili
R.Agladze Institute of Inorganic Chemistry and Electrochemistry of Ivane Javakhishvili Tbilisi State University, 0186, Mindeli st.11, Tbilisi, Georgia

Ore sulfide deposits are significant sources of toxic pollution. Loss of nonferrous and heavy metals from quarry water compounds tens thousands of tons. Ore operations respectively cause serious economic problem and environmental damage of area. Copper sulfide deposit Madneuli is a typical example of deposits existing worldwide. Quarry waters of Madneuli deposit belong to low-concentrated ones and are considered as nonprofitable for extraction of heavy metals. By researches, cleaning-treatment of quarry waters using sulfide methods seems perspective. The method thereby will produce barite-polymetallic sulfide sediment for further processing and quarry water containing metal sulfates being below allowable concentration for reservoirs

Sulfide deposits represent one of the most significant sources of environment pollution by toxic elements. That is caused by migration of heavy and non-ferrous metals into underground waters, where they are dispersed widely and concentrated into various environment objects. Spread scale for some of the components varies in the range of hundreds meters upto several kilometers.

Besides, with quarry waters there are thousands of tons of metals lost, that is serious economical problem for exploitation.

The copper sulfide deposit Madneuli (Bolnisi, Georgia) is a typical example of deposits existing worldwide with similar technocratic impacts on the environment.

According to these researches, the indexes of the contamination of the soils and water objects by toxic elements (Cu,Zn,Cd,Fe), in the range of ~20 km range around deposit, is much greater than maximum permissible concentrations; very high level of sickness rate of population has been revealed; fish has been disappeared in the rivers; Joint-stock company "Madneuli" (currently, Reach Metal Group – RMG) was repeatedly imposed to administrative sanctions [1,2,3,4].

From one side, the waters represent a powerful source for contamination of region hydrographic system, while from the other hand, quarry waters, as valuable raw materials for further technological processing are fled intorivers and tones of heavy and non-ferrous metals are lost, during the years (Table 1).

Table 1.Loss of metal from quarry waters - tones/year
Annual average volume of fled water - 120 m^3/hr

Cu	Fe	Zn	Cd	Pb	Co	Ni	Cr
704	**1198**	**652**	**4.7**	**0.5**	**0.7**	**1.0**	**0.1**

Further problem is that quarry waters of Madneuli deposit, like many other deposits worldwide, belong to low-concentrated ones and are considered as non-profitable for extraction of heavy metals. Nevertheless, it is critical to request purifying quarry waters down to limit of allowable concentration before flowing them into river.

The analysis of existing methods for purification of quarry waters of sulfide deposits shows that at present there is no efficient and economic method for purifying from the ions of heavy metals.

Besides, the effective method for purification of quarry waters and, at the same time, for extraction of metals for further utilization, has not been observed.

Based on researches, processing of quarry waters of copper-pyrite deposits by reagent, namely, sulfide method has been assumed quite perspective.

Development of technology for complex extraction of metals from quarry waters will solve two problems – will purify the deposit waters and will retain the lost heavy metals back to production.

For researches, there have been utilized quarry waters of Madneuli copper-pyrite deposit (Table 2).

For sedimentation there has been used Barium Sulfide. Experiments have been fulfilled at room temperature. During experiments, pH level has been measured by pH-meter with ±0.01 pH accuracy.

Results of water purification have been tested by atomic absorption spectrophotometer, photocolorimeter, chemical analysis and by use of qualitative reaction method for high sensitivity.

There has been set optimal parameters for purification of waters: pH, BaS expenditure, sulfide full sedimentation time.

Based on gained laboratory results, experiments have been done at wide-laboratory scale. In total, there have been purified ~35 l. quarry waters; gained ~460 gr. polimetal supfide sediment.Based on data from chemical analysis, composition of barite-polimetal sulfide sediment has been estimated. Main components of the sediment (%): CuS - 5.14; ZnS -2.71; FeS -2.67; CdS -0.01; $CaSO_4$ – 2.14; $BaSO_4$-75.6.

Table 2. Madneuli quarry water sample composition
(samples have been picked up during one year, once per month)

Sample #	pH	C_{Cu2+}, gr./l	$C_{\sum Fe}$, gr./l	C_{Fe2+}, gr./l	C_{Fe3}^{+}, gr./l	C_{Zn2+}, gr./l	C_{Cd2}^{+}, gr./l
1	3.5	0.43	1.45	0.81	0.81	0.269	0.0034
2	3.5	0.61	1.21	0.73	0.56	0.825	0.0054
3	4.0	0.57	1.17	0.56	0.52	0.769	0.0050
4	4.0	0.72	1.26	0.70	0.47	0.725	0.0049
5	3.0	0.96	1.64	0.46	0.61	0.700	0.0049
6	3.0	2.30	2.21	0.97	0.17	0.562	0.0042
7	4.0	0.91	0.8	0.45	0.37	0.643	0.0043
8	3.5	2.20	2.10	0.97	0.43	0.512	0.0042
9	4.0	1.56	1.47	0.42	0.45	0.758	0.0048
10	4.0	1.23	1.92	0.45	0.67	0.656	0.0042
11	3.0	1.65	1.48	0.69	0.28	0.712	0.0049
12	3.0	1.31	1.32	0.66	0.60	0.587	0.0042
13	3.0	0.63	1.80	0.62	0.51	0.746	0.0047

Concentration of metal sulfates in liquids gained after purification, is below allowed level of concentration in reservoirs.

Based on gained results, there has been worked-out a principal technological scheme for clearing-treatment of quarry waters. It is assumed to cover below stages:

- Sedimentation of sulfides from quarry waters by use of Barium Sulfides;
- Solution sedimentation and directing purified water for technical use or hydrographic network;
- Mixing the sediment to locally produced sulfide deposit enrichment product or delivering it to metallurgic production, after drying.

Technological scheme will be very simple and will not require big capital expenditures.

ლიტერატურა - REFERENCES – ЛИТЕРАТУРА

1. Georgian Strategic Research and Development Center.2006. Newsletter #100. GW-29
2. gardabaniherald. blogpost.com
3. madneuli. blogpost.com
4. Georgian Technical University, International Technical Conference -"Environmental protection and sustainable development". Works. Tbilisi, publishing house "Technical University", 2010. pp.155 -157.

სპილენძ–კოლჩედანური საბადოების კარიერული წყლების გაწმენდა–გადამუშავება

რუსუდან დუნდუა, ნანა ბუთლიაშვილი
ივანე ჯავახიშვილის სახელობის თბილისის სახელმწიფო უნივერსიტეტის რ.აგლაძის არაორგანული ქიმიისა და ელექტროქიმიის ინსტიტუტი, 0186, მინდელის ქ.11, თბილისი, საქართველო

რეზიუმე

სულფიდური მადნების საბადოების კარიერული წყლები წარმოადგენენ ტოქსიკური ელემენტებით გარემოს დაბინძურების ერთ-ერთ მნიშვნელოვან წყაროს. ამავე დროს ფერადი და მძიმე ლითონების დანაკარგები კარიერული წყლებით შეადგენს ათეულ ათასობით ტონას, რაც მადნების ექპლუატაციისას, ეკოლოგიურ ზიანთან ერთად, განაპირობებს სერიოზულ ეკონომიკურ პრობლემებსაც. მადნეულის სპილენძის სულფიდური საბადო ტიპური მაგალითია მსოფლიოში არსებული მსგავსი საბადოებისა. მდგომარეობას ამძიმებს ის გარემოებაც, რომ მადნეულის კარიერული წყლები მიეკუთვნება დაბალკონცენტრირებულს და ითვლება არარენტაბელურად მძიმე ლითონთა ამოწვლილვისათვის. ჩატარებული კვლევების საფუძველზე პერსპექტიულად გვესახება კარიერული წყლების გაწმენდა–გადამუშავება სულფიდური მეთოდის გამოყენებით, რის შედეგადაც მიიღება ბარიტ-პოლილითონური სულფიდური ნალექი შემდგომი გადამუშავებისათვის და კარიერული წყლები, რომლებშიც ლითონთა სულფატების შემცველობები ნაკლებია ზღვრულად დასაშვებ კონცენტრაციებზე წყალსატევებისათვის.

ОЧИСТКА-ПЕРЕРАБОТКА КАРЬЕРНЫХ ВОД МЕДНО-КОЛЧЕДАННЫХ МЕСТОРОЖДЕНИЙ

Р.Г.Дундуа,Н.И. Бутлиашвили
Институт неорганической химии и электрохимии им. Р.И.Агладзе Тбилисского государственного университета им. И.Джавахишвили, 0186, ул. Миндели11, Тбилиси, Грузия

РЕЗЮМЕ

Карьерные воды месторождений сульфидных руд представляют собой один из важных источников загрязнения окружающей среды токсичными элементами. В то же время потери цветных и тяжелых металлов с карьерными водами составляют десятки тысяч тонн, что при эксплуатации руд, вместе с экологическим ущербом, приводит также к серьезным экономическим проблемам. Маднеульское медно-сульфидное месторождение – типичный пример сущетвующих в мире подобных руд. Состояние усугубляется тем, что маднеульские карьерные воды относятся к низко-концентрированным и считаются нерентабельными для извлечения тяжёлых металлов. На основании проведённых исследований считаем перспективным проводить очистку-переработку карьерных вод с применением сульфидного метода, в результате чего получается барито-полиметаллический сульфидный осадок для дальнейшей переработки, и карьерные воды, в которых содержание сульфатов металлов ниже предельно допустимых концентраций для водоёмов.

NEW APPROACHES AND TOOLS FOR REHABILITATION OF CHEMICALLY CONTAMINATED SOILS

M.Kurashvili, T.Varazi, M.Pruidze, G.Adamia, N.Gagelidze,
T.Ananiashvili, M.Gordeziani, G.Khatisashvili
Agricultural University of Georgia, Durmishidze Institute of Biochemistry and Biotechnology, David Agmashenebli Alley 240, Tbilisi, 0159, Georgia, m.kurashvili@agruni.edu.ge

The main idea and novelty of presented work is development a novel approach for rehabilitation of chemically contaminated soils. The approach based on using natural minerals composites which are comprised of natural mineral rocks, natural biosurfactants, microorganism strains having high detoxification ability and plants-phytoremediators. It has been established that soybean and alfalfa together with selected bacterial consortium and natural biosurfactant are the best tools for phytoremediation of soils polluted with oil hydrocarbons.

INTRODUCTION

Nowadays global chemical pollution of the ecosystems biosphere, waters, and soil tops the hazardous level. Succesfully and ecologically friendly method of cleansing of environment is a phytoremediation – selection and purposeful planting of those plants, which roots provide to uptake and enzymes to transform the molecules of toxicants from environment [1].

Phytoremediation in comparison with other nonbiological and biological technologies has great advantages. Nowadays is very actually to use complex approaches, which provides effectiveness and successful of remediation technologies [2, 3].

The goal of the presented work is to elaborate the new technological approach of phytoremediation for soils polluted with petroleum hydrocarbons (crude oil and wax), based on application different tools for improving of this technology: 1) detoxification abilities of microorganisms; 2) plants with high assimilation ability; 3) natural biosurfactant for enhancing long chain hydrocarbons assimilation by plants; 4) natural sorbents for avoid deep contamination of oil. Attention have been paid to enhancement of soil fertility, which improves microorganism and plant growth conditions and is important for bioremediation processes providing soil total rehabilitation.

MATERIALS AND METHODS

Microorganisms

Microorganisms of different taxonomic groups have been screened on solid and liquid areas contained crude oil and wax. Microorganism collection cultures of Durmishidze Institute of Biochemistry and Biotechnology as well as strains freshly isolated from polluted soils have been tested. After incubation in cultivation area the concentration of residual pollutants have been estimated due to the gravimetric, chromatographic and spectrophotometric methods. The criteria of strains selection at screening have been: 1) colony production ability; 2) biomass accumulation potential; 3) pollutants degradation ability; 4) ability to use carbon atoms of toxic compounds as the only carbon source.

Plants

The following plant species were tested as vegetation to be used for purposeful planting during our investigation: alfalfa (*Medicago sativa*) and soybean (*Glycine max*). The plants were cultivated by the hydroponic method, on the running water [4].

Determination of total petroleum hydrocarbons

For analysis of total petroleum hydrocarbons (TPH) content in samples have been measured by Soxhlet extraction and gas chromatography with electron capture (ECD) and flame ionization (FID) detection [5,6].

Investigation of sorbents

Standard methods were applied to define physic-chemical features (volumetric weight, porosity, displacement, filtration characteristics, oil absorption potential, absorption dependence on temperature, pH, etc) of rocks [7].

RESULTS AND DISCUSSIONS

Absorption ability of minerals: Bentonite and Zeolite and their composites for oil were studied. In composites ratio of minerals was the following: oil – B/Z in ratio 2/3. Application of mineral composites is important in case of all types of contamination, as, on the one hand, it is significant from the viewpoint of prevention, and, on the other hand, it creates favorable conditions for growth of vegetation. After introduction of the composites into the upper part of the soil and as a result of subsequent watering, the composites become swollen and stimulate growth and development of vegetation at the corresponding stage of phytoremediation.

As a result of screening 20 strains of bacteria are selected according to their abilities to effectively assimilate oil hydrocarbons at their growth on media containing crude oil or separate individual hydrocarbons (alkanes: C_6H_{14}, C_8H_{18}, $C_{11}H_{24}$, $C_{13}H_{28}$, $C_{14}H_{30}$, $C_{15}H_{32}$ and $C_{16}H_{34}$, arenes: benzene and toluene). The capability of selected strains and their consortia to utilize oil hydrocarbons was determined by their submerge cultivation in nutrient media with crude oil (3%) as the sole source of carbon. Most efficient combination of bacterial cultures is the consortium consisted with *Pseudomonas* and *Rhodococcus* strains. Using of bacterial consortia for bioremediation of soil contaminated by oil hydrocarbons and wax has been tested.

Model experiments. In field experiment the soil polluted as a result of the accidental spill near of Baku-Supsa oil pipeline were used. In these samples were added different amounts of wax. The joint action of plant-microbial consortium for phytoremediation of soils polluted with oil hydrocarbons has been studied in model experiments. Four plant species (alfalfa, maize, ryegrass and soybean) together with bacterial consortium (Rhodococcus sp. MO227, Pseudomonas sp. TP 335) were tested on soils contaminated by oil hydrocarbons with long chains (C_{30}-C_{60}). In tested variants the levels of soil contamination with TPH were equal from 43 000 to 117 000 ppm. Initially, suspension of microorganisms was inoculated in soils. Plant seeds were sowed after 30-35 days of bacteria introduction. Periodically soil samples were analyzed on TPH content (Fig.1 and 2).

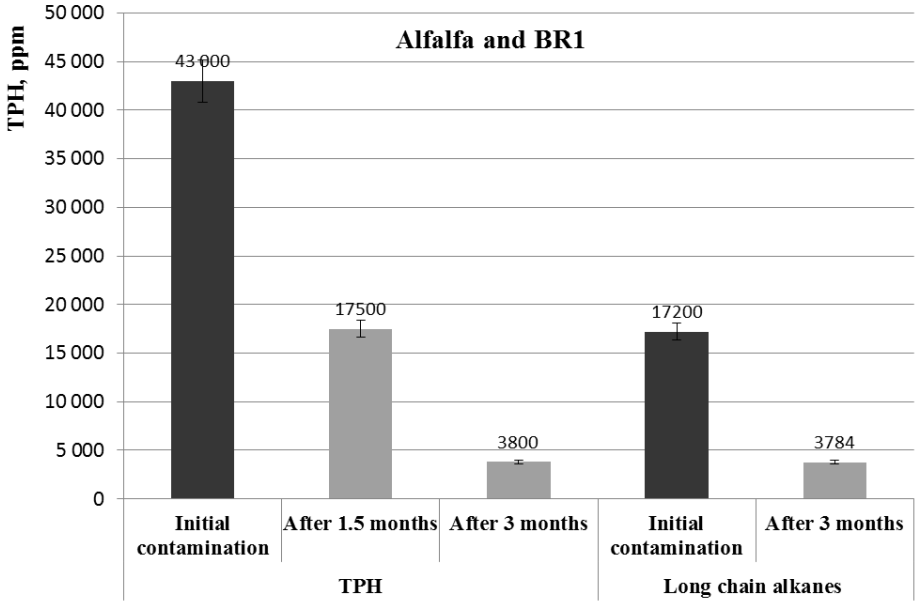

Fig. 1. Model experiment #1: Phytoremediation of soil artificially contaminated with crude oil and wax by using of alfalfa, bacterial consortium (*Rhodococcus* sp. 50 + *Pseudomonas* sp. 6R67) and preparation of BR1 (complex of biosurfactants produced by strain of Rhodococcus sp. 50, concentration – 0.01%). Initial contamination of soil by TPH - 43 000 ppm, by long chain alkanes of wax – 17 200 ppm; duration of experiment – 3 months

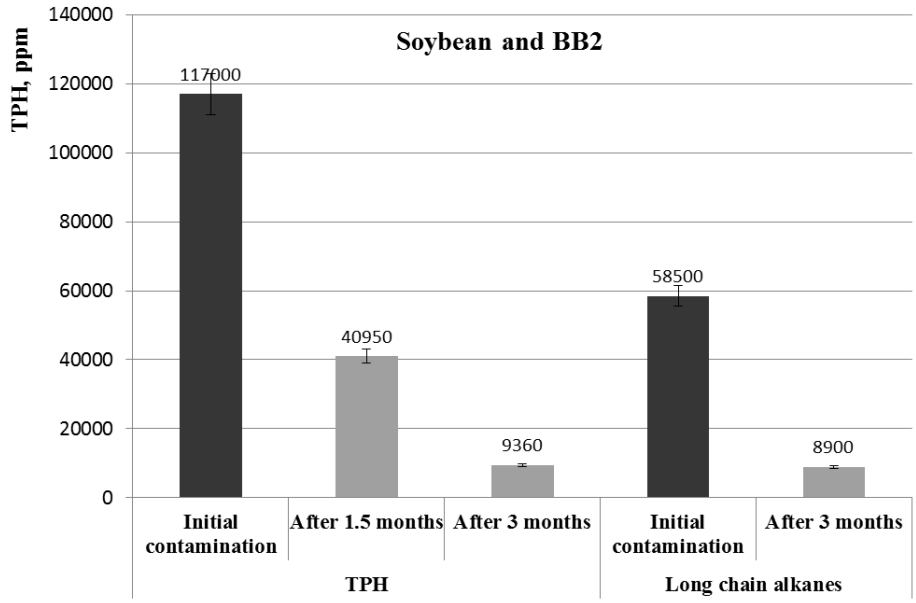

Fig. 2. Model experiment #2: Phytoremediation of soil artificially contaminated with crude oil and wax by using of soybean, bacterial consortium (*Pseudomonas* sp. 6R67 + *Bacillus* spp.) and preparation of BB2 (complex of biosurfactants produced by strain of Baccilus spp., concentration – 0.01%). Initial contamination of soil by TPH was 117 000 ppm, by long chain alkanes of wax – 58 500 ppm; duration of experiment – 3 months

The effect of soil cleaning by presented technology equal 78-92% by **model experiment # 1** and 85-92% by **model experiment #2.** It has been established that soybean and alfalfa together with selected bacterial consortium and natural biosurfactant are the best tools for phytoremediation of soils, polluted with oil hydrocarbons. Bacterial consortium consisting *Rhodococcus* sp. MO227 and *Pseudomonas* sp. TP 335 is best remediation agents among tested microorganisms.

The chromatographic analysis of soil samples (initial contamination – 43 000 ppm of TPH; contaminated soil is treated by bacterial consortium (Rhodococcus sp. MO227 and Pseudomonas sp. TP 335). Duration of remediation: 2 months) show that in case of 43 000 ppm initial contamination in the beginning of remediation the ratio between "light" and "heavy" petroleum hydrocarbons ($C_{8\text{-}15} : C_{16\text{-}35}$) decreased from 87 : 13 to 6 : 94. These results indicate that the assimilation of $C_{8\text{-}15}$ hydrocarbons take place mostly during bioremediation, than phytoremediation.

Periodically, in model experiment the content of microorganisms was controlled. In period of bioremediation (120 day) bacterial content in soil was decreased. It has been supposed that for efficiency of bioremediation process the maintenance of normal level of mineral nutrients – NPK in soil is required.

CONCLUSION

Bacterial consortium consisted with *Rhodococcus* sp. MO227 and *Pseudomonas* sp. TP335 appeared to be the best remediation agent among tested microorganisms and their consortia. In soils contaminated as a result of oil pipeline spills (levels of contamination: from 43 000 to 117 000 ppm) after treatment by this consortium the contamination is decreased by 78-92 %. The assimilation of $C_{8\text{-}15}$ hydrocarbons takes place mostly during bioremediation. It has been established that soybean and alfalfa together with selected bacterial consortium and natural biosurfactant are the best tools for phytoremediation of soils, polluted with oil hydrocarbons.

ACKNOWLEDGMENTS

This work was supported by STCU Partner Project # P499. In addition, Lawrence Livermore National Laboratory is operated by Lawrence Livermore National Security, LLC, for the U.S. Department of Energy, National Nuclear Security Administration under Contract DE-AC52-07NA27344.

ლიტერატურა - REFERENCES – ЛИТЕРАТУРА

1. Salt DE, Blaylock M, Nanda Kumar PBA, Dushenkov VP, Ensley BD, Chet I, Raskin I. Phytoremediation: a novel strategy for the environment using plants. *Biotechnology*, 1998, 13, 468-474.
2. Tsao DT. Phytoremediation. Advances in Biochemical Engineering and Biotechnology. *Berlin Heidelberg New York, Springe*. 2003.
3. Schnoor Dee. Phytoremediation. Technology Evaluation Report TE-98-01. *Ground-Water Remediation Technologies Analysis Center. Ser E. Iowa City*. 1997.
4. Kvesitadze G, Khatisashvili G, Sadunishvili T, Ramsden JJ. Biochemical Mechanisms of Detoxification in Higher Plants. Basis of Phytoremediation. *Berlin Heidelberg New York, Springer*. 2006.
5. Semivolatile organic compounds in soils and solid wastes using thermal extraction/gas chromatography/mass spectrometry. *US EPA Method 3540C Soxhlet Extraction; Method 8572A.* 1996.
6. Characterization of C6-C35 petroleum hydrocarbons in environmental samples. *TNRCC method 1006.* 2000.
7. Fomin GS, Fomin AG. Soil. Control of quantity and ecological safety according to international standards. *Moscow. BNII Standard*. 2001.

ახალი მიდგომები ქიმიურად დაბინძურებული ნიადაგების სარეაბილიტაციოდ

მ.ყურაშვილი, თ.ვარაზი, მ.ფრუიძე, გ.ადამია, ნ.გაგელიძე,
თ.ანანიაშვილი, მ.გორდეზიანი, გ.ხატისაშვილი
საქართველოს აგრარული უნივერსიტეტი, დურმიშიძის ბიოქიმიისა და ბიოტექნოლოგიის ინსტიტუტი, დავით აღმაშენებლის ხეივანი 240, თბილისი, 0159, საქართველო, m.kurashvili@agruni.edu.ge

რეზიუმე

წარმოდგენილი სამუშაოს ძირითად იდეას და სიახლეს შეადგენს ახალი მიდგომების შემუშავება ქიმიურად დაბინძურებული ნიადაგების სარეაბილიტაციოდ. მიდგომა ეფუძნება ბუნებრივი წიაღისეულის კომპოზიტების, რომელიც შედგება ნატურალური მინერალური ქანებისგან, ბუნებრივი ბიოსურფაქტანტების, მაღალი დეტოქსიკაციური უნარის მქონე მიკროორგანიზმთა შტამებისა და მცენარე-ფიტორემედიატორების ერთობლივ გამოყენებას. დადგენილია, რომ სოიას და იონჯას გამოყენება შერჩეული მიკროორგანიზმების კონსორციუმთან და ბუნებრივ ბიოსურფაქტანტებთან ერთად მეტად ეფექტურია ნავთობით დაბინძურებული ნიადაგების ფიტორემედიაციისათვის.

НОВЫЕ ПОДХОДЫ ДЛЯ РЕАБИЛИТАЦИИ ХИМИЧЕСКИ ЗАГРЯЗНЕННЫХ ПОЧВ

М.Курашвили, Т.Варази, М.Пруидзе, Г.Адамиа, Н.Гагелидзе, Т.Ананиашвили, М.Гордезиани, Г.Хатисашвили
Аграрный Университет Грузии, Институт Биохимии и Биотехнологии им. Дурмишидзе, Аллея Д. Агмашенебели 240,Тбилиси, 0159, Грузия, m.kurashvili@agruni.edu.ge

РЕЗЮМЕ

Основная идея и новизна представленной работы – разработка новых подходов для реабилитации химически загрязненных почв. Разработанный подход основан на использовании природных минералов композитов, природных биосурфактантов, штаммов микроорганизмов, обладающих высокой детоксикационной способностью и растений – фиторемедиаторов. Установлено, что использование растений – сои и люцерны, вместе с выбранным бактериальным консорциумом и природными биосурфактантами является очень эффективным инструментом для фиторемедиации почв, загрязненных нефтяными углеводородами.

NUMERICAL SIMULATION OF DISTRIBUTION OF ARSENIC DISCHARGES INTO THE TSKHENISTSKALI AND LUKHUNI RIVERS FROM INDUSTRIAL WASTES

Aleksandre Surmava, Leila Gverdtsiteli*, Nino Bagrationi*
M. Nodia Institute of Geophysics of the I. Javakhishvili Tbilisi State University,
**Georgian Technical University;*
aasurmava@yahoo.com

Numerical simulation of distribution of arsenic discharged into the Tskhenistskali and Lukhuni Rivers will be executed by using non–stationary linear three-dimensional equation of transition-diffusion of substances in continuous medium. Model is intended for the study of distribution of polluting agents in mountain rivers in the first approximation. Distribution of arsenic thrown into those rivers near the Uravi and Koruldashi villages is modeled using numerical experiments in case of stationary sources.

Introduction

The Tskhenitskali River and the Lukhuni (inflow of the R. Rioni) Rivers have an important role in the economy of the Georgian Republics. They are the sources of the drinking water and are intensively used for agricultural and industrial purposes. In the bank of these rivers are located at old abandoned arsenic warehouses, those cause a pollution of waters of those rivers. Therefore, they are the water objects of high ecological risk factor. .

The developed countries widely use the software packages for investigation of surface water pollution and the optimal control systems [1-4]. These packages are mainly elaborated for large water bodies, require a special personnel training and are difficult for the use in case of mountains rivers.

According to [4], in [5], a simple numerical method for calculation of diffusion of passive admixtures to Kura River was elaborated. In the presented work use model [5], is investigated a kinematics of propagation of contaminant in the Tskhenitskali and Lukhuni Rivers.

Formulation of the Problem

For numerical modeling of the pollution distribution the upper parts of the Tskhenitskali and Lukhuni Rivers are divided into 8 and 6 hydrological conventionally uniform sections, accordingly. It is assumed that each of the river's section is a linear canal and river's hydrological parameters are constant along it. Therefore, in this sections the distribution of pollution may be described by transfer-diffusion equation according to [4, 8]

$$\frac{\partial C_i}{\partial t} + u_i \frac{\partial C_i}{\partial x} + w_o \frac{\partial C_i}{\partial z} = \mu_x \frac{\partial^2 C_i}{\partial x^2} + \mu_y \frac{\partial^2 C_i}{\partial y^2} + \mu_z \frac{\partial^2 C_i}{\partial z^2} \qquad (1)$$

where t is time; x, y, and z are the Cartesian coordinates; x axis is horizontally directed along the river flow; y is the horizontal axis directed perpendicularly to the canal; z axis is directed upward vertically from river bottom; u_i is the river's flow velocity at i section along x axis; river flow velocity is equal to zero along y axis; w_o is the velocity of sedimentation of polluting agent; μ_x, μ_y and μ_z are kinematic coefficients of turbulent viscosity along the x, y and z axes, respectively; C_i is the concentration of the contaminant in the i section of river.

The river water velocity u_i in each river section is known, which is constant value along the axis x, and changes along the y and z axes as follows: $u_i(x,y,z) = 1.5U_{i,0} * \sin(\pi y/Y_i)\sin(0.5\pi z/H_i)$. $U_{i,0}$=const is the known value of the river water velocity in the i section. Y_i and H_i are the width and depth of the section i. $U_{i,0}$, Yi, Hi are taken from [6]. Since the values of coefficient of turbulent diffusion for Tskhenitskali and Lukhuni Rivers were not determined on the basis of observation data, we used the values given in [7] as follows: $\mu_x = 5\times 6.4\times 10^{-4}$ m^2/s and $\mu_y = \mu_z = 5\times 5{,}57\times 10^{-3}$ m^2/s for territory with complex mountain relief.

For integrating of equation (1) the corresponding initial and boundary conditions are used: the concentrations of the contaminant in the points of discharge source and at the initial time are known values. The gradient of concentration in the end points of sections $x_i = K_i$, in the river bank, surface and bed

points y_i = 0, 10 and z_i = 0,10 are equal to zero, respectively. The concentrations of the contaminant during the whole interval of time of spilling at the source points are known values. An inflow of tributaries into the rivers are taken into account using change in the parameters $U_{i,0}$, Y_I and H_i.

The numerical integration and solution of equation (1) is made using the split method and balance numerical scheme [8] on the rectangle numerical grid. The grid step along the x axis is equal to 50 m., the grid steps along y and z axes are equal to Yi /11 and Hi /11, respectively.

Results of simulation

For investigation of kinematics of contaminants' propagation in the Tskhenistskali River the series of numerical experiment were conducted. First, were considered the case when the contaminant is discharged into Tskhenistskali River in the points located near village Korundashi. The concentration of the arsenic is equal to 0.006 mg/l in the area of the pollution source during all modeling time. Calculation shows that during the first 6 hours is established quasi-static distribution of the arsenic concentration. In the Fig. 1 the spatial distribution of arsenic Concentration is show. It is shown the concentration is maximal in the areas in vicinity of the two sources of discharge (0,005 mg/l and 0.011 mg/l). The concentration decreases along the river step-by-step in the transition from one section of river to another due to the dilution in the waters of the influx of small rivers and sedimentation. In the result the concentration of the arsenic at the end of 35.6 km section of Tskhenistskali River becomes equal to 0 0.0001mg/l.

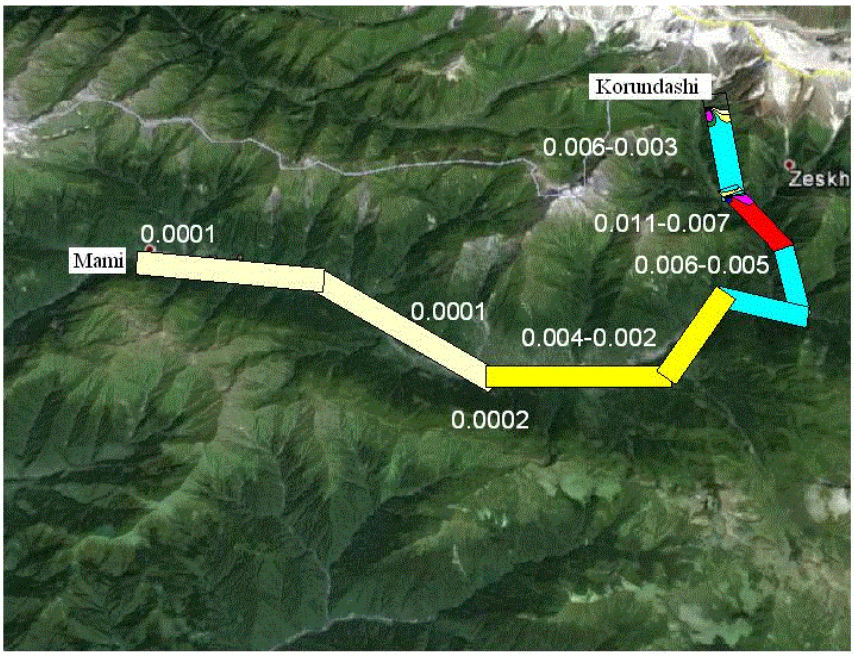

Fig. 1. A distribution of the arsenic concentration (mg/l) in the Tskhenistskali River from Korundashi till Mami

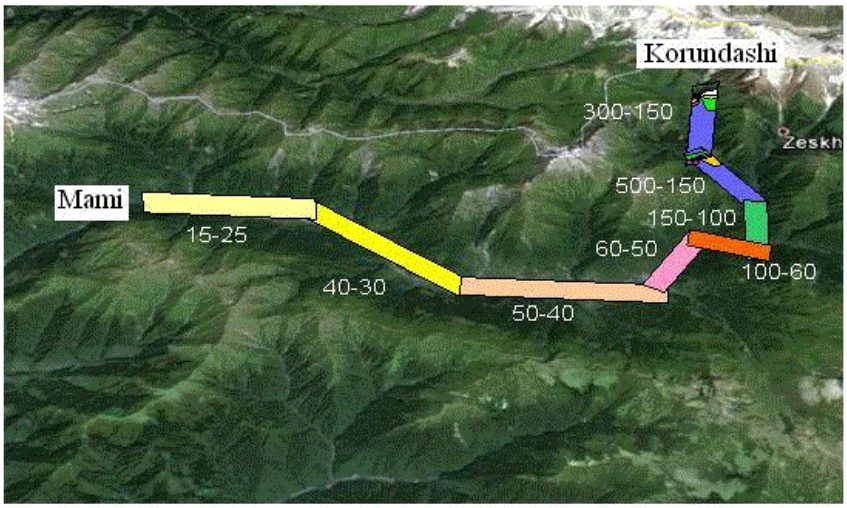

Fig. 2. A distribution of the sediment arsenic surface density (mg/m ^{2}) in the Tskhenistskali from Korundashi till Mami.

In Fig. 2 The distribution of the surface density of the sediment arsenic on the bottom of the river Tskhenistskali during 30 days is showy. By this figure, it is possible to conclude the spatial distribution of the surface density of the sediment arsenic is quality analogical to distribution of the volumetric concentration: the surface density is maximal in two areas in vicinity of of discharge points and gradually decreases along the river flow.

Fig. 3 Shows the arsenic concentration obtained by numerical simulation gradually decreasec from Uravi to Ambrolauri. The maximum concentration 0.011 mg/l is obtained in two points in vicinity of Uravi Village and decreases with removal of these. The rapid decrease of concentration takes place in vicinity of the points of discharge. The area of rapidly decreasing concentration is about 100 m.

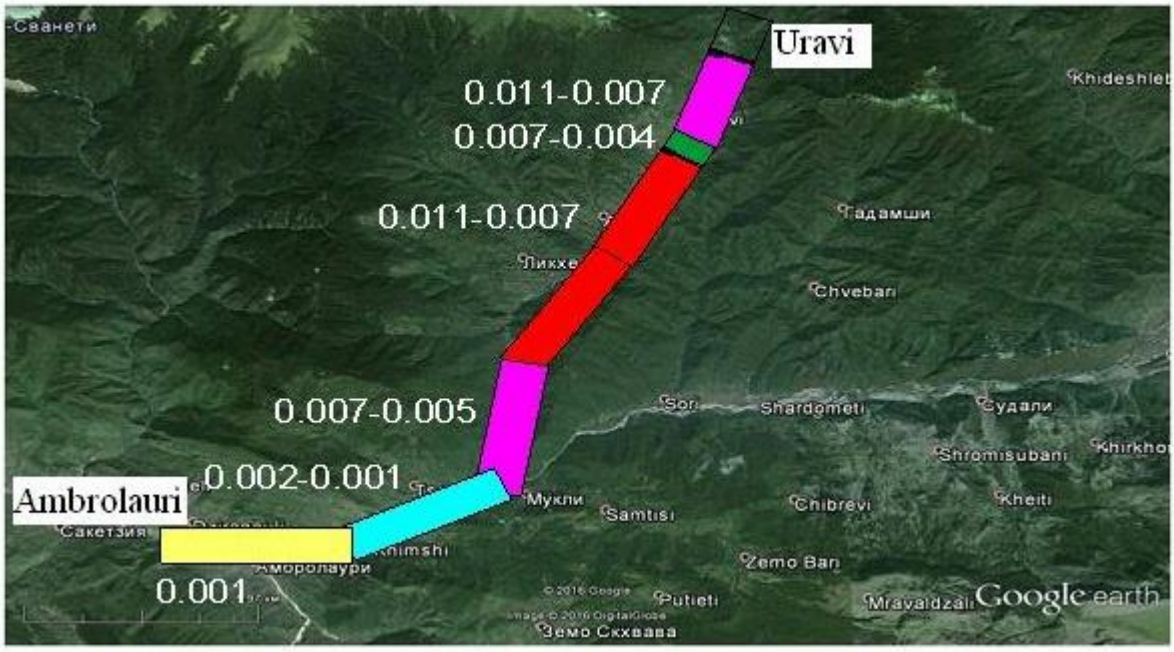

Fig. 3. Distribution of the arsenic concentration (mg/l) in the Lukhuni River from Uravi till Ambrolauri

Discussion.

On the basis of nonstationary three-dimensional equation of mass transfer the numerical model of transfer of carsenic through Tskhenistskali River and Lukhuni River is elaborated. The model is created for the sections of 35,6 km and 23 km length of Tskhenistskali River and Lukhuni, accordingly. The numerical experiments that investigate the kinematic features of distribution of pollution are carried out. Some parameters characterizing the process of pollutants diffusion are obtained by means of these experiments, namely: times necessary for passing separate sections by contaminant and times establishedquasi-static distribution of arsenic.

It should be noted that calculations are carried out for average annual river flow velocity. This fact limits the area of application of this model because the velocity of water flow for mountain rivers may change in wide area in relation with the precipitations taking place in the basin of the separate tributaries. Such limitation can be overcame by two ways: first, for each section the velocity of flow can be calculated using the equation of river water momentum, or second – by database for velocities of flow observed in different situations must be created by means of hydrological observation and these data must be used in equation (1). It is necessary also to obtain semi-empirical formulas for kinematic coefficients of vertical and horizontal turbulence of mountain rivers and to conduct numerical simulation with the using of them.

ლიტერატურა - REFERENCES – ЛИТЕРАТУРА

1. Loucks D. P. and.Van Beek E. Water resources systems planning and management: an introduction to methods, models and applications. 2005, 690 . http://hydrologie.org./BIB/Publ_UNESCO/SR_999_E_2005.pdf.

2. Hatterman F. F. and Kundzewicz Z. (Eds) Water framework directive: model supported implementation. A water manager's guide. IVVA Publishing London, 2010, 268.
3. Pryazhinskaya V. G., Yaroshevsky V. G., Levit-Gurevich L. K. Kompiuternoe modelirovanie v upravlenii vodhimi resursami , Moskva, Fizmatlit, 2002, 496. (in Russian).
4. P. Yu. Pushistov, V. N. Danchev Informatsionno-vichislitelnie kompleksi vodnix obiektov basseina Obi. Chast 1- IVK ,,Severnaia Sosva", Chast 2-IVK ,,Teletskoe Ozero", LAP LAMBERT Academic Publishing. 2013, 160.
5. Surmava A., Intskirveli L., Buachidze N. Numerical Simulation of Distribution of Contaminants Discharged to Kura River. Bulletin of the Georgian National Academy of Sciences, 9, No. 1, 2015, 78-83. http://www.logobook.ru/prod_show.php?object_uid=12563275 (in Russian).
6. Tsomaia V. Sh. (Ed). Resursi poverxnostnikh vod SSSR, t. 9, Zakavkazie I Dagestan. Leningrad. 1974, 579. (in Russian).
7. Socolofsky S. A,. Gerhard H. J. CVEN 489-501: Special topics in mixing and transport in the environment, Texas A&M University, 2005, 184. https://ceprofs.civil.tamu.edu/ssocolofsky/cven489/downloads/book/ch3.pdf
8. G. I. Marchuk (1982), Matematicheskoe modelirovanie v probleme okrughaiei sredi , Moskva, Nauka, 316 p. (in Russian).

მდინარეებში ცხენისწყალი და ლუხუნი სამრეწველო ნარჩენებიდან ჩაღვრილი დარიშხანის გავრცელების რიცხვითი მოდელირება

ალექსანდრე სურმავა, ლეილა გვერდწითელი*, ნინო ბაგრატიონი*
ი.ჯავახიშვილის სახელობის თბილისის სახელმწიფო უნივერსიტეტის მ. ნოდიას სახ. გეოფიზიკის ინსტიტუტი; საქართველოს ტექნიკური უნივერსიტეტის ჰიდრომეტეოროლოგიის ინსტიტუტი
*საქართველოს ტექნიკური უნივერსიტეტი
aasurmava@yahoo.com

რეზიუმე

უწყვეტ გარემოში ნივთიერების გადატანა-დიფუზიის წრფივი სამგანზომილებიანი განტოლების რიცხვითი ინტეგრირებით მოდელირებულია მდ. ცხენისწყალში და მდ. ლუხუნში ჩაღვრილი დარიშხანის გავრცელება. შესწავლილია სოფ. ურავისა და სოფ. კორუნდაშის მიდამოებში ჩაღვრილი დარიშხანის გავრცელება.

ЧИСЛЕННОЕ МОДЕЛИРОВАНИЕ РАСПРОСТРАНЕНИЯ СБРОШЕННОГО ИЗ ПРОМЫШЛЕННЫХ ОТХОДОВ МЫШЬЯКА В РЕКАХ ЦХЕНИСЦКАЛИ И ЛУХУНИ

Александре Сурмава, Леила Гвердцители*, Нино Багратиони*
Институт геофизики им. М. З. Нодиа Тбилисского государственного университета; Институт гидрометеорологии Технического университета Грузии
**Технический университет Грузии.*
aasurmava@yahoo.com

РЕЗЮМЕ

С помощью численного интегрирования линейного трёхмерного уравнения переноса и диффузии вещества в сплошной среде моделировано распространение сброшенного из промышленных отходов мышьяка в реках Цхенисцкали и Лухуни. Изучен перенос мышьяка, сброшенного в окрестностях сёл Урави и Корундаши.

STUDYING THE CONTAMINATION WITH HEAVY METALS AND THE TOXICITY LEVEL OF ARABLE LANDS IN THE INDUSTRIAL REGION OF GEORGIA BOLNISI-KAZRETI USING MODERN TEST METHODS

Rus.Gigauri, Sh.Japaridze, N.Gigauri, T.Gogiberidze

R.Agladze Institute of Inorganic Chemistry and Electrochemistry of Ivane Javakhishvili Tbilisi State University, 0186, Mindeli st.11, Tbilisi, Georgia
gigaurirusudan@gmail.com

The arable lands of Georgia's Kvemo Kartli industrial region Bolnisi-Kazreti (Madneuli Copper and Gold Mine), which are generally irrigated by the River Mashavera, have been studied. The waste water of the above-mentioned mine is discharged into the lands. In spite of the fact that the enterprise is engaged in the water treatment, an average level of contamination with heavy metals is still being observed. Copper tenfold exceeding the MCL is dominant. The constantly accumulating and soluble forms of heavy metals are fixed in soil by the TCLP and WET standard methods. The soil non-irrigation (spring) and intensive irrigation (summer) periods have been studied and compared. The spectral and atomic absorption analysis methods have been used in the study. The currently established ecological monitoring system will, hopefully, further improve the existing situation.

A consumer approach to and improper use of soils contributed to the further worsening of the situation. Almost all Georgian soils are known for a deficiency of a balance of nutrient elements that is so required by plants. Humus, or the general internal structure, is the soil fertility indicator. Our scientists have studied the soil fertility rate (nutrient elements-nitrogen-phosphorus, potassium) in the regions of Georgia. It has been found that poor soils constitute 50% of the total cropland. A subject of global research is the regulation of the cycle of nutrient elements and humus in the soil, study of the preservation and recovery of their contents.The enhancement of the composition indicators of the nutrient areas of soil microorganisms, or nutrient elements is possible with due regard for the relief and scheduled yield [1, 2].

Fig. 1. River Mashavera

Our aim was to determine the contamination with heavy metals and the toxicity level, solubility, valence and acidity of Bolnisi-Kazreti arable lands, their forms and prevalence.These regions of Kvemo Kartli (Bolnisi-Kazreti) have been under emergency conditions for years as one of the industrial regions. A particular example is the Madneuli Copper-Gold Mine, the waste water of which is discharged into the River Mashavera. Another source of contamination is the irrigation system of the River Mashavera, the only source of water supply to the Kvemo Kartli croplands. The soil samples were taken in the spring and autumn, i.e. before and after the irrigation. The maximum allowable concentrations (MAC) of heavy metals in soil are given below as a table.

Table 1. Maximum allowable concentrations of heavy metals in arable lands

	Si	**Al**	**Fe**	**Mn**	**Ni**	**Ti**	**Cu**	**Pb**	**Zn**	**Cd**	**Sn**	**Sb**	**Ag**
MAC	75	8.8	8.0	0.1	-3 5.8-10	0.57	-3 4.7-10	-3 1.6-10	-2 8.3-10	-5 1.3-10	-4 2.5-10	-5 5-10	-6 7-10

At the initial stage, the soil samples under study were subjected to the quantitative spectral analysis for the content of heavy metals. The concentrations of heavy metals were foundto be increased. Below given are the results of the quantitative spectral analysis:

Table 2. Results of the quantitative spectral analysis of soil for percentage of heavy metals before and after irrigation

	#	Si	Al	Fe	Cu	Zn	Pb	Mn	Ti	Ni	Cd	Sb	Au
Soil samples taken in v. Natevani before irrigation	1	70	12	7.0	0.05	0.01	0.001	0.1	1.2	0.02	–	–	–
	3	70	12	7.0	0.10	0.01	0.001	0.14	1.2	0.02	–	–	–
Soil samples taken in v. Natevani after irrigation	1	72	12.5	8	0.10	0.02	0.001	0.1	1.5	0.02	–	–	–
	2	72	12.5	8	0.15	0.02	0.001	0.15	1.3	0.02	–	–	–

If we compare the given data with one another, we shall see that in case the irrigation system of Mashavera River is used, the concentrations of heavy metals are increased. The dominant element - copper - has been distinguished, which is one of the toxic for soil elements. MAC of the following elements is exceeded: Cu-10-20-fold, Al- 1,5-fold, Ni- 3,5-fold, Zn- 1,5-fold, andTi- 2,0-fold. The studies continued to identify the movable or soluble forms in soil, using the test methods (TCLP and WET standards), which implies the heavy metals leaching procedure under conditions of constant mixing with a magnet mixer[3]. The leached solutions were subject to the spectral and atomic absorption analysis. It has been found that heavy metals in the process water are in soluble sulphate forms. When in soil, their solubility is low, which should be caused by the high concentration of calcium. About 80-90% of constantly accumulating heavy metals remain in soil [4].No less dangereous is the constantly accumulating in soil the quantity of heavy metals, which finally leads to the contamination and infertility of soil.

ლიტერატურა - REFERENCES – ЛИТЕРАТУРА

1. I.Tsomaia. Soils and Ecology of Georgia, 2010.
2. T.Urushadze.Agroecology, 2001.
3. EPAtest method 1311- TCLP. Toxicity characteristic leaching procedure 2002.
4. Rus.Gigauri, Sh. Japaridze, T. Gogiberidze, N. Khavtasi The Study of the Toxicity Level of Soils Contaminated with Arsenic in Racha and Svaneti. Annals of Agrarian Science, vol.12, #2,pp.42-44, 2014.

საქართველოს სამრეწველო რეგიონის ბოლნისი-კაზრეთის სახნავ-სათესი ნიადაგების მძიმე მეტალებით დაბინძურების და ტოქსიკურუბის ხარისხის შესწავლა თანამედროვე ტესტმეთოდების გამოყენებით

რუს. გიგაური, შ. ჯაფარიძე, ნ. გიგაური, თ. გოგიბერიძე

ივანე ჯავახიშვილის სახელობის თბილისის სახელმწიფო უნივერსიტეტის რ.აგლაძის არაორგანული ქიმიისა და ელექტროქიმიის ინსტიტუტი, 0186, მინდელის ქ.11, თბილისი, საქართველო

რეზიუმე

საქართველოს სამრეწველო რეგიონის ბოლნისი-კაზრეთის სახნავ-სათეს ნიადაგებში შესწავლილია მძიმე მეტალებით დაბინძურების და ტოქსიკურობის ხარისხი. TCLP და WET სტანდარტების მიხედვით, გამოტუტვის პროცედურამ აჩვენა, რომ მძიმე მეტალები ნიადაგში იმყოფება მცირედ ხსნად ფორმაში. (2-10%). საშუალო ტოქსიკურობის ხარისხითა და გავრცელების არეალით. ნიადაგებში მძიმე მეტალების შემცველობები ბევრად აღემატება ზდკ. დადგენილია, რომ საირიგაციო სისტემების გამოყენების შემდეგ კიდევ უფრო იზრდება მეტელების შემცველობები. ნიადაგში მუდმივად აკუმულირებული რჩება (80-90%).

ИЗУЧЕНИЕ ЗАГРЯЗНЕННОСТИ ТЯЖЕЛЫМИ МЕТАЛЛАМИ И СТЕПЕНИ ТОКСИЧНОСТИ ПАХОТНО-ПОСЕВНЫХ ПОЧВ БОЛНИСИ-КАЗРЕТСКОГО РАЙОНА ГРУЗИИ СОГЛАСНО СТАНДАРТНЫМ ТЕСТАМ

Р. Гигаури, Ш. Джапаридзе, Н. Гигаури, Т. Гогиберидзе

Институт неорганической химии и электрохимии им. Р.И.Агладзе Тбилисского государственного университета им. И.Джавахишвили, 0186, ул. Миндели11, Тбилиси, Грузия

РЕЗЮМЕ

В промышленном Болниси-Казретском регионе Грузии, при помощи стандартных тестов TCLP и WET, был изучен уровень загрязненности пахотно-посевных почв тяжелыми металлами и их токсичности. Процедуры выщелачивания показали, что тяжелые маталлы в почве находятся в растворимой форме (2-10%) и отличаются средней токсичностью и средним уровнем распространения. Концентрация тяжелых металлов в почве во многом превышает ПДК. Установлено, что после использования ирригационных систем концентрация тяжелых металлов возрастает еще больше. Около 80-90% тяжелых металлов постоянно аккумулируются в этих почвах.

CHEMICAL COMPOSITION OF MINERAL WATER ASHARI OF VILLAGE BABILI, LENTEKHI DISTRICT

Manuchar Chikovani, Mariam Kurasbediani

A.Tsereteli Kutaisi State University
Kutaisi, Georgia, e-mail: atsu@atsu.edu.ge

Concentration of ions in the mineral water of village Babili, Lentekhi District, was determined by use of various methods, namely complexonometric titration for Ca^{2+} and Mg^{2+}, mercurometric titration and acidometric method for Cl^- and HCO_3^-, Reznikov's method for I^-. Concentrations of biogenic substances were determined by means of photometric analysis: Nessler's reagent was used for determination of NH_4^+, Griess reagent for NO_2^-, diphenylamine for NO_3^-, ammonium phosphomolybdate for PO_4^{3-}. No biogenic substances were discovered in the selected water samples. Concentration of dissolved oxygen was determined by iodometric titration. Total concentration of organic substances was determined by the method of permanganometry (oxidation-reduction titrations). The concentration of abovementioned ions is within a normal range and the water can safely be used for human consumption.

Humans strived for perceiving the nature of mineral water scince ancient times. Production of natural mineral waters is one of the most leading sectors of Georgia's industry, which can significantly contribute to the development of the whole economy.

Lentekhi district is located in West Georgia, at the southern slopes of Central Caucasus, namely Svaneti Ridge, in the upper part of Tskhenistskali River basin. The district is distinguished with humid climate with cold winter and quite long cool summer. Mountainous relief is conditioned by ramification of neghbouring ridges. Lower areas represent river gorges, mainly characterized by mountanous subtropical and glacial relief. The northern border of the district passes by Main Caucasus (dividing) Ridge. Altitudional zonation is observed due to the mountanous relief of the district with humid and cold climate and abundant snowfalls in the highest altitudes.

The main river of Lentekhi District is Tskhenistkali, the head of which is located in the Main Caucasus Range. The floods are observed on springs and conditioned by melting of snow in mountains. Mainly mountain-meadow soils are observed in the area. Village Babili is located in Lentekhi Community (3 km. from Lentekhi) on the south slope of Svaneti Ridge, on the right bank of the river Tskhenistskali [1].

Water is an invaluable resource and always was considered as a source of life on the Earth. Today humans use the recourses of biosphere for development of production and building a welfare society. In its turn the technical progress gives rise to deep changes in biosphere, which may affect human health .

There is no chemically pure water in the nature. On the way through the earth's crust to the surface groundwater dissolves various substances. The natural water represents a solution, which contains the substances of various nature and condition. Hence, the study of natural waters requires knowledge of main characteristics of solutions.

Before using water for human consumption it needs to be deeply analyzed. In order to assess water quality it is necessary to determine its physical-mechanical properties and chemical composition, carry out organoleptic evaluation [2].

In order to study therapeutic activity of natural mineral waters and their influence on the human organisms first of all it is necessary to determine water characteristics. The main parameters are ionic and gas composition, temperature, and radioactivity. As soon as these parameters are known, it is necessary to determine the content of unique microcomponents in order to establish functional relationship between these microcomponents and other substances of mineral water. Mineral waters are formed deep underground and reach the surface due to hydrostatic or gas pressure.

One of the most important subjects is the stages of formation of mineral water. The same mineral water formed under influence of different environmental and natural processes may significantly vary in its chemical composition. The mineral waters formed deep underground and closer to the surface may differ in content of specific microcomponents. The high temperature of the mineral water may not be accepted as

a proof of formation in deeper earth layers as surface waters may as well infiltrate into ground and respectively the temperature of such water becomes much higher. Physical and chemical processes undergoing in the Earth's crust do noticeably change chemical composition of mineral waters. Namely these processes determine the difference in composition of various mineral waters [3].

The population of village Babili for drinking purposes consumes the Ashari mineral water and it is very important to determine its chemical content.

The aim of the study was to investigate hydrochemical characteristics of mineral water of village Babili, Lentekhi District, wich was carried out according to international standards.

The analysis was carried out at the Laboratory of Analytical Chemistry of the A. Tsereteli Kutaisi State University with the application of well-known and approved methods of hydrochemical analysis of groundwaters [4].

pH of the water samples was measured by use of potentiometric titration.

Concentration of chlorine ions was established by application of mercurometric titration (indicator diphenylcarbazone).

Content of bicarbonates was determined by use of acidimetry (indicator methyl-orange).

Concentration of calcium and magnesium ions and general hardness of water was determined by means of complexonometric titration. The impact of heavy metals was avoided by adding sodium sulfide.

Content of biogenic substances was established by application of photometric analysis: Nessler's reagent was used for determination of NH_4^+, Griess reagent for NO_2^-, diphenylamine for NO_3^-, ammonium phosphomolybdate for PO_4^{3-}. Reznikov's method was applied for determination of iodide ion I^- [5].

Total concentration of organic substances was determined by the application of permanganate and bichromatic oxidation. Concentration of dissolved oxygen was determined by means of iodometric titration.

Content of SO_4^{2-} ions in the water samples was determined by means of gravimetric analysis (sediment $BaSO_4$). The results of analysis are given in the Table 1.

Table 1. Concentration of some ions in the Ashari mineral water of village Babili, Lentekhi District

pH	Concentration of ions, mg/l											μg /l
	Oxidability	Dissolved oxygen	Mg^{2+}	Ca^{2+}	HCO_3^-	Cl^-	NO_2^-	NO_3^-	NH_4^+	PO_4^{3-}	SO_4^{2-}	I^-
5.6	1.92	0.98	17.25	3.45	19.96	0.73	-	-	-	-	0.0034	0.85

According to the results of analysis NO_2^-, NO_3^-, NH_4^+, PO_4^{3-} ions were not discovered in the water of village Babili. The concentration of the remaining ions was as follows: Mg^{2+} - 17.25 mg/l, Ca^{2+} - 3.45 mg/l, HCO_3^- - 19.96 mg/l, Cl^- - 0.73 mg/l, SO_4^{2-} - 0.0034 mg/l, I^- - 0.85 μg /l. Content of dissolved oxygen – 0.98 mg/l, oxidability – 1.92 mg/l. The concentration of abovementioned ions in water samples is within a normal range and the water can safely be used for human consumption.

ლიტერატურა - REFERENCES – ЛИТЕРАТУРА

1. Georgian Soviet Encyclopaedia. 1986, vol. 6, 189.
2. Bregvadze U., Natidze M., Mamulashvili Z. Chemistry and microbiology of water. Tbilisi. 1987, 5.
3. Eristavi D. Mineral water and its chemical analysis. Tbilisi. 1945, 14-25
4. Standard methods of water analysis. Moscow. 1973.
5. Reznikov A., Mulikovskaya E., Sokolov I. Methods of analysis of natural waters. M. 1970, 261.

ლენტეხის რაიონის სოფელ ბაბილის აშარის მინერალური წყლის ქიმიური შედგენილობის განსაზღვრა

მანუჩარ ჩიქოვანი, მარიამ ქურასბედიანი
ქუთაისის აკაკი წერეთლის სახელმწიფო უნივერსიტეტი
ქუთაისი, საქართველო, ელ-ფოსტა: atsu@atsu.edu.ge

რეზიუმე

ლენტეხის რაიონის სოფელ ბაბილის აშარის მინერალური წყალში ჩვენს მიერ პირველად იქნა განსაზღვრული ზოგიერთი იონები: მაგნიუმი და კალციუმი განსაზღვრული იქნა მარტივი და სწრაფი კარგი განმეორებადობის მქონე კომპლექსონომეტრული მეთოდით. ქლორიდების და ჰიდროკარბონატები შემცველობა დადგენილი იქნა მერკერომეტრული და აციდომეტრული მეთოდებით, იოდიდ-იონები განსაზღვრული იქნა რეზნიკოვის მეთოდით. ბიოგენური ნივთიერებების შემცველობა დადგენილ იქნა ფოტომეტრული მეთოდებით: NH_4^+ - ნესლერის რეაქტივით, NO_2^- - გრისის რეაქტივით, NO_3^- - დიფენილამინით, PO_4^{3-} – ამონიუმის ფოსფორმოლიბდატით. ჩვენს მიერ კვლევისათვის შერჩეულ აშარის მინერალურ წყალში ბიოგენური ელემენტები არ აღმოჩნდა. გახსნილი ჟანგბადი განსაზღვრულ იქნა იოდომეტრულად, ორგანული ნივთიერებების ქიმიური კონცენტრაცია დადგენილ იქნა პერმანგანატომეტრული და ბიქრომატული ჟანგვადობების მეთოდით, სულფატ-იონები გრავიმეტრული მეთოდებით. ზემოთ აღნიშნულ იონთა შემცველობა ნორმის ფარგლებშია და მისი გამოყენება სასმელად მიზანშეწონილია.

ОПРЕДЕЛЕНИЕ ХИМИЧЕСКОГО СОСТАВА МИНЕРАЛЬНОЙ ВОДЫ АШАРИ СЕЛА БАБИЛИ ЛЕНТЕХСКОГО РАЙОНА

М.Чиковани, М. Курасбедиани
Кутаисский Государственный Университет им. А. Церетели
Кутаиси, Грузия, эл-почта: atsu@atsu.edu.ge

РЕЗЮМЕ

Впервые была определена концентрация некоторых ионов в минеральной воде Ашари, села Бабили, Лентехского района. Содержание магния и кальция было определено с помощью простого и быстрого комплексонометрического анализа, отличающегося хорошей повторяемостью. Концентрацию хлоридов и гидрокарбонатов определили меркурометрическим и ацидометричеким методами анализа, иодид-ионов – методом Резникова. Содержание биогеных веществ определили фотометрическим методом анализа: для NH_4^+ использован реактив Несслера, для NO_2^- – реактив Грисса, для NO_3^- - дифениламин, для PO_4^{3-}– фосфомолибдат аммония. Во взятых пробах воды никаких биогенных элементов обнаружено не было. Концентрация растворенного кислорода была определена методом иодометрии, химическая концентрация органических веществ – методами перманганатного и бихроматного окисления, содержание сульфат-ионов – методом гравиметрии. Концентрация вышеперечисленных ионов находится в пределах нормы и минеральная вода может быть использована для питьевых нужд.

ANTIMICROBIAL METABOLITES OF ENDOPHYTIC YEAST FUNGI AFFECTING THE TASTE AND SPOILAGE OF WINES

Natia Barbakadze, Liparit Dolidze, Nino Kavtaradze, Tamar Dgebuadze, Maia Japaridze, Avtandyl Dolidze
Petre Melikishvili Institute of Physical and Organic Chemistry at Iv. Javakhishvili Tbilisi State University

Volatile phenols, which are related to the wine production and are responsible for the aroma of the wine, were early extracted from the yeast fungi. Lately it was proved that the yeast fungus Picchia Guilermondi that grows on the plant Paris Polyphylla var. yanasesis, is able to yield the same metabolites in the process of fermentation, which simultaneously lead to wine spoilage. Besides, antimicrobial activity of these metabolites has been confirmed, which is perspective with the view of their further application.

The biologically active substance "Paclitaxel" that was declared as the "gold" in the final decade of the last century (1993) was successfully extracted from the fungus *Taxomyces andreanae. Many* researchers devoted their researches to endophytic fungi and consequently many biologically active substances were extracted and investigated which were characterized by valuable antimicrobial, insecticidal, cytotoxical and anticancer activity. In its turn, endophyte fungi are fungal microorganisms, which along their whole life-cycle or its section form external- or inner-cellular colonies on parent-plant tissues not inciting plant diseases [1,2]. Lately endophytic fungus *Pichia guilliermondii* extracted from medicinal herb *Paris polyphylla var.yunnanen* has attracted specific attention. Metabolites of this yeast are widely used in wine-making and are known for their specific antimicrobial activity.

Paris polyphylla var.yunnanensis **(rhizoma)**

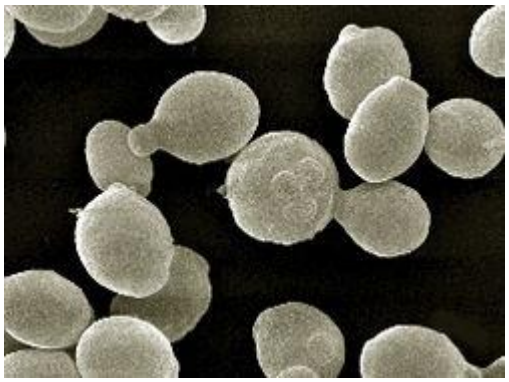

Pichia guilliermondii **under microscope**

The role of the endophytic fungus *Pichia guilliermondii* for wine taste improvement should be emphasized. In recent years wine is intensely considered in special scientific literature as a food product and while assessing its quality the greatest significance is attributed to biologically active substances – phenol compounds, organic acids, amino acids, aromas (congenital, fermentation or acquired), sugars

according to the contents of which the wine types are distinguished, carbon dioxide , which affects taste properties, proteins, which threaten wine with turbidity and destruct wine stability, various extracted substances, which are nonvolatile compounds and guarantee high quality of wine. Phenol compounds and the products of their transformation actively participate in the process of wine type formation at all stages of its making and storing and directly affect its taste, its flavor, color, transparency. While somewhat high content of phenol compounds is necessary and makes positive impact on the formation of taste qualities of fortified, dessert or some other types of wine, their excess concentration makes adverse effect on the quality of Champagne type wine materials, results in their oxidation and alters their taste.

At the initial stage of wine fermentation the yeast fungi, and in particular *Pichia guilliermondii* are capable to form volatile phenol compounds, which, as it was noted above, provide for wine taste properties. Yeast and bacterial biota metabolism somewhat change wine organoleptic properties at the fermentation, ageing and storing processes [4]. In their turn, volatile phenols are formed from the main components accompanying grape syrup, alpha cumarine, caffeine and ferulic acid. These acids can be metabolized at the impact of various microorganisms into 4-vinyl derivatives, which can be transformed into 4-ethyl derivatives by means of enzymes –hydroxycinnamate carboxylase and vinyl phenol reductase [6]. Hydroxycinnamate carboxylase is in great quantity in various yeasts and other microorganisms, while vinyl phenol reductase till present was associated only with the species *Dekkera bruxellensis* and *Dekkera anomala*. Currently activity of phenol reductase is also associated with the *Candida Versatilis, Candida fermentatic and Pichia guilliermonii* species. In distinct from *D.bruxellensis* ability of this variety to form volatile phenols in enologic conditions is scarcely studied. According to the available literature data phenol aroma is sharply felt in the new red wine, which is in immediate relation with high possibility of formation of *Pichia guilliermondii* colonies at the initial state, at spontaneous fermentation [7].

Besides, 3 steroids and 1 triterpenoid of antimicrobial activity have been obtained from *Pichia guilliermondii.* They belong to innovative source of natural significant biologically active substances for agriculture, medicine and food industry. Identity of biologically active substances isolated from endophytic fungi was determined by physical-chemical and spectrometric methods Helvolic acid revealed the highest antimicrobial activity towards wide spectrum of microorganisms, such as: *Bacillus subtilus, Escherichia coli, Helicobacter pylori, Pseudomonas vesicatoria)* as well as anti fungal activity to *Aternariabrassicae, Botrytis cinerea, Candida albicans, Colletotirchum gloesporioides, Fusarium graminearum, Phytophtora capsici and Valsa mali* [3-4]. Helvolic acid extracted from *Pichia guilliermonii* is the main antimicrobial component of endophytic fungus. In all 27 perspective compounds were extracted from the above stated endophytic fungus, which can be used further.

The above referred properties of the endophytic fungi metabolites are perspective for food industry and medicine and many branches of science with the view of their practical application, which still greater increases the interest to these metabolites and contributes to intensification of researches towards the study of the mechanism of the action of antimicrobial substances, physiological role of these fungi, content of metabolites and strategic resolution of terms for development of fungal cultures, while on the base of the available data we can state convincingly, that the practical role of metabolites of endophytic fungi is important for the progress of many branches.

Paris polyphylla spread in Georgia and many endemic herbs were found this year on the territory of Tbilisi National Park (village Saguramo). Preliminary experiments proved the feasibility of practical application of the taste properties and anti-spoilage effect of extracts obtained from these plants.

ლიტერატურა - REFERENCES – ЛИТЕРАТУРА

1. Tan, R.X.; Zhou, W.X. Endophytes: a rich source of functional metabolites. Nat. Prod. Rep. 2001, 18, 448-459;
2. Rodriguez, R.J.; White, J.F.; Arnold, A.E.; Redman, R.S. Fungal endophytes: diversity and functional roles. New Phytol. 2009, 182, 314-330;
3. Zhang, M.; Wang, W.L.; Fang, Y.C.; Zhu, T.J.; Gu, Q.Q.; Zhu, W.M. Cytotoxic alkaloids and antibiotic nordammarane triterpenoids from the marine-derived fungus Aspergillus sydowi. J. Nat. Prod. 2008, 71, 985-989;
4. Feng, C.; Ma, Y. Isolation and anti-phytopathogenic activity of secondary metabolites from Alternaria sp. FL25, an endophytic fungus in Ficus carica. Chin. J. Appl. Environ. Biol. 2010, 16, 76-78;

5. Li, Y.; Song, Y.C.; Liu, J.Y.; Ma, Y.M.; Tan, R.X. Anti-Helicobacter pylori substances from endophytic fungal cultures. World J. Microbiol. Biotechnol. 2005, 21, 553-558;
6. Lambrechts MG. Pretorius IS. Yeast and its importance to wine aroma: a review. S Afr J Enol Vitic 2000; 21: 97-129;
7. Lopes CA, Lavalle TL, Querol A, Caballero AC. Combined use of killer biotype and mtDNA-RFLP patterns in a Patagonian wine Saccharomyces cerevisiae diversity study. Antonie van Leeuwenhoek 2006; 89: 147-56.

ღვინის გემურ თვისებებზე და გაფუჭებაზე მომძმედი ენდოფიტური საფუარი სოკოების ანტიმიკრობული მეტაბოლიტები

ნათია ბარბაქაძე, ლიპარიტ დოლიძე, ნინო ქავთარაძე, თამარ დგებუაძე, მაია ჯაფარიძე, ავთანდილ დოლიძე
ივ. ჯავახიშვილის სახელობის თბილისის სახელმწიფო უნივერსიტეტი/პეტრე მელიქიშვილის ფიზიკური და ორგანული ქიმიის ინსტიტუტი

რეზიუმე

ღვინის წარმოებასთან დაკავშირებული საფუარი სოკოებიდან ადრე გამოყოფილი იყო აქროლადი ფენოლები, რომლებიც გავლენას ახდენენ ღვინის არომატზე. ასევე დადასტურებულია ამ მეტაბოლიტების ანტიმიკრობული აქტივობა, რაც პერსპექტიულია შემდგომში გამოყენების თვალსაზრისით. არსებული მონაცემების საფუძველზე ცალსახად შეიძლება აღინიშნოს, რომ ენდოფიტური სოკოების მეტაბოლიტების პრაქტიკული როლი მნიშვნელოვანია მრავალი დარგის განვითარებისათვის. მიმდინარე წელს თბილისის ეროვნული პარკის ტერიტორიაზე (სოფ. საგურამო) მოძიებულ იქნა საქართველოში გავრცელებული ყვავისთვალა *Paris polyphylla* და სხვა ენდემური მცენარეები. წინასწარი ცდებით დადასტურებულია ამ მცენარეების ექსტრაქტების გემური თვისებებისა და გაფუჭების საწინააღმდეგო მოქმედების პრაქტიკული გამოყენების შესაძლებლობის შესახებ.

АНТИМИКРОБНЫЕ МЕТАБОЛИТЫ ЭНДОФИТНЫХ ДРОЖЖЕВЫХ ГРИБОВ, ВЛИЯЮЩИЕ НА ВКУСОВЫЕ КАЧЕСТВА И ПОРЧУ ВИНА

Н.Г.Барбакадзе, Л.А.Долидзе, Н.А.Кавтарадзе, Т.А.Дгебуадзе, М.З.Джапаридзе, А.В.Долидзе
Тбилисский Государственный Университет им. Ив. Джавахишвили, Институт физической и органической химии им. Петре Меликишвили

РЕЗЮМЕ

Летучие фенолы, которые связаны с производством вина и влияют на аромат вина, раннее были экстрагированы из дрожжевых грибов. Подтверждается, что антибактериальная активность этих метаболитов также является перспективным для их дальнейшего использования. Основываясь на существующих данных, роль метаболитов эндофитных грибов значительна в развитии различных областей. В этом году, на территории Национального Парка Тбилиси (вблизи с. Сагурамо) нами был найден *Paris Polyphylla* и другие эндемические растения. По предварительным экспериментам подтверждено, что экстракты этих растений влияют на вкусовые качества и сохранность вина, что очень важно для практического использования.

DEVELOPMENT OF INNOVATIVE NUTRITIONAL FUNGICIDE COMPOSITE WITHOUT COPPER

Ketevan Kochiashvili, Natia Barbakadze, Maia Japaridze, Maia Stepanishvili, Liparit Dolidze, Rusudan Tsiskarishvili, Avtandyl Dolidze
Petre Melikishvili Institute of Physical and Organic Chemistry at Iv. Javakhishvili Tbilisi State University

Development of modern fungicides of nutritive properties is a top priority for the progress of agriculture. Application of natural resources guarantees ecological security and reasonable price of the composite. Besides, application of phosphites and phosphates contributes to the reduction of migration of undesirable compounds in the soil and prevents their transition to human food cycle. On the basis of preliminary experiments, samples of natural phosphorite formations of Georgia have been selected and feasibility of preparation of optimal concentration composites has been proved.

Presence of heavy metals in food is one of the urgent problems of the modern world and is rather acute for Georgia too. Heavy metals fall into food through various ways, inclusive preparations used for plany protection against pests and diseases. Fungicide mixtures used in plant protection, which contain the second class dangerous heavy metal, copper are of contact effect. In case of precipitation the preparation is washed –off (leached) into soil. Besides, copper is accumulated in the soil, plant and fruit. Systematic application of Bordeaux mixture for decades resulted in excessive accumulation of copper, which finally was expressed on wine materials too. Therefore it became necessary to develop new fungicides void of metals to replace copper in it. With this in view, it is possible to use phosphor containing natural resources which will improve plant nutrition and will have fungicidal properties simultaneously. Preparations made on the base of phosphorites efficiently act as fertilizers and fungicides, simultaneously.

It is universally know that there are rather abundant reserves of phosphorites in the world and their transformation into phosphites is not a problem. In Israel, in the coastal zone of the Dead Sea, as well as in other countries phosphorite strata were exposed which have been used for production of phosphorous fertilizers and phosphoric acid. This practice is used in other European countries too [1]. We have to note that phosphorites are found at the Azerbaijan-Georgia border, along the river Iori, on Eldar valley (according to the data of 1927) [2-5]. Later these data were still more précised and specified. Phosphorus-containing strata on the Eldar valley are divided into separate horizons. Phosphor-containing rocks are also found in the west Georgia, in Tsageri and Ambrolauri regions, in the basins of Tskhenistskali, Lajanuri and Rioni rivers. Information is available about presence of phorphsorite reserves on the territories of Adjara, Godogani (Imereti) and Lechkhumi-Kvemo Svaneti [6]. Experiments proved that deposits exposed in west Georgia are not less interesting with the view of phosphor-containing rocks. Irrespective of the fact that useful industrial properties of this material were proved back in 60ies of the last century, phosphorite deposits of Georgia have never been extracted.

Phosphor-containing substances are very significant sources for plant nutrition. Phosphates $(PO_4)^{3-}$ are used namely with this purpose. Phosphites $(PO_3)^{3-}$ resemble very much the phosphates, but phosphite, in distinct from the phosphate is not assimilated by the plant as a source of phosphor, therefore its application for phosphor-deficient plants is not recommended. Chemically these compounds are similar, but phosphate has one more oxygen atom, which absolutely changes its properties and reactivity. Phosphates are phosphorous salts and ethers. There are orthophosphates and condensed phosphates, which contain more than one phosphor atom, create bond P-O-P [7]. Phosphates are widely used in production of phosphorous fertilizers, synthetic detergents and some medicinal preparations. Phosphor-containing natural rocks are also used in the world practice for *in situ* fixation of harmful wastes.

Phosphates form insoluble compounds in the soil as a result of which only small portion of phosphor is consumed by plants. Similarly complex is assimilation of phosphor by plant leaves (spraying), since it hardly passes through cuticle layer (in case of potassium phosphate). Phosphite compounds (potassium phosphate) are generally used as water solution. Elevation of phosphor mobility in plant tissues and soil proceeds thanks to three oxygen atoms. They can affect all parts of a plant: leaf, stem and roots. Passing

xylem and phloem it reaches all bodies of a plant and phosphites are easily consumed by the whole plant [8]. Experiments proved that regular and stage-wise application of phosphites as a part of complex approach for the struggle against plant diseases significantly reduces cases of diseases and gravity of the progress of diseases. Phosphites obtained from phosphoric acids are distinguished by their phototoxic action. This is why prior to their application they are treated with neutralizing substrate (potassium hydroxide) that results in the formation of potassium phosphite. Assimilation of potassium contributes to the improvement of plant nutrition. This compound is a good bio-stimulator and significantly reduces formation of *Microdochium nivale*.

In 2010, experimental land plots were created in Russia (Moscow) where supervision was performed over three lawn grasses, together with the assessment of plant diseases and grass quality. According to the data obtained on the basis of field and laboratory experiments, in case of application of potassium phosphate incidents of diseases were reduced at 50%.

Application of the widely used fungicide Chipco Green jointly with the organic fertilizers PK Plus hinders to disease formation, and alongside with it, shows various forms of disease inhibition and possible synergic effect. Sharp improvement of quality index was observed on all sections treated with phosphites. There are two versions of action of phosphites on plants: direct, as a fungicide and indirect, as a stimulator through plant protection mechanism. It was shown, that in case of application of 100 mkg/L phosphate concentration the mycelium growth is blocked completely, while at the application of a weaker concentration destruction of hyphae was observed. It was shown that after leaf-feeding of the plant by phosphites, energy was actively assimilated and accumulated in leaves. The complete systemic mobility of tissues and the fact that in plants phosphite was not transformed into phosphate was also observed. [9].

Lately the preparation "Quantum-Phytos" (Stop-Phytophtora) was developed in the Ukraine containing potassium and phosphor forms easily assimilated by plants, which are vital for plant growth and development. At the expense of the preparation activity, plants develop natural stable resistance to pathogens; at the same time stimulation of protecting mechanism against phytophtora, fuzarioses, rhizoctonioses, pitium and other diseases takes place. The preparation supports the plant in the creation of immune system. These fertilizers are distinguished by specific efficiency for prevention of diseases. Addition of organic acids to phosphor and potassium special formulations enables the plant to use efficiently nutrients, improve root system develop and absorb nutrients from soil. It is the accessible source for potassium and phosphor and simultaneously the efficient means for the struggle against plant diseases.

On the basis of preliminary experiments the specimens of natural phosphorite rocks were selected, which after due treatment were used for development of nutritive-fungicidal composites. Their application as phosphorous fertilizers (Kakheti, Adjara, Lechkhumi) contributed to sharp increase of the yield. Repeated check up of fungicidal properties is planned. At the same time some versions of the composite formulation will be précised and the economically profitable formulation will be selected for its practical application.

ლიტერატურა - REFERENCES – ЛИТЕРАТУРА

1. T.R. Yager. The mineral industry of Israel. USGS, Minerals Yearbook, Israel, 2012,March, 50.1-50.5;
2. Akentjev S. Geological review of Eldar. Manuscript, report for ""Gruzvodkhoz" №469.1929
3. Akentjev S. Draft review about geological prospecting on Eldar. Manuscript,.1931.
4. Akentjev S. Reports-accounts about phosphorites in west Georgia (manuscripts from 1931).
5. Bogachev V. Problem of r.Kura valley. Proceedings of the Caucasus Museum; vol. 8, 1913.
6. G. Dzotsenidze. Development of magma phenomena in Kutaisi region. Tbilisi. Transactions of the Institute of Geology and Mineralogy, Tbilisi, 1951, p. 49-50;
7. Crystal chemistry of inorganic phosphites, J. Loub, Acta Cryst. (1991), B47, 468-473, DOI:10.1107/S0108768191002380;
8. Chemistry 9. — M.,: Ventana-Graf, 2010. — pp. 287.
9. Greenwood, Norman N.; Earnshaw, Alan. (1997), Chemistry of the Elements (2nd ed.), Oxford: Butterworth-Heinemann, ISBN 0-08-037941-9.

ინოვაციური მკვებავი ფუნგიციდური კომპოზიციის შემუშავება სპილენძის გარეშე

ქეთევან ქოჩიაშვილი, ნათია ბარბაქაძე, მაია ჯაფარიძე, მაია სტეფანიშვილი, ლიპარიტ დოლიძე, რუსუდან ცისკარიშვილი, ავთანდილ დოლიძე
ივ. ჯავახიშვილის სახელობის თბილისის სახელმწიფო უნივერსიტეტი/პეტრე მელიქიშვილის ფიზიკური და ორგანული ქიმიის ინსტიტუტი

რეზიუმე

მძიმე მეტალების შემცველობის გარეშე თანამედროვე ფუნგიციდების შემუშავება პრიორიტეტული ამოცანაა. პრეპარატებს ფუნგიციდურ თვისებებთან ერთად უნდა გააჩნდეთ სასუქის თვისებებიც. მულტიფუნქციონალური პრეპარატების შემუშავება ხელს შეუწყობს სასოფლო-სამეურნეო წარმოების რენტაბელობის ამაღლებას. ბუნებრივი ნედლეულის გამოყენება განაპირობებს ეკოლოგიურ უსაფრთხოებას და პრეპარატის მისაღებ ღირებულებას. ამასთან ერთად მნიშვნელოვანია ფოსფიტების და ფოსფატების გამოყენება ნიადაგში არასასურველი ნივთიერებების მიგრაციის შესამცირებლად, რათა არ მოხდეს მათი გადასვლა ადამიანის კვების ციკლში. წინასწარი გამოცდების შედეგად შერჩეულია საქართველოს ბუნებრივი ფოსფორიტული პლასტების ნიმუშები და დადასტურებულია პრეპარატის ოპტიმალური კომპოზიციის მიღების შესაძლებლობა.

РАЗРАБОТКА ИННОВАЦИОННОЙ ПИТАТЕЛЬНОЙ ФУНГИЦИДНОЙ КОМПОЗИЦИИ БЕЗ МЕДИ

К.Н. Кочиашвили, Н.Г.Барбакадзе, М.З.Джапаридзе, М.А.Степанишвили, Л.А.Долидзе, Р.П.Цикаришвили, А.В.Долидзе
Тбилисский Государственный Университет им. Ив. Джавахишвили, Институт физической и органической химии им. Петре Меликишвили

РЕЗЮМЕ

Разработка современных фунгицидов без содержания тяжелых металлов является приоритетной задачей. Препараты вместе с фунгицидными свойствами должны иметь характер удобрений. Разработка мультифункциональных препаратов будет способствовать повышению рентабельности сельскохозяйственного производства. Использование природного сырья обусловливает экологическую безопасность и приемлемую стоимость препарата. Важнейшим фактором является использование фосфатов для уменьшения миграции нежелательных веществ в почве и их перехода в пищевой цикл человека. На основе предварительных испытаний отобраны образцы природных фосфоритных пласт Грузии и доказаны их питательные и фунгицидные свойства. Проводятся практические работы по разработке и испытаний композиций оптимального состава.

ANALYSIS OF SCIENTIFIC PRODUCTIVITY AT THE MESO- AND MACRO-LEVELS

Levon Chobanyan, Teimuraz Chubinishvili, Nelly Makhviladze, Alexander Phatsatsia

Georgian Technical University, Institute TECHINFORMI, Tbilisi, Georgia,
tech@caucasus.net

The most important instrument for solving science management problems is analysis of scientific activity efficiency at both the microlevel and the mezo- and microlevels. Upon analysis of the scientific activity of researchers based on individual quantitative parameters, such as publishing activity (number of published works in high-ranking journals), citation index, taking into account of the scientific direction of a researcher or a research team acquires a particular interest. For example, an average number of citations per journal in the world flow of publications for different fields of chemistry can differ 5-6 times. For a scientometric analysis, taking into account scientific directions of an individual researcher and the research team, the effective citation indexes H* and I* have been introduced.

The most important instrument for solving science management problems is analysis of scientific activity efficiency at both the microlevel, that is for an individual researcher as well as at the meso- and macrolevels:for scientific groups and departments, large scientific collectives (universities, institutes, etc.) and the State as a whole.[1-5]

During the last decades, in general, an analysis of scientific activity of researchers based on individual quantitative parameters, such as publishing activity (number of published works in high-ranking journals) and citation index, has become rather popular.[6-9]

As pracice shows, the formal analysis on the basis of such quantitative parameters can produce a distorted picture of the scholar's scientific activity. In order to obtain a real characteristic of the researcher's activity independent expert opinions need to be used[10-11], whereas in calculating the quantitative scientometeric characteristics, of most importance is to take into account such parameters as self-citation (direct and indirect), number of co-authors, time distribution of published works, etc.[12,13]

In our opinion, of special importance is the taking into account the scientific field/discipline of the researcher. For example, an average number of citations per article in the world flow of publications can, depending on the discipline, differ more than seven times. As a result, the average citation indexes of scholars working in different scientific fields will significantly differ and formal analysis of their activity will give a distorted account.[14,15]

Similar problems arise when comparing scientific activity characteristics for different chemistry branches.

Underlying Table gives data on the average citation per paper for Georgian scientists working in different branches of Chemistry. The Data is based on the Database of Web of Science (WOS). The average is calculated for the following three time intervals: 1960-2015, 2005-2015 and 2010-2015.

	1	2	3	4	5	6	7	8	9	10	11	12	13	14	15
1960 – 2015															
TC	2152	100	252	77	194	177	296	522	307	89	156	32	132	168	82
ATC	5.8	27.9	17.5	1.7	4.8	4.6	5.7	2.7	4.6	6.9	3.0	2.2	7.8	6.2	5.5
2005 – 2015															
TC	2102	49	85	35	38	127	76	138	70	16	35	6	50	41	21
ATC	5.8	17.4	13.5	3.2	6.1	3.7	5.0	2.7	3.4	6.2	3.3	1.3	4.2	6.0	4.1
2010 – 2015															
TC	2093	32	56	24	15	52	35	54	33	7	17	1	30	16	9
ATC	5.8	14.0	11.5	1.8	3.9	1.6	2.8	1.9	2.4	1.4	0.8	5.0	5.0	2.0	5.0

In Table we denote: TC – accumulative citation value and ATC Average Time Cited per one article for some Chemistry branch. Also we denote Column 1 for All Chemistry branches, 2 - Biochemical Research Methods, 3 - Chemistry, Analytical, 4 - Chemistry, Applied, 5 - Chemistry, Inorganic & Nuclear, 6 - Chemistry, Medicinal, 7 - Chemistry, Multidisciplinary, 8 - Chemistry, Organic, 9 - Chemistry, Physical, 10 - Crystallography, 11 - Electrochemistry, 12 - Engineering, Chemical, 13 - Physics, Atomic, Molecular & Chemical, 14 - Polymer Science, 15 - Spectroscopy

The table shows that the average number of citation per paper depends significantly on the research branches.

In particular for the branches BIOCHEMICAL RESEARCH METHODS and CHEMISTRY, ORGANIC the average citation differs by more than 6 times.

In addition, we think that in a number of publications, upon comparison of the scientometric characteristics at the macrolevel, the scientometricindexes used at the microlevel are being applied totally unfoundedly. This leads to serious mistakes in analysis and distortion of the real picture.

Theauthorsofthearticlehaveintroducedascientometric index – the effective individual h-index (Hirsch)$\mathbf{H_j^*}$**,** taking into account the scientific field of a researcher [15] and developed the effective citation index methodology/procedure. Further, in a linear approximation of the function of dependence of the number of citations of a publication on its number in the list ordered according to the number of citations/quotations**Q(n)**, the ratio of the effective citation h-index to the standard h-index was obtained:

$$\mathbf{H^*/\,H} = \frac{l+1}{l+1/\mathbf{K}_j},$$

where l is the tangent of *(n) slope*, and $\mathbf{K}_j$ is the ratio inversely proportional to the average number of citations per article in the J-scientific field.

The linear approximation of the function *Q(n***)** does not lead to a reduction in the accuracy of results, because the behavior of the function *Q(n)* in the point n=H is what finally constitutes our interest.

The produced expression coincides with the result receivable with the frequently used hyperbolic approximation of the function *Q(n)*.

The computations made on the experimental *Georgian Scientists* data file demonstrated that a difference of the guess of the value $\mathbf{H_j^*/\,H}$ from its denotation does not exceed 20%, while the mean error makes 8%.

As an example, for a researcher working in the scientific fieldMATERIALSSCIENCE and whose h-index is H=3, the H* computation results will be$l$=0.47, andk_j=4.03. Asaresult, forthe effective value of the h-index we shall receive**H*=6.**

The developed methodology of introducing the effective individual citation indexes can be also applied to other individual bibliometric citation-related indexes: *e-index, g-index, hc-index , hi-index*.[18-20]

On the basis of conducted experimental research we have arrived to a conclusion that the effective citation index I* obtainable by modernization of the I-index concurrently introduced by Kosmulski [16] and Prathap [17] is the most expedient for analyzing the efficiency of scientific activity at the mezo- and micro-levels.

The I-citation index is determined as follows: a scientific institute or a group of scientists have the I-index equaling *m*, where *m* is the maximum number of the set {n}, whose every element satisfies the condition:the team membership includes *n*researchers whose individual h-index is no less than *n*.

For accounting scientific fields where in the members of a group are engaged, it is necessary that the effective value of the h-index rather than its individual value be used for each group member.

Thus, determination of the effective citation index I* will look as follows:

The citation index I* is determined as follows: a scientific institute or a group of scientists has the I*-index equal to *m*, where *m*is the maximum number of the set {n}, each element of which fits the condition: there are *n* researchers in the group with the individual effective h-index not less than *n*.

At the further stages of research our aimis to investigate the effective values of the I*-index, being based on other types of individual citation indexes for the approximate calculation of I*-indexes. The possibility of approximate calculation is important for facilitating analysis of the effective characteristics based on the output data of the international science citation indexes.

Further, the results obtained for the experimental groups of scientists should be compared with the independent expert opinions.

The aforesaid procedures of scientometric analysis were realized on the following database:

Bibliographic descriptions of Georgian scientists' publications in the databases: Web of Science, Scopus/Google Scholar,as well as on the basis of statistical data on the world flows of scientific periodicals in the subsystemWebofScience – Essential Science Indicators.

However, a complete solution of a problem of scientometric support of the Georgian science management system requires that the articles published by Georgian scientists in the Georgian scientific periodicals need also be analyzed.

This will require standardization of the processes of preparation and publication of the Georgian scientific periodicals as well as the development of a Georgian Science Citation Index.

The developments should be carried out based on the generated databases of *DOI* (digital object identifier) [21] and ORCID (Open Researcher and Contributor ID systems) [22]. The information contained in the DOI electronic document contains its location indicator (e.g., URL), its name, and other object identifiers. ORCID is a register of unique identifiers of researchers. ORCID is an instrument connecting the scientific activity of researchers with their identifiers.

In addition, documents in a database should be indexed on the basis of standard international classifiers of scientific periodical.

The works on the implementation of the aforesaid tasks are intended to start on the basis of scientific periodical published in the Georgian Technical University and to be extended, in the future, to the publications of other universities, research centers and publishers of Georgia.

ლიტერატურა - REFERENCES – ЛИТЕРАТУРА

1. Glanzel W. The need for standards in bibliometric research and technology, S*cientometrics*.35(2), 1996, 167-176.
2. Moed H. F. Citation analysis in research evaluation. Dordrecht: Springer, 2005.
3. Price D. de Solla. *Little Science, Big Science*, Columbia Univ. Press, New York, 1963.
4. Frame J.D. Mainstream research in Latin America and the Caribbean, *Interciencia*, 2, 1977, 143-148.
5. Schbert A., Glanzel W., Braun T. World flash on basic research: Scientometricdatafiles. A Comprehensive set of indicators on 2649 journals and 96 countries in all major science fields and subfields, 1981-1985, *Scientometrics*, 16(1-6), 1989, 3-478.
6. HirschJ. E. An index to quantify an individual's scientific research output. Proc. Natl. Acad. Sci. U. S. A. 102(46), 2005, 165-169
7. AdlerR., Ewing J., and Taylor P.Citation statistics. http://www.mathunion.org/fileadmin/IMU/Report/CitationStatistics.pdf
8. Jones T. Huggett, S., Kamalski J. Finding a Way Through the Scientific Literature: Indexes and Measures. WorldNeurosurgery 76: 36. doi:10.1016/j.wneu.2011.01.015, 2011.
9. Google Scholar Metrics for Publications - Google Scholar Blog. googlescholar.blogspot.com.br.
10. Polyanin A.On the Hirsch index and other scientometric indicators. http://eqworld.ipmnet.ru/ru/info/sci-edu/Polyanin-IndexH-2013.html. CitedNovember 22, 2014
11. KholodovA.S. Onscientificworkcitationindexes. Bulletin of the Russian Academy of Sciences., 2015, 310-320.
12. Lawrence P. A. Lost in publication: How measurement harms science, Ethics in Science and Environmental Politics 8, 9 (2008). http://www.int-res.com/articles/esep2008/8/e008p009.pdf CrossRef
13. CampbellP. Escape from the impact factor, Ethics in Science and Environmental Politics 8, 5 2008.http://www.int-res.com/articles/esep2008/8/
14. Chobanyan L, Magradze V., Makhviladze N., Shatberashvili O., Tsotskolauri P. Development of bibliometrictools and their adaptation to the study of Georgian scientific products. The International Scientific Conference Devoted to the 80th anniversary of Academician I.V. Prangishvili - Information and Computer Technologies, Modeling, Control. Tbilisi, Georgia, 2010. p.167.
15. Chobanyan L., Makhviladze N., Shatberashvili O., Tsotskolauri P. The unification of bibliometricindexes to assess the level of scientific productivity at the micro- and mezo levels. Georgian Engineering News, 2013, 3, pp.28-30.
16. Kosmulski M. I—a bibliometric index. ForumAkademickie 11: 31., 2006.

17. Prathap G. Hirsch-type indexes for ranking institutions' scientific research output. CurrentScience 91 (11): 1439, 2006.
18. Cronin B., Meho L. Egghe LeoTheory and practice of the g-index, Scientometrics, vol. 69, No 1, pp. 131–152,2006. Using the h-Index to Rank Influential Information Scientists, *Journal of the American Association for Information Science and Technology*, vol. 57, no. 9, 2006, pp. 1275-1278.
19. Egghe L., Rousseau R. An informetric model for the Hirsch-index, *Scientometrics*, vol. 69, no. 1, 2006, pp. 121-129.
20. Sidiropoulos A., Katsaros C., Manolopoulos Y. Generalized h-index for disclosing latent facts in citation networks, *arXiv:cs.DL/0607066* v1 13 Jul, 2006
21. Paskin N.Digital Object Identifier (DOI®)system. *Encyclopedia of Library and Information Sciences* (Taylor & Francis Group), 2010.
22. Ten things you need to know about ORCID right now. *ImpactStory. 10 April 2014. Retrieved 15 April 2014.*

სამეცნიერო პროდუქტიულობის ანალიზი მეზო და მაკრო დონეზე

ლევონ ჩობანიანი, თეიმურაზ ჩუბინიშვილი, ნელი მახვილაძე, ალექსანდრე ფაცაცია
საქართველოს ტექნიკური უნივერსიტეტი, ინსტიტუტი ტექინფორმი, თბილისი, საქართველო
tech@caucasus.net

რეზიუმე

მეცნიერების მართვის ამოცანათა გადაჭრის ერთ-ერთ მთავარ ინსტრუმენტს წარმოადგენს სამეცნიერო მუშაობის ეფექტურობის ანალიზი როგორც მიკრო, ასევე მეზო და მაკრო დონეებზე. მკვლევართა სამეცნიერო მოღვაწეობის ანალიზისათვის ისეთი ინდივიდუალური რიცხვითი პარამეტრების საფუძველზე როგორიცაა პუბლიკაციების აქტიურობა, ციტირების ინდექსი განსაკუთრებული მნიშვნელობა ენიჭება მეცნიერის ან მეცნიერთა კოლექტივის კვლევის მიმართულების გათვალისწინებას. მაგალითად, ქიმიურ მეცნიერებათა სხვადასხვა დარგში ცალკეული სტატიების ციტირების საშუალო რაოდენობების შეფარდება აღწევს ხუთს, და ზოგჯერ ექვსაც კი. ინდივიდუალური მეცნიერის, ან მეცნიერთა კოლექტივის კვლევითი მოღვაწეობის ეფექტური მეცნიერებათმზომილობითი ანალიზისათვის ჩვენ შემოგვყავს ციტირების ეფექტური კოეფიციენტები H* და I*, რომლებიც ითვალისწინებენ დარგების ასეთ სპეციფიკას და გვაძლევს საშუალებას გარკვეული აზრით შევადაროთ სხვადასხვა დარგებში მომუშავე მკლევართა სამეცნირო პროდუქტიულობა.

АНАЛИЗ НАУЧНОЙ ПРОДУКТИВНОСТИ НА МЕЗО И МАКРО УРОВНЯХ

Левон Чобанян, Теймураз Чубинишвили, Нелли Махвиладзе, Александр Пацация
Грузинский Технический Университет, Институт Техинформи, Тбилиси, Грузия
tech@caucasus.net

РЕЗЮМЕ

Важнейшим инструментом для решения задач управления наукой является анализ эффективности научной деятельности как на микро-уровне, так и на мезо и макро-уровнях. При анализе научной деятельности ученых на основе индивидуальных численных параметров, таких как активность публикации, индекс цитирования, особое значение имеет учет научного направления деятельности ученого или научного коллектива. Например, среднее количество цитирований на одну статью в мировом потоке публикаций, для разных областей химии может отличаться в 5-6 раз. Для наукометрического анализа, учитывающего научные направления деятельности отдельного ученого и для научного коллектива, введены эффективные индексы цитирования: H* и I*.

სპარტაკ უროტაძის ხსოვნას

საქართველოს ქიმიური საზოგადოება ღრმა მწუხარებას გამოთქვამს წარმატებული მეცნიერის, შესანიშნავი მამულიშვილისა და კოლეგის, უაღრესად გულთბილი და სიკეთით სავსე ადამიანის გარდაცვალების გამო.

მოულოდნელად წავიდა ჩვენგან **სპარტაკ უროტაძე,** პეტრე მელიქიშვილის ფიზიკური და ორგანული ქიმიის ინსტიტუტის აგრარული ქიმიის პრობლემათა ლაბორატორიის გამგე, მთავარი მეცნიერ თანამშრომელი, ქიმიის მეცნიერებათა დოქტორი. იგი დაიბადა 1943 წლის 25 ივნისს, 1967 წელს დაამთავრა თბილისის სახელმწიფო უნივერსიტეტის ქიმიის ფაკულტეტი და ამავე წელს დაიწყო მუშაობა საქართველოს მეცნიერებათა აკადემიის პეტრე მელიქიშვილის სახელობის ფიზიკური და ორგანული ქიმიის ინსტიტუტის ფიზიკური ქიმიის ლაბორატორიაში.

1978 წელს მან წარმატებით დაიცვა საკანდიდატო დისერტაცია თემაზე: „ბუნებრივი კლინოპტილოლითების ადსორბციული თვისებების კვლევა“, ხოლო 2003 წელს სადოქტორო დისერტაცია - „საქართველოს ბუნებრივი ცეოლითების სკოლეციტისა და ლომონტიტის ფიზიკურ-ქიმიური შესწავლა და პრაქტიკული რეკომენდაციები“, რომლის სამეცნიერო კონსულტანტი იყო აკადემიკოსი გიორგი ციციშვილი.

სპარტაკ უროტაძე წლების განმავლობაში იყო ფიზიკური და ორგანული ქიმიის ინსტიტუტის სამეცნიერო-ტექნიკური განყოფილების გამგე, დირექტორის მოადგილე სამეცნიერო-ტექნიკურ დარგში, 2006 წლიდან - აგრარული ქიმიის პრობლემათა ლაბორატორიის გამგე.

დიდია ბ-ნი სპარტაკის წვლილი საქართველოს მეცნიერების განვითარებაში. იგი წარმატებით მუშაობდა სხვადასხვა სამეცნიერო მიმართულებით, როგორებიცაა: სორბციული და სხვა ზედაპირული პროცესები, ქრომატოგრაფია, სინთეზური და ბუნებრივი ცეოლითების ფიზიკურ-ქიმიური თვისებების კვლევა, ბუნებრივი ცეოლითების გამოყენება მეცხოველეობასა და სოფლის მეურნეობაში, აგრეთვე გარემოს დაცვის პრობლემების გადაჭრის საქმეში. განსაკუთრებით აღსანიშნავია სპარტაკ უროტაძის მონაწილეობა საქართველოს ბუნებრივი ცეოლითების სკოლეციტისა და ლომონტიტის იონმიმოცვლითი თვისებების კვლევაში, სადაც მან წარმატებით გამოიყენა იონური ქრომატოგრაფიისა და სხვა თანამედროვე ფიზიკურ-ქიმიური მეთოდები, მიიღო ორიგინალური შედეგები და შექმნა მიმდინარე პროცესების მარტივი მათემატიკური მოდელი, რის საფუძველზე შეიმუშავა რეკომენდაციები სორბენტებისა და იონმიმომცვლელების სახით აღნიშნული ბუნებრივი ცეოლითების პრაქტიკული გამოყენების შესახებ. კვლევების განხორციელებისას და მიღებული შედეგების განსჯისას სპარტაკ უროტაძე ყოველთვის იყო უშუალო კონტაქტში დარგის წამყვან მეცნიერებთან, პირველ რიგში თავის მასწავლებელთან, აკადემიკოს გიორგი ციციშვილთან, სხვა ქართველ (აკადემიკოსები თეიმურაზ ანდრონიკაშვილი და ნიკოლოზ სხირტლაძე), რუს (აკადემიკოსი მ.მ.დუბინინი, პროფესორები ვ.ნ.კელცევი, ნ.ს.პოლიაკოვი და კ.ი.საკოდინსკი), ჩეხ (ირჟი კადლეცი და ვერა პაცელოვა), გერმანელ (ვალტერ შირმერი და მარტინ ბიულოვი), ბულგარელ

(გიორგი კიროვი და ლუდმილა ფილიზოვა), იტალიელ (დიეგო გატა), ამერიკელ (სტეგენ ბაიცინგერი), ლატვიელ (ლივია ზარინა) და სხვა ქვეყნების მეცნიერებთან.

სპარტაკ უროტაძე 150-მდე სამეცნიერო ნაშრომის, 4 საავტორო მოწმობის გამოგონებაზე, 7 პატენტის ავტორი და თანაავტორია. მას მონაწილეობა აქვს მიღებული მრავალი სამეცნიერო ფორუმის მუშაობასა და ორგანიზებაში. განსაკუთრებით აღსანიშნავია მისი დაუღალავი და ნაყოფიერი მუშაობა თბილისში, სოხუმსა და საქართველოს სხვა ქალაქებში ჩატარებული კონფერენციების ორგანიზებაში: ადსორბციასა და ქრომატოგრაფიაში (1970-80-იან წლები); ბუნებრივი ცეოლითების მოპოვებისა, კვლევისა და გამოყენების მიმართულებებით (1993, 1997, 2002). საკმაოდ დიდი ინტერესი და მრავალი გამოხმაურება დაიმსახურა სპარტაკ უროტაძის მოხსენებებმა მსოფლიო კონგრესებზე ბუნებრივი ცეოლითების კვლევა-მოპოვება-გამოყენების დარგში (2002, თესალონიკი, საბერძნეთი; 2010, სოფია, ბულგარეთი).

ბიოლითონების კოორდინაციული ნაერთების და ბუნებრივი ცეოლითების კომპოზიციების საფუძველზე მომზადებული პრემიქსების კვლევას ეძღვნება ბატონი სპარტაკ უროტაძის ხელმძღვანელობით განხორციელებული პროექტი: „ბიოლითონებისა და ბუნებრივი ცეოლითების შემცველი ახალი თაობის პრემიქსები“. პროექტი დაფინანსდა უკრაინის მეცნიერებისა და ტექნოლოგიების ცენტრის (უმტც) მიერ და მიმდინარეობდა 2011-2014 წლებში.

თეორიისა და პრაქტიკის აზრიანად შერწყმით ს.უროტაძეს თავისი კვლევები ყოველთვის მიჰყავდა ორიგინალურ გადაწყვეტამდე და მათ პრაქტიკაში აუცილებელ გამოყენებამდე. მის მრავალ სამუშაოს გამოყენებითი ხასიათი გააჩნია. ესაა ბუნებრივი ცეოლითების გამოყენება მრეწველობის სხვადასხვა დარგებში. განსაკუთრებით საინტერესოა სამუშაოები ბუნებრივი ცეოლითების გამოყენების შესახებ მიწათმოქმედებასა და მეცხოველეობაში.

აგრარული ქიმიის პრობლემათა ლაბორატორიაში 2013-2015 წწ.-ში შ.რუსთაველის ეროვნული სამეცნიერო ფონდის დაფინანსებით განხორციელდა პროექტი „ხელატები სოფლის მეურნეობაში“.

პროექტის ფარგლებში, სპარტაკ უროტაძის ხელმძღვანელობით, ლაბორატორიაში სინთეზირებული ხელატური ნაერთების საფუძველზე შექმნილი პრემიქსი გამოცდილი იქნა ბროილერზე და კვერცხმდებელ ფრინველზე, ხოლო სასუქი სიმინდის კულტურაზე. სასუქის 5%-იანი მუშა ხსნარის გამოყენებამ უზრუნველყო: მოსავლიანობის რაოდენიბრივი და ხარისხობრივი მაჩვენებლის ზრდა; N,P,K-ს შეთვისების მაღალი ხარისხი; ფიზიოლოგიური მდგომარეობის და მეტაბოლური პროცესების გაუმჯობესება; სასუქის გახანგრძლივებული მოქმედება; ნიადაგის გაკეთილშობილება და სტრუქტურის გაუმჯობესება.

გარდა აღნიშნული პროექტებისა გეგმის მიხედვით მიმდინარე სამუშაოების შესრულებისათვის ლაბორატორიასა და ი.ლომოურის მიწათმოქმედების, ასევე ანასეულის ჩაისა და სუბტროპიკული კულტურების სამეცნიერო კვლევით ინსტიტუტებს შორის დადებული ხელშეკრულების ფარგლებში, ლაბორატორიაში მომზადებული ხელატური სასუქები გამოცდილი იყო საველე პირობებში სხვადასხვა სასოფლო-სამეურნეო კულტურებზე (ხორბალი, ბოსტნეული, სოიო, ლობიო, სიმინდი, ციტრუსები). ხოლო

პრემიქსები გამოცდილი იქნა მეფრინველეობის ფაბრიკებში: შპს.“პატარძეული“, შპს. „ალგეთი“, შპს. „როსტერი“ და მებოცვრეობის ფერმაში შპს. „ბუკარა“.

ლაბორატორიაში სინთეზირებული ბიოკოორდინაციული ნაერთების ფიზიკურ-ქიმიური და ბიოლოგიური აქტივობის კვლევების საფუძველზე მიღებული შედეგები ასახულია პატენტებსა და სამეცნიერო პუბლიკაციებში, რომლებიც მოხსენებული და გამოქვეყნებულია როგორც ადგილობრივ, ისე საერთაშორისო კონფერენციებსა და ჟურნალებში.

ძირითადი საქმიანობის გარდა, სპარტაკ უროტაძე ყოველთვის აქტიურად იყო ჩართული საზოგადოებრივ საქმიანობაში. სხვადასხვა დროს იგი იყო სამეცნიერო ხარისხების მიმნიჭებელი სპეციალიზირებული სამეცნიერო საბჭოს წევრი, მრავალი წლის განმავლობაში კი ინსტიტუტის სამეცნიერო საბჭოს წევრი.

ბატონი სპარტაკი მრავალმხრივი ნიჭით დაჯილდოებული პიროვნება იყო, შესანიშნავი მეუღლე, მამა, ბაბუა, გულისხმიერი მეგობარი, კორექტური ხელმძღვანელი. თავისი პატიოსნებით, მაღალი ზნეობით, სიკეთით, ვაჟკაცობით იყო უზომოდ შრომისმოყვარე და ნიჭიერი პიროვნება.

საქართველოს მეცნიერებათა ეროვნულმა აკადემიამ, იუნესკოს მიერ დაწესებული მეცნიერების მსოფლიო დღესთან დაკავშირებით ქიმიის დარგში სამეცნიერო მიღწევებისათვის, ქიმიის მეცნიერებათა დოქტორი სპარტაკ უროტაძე დაჯილდოვა საპატიო სიგელით.

მას უზომოდ უყვარდა თავისი ახლობლები, ნათესავები და მეგობრები. გამორჩეულად უყვარდა თავისი მეუღლე ქალბატონი ნანა, რომელიც ღირსეულად ედგა მხარში ბატონ სპარტაკს მთელი ცხოვრების მანძილზე.

ძნელია და დღესაც გვიჭირს იმასთან შეგუება, რომ ჩვენს შორის აღარ არის ბატონი სპარტაკი. მისი მოგონება მარად იცოცხლებს ჩვენს ხსოვნაში.

პეტრე მელიქიშვილის ფიზიკური და ორგანული ქიმიის ინსტიტუტი

CONDOLENCE

Petre Melikishvili Institute of Physical and Organic Chemistry mourns the loss of the head of the laboratory of agrarian chemistry, Doctor of Chemical Sciences Spartak Urotadze (25.06.1943-28.09.2016), which was an outstanding scientist, faithul friend and helpful responsive person, and expresses its condolences to his family, friends and colleagues.

СОБОЛЕЗНОВАНИЕ

Институт физической и органической химии им. П.Г.Меликишвили скорбит по поводу утраты заведующего лабораторией проблем аграрной химии, доктора химических наук Спартака Левановича Уротадзе (25.06.1943-28.09.2016), выдающегося учёного, верного друга и отзывчивого человека, и выражает соболезнование его семье, друзьям и коллегам.

ინფორმაცია ავტორებისათვის

ჟურნალი "**საქართველოს მეცნიერებათა ეროვნული აკადემიის მაცნე. ქიმიის სერია**" აქვეყნებს სტატიებს ქიმიური მეცნიერების დარგში ქართულ, ინგლისურ და რუსულ ენებზე; მიმოხილვებისა და ინფორმაციული ხასიათის მასალების წარმოდგენა შესაძლებელია სარედაქციო კოლეგიასთან შეთანხმებით. გამოსაქვეყნებელი მასალის მოცულობა, ფორმატი და მისი წარმოდგენის სხვა პირობები შეთანხმებული უნდა იყოს პასუხისმგებელ მდივანთან, ავტორებმა ტექსტი უნდა წარმოადგინონ ელექტრონულ ფორმაში, Microsoft Word ფაილის (*.doc ან *.rtf) სახით, ნახაზები და სურათები – შავ-თეთრი გრაფიკული (*.bmp, *.dib, *.jpg, *.gif და სხვ.) ფაილების სახით. სამეცნიერო სტატიების ავტორების დასახმარებლად რედაქციის მიერ გათვალისწინებულია როგორც სტანდარტული ელექტრონული ფორმატები სამივე ენაზე, ისე სხვა ტექნიკური მომსახურება. Chemical Abstracts-სა (ინგლისურ ენაზე) და საქართველოს რეფერატულ ჟურნალში (ქართულ და ინგლისურ ენებზე) სტატიის რეფერირებისათვის ავტორი ვალდებულია გაითვალისწინოს შინაარსობრივი რეზუმეების მომზადება ორივე ენაზე.

სარედაქციო კოლეგიასთან შეთანხმებული საფასური უნდა იყოს გადარიცხული სსიპ საქართველოს მეცნიერებათა ეროვნული აკადემიის ანგარიშზე, მიმღები ბანკი – სახელმწიფო ხაზინა, მიმღების დასახელება – ხაზინის ერთიანი ანგარიში, ბანკის კოდი – TRESGE22, მიმღების სახაზინო კოდი – 708777499, დანიშნულება – ჟურნალ "მაცნეს" ქიმიის სერიაში სტატიის გამოქვეყნების ჰონორარი. აუცილებელია მიეთითოს ავტორის გვარი ვინც იხდის თანხას.

INFORMATION for AUTHORS

The journal "**Proceedings of the Georgian National Academy of Sciences. Chemical series**" is publishing articles in a field of chemical sciences in Georgian, English, and Russian, reviews and informational/advertizing materials may be submitted after consultations with the Editorial Board. Volume, format, and other details of contribution are to be discussed with the Executive Secretary; Authors submit texts of articles in a form of Microsoft Word files (***.doc or ***.rtf), figures and pictures – as monochrome (*.bmp, *.dib) or black/white (*.jpg, *.gif, etc.) files. To help Authors of scientific articles, standard Georgian, English, and Russian formats are provided as well as other techical service and support. For references of the article in the Chemical Abstracts (in English) and in the Georgian Abstracts Journal (in Georgian and in English) authors are obliged to foresight substantial summaries in both languages.

Agreed with the Editorial Board publishing expences are to be paid at the Tresury of Georgia (bank code TRESGE22) on the account of the Georgian National Academy of Sciences (receiver code 708777499).

ИНФОРМАЦИЯ ДЛЯ АВТОРОВ

Журнал "**Известия Национальной Академии наук Грузии. Серия химическая**" публикует статьи и краткие сообщения в области химических наук на грузинском, английском и русском языках; обзорные статьи и материалы информационного характера публикуются по предварительному согласованию с редакционной коллегией. Объем, формат и условия представления материала для публикации следует согласовать с ответственным секретарем; авторы должны представить тексты в виде файлов Microsoft Word (***.doc или ***.rtf), а рисунки, чертежи и фотоснимки – в виде черно-белых графических (*.bmp, *.dib, *.jpg, *.gif и др.) файлов. Для оказания помощи авторам научных статей, редакция предусматривает стандартные электронные формы на всех трех языках, а также другую техническую поддержку. Для реферирования статьи в Chemical Abstracts (на английском языке) и Грузинском реферативном журнале (на английском и грузинском языках) авторам следует предусмотреть содержательные резюме на обоих языках.

Оплата расходов по публикации производится перечислением согласованной с коллегией суммы на счёт Национальной Академии наук Грузии в Казначействе Грузии (код банка TRESGE22, код получателя 708777499).